Complexes of Rhenium and Technetium with Multidentate Phosphine Ligands

Department of Biology, Chemistry and Pharmacy
Freie Universität Berlin
PhD Dissertation

Ali Barandov
Berlin, March 2009

1. Supervisor: Prof. Dr. Ulrich Abram
2. Supervisor: Prof. Dr. Konrad Seppelt

Date of the oral presentation: 30.04.2009

Acknowledgment

I would like to acknowledge my supervisor Prof. Dr. U. Abram whose help, suggestions and encouragement assisted me in all the time of research.

I gratefully thank Prof. Dr. K. Seppelt for being my second supervisor.

I would like to thank Prof. Dr. B. Koksch for her collaboration in the solid-phase labelling project.

I would like to express my deepest sense of appreciation to my wife Rahele Rezaei-Araghi. Her support and patience were undeniably the greatest encouragement. Moreover, I acknowledge her productive collaboration in the solid-phase labelling project.

I thank Dr. Adelheid Hagenbach for her constructive crystallographic discussions and X-ray measurements.

I am very grateful for the friendship of Jacqueline Grewe, Nguyen Hung Huy, Dr. Alexander Jagst, Jennifer Schroer and Stephan Meyer with whom I worked closely and puzzled over many of the same problems.

I gratefully acknowledge a PhD scholarship of the German Academic Exchange Service (DAAD).

I would like to sincerely thank the Institute of Chemistry and Biochemistry of the Freie Universität Berlin, the analytical services and particularly Mrs. Doris Plewinsky for uncounted elemental analyses.

I would like to acknowledge support and help of all my colleagues and friends, Elisabeth Oehlke, Bernd Kuhn, Detlef Wille, Dr. Sonia Saucedo Anaya.

I would like to thank my project students, Carolin Nietzold, Dennis Wiedemann, Farhad Tamadon, Lars Kirsten, Christian Gröschl for their enthusiasm and hardworking.

Summary of contents

Abbreviations

Bu	Butyl
Calcd.	Calculated
d	Doublet
Et	Ethyl
EtOH	EtOH
IR	Infrared
m	Medium
Me	Methyl
Me_2CO	Acetone
MeOH	Methanol
MS	Mass Spectrometry
NBu_4	Tetrabutylammonium
NEt_4	Tetraethylammonium
NMR	Nuclear Magnetic Resonance
Ph	Phenyl
s	Singlet
st	Strong
t	Triplet
temp.	Temperature
THF	Tetrahydrofurane
w	Weak

Abstract

This thesis contains synthesis and structural characterization of novel technetium and rhenium complexes with polydentate phosphine-containing ligand systems, which have been designed: (i) for the synthesis of metal complexes of high stability and (ii) as starting materials for bioconjugation purposes. Therefore, derivatives with linking groups such as carboxylic or hydroxylic groups were prepared and tested in typical bioconjugation procedures with small peptides such as triglycine or natural peptides such as Substance P.

Chapter 1

Introduction

1.1 Introduction

Technetium and rhenium coordination chemistry is of particular interest due to the favorable nuclear properties of ^{99m}Tc ($E\gamma$ = 140 keV, $t_{1/2}$ = 6.02 h) which makes this isotope the workhorse for diagnostic nuclear medicine [1]. The β-emitting rhenium nuclides ^{186}Re and ^{188}Re are under investigation for possible applications in radioimmunotherapy [2]. Fundamental chemical studies are possible with the naturally occurring rhenium (^{185}Re, 37.07%; ^{187}Re, 62.93%) or the long-lived technetium isotope ^{99}Tc (weak β-emitter, E_{max} = 0.3 MeV, $t_{1/2} = 2.12 \times 10^5$ a) which allows conventional laboratory techniques.

Common metal-containing radiopharmaceuticals base on stable or kinetically inert complexes: either with strong chelating or tightly bonded monodentate ligands. Remarkable examples of such complexes are the clinically used ^{99m}Tc-based imaging agents Tc-(HMPAO) (HMPAO = hexamethylpropyleneamine oxime) [3], and Tc(MIBI) (MIBI = 2-methoxy-2-methylpropyl-isonitrile) [4], which are applied in cerebral or myocardial imaging.

Modern medicine demands progressively more sophisticated methods which are able to target specific receptor sites in the body. This is achieved by using a bifunctional chelating agent which strongly binds to the radioactive metal and is equipped with a second molecular site, which can be covalently attached to a targeting molecule, such as a monoclonal antibody, a peptide, or other biologically active molecules.

Heterofunctionalized phosphines with additional oxygen or nitrogen donor sites attract growing interest in the coordination chemistry of rhenium and technetium. The reduction potential of phosphines and the strong chelate formation tendency due to the mixed hard/soft donor set make heterofunctionalized phosphines good candidates for kit preparation procedures [5].

Multidentate Schiff bases with PNO and PNS donor sets derived from (2-formyl phenyl)diphenylphosphine are of great interest in the coordination chemistry of transition metals. Complexes of such compounds with the first [6], second [7], and third [8] row of the transition metals are well studied. Structurally characterized complexes of rhenium and technetium with this class of ligands are restricted to complexes with the metal ions in lower oxidation states and to bidentate chelating ligands. Complexes of the compositions $[Re(CO)_3X(L)]$ (X = Cl, Br; L = $Ph_2PC_6H_4$-2-CH=NPh) [9] and $[Re(CO)_3Br(L)]$ {L = 2-(2-(diphenylphosphino)phenyl)oxazoline} [10] were isolated and characterized by X-ray diffraction.

(2-Benzylamino)phosphines, $Ph_{3-n}P(C_6H_4\text{-}2\text{-}CH_2NHR)_n$ (n = 1 – 3, R = aryl, alkyl) can be synthesized by the reduction of the related Schiff bases [11] or *in situ* reduction of the reaction mixtures of primary amines and (2-formylphenyl)phosphines [12]. Some complexes of the multidentate (2-benzylamino)phosphines are known with main group [13] and transition metals [14]. Such compounds are versatile reagents for synthetic organic and organometallic chemistry. Structurally characterized complexes of (2-benzyl amino)phosphines with rhenium and technetium are rare. According to the Cambridge Structural Database (CSD), there are two rhenium complexes of the composition $[Re(CO)_3Br(PN)]$, where PN are bidentate neutral (2-benzylamino)phosphines [9,15].
(2-Aminophenyl)phosphines, $Ph_{3-n}P(C_6H_4\text{-}2\text{-}NHR)_n$ (n = 1 – 3, R = H, Aryl, Alkyl) are multipurpose compounds in the coordination chemistry. Complexes of (2-aminophenyl) phosphines with primary amines are restricted to compounds with (2-aminophenyl) diphenylphosphine, as a bidentate chelating ligand. Such rhenium and technetium complexes were reported with the metal ions in their higher oxidation states and with oxo-, imido-, and nitridorhenium(V) and -technetium(V) cores [16]. However, (2-aminophenyl)phosphines with secondary amines, which were reported as potentially bidentate [P,N] [17], tridentate, [P,N,O/P] [18] and tetradentate [P,N,N,P] [19] ligand systems for a number of metal ions are almost unknown in the rhenium and technetium coordination chemistry. There is only little information about complexes with the tetradentate $\{(Ph_2PC_6H_4\text{-}2\text{-}NHCH_2)_2CH_2\}$ ligand [20].
Phosphine ligands with additional oxygen donors have attracted significant interest due to the application of their transition metal complexes in organometallic and polymer chemistry [21]. Some rhenium and technetium complexes of (2-hydroxyphenyl)phosphines, $Ph_{3-n}P(C_6H_4\text{-}2\text{-}OH)_n$, have recently been studied because of their potential applications in the development of new radiopharmaceuticals [22].

This thesis will introduce four novel classes of heterofunctionalized phosphines:

- (2-benzylimino)phosphines
- (2-benzylamino)phosphines
- (2-aminophenyl)phosphines
- {2-(hydroxymethyl)phenyl}phosphines.

These compounds were designed for the synthesis of stable complexes of rhenium and technetium, which can potentially be used in nuclear medicine. In order to fulfill this aim, polydentate heterofunctionalized phosphines with up to seven donor atoms were synthesized. This will allow to either encapsulate the whole metal ion within one ligand or cover the labile

coordination sites of a stable core such as "$\{M(CO)_3\}^+$" (M = Re, Tc). Consequently, this will prevent probable interactions between the metal ion and its environment, which normally contains a manifold of competing ligand system. Such studies play a key role in the fundamental chemistry of metal-based radiopharmaceuticals.

With the aim of labelling natural polypeptides such as neurotransmitters by the resulting stable complexes, bifunctional phosphines were designed by keeping the main molecule architecture of favorable ligand system which have found during the basic chemical studies. The attachment of carboxylic groups to the backbone of such ligand allows bioconjugation reactions with the help of liquid-, and solid-phase peptide synthesis techniques.

1.2 References

[1] a) Alberto, R. *Technetium, Comprehensive Coordination Chemistry II, Elsevier*, **2004**, 126; b) Clarke, M. J.; Podbielski, L. *Coord. Chem. Rev.*, **1987**, *78*, 253.

[2] Abram, U. *Rhenium, Comprehensive Coordination Chemistry II, Elsevier*, **2004**, 271.

[3] a) Morrissey, G. J.; Powe, J. E. *J. Nucl. Med*., **1993**, *34*, 151; b) Nakamura, K.; Tukatani, Y.; Kubo, A.; Hashimoto, S.; Terayama, Y.; Amano, T.; Goto, F. *Eur. J. Nucl. Med.*, **1989**, *15*, 100.

[4] Delmon-Moingeon, L. I.; Piwnica-Worms, D.; Van den Abbeele, A. D.; Holman, B. L.; Davison, A.; Jones, A. G. *Cancer Res.*, **1990**, *50*, 2198.

[5] a) Greenland W. E. P; Blower P. J. *Bioconjugate Chem.*, **2005**, *16*, 939; b) Bolzati, C.; Benini, E.; Cavazza-Ceccato, M.; Cazzola, E.; Malago, E.; Agostini, S.; Tisato, F.; Refosco, F.; Bandoli, G. *Bioconjugate Chem.*, **2006**, *17*, 419.

[6] a) Tang, X.; Zhang, D.; Jie, S.; Sun, W.; Chen, J. *J. Organomet. Chem.*, **2005**, *690*, 3918; b) Hou, J.; Sun, W.; Zhang, S.; Ma, H.; Deng, Y.; Lu, X. *Organometallics*, **2006**, *25*, 236.

[7] a) Reddy, K. R.; Tsai, W.; Surekha, K.; Lee, G.; Peng, S.; Chen, J.; Liu, S. *J. Chem. Soc., Dalton Trans.*, **2002**, 1776; b) Song, H.; Zhang, Z.; Mak, W. T. C. *Polyhedron*, **2002**, *21*, 1043.

[8] a) Garcia-Yebra, C.; Janssen, J. P.; Rominger, F.; Helmchen, G. *Organometallics*, **2004** , *23*, 5459; b) Carmona, D.; Vega, C.; Garcia, N.; Lahoz, F. J.; Elipe, S.; Oro, L. A.; Lamata, M. P.; Viguri, F.; Borao, R. *Organometallics*, **2006**, *25*, 1592.

[9] Chen, X.; Femia, F. J.; Babich, J. W.; Zubieta, J. *Inorg. Chim. Acta,* **2001**, *315*, 147.

[10] Kniess, T.; Correia, J. D. G.; Domingos, A.; Palma, E.; Santos, I. *Inorg. Chem.*, **2003**, *42*, 6130.

[11] Correia, I.; Pessoa, J.; Duarte, M. T.; Da Piedade, M. F.; Jackush, T.; Kiss, T.; Castro, M. M. C. A.; Geraldes, C. F. G. C.; Avecilla, F. *Eur. J. Inorg. Chem.*, **2005**, *4*, 732.

[12] Del Zotto, A.; Baratta, W.; Ballico, M.; Herdtweck, E.; Rigo, P. *Organometallics*, **2007**, *26*, 5636.

[13] a) Izod, K.; O'Shaughnessy, P.; Clegg, W. *Organometallics* , **2002**, *21*, 641, b) Clegg, W.; Doherty, S. N; Izod, K.; Kagerer, H.; O'Shaughnessy, P.; Sheffield, J. M. *J. Chem. Soc., Dalton Trans.*, **1999**, 1825.

[14] a) Ainscough, E. W.; Brodie, A. M.; Burrell, A. K.; Kennedy, S. M. F. *J. Am. Chem. Soc.,* **2001**, *123*, 10391; b) Watkins, S. E.; Craig, D. C.; Colbran, S. B. *J. Chem. Soc., Dalton Trans.*, **2002**, 2423.

[15] Palma, E.; Correia, J. D. G.; Domingos, A.; Santos, I.; Alberto, R.; Spies, H. *J. Organomet. Chem*., **2004**, *689*, 4811.

[16] a) Bolzati, C.; Tisato, F.; Refosco, F.; Bandoli, G.; Dolmella, A. *Inorganic Chem.* **1996**, *35*, 6221; b) Refosco, F.; Bolzati, C.; Tisato, F.; Bandoli, G. *J. Chem. Soc., Dalton Trans.*, **1998**, 923; c) Refosco, F.; Tisato, F.; Moresco, A.; Bandoli, G. *J. Chem. Soc., Dalton Trans.*, **1995**, 3475.

[17] a) Lan-Chang, L.; Wei-Ying, L.; Chi-Chun, Y. *Organometallics*, **2004**, *23***,** 3538; b) Dahlenburg, L.; Herbst, K. *Chem. Ber.*, **1997**, *130*, 1693.

[18] a) Wei-Qiu, H.; Xiu-Li, S.; Cong,W.; Yuan, G.; Yong, T.; Li-Ping, S.; Wei, X.; Jie, S.; Hou-Liang, D.; Xiao-Qiang, L.; Xiao-Li, Y.; Xing-Ren, W. *Organometallics*, **2004**, *23*, 1684; b) Ainscough, E. W.; Brodie, A. M.; Burrell, A. K.; Kennedy, S. M. F. *J. Am. Chem. Soc.,* **2001**, *123*, 10391.

[19] Tisato, F.; Refosco, F.; Bandoli, G.; Pilloni, G.; Corai, B. *J. Chem. Soc., Dalton Trans.*, **1994**, 2471.

[20] Tisato, F.; Refosco, F.; Moresco, A.; Bandoli, G.; Dolmella, A.; Bolzati, C. *Inorg. Chem.*, **1995**, *34*, 1779.

[21] Marciniec, B.; Lawicka, H.; Dudziec, B. *Organometallics,* **2008**, *27*, 235.

[22] Bolzati, C.; Tisato, F; Bandoli, G. *Inorg. Chim. Acta*, **1996**, *247*, 125.

Chapter 2

2-(Benzylimino)phosphines and their reactions with oxorhenium(V) complexes

2.1 Synthesis of 2-(benzylimino)phosphines

2.1.1 Synthesis of (2-formylphenyl)phosphines

A common way for the synthesis of multidentate ligands is the imine condensation. The resulting compounds, so called "Schiff bases" [1], can readily be achieved by reactions between aldehydes (or ketones) and primary amines or similar compounds such as hydrazine derivatives. Many Schiff base ligand systems such as H_2Salen, (o-$C_6H_4HC{=}N\text{-}CH_2\text{-})_2$, are obtained from salicylaldehyde and their complexes with rhenium and technetium have been well studied during the recent years [2].

(2-Formylphenyl)diphenylphosphine (**V**) is a versatile starting material for the synthesis of ligand systems which comprise mixed soft (P) and hard (N/O) donor atoms [3]. Bis- and tris(2-formylphenyl)phosphines (**VI, VII**) can be used for the synthesis of ligand systems with high numbers of denticity owing to two or three formyl groups.

(2-Formylphenyl)phosphines (**V - VII**) are prepared by two synthetic pathways with moderate overall yields, Scheme 2.1.

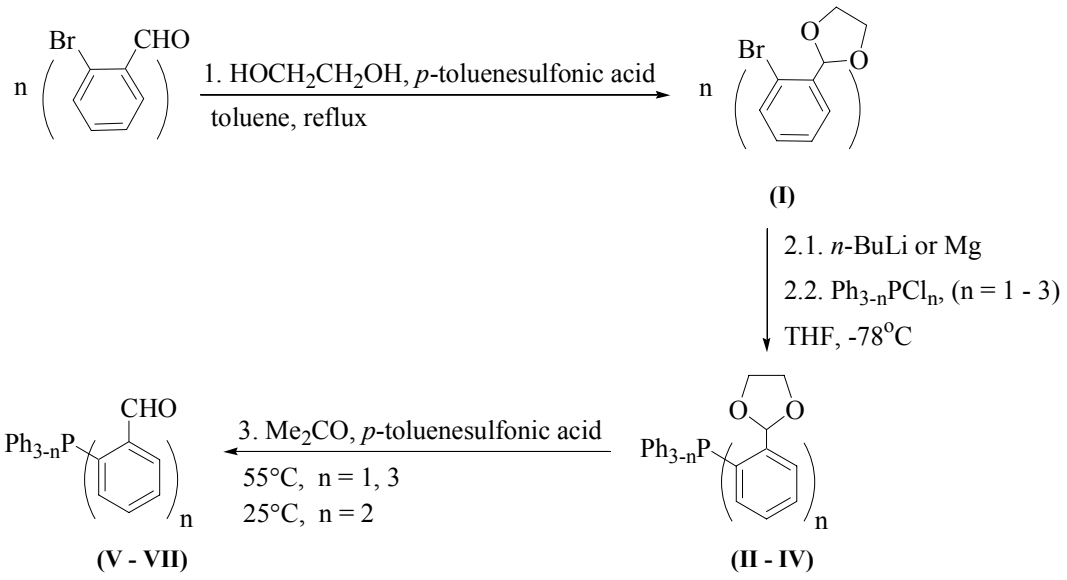

Scheme 2.1 General synthetic pathway for the synthesis of (2-formylphenyl)phosphines (**V – VII**)

The first method bases on ortholithiation of 2-bromophenyl-1,3-dioxolane (**I**). The general procedure was adopted from the report of Kaack *et al.* [4] except of some modifications in the deprotection step (Scheme 2.1, step 3), which improves the yield of the reaction. The second synthetic pathway bases on the standard Grignard orthometalation of 2-bromophenyl-1,3-dioxolane (**I**) in dry diethylether at 30°C. The orthometalated species were reacted with $Ph_{3-n}PCl_n$ (n = 1 - 3) under formation of [2-(1,3-dioxolane-2-yl)phenyl]phosphines (**II - IV**), which were obtained as colorless crystalline solids in moderate yields.

The ^{31}P-{H} NMR spectra of **II - IV** show single resonances of the phosphines between −20.0 and −35.0 ppm. The ^{1}H NMR spectra of **II - IV** present a doublet at 6.1 ppm, which is assigned to the methine proton (CH). The splitting pattern of the signal is due to the coupling with the phosphorus atom, J_{PH} = 5.2 Hz.

As shown in Scheme 2.1, the deprotection of bis-[2-(1,3-dioxolane-2-yl)phenyl]phenyl phosphine (**III**) must be carried out at room temperature to avoid different side reactions reported by Rauchfuss *et al.* [5].

All the three (2-formylphenyl)phosphines (**V - VII**) were isolated as orange yellow micro-crystalline compounds. The ^{13}P-{H} NMR spectra of the isolated (2-formylphenyl)phosphines show single resonances at −10.1 ppm for **V,** −15.2 ppm for **VI** and −20.1 ppm for **VII**. The ^{1}H NMR spectra confirm the supposed formyl functions by doublets at 10.2 ppm. The IR spectra present strong absorptions in the range of 1670 to 1690 cm^{-1} due to the carbonyl stretching vibrations.

The 2-(benzylimino)phosphines were synthesized by heating mixtures of primary amines and (2-formylphenyl)phosphines in EtOH. The products were obtained in solid form directly from the reaction mixtures, Scheme 2.2.

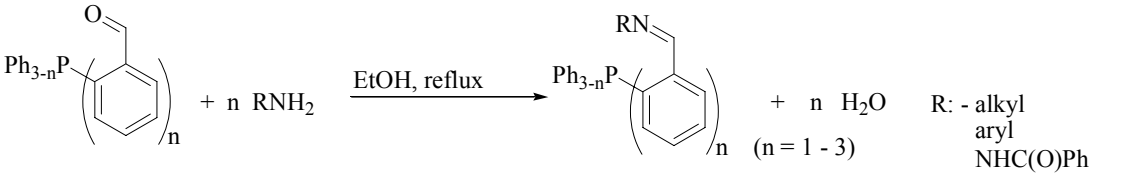

Scheme 2.2 General synthetic pathway for 2-(benzylimino)phosphines

2.1.2 Synthesis of the tetradentate 2-(benzylimino)phosphines derived from 1,2-diaminocyclohexane and 1,2-diaminoethane

The 2-(benzylimino)phosphines L^{11} and L^{21} were synthesized based on the reported procedures in good yields [6,7], Scheme 2.3.

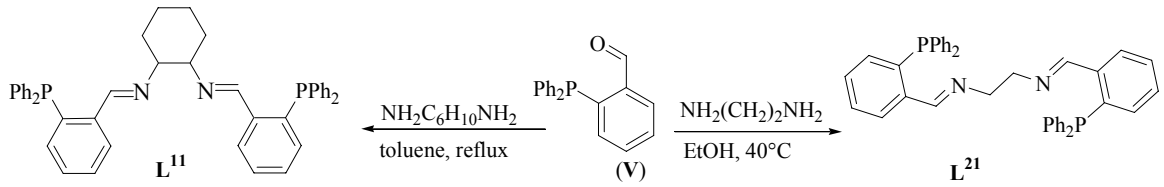

Scheme 2.3 Synthesis of the 2-(benzylimino)phosphines L^{11} and L^{21}

The ^{31}P-{H} NMR spectra of the compounds L^{11} and L^{21} show single resonances at about −13.1 ppm as is expected for compounds with two magnetically equivalent phosphorus atoms. The ^{1}H NMR spectra present doublets at about 8.7 ppm, which confirm the imine function of L^{11} and L^{21}. Intense IR absorptions at about 1637 cm^{-1} were assigned to the stretching vibrations of the imine groups. The FAB^{+} mass spectra of both compounds are consistent with the supposed molecular structures by presenting the molecular ions of L^{11} (*m/z* = 659.0 amu) and L^{21} (*m/z* = 604.7 amu).

2.1.3 Syntheses of hydrazonic Schiff bases

Hydrazine derivatives such as benzoylhydrazine and semicarbazides are versatile compounds in the coordination chemistry of the d- and f-block metals [8,9]. Benzoylhydrazine and 4-phenylsemicarbazide react with (2-formylphenyl)diphenylphosphine (**V**) in EtOH under reflux to give HL^{31} and HL^{41} as colorless solids in good yields, Scheme 2.4.

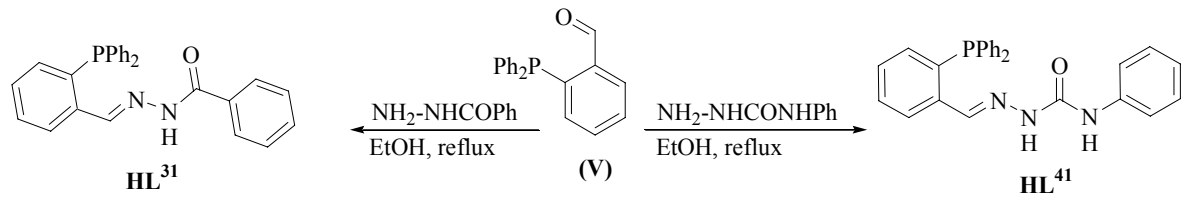

Scheme 2.4 Synthesis of the hydrazonic Schiff bases HL^{31} and HL^{41}

^{31}P-{^{1}H} NMR spectra of HL^{31} and HL^{41} show single resonances of phosphines at about −15.0 ppm. The ^{1}H NMR spectra of both compounds show doublets at 9.15 ppm for HL^{31} and 8.56 ppm for HL^{41}, which support the presence of the imine functions. Moreover, the spectrum of HL^{31} exhibits a singlet at 12.02 ppm related to the NH group, which appears at

higher chemical shift values compared to that of HL^{41} at 10.86 ppm. This implies a higher acidity of the NH group of HL^{31}. The amide hydrogen atom (Ph*H*NCO) of HL^{41} was detected as a singlet at 8.80 ppm. The IR spectrum of HL^{31} shows a weak absorption at 3209 cm^{-1} while for HL^{41} two weak bands at 3344 and 3317 cm^{-1} are found for the NH stretching vibrations.

2.1.4 Synthesis of the bi- and tridentate Schiff bases derived from 2-aminophenol

$HL^{51}P$ was synthesized from the reaction of (2-formylphenyl)diphenylphosphine (**V**) with an equimolar amount of 2-aminophenol in EtOH under reflux. The product was isolated as an orange yellow solid. $HL^{51}PO$ was synthesized by the reaction of $HL^{51}P$ with an excess amount of H_2O_2 (30% wt) in EtOH. $HL^{51}PO$ was obtained as a microcrystalline solid. The isolated product was recrystallized from a mixture of CH_2Cl_2/*n*-hexane at −10°C, Scheme 2.5.

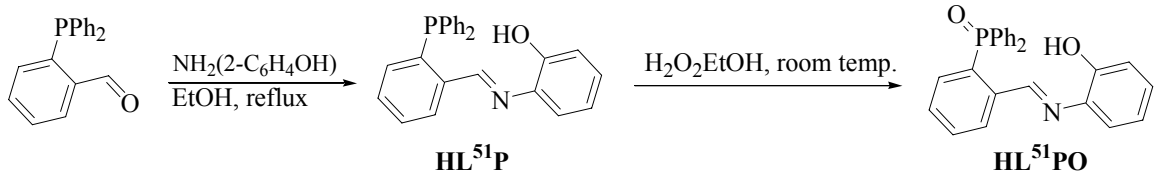

$HL^{51}P$ **$HL^{51}PO$**

Scheme 2.5 Synthesis of the 2-(benzylimino)phosphines, $HL^{51}P$ and $HL^{51}PO$.

The ^{31}P-{^{1}H} NMR spectra show single resonances at −12.9 ppm for $HL^{51}P$ and at 31.6 ppm for $HL^{51}PO$. The low-field shift of the signal of $HL^{51}PO$ compared to that of HL^{51} is consistent with the molecular structures of the compounds. The imine group signals in the ^{1}H NMR spectra are detected as a doublet at 9.1 ppm for $HL^{51}P$ and a singlet at 10.0 ppm for $HL^{51}PO$. Intense IR absorptions at 1631 cm^{-1} for HL^{51} and 1693 cm^{-1} for $HL^{51}PO$ are due to the stretching vibrations of the imine groups.

2.2 Reactions of 2-(benzylimino)phosphines with oxorhenium(V) complexes

2.2.1 Reactions of L^{11} and L^{21} with $(NBu_4)[ReOCl_4]$

Despite the fact that complexes of the 2-(benzylimino)phosphines L^{11} and L^{21} were studied with different d-block transition metals [10], nothing is known about their rhenium complexes.

$(NBu_4)[ReOCl_4]$ reacts with L^{11} in MeOH at ambient temperature under formation of two unexpected complexes: $[ReOCl(L^{11b})_2]$ (**1**) and $[ReOCl(L^{11a})](\mu\text{-}O)[ReOCl_2(L^{11b})]$ (**2**), Scheme 2.6.

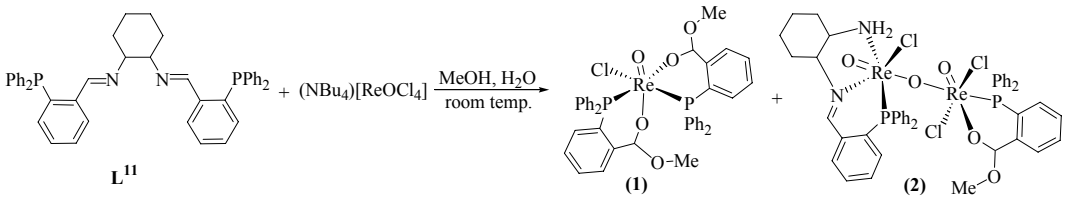

Scheme 2.6 The reaction between $(NBu_4)[ReOCl_4]$ and L^{11}

The molecular structure of the main product **1** is presented in Fig. 2.1 and selected bond lengths and angles in Table 2.1. $[ReOCl(L^{11b})_2]$ (**1**) is a neutral oxorhenium(V) complex. The coordination sphere of the rhenium atom is occupied by two of the unexpectedly formed bidentate chelating ligand $(L^{11b})^-$, a chloro, and the terminal oxo ligands. Surprisingly, L^{11b} possesses a hemiacetal group, which is formed during the complex formation reaction. Similar *in situ* formation of hemiacetal was reported by *Alberto et al.* for the reaction of 2-pyridine aldehyde with $[Re(CO)_3Br_3]^{-2}$ [11]. However, this can be explained by the equilibrium between aldehydes and hemiacetals in alcohols [12]. The formation of **1** is the first example of the formation of a hemiacetal from an imine. The coordination environment the rhenium atom is distorted octahedral with a Re-O(10) distance of 1.686(9) Å and a Re-Cl bond of 2.418(5) Å. The chelating ligands $(L^{11b})^-$ are bonded mutually *cis* with O(3) (oxygen atom of the hydroxyl group of one of the hemiacetals) *trans* to the oxo ligand. The O(10)-Re-O(1) angle of 103.7(5)° is bigger than the ideal value of 90°, which results from the repulsion of the π-electrons of the terminal oxo ligand and the donor atoms in the equatorial plane. The O(1)-C(7) bond length of 1.39(2) Å as well as the O(1)-C(7)-O(2) angle of 107.3(1)° suggest sp^3 hybridization for C(7). This supports the hemiacetal functionality and is contrary to the presence of an ester or a carboxylic group [13].

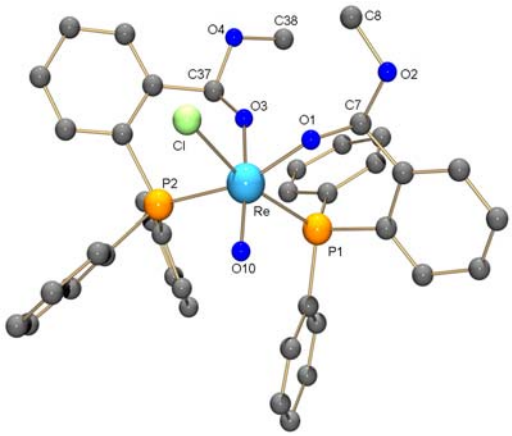

Fig. 2.1 Molecular structure of [ReOCl(L^{11b})$_2$] (**1**). The hydrogen atoms were omitted for clarity.

Table 2.1 Selected bond lengths and angles of [ReOCl(L^{11b})$_2$] (**1**)

Bond Lengths [Å]:					
Re-O(10)	1.686(9)	Re-O(1)	1.97(1)	Re-O(3)	1.95(1)
Re-Cl	2.418(5)	Re-P(1)	2.491(6)	Re-P(2)	2.449(6)
O(1)-C(7)	1.39(2)	C(7)-O(2)	1.43(2)	O(2)-C(8)	1.44(2)
Bond Angles [°]:					
O(10)-Re-O(1)	103.7(5)	O(10)-Re-O(3)	168.0(5)	O(1)-Re-O(3)	87.2(4)
Cl-Re-P(1)	168.1(2)	C(7)-O(2)-C(8)	115.3(1)	C(37)-O(4)-C(38)	116.2(2)

The ^{1}H NMR spectrum of **1** exhibits two singlets at about 1.7 ppm (6H) for two methyl groups. A multiplet at 7.2 ppm with the integration of two protons is related with the methine protons, HC(7), HC(37) of the hemiacetal groups. Similar chemical shift values were observed for the hemiacetals derived from substituted benzaldehydes [14-15]. The IR spectrum supports the molecular structure by an intense band at 984 cm^{-1} for the Re=O stretching vibration. The absence of any absorption between 1600 and 2100 cm^{-1} confirms the absence of an ester group. The MS(ESI) spectrum shows the base peak at *m/z* = 881 amu with the expected isotopic pattern for the [M+H]$^+$ fragment.

Fig. 2.2 depicts the molecular structure of the dinuclear rhenium(V) complex [ReOCl(L^{11a})](μ-O)[ReOCl$_2$(L^{11b})] (**2**). Selected bond lengths and angles are summarized in Table 2.2. The compound contains two rhenium(V) centers connected by an oxo ligand. Surprisingly, the terminal oxo ligands, O(10) and O(30), are *trans* and *cis* to the bridging oxygen atom O(20), which is an extremely rare example in the coordination chemistry of rhenium. The bridging oxygen has Re-O bond distances of 1.83(1) Å for Re(1)-O(20) and 2.02(1) Å for Re(2)-O(20). Presumably, the intense difference in bond distances between the rhenium atoms and the bridging oxo ligand is induced by two effects:

- The electron transfer from the terminal oxo ligand to the mutually *trans* coordinated oxygen atom O(20) shortens the Re(1)-O(20) distance
- The strong *trans* influence of the phosphine group lengthens the Re(2)-O(20) distance.

Similar observation has been reported by Volkert *et al.*, where $[Re(O)(\mu\text{-}O)(P\{CH_2OH\}_3)(\mu\text{-}\eta^2\text{-}P\{CH_2OH\}_2CH_2O)]_4$ shows the *trans* μ-oxo bond lengths are much shorter as compared to the *cis* μ-oxo ones [16].

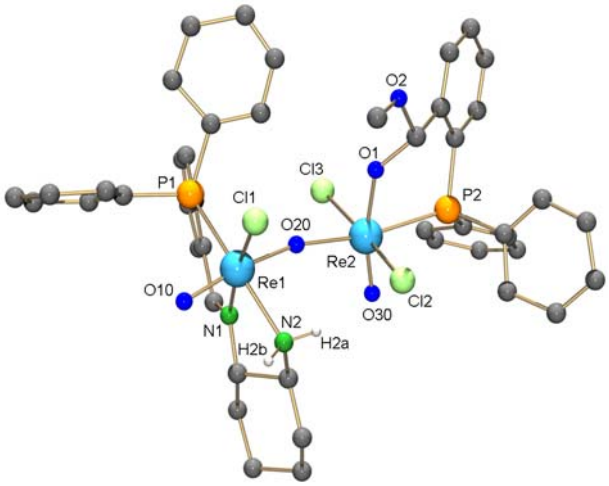

Fig. 2.2 Molecular structure of $[ReOCl(L^{11a})](\mu\text{-}O)[ReOCl_2(L^{11b})]$ (**2**). The hydrogen atoms bonded to carbon atoms were omitted for clarity.

Table 2.2 Selected bond lengths and angles of $[ReOCl(L^{11a})](\mu\text{-}O)[ReOCl_2(L^{11b})]$ (**2**)

Bond lengths [Å]:					
Re(1)-O(10)	1.67(1)	Re(1)-O(20)	1.83(1)	Re(1)-N(1)	2.12(2)
Re(1)-N(2)	2.19(1)	C(7)-N(1)	1.27(3)	Re(2)-O(20)	2.02(1)
Re(2)-O(30)	1.69(1)	Re(2)-P(2)	2.454(4)	O(1)-C(47)	1.41(2)
O(2)-C(47)	1.42(2)	O(2)-C(48)	1.42(3)		
Angles [°]:					
O(10)-Re(1)-O(20)	170.7(5)	Re(1)-O(20)-Re(2)	166.4(6)	O(30)-Re(2)-O(20)	102.8(5)

Hydrogen bonds:				
D-H...A	d(D-H)	d(H...A)	d(D...A)	<(DHA)
N(2)-H(2B)...O(10)[a]#1	0.90	2.23	3.11(2)	168.4

a) Symmetry transformations used to generate equivalent atoms: #1 -x+2,-y+1,-z+2

The nitrogen atom N(2) establishes a hydrogen bond via H(2B) to O(10) in the adjacent molecule with a donor-acceptor distance of 3.11(2) Å. The N(1)-C(7) bond length of 1.27(3) Å is consistent with a double bond. Since the purity of L^{11} was proved by means of the different analytical methods before being used for the complex formation reaction, the resulting fragments L^{11a} and L^{11b} must be formed by the dissociation of the imine group during the reaction.

A comparison between the molecular structure of **1** and **2** indicates that **2** should be an intermediate compound for the formation of the major product $[ReOCl(L^{11b})_2]$ (**1**). Scheme 2.7 exhibits the suggested reaction pathway.

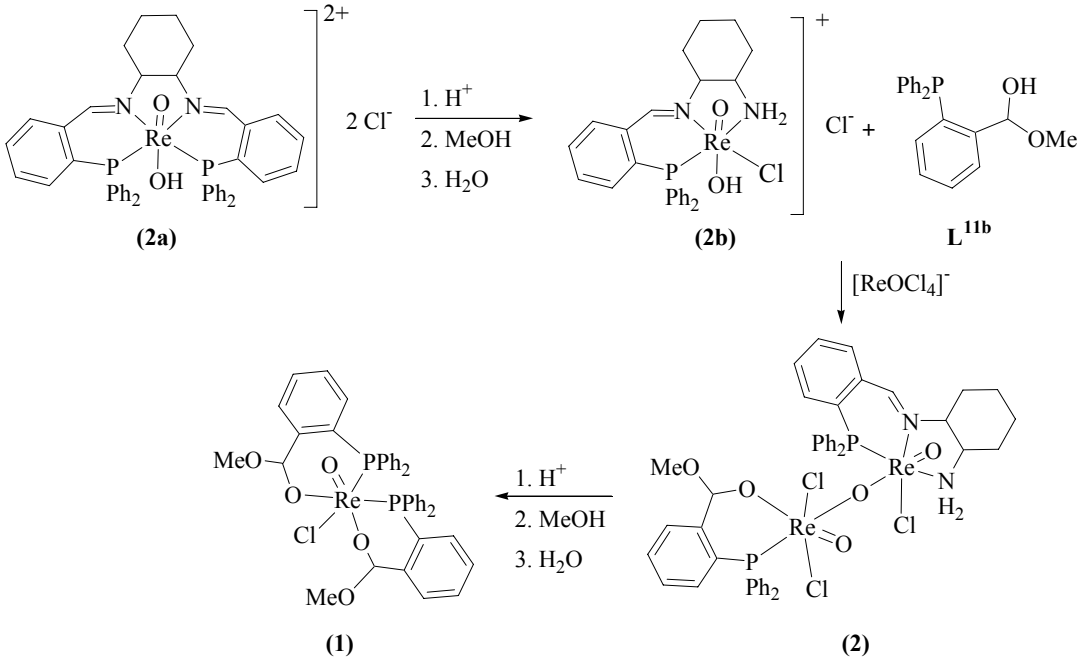

Scheme 2.7 The suggested reaction pathway for the formation of $[ReOCl(L^{11b})_2]$ (**1**)

It is supposed that L^{11} reacts with $(NBu_4)[ReOCl_4]$ under formation of the intermediate complex **2a**. After consecutive acidic solvolysis and hydrolysis of **2a**, the *in situ* formed compounds L^{11b} and **2b** react with $(NBu_4)[ReOCl_4]$ under formation of **2**. The second imine group of $[ReOCl(L^{11a})](\mu\text{-}O)[ReOCl_2(L^{11b})]$ (**2**) undergoes the next consecutive acidic solvolysis and hydrolysis to give **1** in a moderate yield. The suggested reaction mechanism is supposed basing on the molecular structures of **1**, **2** and the applied reaction conditions.

Contrary to L^{11}, which possesses a rigid configuration because of its cyclic backbone, L^{21} is flexible and can principally form monomeric and dimeric complexes by rotating around the C-C bond of ethylene group, Fig.2.3.

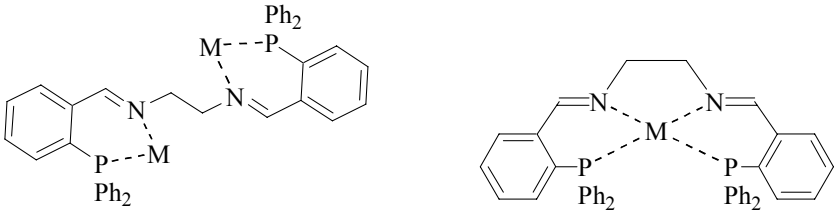

Fig. 2.3 Possible coordination modes of L^{21}

The reaction between the 2-(benzylimino)phosphine L^{21} and two equivalents of $(NBu_4)[ReOCl_4]$ in methanol at ambient temperature results in precipitation of $[\{ReOCl_2(OMe)\}_2(\mu\text{-}L^{21})]$ (**3**). Fig. 2.4 presents the molecular structure of **3**, where L^{21} coordinates to two oxorhenium(V) cores in a bidentate [P,N] mode. The rest of the coordination sites are occupied by each two chloro ligands in the equatorial plane and a methoxo groups *trans* to the oxo ligands. Selected bond lengths and angles of **3** are presented in Table 2.3.

A centre of inversion is located in the center of the C-C bond of ethylene group. The C(7)-N(1) bond length of 1.29(1) Å is in the range of a carbon-nitrogen double bond [17]. Moreover, the C(6)-C(7)-N(1) and C(7)-N(1)-Re angles of 130.5(9)° and 128.2(6)° elucidate a planar geometry about C(7), which is consistent with the imine functionality of L^{21}.

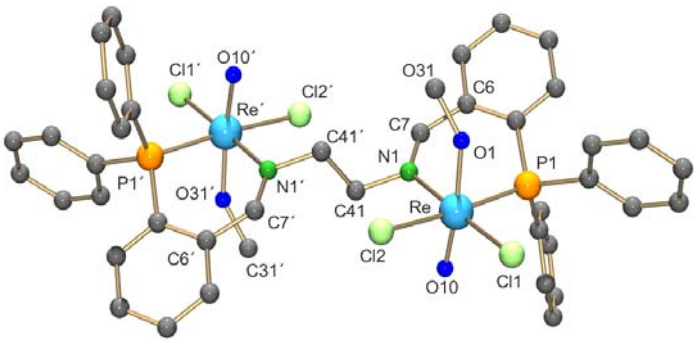

Fig. 2.4 Molecular structure of $[\{ReOCl_2(OMe)\}_2(\mu\text{-}L^{21})]$ (**3**). The hydrogen atoms were omitted for clarity.

Table 2.3 Selected bond lengths and angles of $[\{ReOCl_2(OMe)\}_2(\mu\text{-}L^{21})]$ (**3**)

Bond Lengths [Å]:					
Re(1)-O(10)	1.728(7)	Re(1)-O(1)	1.874(7)	Re(1)-P(1)	2.391(2)
Re(1)-Cl(1)	2.363(2)	Re(1)-Cl(2)	2.464(2)	Re(1)-N(1)	2.163(8)
Bond Angles [°]:					
O(10)-Re(1)-O(1)	168.2(3)	O(10)-Re(1)-P(1)	92.8(2)	Cl(1)-Re(1)-N(1)	178.5(2)
O(10)-Re(1)-Cl(1)	97.2(2)	O(1)-Re(1)-P(1)	85.4(2)	C(6)-C(7)-N(1)	130.5(9)

The Re(1)-O(10) distance of 1.728(7) Å is in the range of a rhenium-oxygen double bond [18] and the Re-O(1) bond length of 1.874(7) Å is consistent with the alkyloxo-Re bond *trans* to the terminal-oxo ligand [19]. This implies a high degree of electron transfer from the terminal oxo ligand O(10) to its *trans* position. The difference between the bond lengths of Re(1)-Cl(1) of 2.363(2) Å and Re(1)-Cl(2) of 2.464(2) Å reflects a stronger *trans* influence of the phosphine group compared to an imine.

The intense absorptions at 1616 and 948 cm^{-1} in the IR spectrum of **3** are characteristic for the C=N and Re=O vibrations, where the $\nu_{C=N}$ shows a 16 cm^{-1} bathochromic shift compared to the uncoordinated L^{21}. The ^{31}P-$\{^1H\}$ NMR spectrum of **3** shows a single resonance at 23.2 ppm suggesting a coordinated phosphine.

2.2.2 Reactions of hydrazonic Schiff bases with oxorhenium(V) complexes

Hydrazonic Schiff bases, such as benzoylhydrazones and semicarbazones, are versatile ligands, the complexes of which found attention in analytical and medical applications. These ligands coordinate as neutral or anionic chelators commonly via their azomethine nitrogen and the oxygen atoms [20].

HL^{31} reacts with $(NBu_4)[ReOCl_4]$ in MeOH without addition of a supporting base under formation of *mer*-$[ReOCl(OMe)(L^{31})]$ (**4**) in high yield, Scheme 2.8. The reaction must be carried out at ambient temperature, since heating results in the formation of unexpected products, which are formed by either decomposition or rearrangement of the ligand [21].

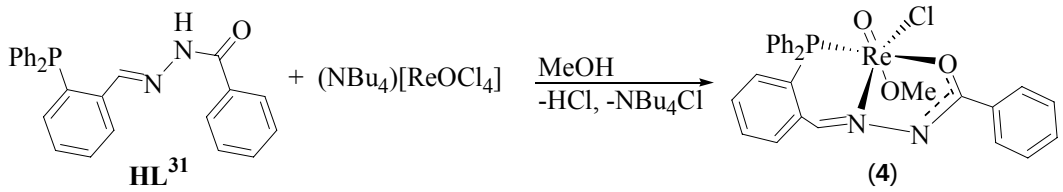

Scheme 2.8 The reaction of HL^{31} with $(NBu_4)[ReOCl_4]$

Fig. 2.5 illustrates the molecular structure of *mer*-$[ReOCl(OMe)(L^{31})]$ (**4**). The equatorial plane of the neutral complex is occupied by $(L^{31})^-$ and a chloro ligand and the axial position *trans* to the terminal oxo O(10) is occupied by a methanolato ligand. The rhenium atom is located 0.136 Å above the equatorial plane. The bond lengths C(30)-O(1) of 1.30(2) Å and C(30)-N(2) of 1.35(2) Å are between C-O single and double bonds, which implies the delocalization of the π-electrons between these atoms. The C(7)-N(1) bond length of 1.27(2) Å is consistent with the characteristic double bond reported for similar hydrazones [22].

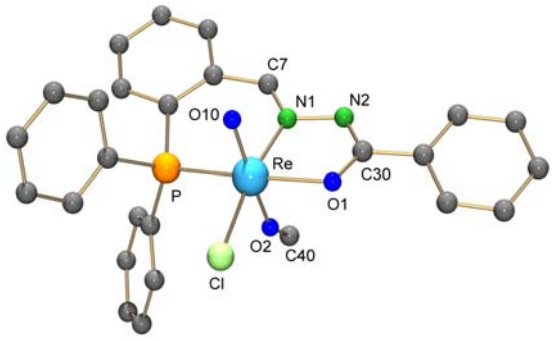

Fig. 2.5 Molecular structure of *mer*-[ReOCl(OMe)(L^{31})] (**4**). The hydrogen atoms were omitted for clarity.

Table 2.4 Selected bond lengths and angles of [ReOCl(OMe)(L^{31})] (**4**)

Bond Lengths [Å]:					
Re-O(10)	1.69(1)	Re-O(1)	2.08(1)	Re-N(1)	2.07(1)
Re-P	2.392(4)	Re-O(2)	1.89(1)	Re-Cl	2.390(5)
N(1)-N(2)	1.42(2)	C(30)-O(1)	1.30(2)	N(2)-C(30)	1.35(2)
Bond Angles [°]:					
O(10)-Re-O(1)	96.4(5)	O(10)-Re-P	89.1(4)	C(7)-N(1)-N(2)	114.5(1)
O(2)-Re-O(1)	86.1(5)	O(10)-Re-O(2)	170.0(5)		

The ^{31}P-{^{1}H} NMR spectrum presents a single resonance at 6.5 ppm. The ^{1}H NMR spectrum of **4** presents a singlet at 2.3 ppm, which can be assigned to the methoxo group. The signal of the imine proton appears at 9.0 ppm. Deprotonation of the ligand is confirmed by the absence of the NH absorption in the IR spectrum of the compound, which appears at 3209 cm^{-1} for the uncoordinated HL^{31}. Coordination of the imine group is supported by a strong band at 1493 cm^{-1}. The mass spectrum presents a base peak at *m/z* = 641 amu, which is associated with the $[M\text{-}Cl]^{+}$ fragment.

In order to exchange the labile Cl^{-} and $(CH_3O)^{-}$ ligands with a bidentate chelating ligand to form more stable complexes, **4** was reacted with N,N-diethyl-N'-benzoylthiourea, HEt_2btu, in a mixture of CH_2Cl_2/MeOH in the presence of a supporting base. Red blocks of [ReO(Et_2btu)(L^{31a})] (**5**) (L^{31a} = (Ph_2P{2-C_6H_4[$CH(OCH_3)$(N-NCOPh]}) were obtained in a good yield, Scheme 2.9.

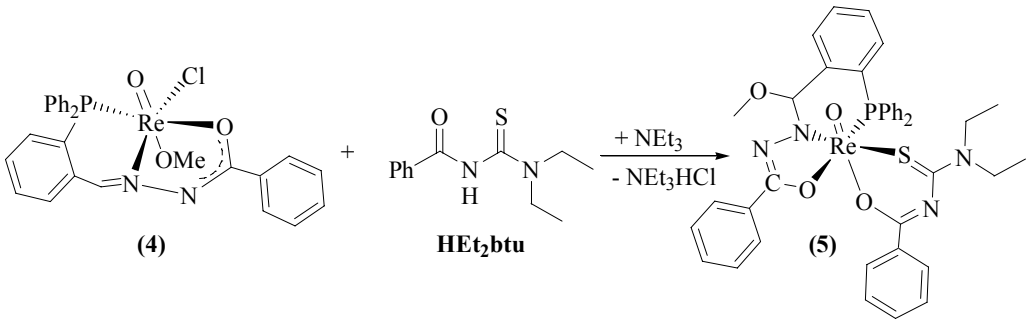

Scheme 2.9 The reaction between [ReOCl(OMe)(L^{31})] (**4**) and HEt_2btu

Fig. 2.6 illustrates the molecular structure of [ReO(Et_2btu)(L^{31a})] (**5**) and Table 2.5 contains selected bond lengths and angles. The coordination sphere of the rhenium atom is occupied by the unexpected tridentate phosphine $(L^{31a})^{2-}$, a bidentate $(Et_2btu)^-$, and the terminal oxo ligands. The molecular structure of **5** confirms that the carbon atom C(7) of the hydrazonic Schiff base $(L^{31})^-$ reacted with a methanol molecule under a nucleophilic addition reaction and formation of $(L^{31a})^{2-}$. The bond lengths C(7)-O(3) of 1.42(2) Å and C(7)-N1(1) of 1.51(2) Å confirm C-N/O single bonds between these atoms. The bond angle O(3)-C(7)-N(1) of 109.9(1)° fits fully with the sp^3 hybridization of C(7) and is consistent with the single bonds between C(7) and its neighboring atoms. A comparison of the bond lengths N(2)-C(17) of 1.30(2) Å and C(17)-O(1) of 1.34(2) Å affirms the localization of the π-electrons mostly between N(2) and C(17) atoms.

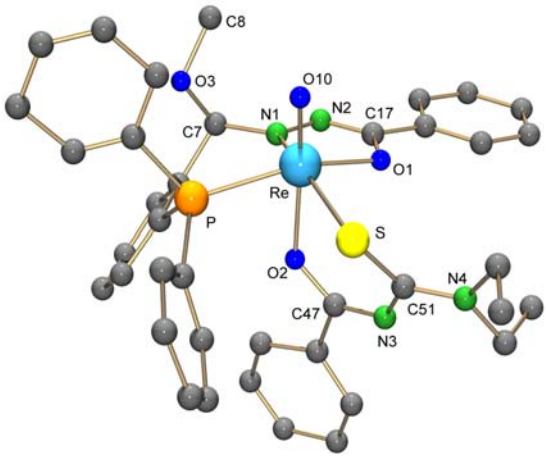

Fig. 2.6 Molecular structure of [ReO(Et_2btu)(L^{31a})] (**5**). The hydrogen atoms were omitted for clarity.

Table 2.5 Selected bond lengths and angles of [ReO(Et_2btu)(L^{31a})] (**5**)

Bond Lengths [Å]:					
Re-O(10)	1.685(9)	Re-O(1)	2.01(1)	Re-N(1)	1.92(1)
Re-P	2.434(4)	Re-S	2.483(4)	Re-O(2)	2.140(9)
N(1)-N(2)	1.37(2)	C(7)-O(3)	1.42(2)	C(7)-N(1)	1.51(2)
C(17)-O(1)	1.34(2)	C(17)-N(2)	1.30(2)		

Bond Angles [°]:					
O(10)-Re-O(2)	166.9(5)	O(1)-Re-P	158.2(2)	N(1)-Re-S	158.6(4)
O(10)-Re-O(1)	106.1(5)	S-Re-O(1)	89.6(3)	P-Re-O(2)	77.8(4)
O(3)-C(7)-N(1)	109.9(1)	C(7)-N(1)-N(2)	111.6(1)	N(2)-C(17)-O(1)	120.2(1)

The exact reaction pathway is not clear. It is supposed that [ReOCl(OMe)(L^{31})] (**4**) reacts with the HEt_2btu ligand under formation of the cationic intermediate complex [ReO(Et_2btu)(L^{31})]$^+$ (**4a**). This undergoes a nucleophilic addition reaction with a methanolato anion $(CH_3O)^-$ and forms the final product **5** in a good yield, Scheme 2.10.

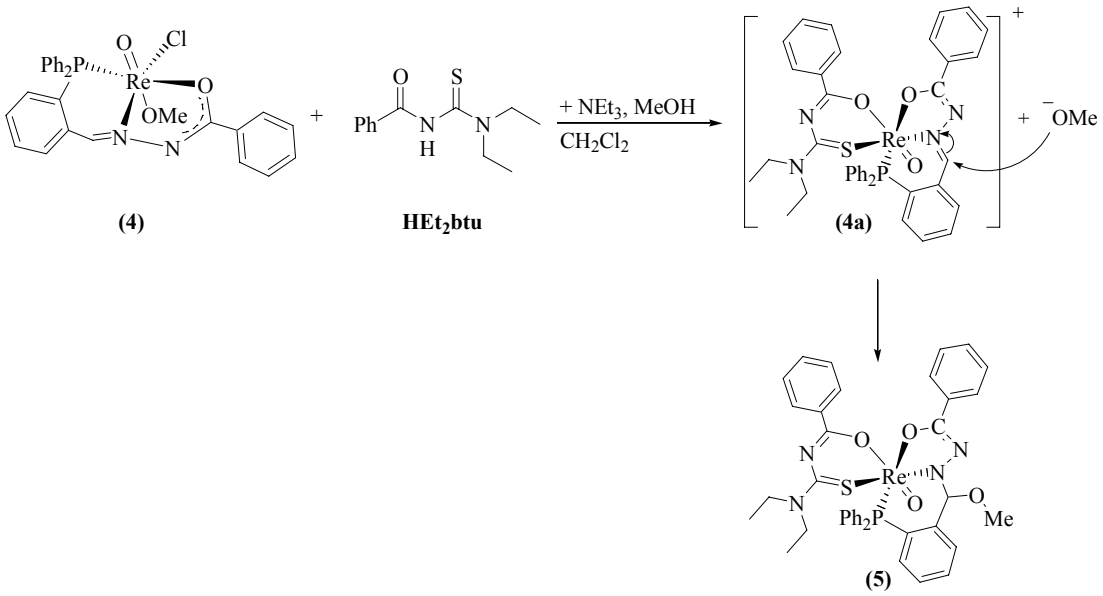

Scheme 2.10 The supposed reaction pathway for the formation of [ReOl(Et_2btu)(L^{31a})] (**5**)

The ^{1}H NMR spectrum of **5** shows two triplets at about 1.3 ppm for the methyl groups of the bidentate HEt_2btu ligand. A singlet at 2.3 ppm with integration of three hydrogen atoms supports the presence of the methoxo group. A singlet at 6.4 ppm is assigned to the methine proton, Fig. 2.7. The single resonance at 23.6 ppm in the ^{31}P-{^{1}H} NMR spectrum of the compound suggests the presence of the coordinated phosphine. The IR spectrum of **5** confirms the Re=O core by an absorption at 933 cm^{-1}.

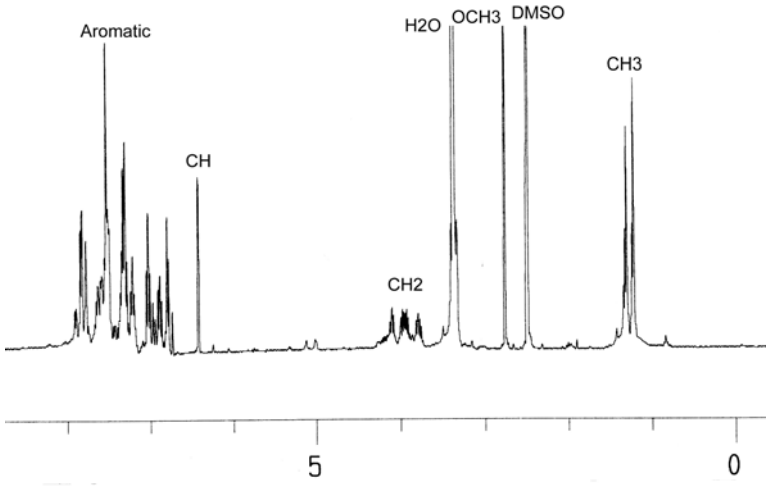

Fig. 2.7 The ^{1}H NMR spectrum of [ReOl(Et_2btu)(L^{31a})] (**5**)

HL^{41} reacts with $(NBu_4)[ReOCl_4]$ in methanol under single deprotonation and formation of the neutral oxorhenium(V) complex **6**. The product precipitates as a red, microcrystalline solid directly from the reaction mixture. It is readily soluble in chloroform or dichloromethane and can be recrystallized from a CH_2Cl_2/MeOH mixture to give large red blocks, Scheme 2.11.

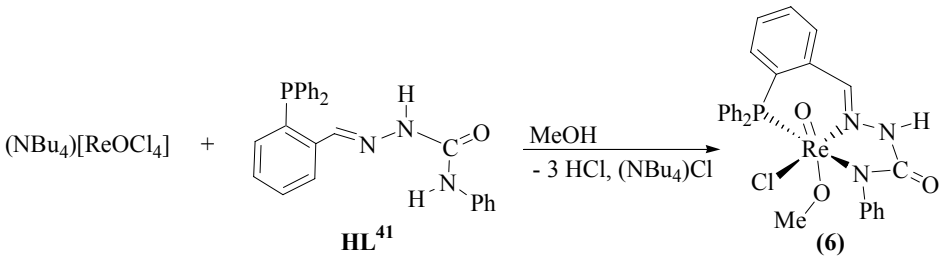

Scheme 2.11 The reaction of the phosphinosemicarbazone HL^{41} with $(NBu_4)[ReOCl_4]$

The rhenium atom in [ReOCl(OMe)(L^{41})] (**6**) possesses a distorted octahedral coordination environment with the tridentate semicarbazonato ligand $(L^{41})^-$ in the equatorial plane. The molecular structure is shown in Fig. 2.8. Selected bond lengths and angles are given in Table 2.6. The axial positions are occupied by the oxo and a methoxo ligands. The rhenium atom is located 0.121 Å above the equatorial plane towards the oxo ligand. The relatively short Re-O(2) bond of 1.90(7) Å reflects a considerable degree of transfer of electron density from the Re=O double bond to its *trans* position and goes along with a slight lengthening of the Re–O(10) bond (1.71(7) Å), which is at the upper limit for Re(V) oxo complexes [23]. The observed N,N' coordination is to the best of my knowledge without precedent in the coordination chemistry of semicarbazones. The conventional chelate formation for semicarbazones is via the carbonyl oxygen and azomethine nitrogen atoms [24], which has recently also been found for the only hitherto structurally characterized rhenium complex with

a semicarbazonato ligand [25]. Two entries in the Cambridge Crystallographic database (DAPSNI and DAPSCU), which suggest a N,N' coordination mode are not correct and the corresponding copper(II) and nickel(II) complexes with 2,6-diacetylpyridine bis-(semicarbazone) are clearly N,O coordinated [26].

The hydrogen bond between N(2) and O(2) in adjacent molecule generated by the symmetry element (-x+2,-y,-z+1) confirms the deprotonation situation of the ligand. The bond lengths between N(1)-N(2) of 1.38(1) Å, N(2)-C(10) of 1.39(1) Å and C(10)-N(3) of 1.34(1) Å are slightly shorter than normal single bonds, which suggest the delocalization of π-electrons between these atoms N(1), N(2), C(10) and N(3). The distance between C(10)-O(1) of 1.26(1) Å is consistent with the carbon-oxygen double bond characteristics for the carbonyl function.

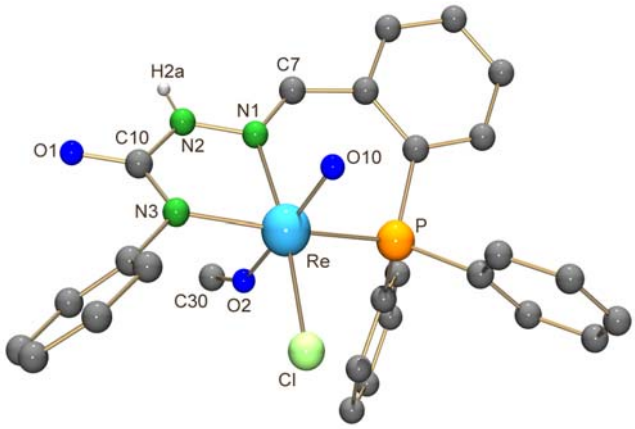

Fig. 2.8 Molecular structure of [ReOCl(OMe)(L^{41})] (**6**). The hydrogen atoms bonded to carbon atoms were omitted for clarity.

Table 2.6 Selected bond lengths and angles of [ReOCl(OMe)(L^{41})] (**6**)

Bond Lengths [Å]:					
Re-O(10)	1.706(7)	Re-O(2)	1.896(7)	Re-N(3)	2.098(8)
Re-N(1)	2.104(8)	C(7)-N(1)	1.30(1)	N(1)-N(2)	1.38(1)
N(2)-C(10)	1.39(1)	C(10)-O(1)	1.26(1)	C(10)-N(3)	1.34(1)
Bond Angles [°]:					
O(10)-Re-O(2)	167.2(3)	N(1)-Re-P	90.6(2)	N(3)-Re-N(1)	78.0(3)
N(1)-N(2)-C(10)	119.9(9)	O(1)-C(10)-N(3)	128.7(1)		

Hydrogen bond:				
D-H...A	d(D-H)	d(H...A)	d(D...A)	<(DHA)
N(2)-H(2a)...O(2)#1[a]	0.86	1.98	2.73(1)	144.1

a) Symmetry transformations used to generate equivalent atoms: #1 -x+2,-y,-z+1

The coordination of the phosphorus atom of $(L^{41})^-$ is confirmed by a shift of the ^{31}P-$\{^1H\}$ NMR resonance of HL^{41} at −14.04 ppm to a value of 0.68 ppm in the spectrum of the complex. A weak absorption at 3425 cm^{-1} in the IR spectrum of **6** is assigned to the stretching vibrations of the NH group and the related deformation vibrations appears at 1596 cm^{-1} as a meddium intense band. The $\nu_{C=O}$ and $\nu_{C=N}$ bands of the uncoordinated semicarbazone are bathochromically shifted in the spectrum of the complex and appear at 1635 and 1531 cm^{-1}.

2.2.3 Reactions of the 2-(benzylimino)phosphines derived from 2-aminophenol with oxorhenium(V) complexes

HL^1P reacts with oxorhenium(V) precursors such as $[ReOCl_3(PPh_3)_2]$ or $(NBu_4)[ReOCl_4]$ as is indicated by almost immediate change of the colors of the reaction mixtures. However, all our attempts to isolate crystalline products from such mixtures failed. ^{31}P-$\{^1H\}$ NMR studies of the reaction solutions showed several new signals at negative and positive chemical shift values for each reaction. Number and positions of the signals were strongly dependent on the solvent and the reaction time, which indicates an ongoing decomposition of HL^1P and/or oxidation of the phosphine under formal reduction of the metal atom. The latter type of reaction is not without precedent and has frequently been observed during the interaction of oxorhenium(V) compounds and phosphines, and can principally simply be initiated by released PPh_3 [23]. A detailed analysis of such oxygen transfer reactions has been carried out by *Conry* and *Mayer* [27].

In order to simplify the reaction and to minimize the risk of the formation of Re(III) products by a reaction of HL^1P with the oxo oxygen and subsequent formation of HL^1PO in the reaction mixture, we used the phosphine oxide directly. While the course of even this reaction with $(NBu_4)[ReOCl_4]$ remained unclear, HL^1PO reacted within 1 h in boiling THF with the sparingly soluble $[ReOCl_3(PPh_3)_2]$ under formation of a clear green solution from which two crystalline products, the red $[ReOCl_2(PPh_3)(L^1PO\text{-}O,N)]$ (**7**) and the green $[Re(NC_6H_4OH)Cl_3(PPh_3)_2]$ (**8**), could be isolated in an approximate ratio of 1:2. The amount of compound **8** can be increased by a prolonged reaction time, Scheme 2.12.

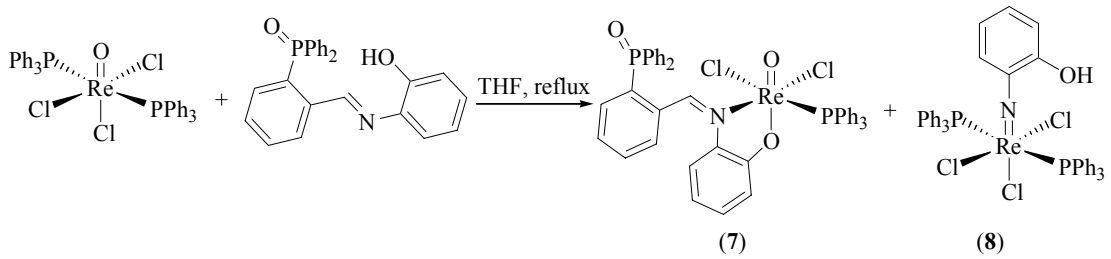

Scheme 2.12 The reaction of $HL^{51}PO$ with $(NBu_4)[ReOCl_4]$

Fig. 2.9 shows the molecular structure of **7**. Selected bond lengths and angles are summarized in Table 2.7. The coordination sphere of the complex is a distorted octahedron with the Schiff base as a singly deprotonated O,N chelating ligand binding via the imine nitrogen and the phenolic oxygen atoms. The oxygen atom O(2) is found in *trans* position to the oxo ligand. Such a coordination mode is typical for chelating ligand systems with oxygen donor atoms [23] and goes along with a considerable transfer of electron density from the terminal Re=O bond into the relatively short Re-O(2) bond of 1.958(6) Å. The phosphine oxide unit does not contribute to the coordination of the metal atom. This results in a bulky complex molecule, which produces relatively large voids between the molecules, which is also expressed by the relatively low density of the rhenium complex of 1.48 g/cm^3.

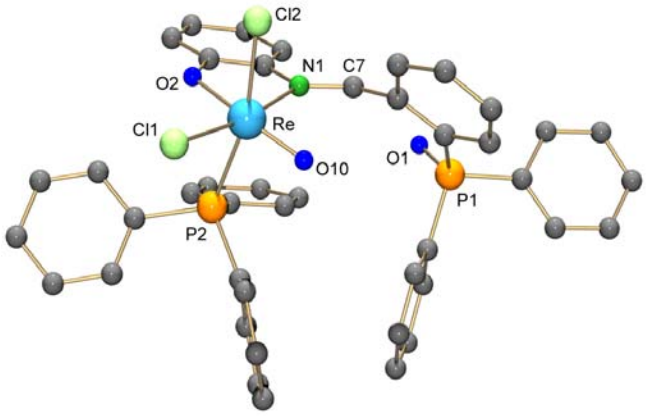

Fig. 2.9 Molecular structure of $[ReOCl_2(PPh_3)(L^{51}PO)]$ (**7**). The hydrogen atoms were omitted for clarity.

Table 2.7 Selected bond lengths and angles for $[ReOCl_2(PPh_3)(L^{51}PO)]$ (**7**)

Bond Lengths [Å]:					
Re-O(10)	1.657(6)	Re-O(2)	1.958(6)	Re-N(1)	2.192(7)
Re-Cl(1)	2.346(2)	Re-Cl(2)	2.386(2)	Re-P(2)	2.469(2)
N(1)-C(7)	1.29(1)				
Bond Angles [°]:					
O(10)-Re-O(2)	161.2(3)	O(10)-Re-N(1)	87.9(3)	O(10)-Re-Cl(1)	102.4(2)
C(7)-N(1)-Re	130.0(6)	O(2)-Re-N(1)	76.3(3)	Cl(2)-Re-P(2)	165.80(9)

The ^{31}P-{^{1}H} NMR spectrum of **7** exhibits two resonances at 26.8 and 29.4 ppm indicating the presence of $L^{1}PO^{-}$ and coordinated PPh_3. The $\nu_{C=N}$ band of the uncoordinated imine compound is bathochromically shifted in the spectrum of the complex and appears at 1566 cm^{-1}. The ^{1}H NMR spectrum of **7** presents a singlet at 10.5 ppm for the imine group the frequency of which shows a 1.5 ppm low-field shift compared to the uncoordinated $HL^{51}PO$. The MS (FAB^{+}) spectrum of **7** shows a peak at *m/z* = 896 amu with the expected isotopic pattern associating with $[M\text{-}Cl]^{+}$ fragment.

The formation of the green phenylimido complex **8** is an unexpected feature of the reaction, but confirms the decomposition of $HL^{1}PO$ during the reaction with $[ReOCl_3(PPh_3)_2]$. The fact that the amount of **8** formed increases with a prolonged reaction time, also indicates a considerable instability of **7**. The presence of the metal complex is mandatory for the observed ligand decomposition, and all our attempts to decompose pure $HL^{1}PO$ in boiling THF failed. The compound resisted such a treatment for 5 h without degradation as has been proven by ^{31}P-{^{1}H} NMR and TLC experiments. The released 2-aminophenol finally reacts with the oxorhenium core under formation of a phenylimido unit. Such reactions are common and many phenyimido complexes have been prepared from reactions of oxo complexes with anilines, but there are only a few structurally characterized examples of rhenium compounds with 2-hydroxyphenylimido ligands [28]. Fig. 2.10 depicts the molecular structure of **8**. Selected bond lengths and angles are given in Table 2.8. Main structural features of the compound are similar to the corresponding "parent complex" $[Re(NPh)Cl_3(PPh_3)_2]$ [29]. The only remarkable feature in the molecular structure of **8** is an intramolecular hydrogen bond (O1-H1: 0.82 Å, H1…Cl2: 2.25 Å, O1…Cl2: 3.037(7) Å, O1-H1-Cl2: 161.3°), which is established between the phenolic oxygen atom and one of the chloro ligands.

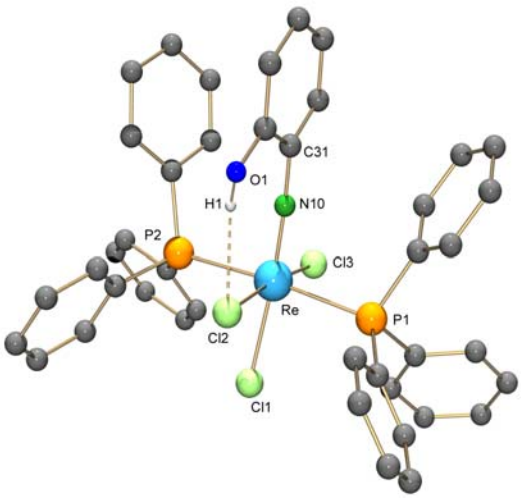

Fig. 2.10 Molecular structure of $[Re\{N(2\text{-}C_6H_4OH)\}Cl_3(PPh_3)_2]$ (**8**). The hydrogen atoms bonded to carbon atoms were omitted for clarity.

Table 2.8 Selected bond lengths and angles for [Re{N(2-C_6H_4OH)}$Cl_3(PPh_3)_2$] (**8**)

Bond Lengths [Å]:					
Re-N(10)	1.722(6)	Re-Cl(1)	2.403(2)	Re-Cl(3)	2.406(2)
Re-Cl(2)	2.425(1)	Re-P(2)	2.489(2)	Re-P(1)	2.500(2)
Bond Angles [°]:					
N(10)-Re-Cl(1)	173.6(2)	N(10)-Re-Cl(3)	95.7(2)	N(10)-Re-P(2)	92.0(2)
P(2)-Re-P(1)	174.18(5)	C(31)-N(10)-Re	174.9(5)		
Hydrogen bond:					
D-H...A	d(D-H)	d(H...A)	d(D...A)	<(DHA)	
O(1)-H(1)...Cl(2)	0.82	2.25	3.037(7)	161.3	

The coordinated PPh_3 gives a singlet at −20.7 ppm in the ^{31}P-{^1H} NMR spectrum of **8,** which is similar to that of *trans*-[$ReCl_3(NPh)(PPh_3)_2$] [30]. The ^1H NMR shows resonances of aromatic protons in the range of 6.17 - 7.87 ppm. A medium intense band in the IR spectrum of **8** at 1092 cm^{-1} confirms the presence of the phenylimido $[Re{=}NPh]^{3+}$ core. The broad band at 3132 cm^{-1} is due to the stretching vibration of the hydroxyl group.

2.3 Summary and Conclusions

The Schiff bases derived from (2-formylphenyl)diphenylphosphine are versatile compounds due to the ease of synthesis and mixed soft/hard donor atoms. They can readily be synthesized by reactions of (2-formylphenyl)diphenylphosphine with primary amines, or hydrazine derivatives. The products were isolated in solid form directly from the reaction mixtures.

The molecular structure of the products, obtained from the complex formation reactions of the aforementioned Schiff bases with oxorhenium(V) complexes, depends on several factors:

- Type of the Schiff base
- Reaction temperature
- Solvent
- pH value
- Overall charge of the intermediate complexes; etc.

The Schiff bases synthesized based on the hydrazine derivatives such as benzoylhydrazones HL^{31} and semicarbazones HL^{41} show higher stability than those derived from primary amines like L^{11} and $HL^{51}P(O)$, due to the resonance of the π–electrons.

The complex formation reactions should be preferably carried out at room temperature. The reactions between $(NBu_4)[ReOCl_4]$ with the hydrazonic Schiff bases HL^{31} and HL^{41}, as well as with the amine-based $HL^{51}P(O)$ under heating of the reaction mixtures give unexpected complexes, which contain fragments of the initial Schiff bases. The hydrazonic Schiff bases HL^{31} and HL^{41} react with $(NBu_4)[ReOCl_4]$ at ambient temperature under formation of the expected complexes **4** and **5,** while the reactions of L^{11} or $HL^{51}P$ with $(NBu_4)[ReOCl_4]$ at room temperature result in the decomposition of the ligands. Heating of the reaction mixture of $HL^{51}PO$ and $[ReOCl_3(PPh_3)_2]$ results in the dissociation of the imine group to the related amine and carbonyl units. The released amine, 2-aminophenol, reacts with the oxorhenium(V) intermediate compound under formation of **8** in a moderate yield.

Alcohols stabilize oxorhenium(V). L^{21} reacts with $(NBu_4)[ReOCl_4]$ in methanol under formation of the dimeric $[ReO(OMe)Cl_2]_2(\mu\text{-}L^{21})$ (**3**) in a good yield. The same reaction in chlorinated solvents failed.

Charged intermediate complexes of the Schiff bases L^{11} or HL^{31} shows low stability against the nucleophilic solvents such as water or alcohols.

L^{11} reacts with $(NBu_4)[ReOCl_4]$ under formation of **1** as the main product. The molecular structure of the side product **2** suggests that a consecutive solvolysis and hydrolysis of the charged intermediate compound **2a** give **1** in a moderate yield. The solvolysis and hydrolysis

of the ligand L^{11} should occur by a nucleophilic addition of a metanolato and hydroxo groups to the electropositive carbon atom of the Schiff base. The positively charged intermediate complex **4a** form the reaction of **4** with the mononegative bidentate ligand $(Et_2btu)^-$ in methanol undergoes a nucleophilic addition reaction with a methanolato anion and gives the oxorhenium(V) complex **5** with a rare tridentate ligand L^{31a}.

Although the abovementioned compounds (and discussions) declare that the Schiff bases derived from (2-formylphenyl)diphenylphoshine are remarkable ligands due to the mixed set of donor atoms, but their low stability restricts the application of these ligands.

2.4 References

[1] Bloch, R. *Chem. Rev*., **1998**, *98*, 1407.

[2] a) Winpenny, R. E. P. *Chem. Soc. Rev.*, **1998**, 27, 447; b) Francesco, T.; Fiorenzo, R.; Giuliano, B. *Coord. Chem. Rev.*, **1994**, *135*, 325; c) Guodong, D.; Fanwick, P. E.; Abu-Omar, M. M. *Inorg. Chim. Acta*, **2008**, *361*, 3184; d) Ison, E. A.; Cessarich, J. E.; Travia, N. E.; Fanwick, P. E.; Abu-Omar, M. M. *J. Amer. Chem. Soc.*, **2007**, *129*, 1167; e) Dilworth, J. R.; Jobanputra, P.; Thompson, R.M.; Povey, D. C.; Archer, C. M.; Kelly, J. D. *Dalton Trans.*, **1994**, 1251.

[3] Wencel, J.; Rix, D.; Jennequin, T.; Labat, S.; Crevisy, C.; Mauduit, M. *Tetrahedron*, 2**008**, *19*, 1804.

[4] Schiemenz, G. P.; Kaack, H. *Liebigs. Ann. Chem.,* **1973**, 1480.

[5] Landvatter, F. E; Rauchfuss, B. T. *Chem. Commun.*, **1982**, 1170.

[6] Rancurel, C.; Daro, N.; Borobia, O. B.; Herdtweck, E.;Sutter, J. P. *Eur. J. Org. Chem.,* **2003**, 167.

[7] Jeffery, J. C.; Rauchfuss, B. T.; Tucker, A. P. *Inorg. Chem.,* **1980**, 19, 3306.

[8] Matoga, D.; Szklarzewicz, J.; Stadnicka, K.; Shongwe, M. S. *Inorg. Chem.,* **2007**, *46*, 9042.

[9] Padhye, S. *Coord. Chem. Rev*., **1985**, *63*, 127.

[10] Bachmann, S.; Furler, M.; Mezzetti, A. *Organometallics,* **2001,** *20,* 2102.

[11] Wang, W.; Spingler, B.; Alberto, R. *Inorg. Chim. Acta.,* **2003**, *355*, 386.

[12] McMurry, J. E.; Simanek, E. E. *Fundamentals of Organic Chemistry*, Brooks Cole, **2003**.

[13] Correia, J. D. G.; Domingos, A.; Santos, I.; Bolzati, C.; Refosco, F.; Tisato, F. *Inorg. Chim. Acta*, **2001**, *315*, 213.

[14] Crampton, Michael R. *Perkin Trans. 2: Phys. Org. Chem.*, **1975**, *3*, 185.

[15] Brianese, N.; Casellato, U.; Tamburini, S.; Tomasin, P.; Vigato, P. A. *Inorg. Chim. Acta* , **1998**, *272*, 235.

[16] Berning, D. E.; Katti, K. V.; Barbour, L. J.; Volkert, W. A. *Inorg. Chem.*, **1998**, *37*, 334.

[17] Wong, W.; Gao, J. G.; Zohu, Z. Y.; Mak, T. C. W. *J. Chem. Soc., Dalton Trans.,* **2000**, 1397.

[18] Bandoli, G.; Dolmella, A.; Gerber, T. I. A.; Mpinda, J.; Perils, D.; Du Preez, J. G. H. *J. Coord. Chem*., **2002**, *55*, 823.

[19] Kirillov, A. M.; Haukka, M.; Pombeiro, A. J. L. *Inorg. Chim. Acta*, **2006**, *359*, 4421.

[20] Iskander, M. F.; Khalil, T. E.; Haase, W.; Werner, R.; Svoboda, I.; Fuess, H. *Polyhedron*, **2001**, *20*, 2787.

[21] Bartz, T. *Diploma Thesis (Freie Universität Berlin)*, **2005**.

[22] Barbazan, P.; Carballo, R.; Abram, U.; Pereiras-Gabian, G.; Vazquez-Lopez, E. M. *Polyhedron*, **2006**, *25*, 3343.

[23] Abram, U. *Comprehensive Coordination Chemistry II*, Vol. V, Elsevier, **2004**, 271 and refs. cited therein.

[24] Casas, J. S.; Garcia-Tasende, M. S.; Sordo, J. *Coord. Chem. Rev*., **2000**, *209*, 197.

[25] Otero, L.; Noblia, P.; Gambino, D.; Cerecetto, H.; Gonzalez, M.; Sanchez-Delgado, R.; Castellano, E. E.; Piro, O. E. *Z. Anorg. Allg. Chem.,* **2003**, 629, 1033.

[26] Wester, D.; Palenik, G. J. *J. Am. Chem. Soc*., **1974**, *96*, 7565.

[27] Conry, R. R.; Mayer, J. M. *Inorg. Chem.*, **1990**, *29* , 911.

[28] (a) Gerber, T. I. A.; Luzipo, D.; Mayer, P. *Inorg. Chim. Acta*, **2004**, *357*, 429; (b) Bandoli, G.; Gerber, T. I. A.; Perils, J.; Preez, J. G. H. *Inorg. Chim. Acta*, **1998**, *278*, 96; (c) Gerber, T. I. A.; Luzipo, D.; Mayer, P. *J. Coord. Chem.,* **2006**, *59*, 1055.

[29] (a) Forsellini, E.; Casellato, U.; Graziani, R.; Carletti, M. C.; Magon, L. *Acta Crystallogr. C*, **1984**, *40*, 1795; (b) Wittern, U.; Strähle, J.; Abram, U. *Z. Naturforsch., B,* **1995**, *50*, 997.

[30] Bereau, V. M.; Khan, S. I.; Abu-Omar, M. M. *Inorg. Chem*., **2001**, *40*, 6767.

Chapter 3

2-(Benzylamino)phosphines and their reactions with rhenium and technetium complexes

---

3 Synthesis of 2-(benzylamino)phosphines and their reactions with rhenium and technetium complexes

The increasing interest in the coordination chemistry of multidentate ligands containing [P,N,O] donor atoms is due to their remarkable properties such as the stabilization of a variety of metal ions and their bioconjugation potential [1]. Additionally, the phosphines can act as a reducing agents [2], which can be an advantage for kit preparation procedures. Despite the existence of numerous phosphine containing ligand systems, the designing and synthesis of such a class of compounds is still a serious challenge.

3.1 2-(Benzylamino)phosphines derived from 2-aminophenol and their rhenium and technetium complexes

3.1.1 Synthesis of the 2-(benzylamino)phosphines derived from 2-aminophenol

The 2-(benzylimino)phosphines introduced in Chapter 2 are versatile ligand systems, due to the combination of the hard and soft donor set, but the imine function in many cases does not show sufficient stability during heating or under acidic conditions. However, reduction of the imine group to a secondary amine [3] gives ligand systems, which have similar skeletons like the related 2-(benzylimino) phosphines and show a higher stability, Scheme 3.1.

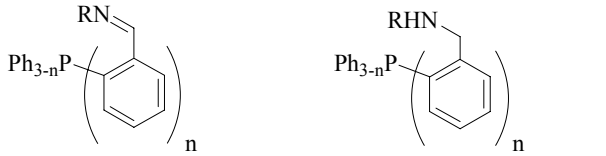

2-(benzylimino)phosphines **2-(benzylamino)phosphines**

(n = 1 - 3; R= Any aliphatic or aromatic group)

Scheme 3.1 General formulae of 2-(benzylimino)phosphines and 2-(benzylamino)phosphines

Some of the advantages of 2-(benzylamino)phosphines, compared to 2-(benzylimino) phosphines are expected:

- Higher chemical stability due to the saturated carbon-nitrogen bond
- Higher flexibility induced by the methylene group instead of the rigid C=N bond
- Higher number of potential deprotonation positions

In order to synthesize 2-(benzylamino)phosphines by reduction of 2-(benzylimino) phosphines, the rest of the backbone of the molecule must be resistant against reduction.

Therefore, the 2-(benzylimino)phosphines derived from 2-aminophenol, $HL^{51}P$ (see 2.1.4.), were chosen as first candidates to be reduced since:

- They have no competitive group which can be reduced
- The chelating system can be expanded by the use of bis- and tris(formylphenyl) phosphines which provides the possibility of penta- and heptadentate ligands

The bis- and tris-{2-(benzylimino)}phosphines are synthesized based on the synthesis of $HL^{51}P$ (see 2.1.4.) and 2-(benzylamino)phosphines, $H_{2n}L^{5n}$ (n = 1 - 3), are synthesized by the reduction of the related 2-(benzylimino)phosphines $H_nL^{5n}P$ (n = 1 - 3) with an excess of $NaBH_4$ in EtOH. The products H_2L^{51}, H_4L^{52} and H_6L^{53} can be isolated as colorless solids, which are soluble in THF, CH_2Cl_2 and $CHCl_3$ but insoluble in alcohols, Scheme 3.2.

The $^{31}P-\{^1H\}$ NMR spectra of $H_2L^{52}P$ and $H_3L^{53}P$ show resonances at −18.8 ppm and −25.5 ppm, respectively. The corresponding ^1H NMR spectra exhibit doublets at 9.1 ppm and 9.2 ppm due to the imine groups. The observed splittings result from couplings between hydrogen atoms of the imine components with the phosphorus atom with a coupling constant of J_{PH} = 5.2 Hz. The phenolic OH groups are detected by IR spectroscopy with stretching vibrations at about 3300 cm^{-1}. The stretching vibrations of the imine groups are detected at 1624 cm^{-1}. The elemental analyses support the molecular formulae of the compounds $H_2L^{52}P$ and $H_3L^{53}P$.

$^{31}P-\{^1H\}$ NMR spectra of the 2-(benzylamino)phosphines $H_{2n}L^{5n}$ (n = 1 - 3) present single resonances of the phosphorus atoms at −16.6 ppm for H_2L^{51}, −27.4 ppm for H_2L^{51} and −37.05 ppm for H_6L^{53} respectively. These resonances appear at higher field compared to those of $H_nL^{5n}P$, which is due to electron donation from the methylene group. ^1H NMR spectra of $H_{2n}L^{5n}$ exhibit doublets at 4.3 ppm with each coupling constants of J_{HH} = 5.2 Hz due to the coupling with the protons of the methylene groups. The hydrogen atoms of the secondary amines, $H_{2n}L^{5n}$, are detected as triplets at 5.4 ppm (J_{HH} = 5.6 Hz). The IR spectra support the molecular structures of $H_{2n}L^{5n}$ by medium bands at about 3425 cm^{-1} and strong absorptions at 1601 cm^{-1} from stretching and deformation vibrations of the NH groups.

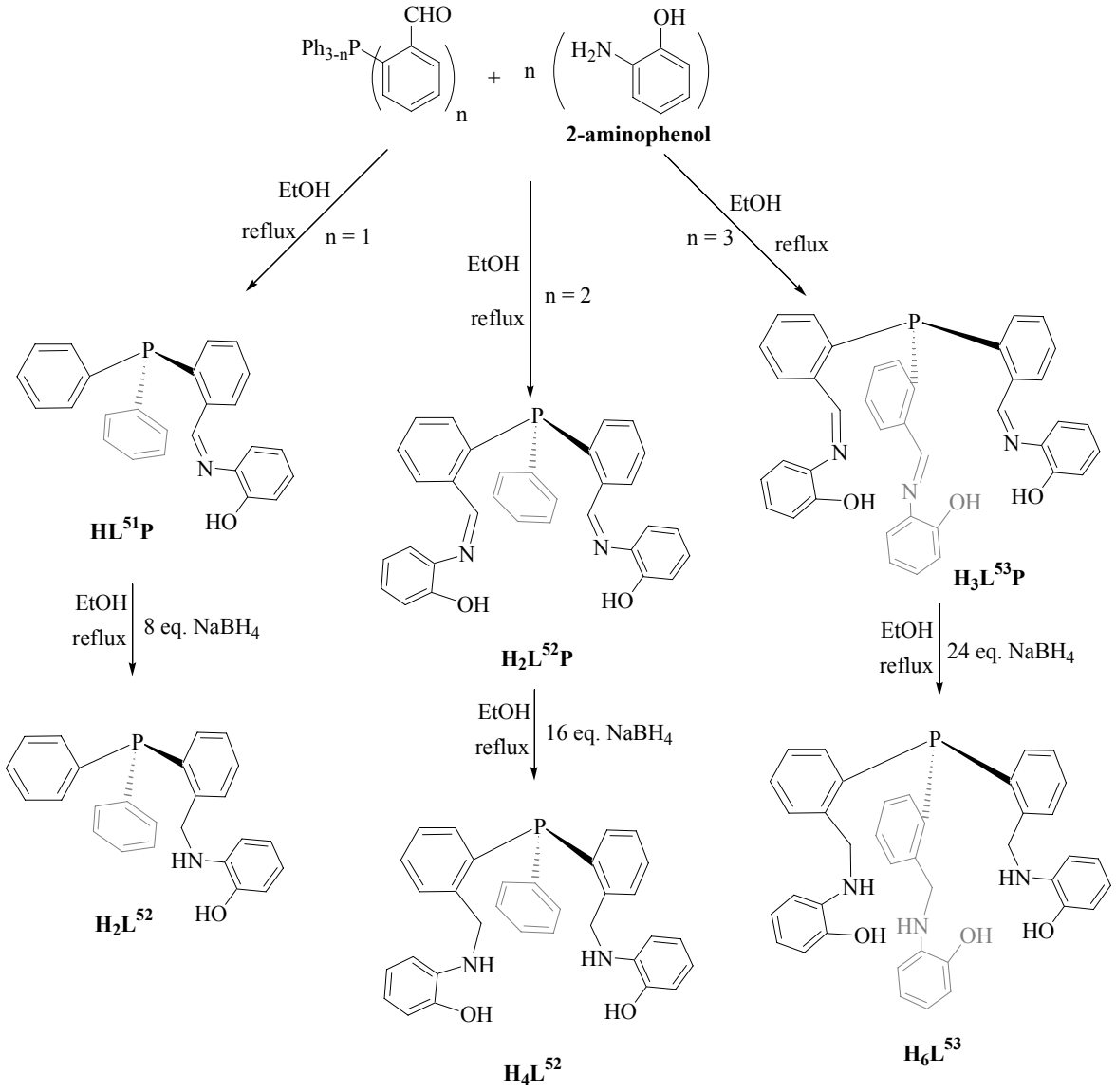

Scheme 3.2 Synthesis of the multidentate 2-(benzylamino)phosphines H_nL^{5n} (n = 1 - 3) derived from 2-amino phenol

3.1.2 Reactions of the 2-(benzylamino)phosphines, $H_{2n}L^{5n}$, with rhenium and technetium complexes

3.1.2.1 Reactions of H_2L^{51}

H_2L^{51} reacts with $(NBu_4)[ReOCl_4]$ in MeOH at ambient temperature under formation of *fac*-$[ReOCl_2(HL^{51})]$ (**9**) as a microcrystalline olive-green solid. The same product can be obtained from the reaction of $[ReOCl_3(PPh_3)_2]$ with H_2L^{51} in refluxing THF, Scheme 3.3.

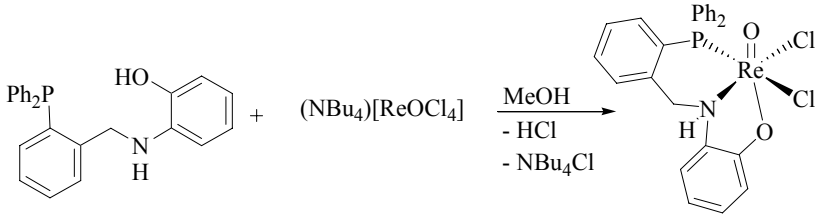

H_2L^{51} **(9)**

Scheme 3.3 Synthesis of *fac*-$[ReOCl_2(HL^{51})]$ (**9**)

fac-$[ReOCl_2(HL^{51})]$ (**9**) is a neutral oxorhenium(V) complex. The phenolic oxygen atom of the tridentate ligand coordinates *trans* to the terminal axial oxo ligand. The other two donor atoms (P and N) occupy the equatorial plane. The coordination sphere is completed by two chloro ligands.

The molecular structure of *fac*-$[ReOCl_2(HL^{51})]$ (**9**) is presented in Fig. 3.1 and selected bond lengths and angles are reported in Table 3.1. The compound is a distorted octahedral rhenium(V) complex. The rhenium atom is located 0.149 Å above the equatorial plane. The Re-N(1) bond length of 2.195(4) Å is in the range of the metal-nitrogen single bond (2.0 – 2.2 Å) [4]. The Re-N(1)-C(11) and C(11)-N(1)-C(7) angles of 109.3(3)° and 112.2(4)° define the tetrahedral environment of the nitrogen atom. The hydrogen atom H(1) establishes an intermolecular hydrogen bond with the Cl(2) ligand of a neighboring molecule generated by the symmetry element (-x+2,-y+2,-z+1).

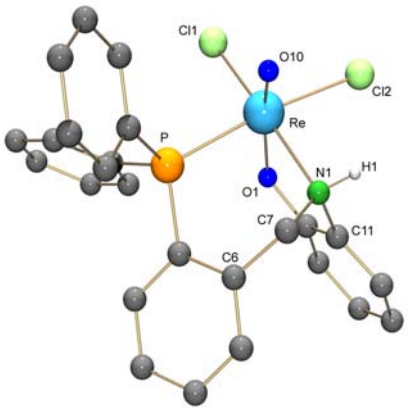

Fig. 3.1 Molecular structure of *fac*-[$ReOCl_2(HL^{51})$] (**9**). The hydrogen atoms bonded to carbon atoms were omitted for clarity.

Table 3.1 Selected bond lengths (Å) and angles (°) of *fac*-[$ReOCl_2(HL^{51})$] (**9**)

Bond lengths [Å]:					
Re-O(10)	1.679(4)	Re-O(1)	1.976(3)	Re-N(1)	2.195(4)
Re-P	2.414(1)	Re-Cl(1)	2.344(1)	Re-Cl(2)	2.428(1)
C(7)-N(1)	1.500(7)	N(1)-C(11)	1.469(7)		
Angles [°]:					
O(10)-Re-O(1)	163.2(2)	Cl(1)-Re-N(1)	169.3(1)	P-Re-Cl(2)	171.63(4)
Re-N(1)-C(11)	109.3(3)	C(7)-N(1)-C(11)	112.2(4)		
Hydrogen bridge:					
D-H...A	d(D-H)	d(H...A)	d(D...A)	<(DHA)	
N-H(1)...Cl(2)#1[a]	0.91	2.54	3.299(5)	140.8	

(a) Symmetry transformations used to generate equivalent atoms: #1 -x+2,-y+2,-z+1

A single resonance at −4.6 ppm in the ^{31}P-{^{1}H} NMR spectrum of **9** proves the coordination of the phosphine. The recorded values correspond to a 15.0 ppm low field shift compared to the uncoordinated H_2L^{51}. The ^{1}H NMR spectrum shows two doublets at 5.0 and 5.6 ppm with coupling constants of 11 Hz, which is characteristic for *HH* geminal couplings. The hydrogen atom of the amine group is detected as a multiple resonance at 6.0 ppm. The IR spectrum contains a medium intense absorption at 968 cm^{-1}, which is assigned to the Re=O vibration. The broad band at 3452 cm^{-1} is consistent with the stretching vibration of NH and the broadening of this band supports the hydrogen bond found in X-ray analysis. The $[M\text{-}Cl]^+$ fragment was detected in the MS(FAB^+) spectrum at m/z = 621.2 amu with the expected isotopic pattern for $C_{25}H_{21}NO_2PClRe$.

The labile chloro ligands can be replaced by bidentate chelating ligands under formation of so called "3+2" oxorhenium complexes. Therefore, a reaction of *fac*-[$ReOCl_2(HL^{51})$] (**9**) with *N,N*-diphenylbenzoylthiourea, HPh_2btu, was performed. NEt_3 was added to facilitate the deprotonation of H_2L^{51} and HPh_2btu.

After working up the reaction mixture the product *mer*-[$ReO(L^{51})(Ph_2btu)$] (**10**) was isolated as a red-brown solid. The complex is soluble in CH_2Cl_2 and $CHCl_3$, but insoluble in alcohols, Scheme 3.4.

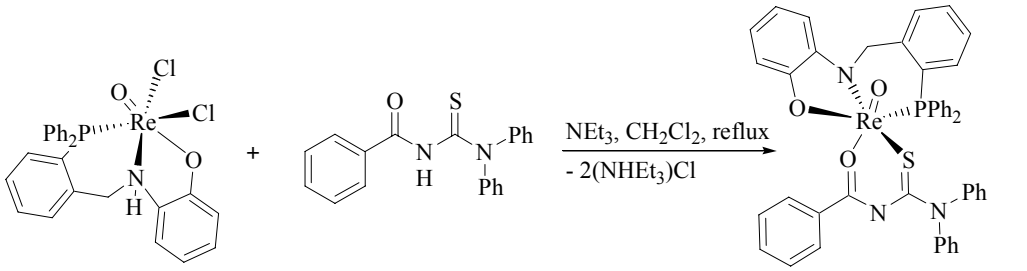

***fac*-[$ReOCl_2(HL^{51})$] (9)** **HPh_2btu** ***mer*-[$ReO(Ph_2btu)(L^{51})$] (10)**

Scheme 3.4 Synthesis of *mer*-[$ReO(L^{51})(Ph_2btu)$] (**10**)

Unlike in **9**, the tridentate 2-(benzylamino)phosphine ligand in **10** is deprotonated twice. Deprotonation of the amine function by the addition of the supporting base NEt_3 is accompanied by the transfer of the hemilabile phenolic oxygen atom to the equatorial plane. The empty axial position *trans* to the terminal oxo ligand is then occupied by the oxygen atom of the bidentate $(Ph_2btu)^-$ ligand, which results in the formation of the neutral complex *mer*-[$ReO(Ph_2btu)(L^{51})$] (**10**).

The molecular structure of *mer*-[$ReO(L^{51})(Ph_2btu)$] (**10**) is shown in Fig. 3.2 and selected bond lengths and angles in are given Table 3.2. The oxygen atom O(1) is located 0.075 Å above themean least-square plane of the atoms C(7), N(1), C(11) and Re. The C(7)-N(1)-C(11) angle of 118.5(6)° confirms a planar environment for N(1). The N(1)-C(7) and N(1)-C(11) bond lengths of 1.469(8) Å and 1.411(8) Å are in the range of a carbon-nitrogen single bond. Therefore, the planarity about the N(1) is originated from the conjugation of the lone pair of N(1) with the metal orbitals, which shortens the Re-N(1) bond length to 1.952(6) Å. The Re-O(2) distance of 2.146(4) Å is in the range of other rhenium complexes with *N,N*-dialkylbenzoylthioureas [5]. The relatively long Re-O(2) bond length results from the *trans* influence of the terminal oxo ligand. The atoms O(2), C(47), N(2), C(48) and S are all in one plane, while C(47) is located 0.16 Å above the meanplane. The planar chelate ring is formed by delocalization of the π – electrons between these atoms. This is confirmed by the bond lengths between the mentioned atoms, which are between values expected for single and double bonds, Table 3.2.

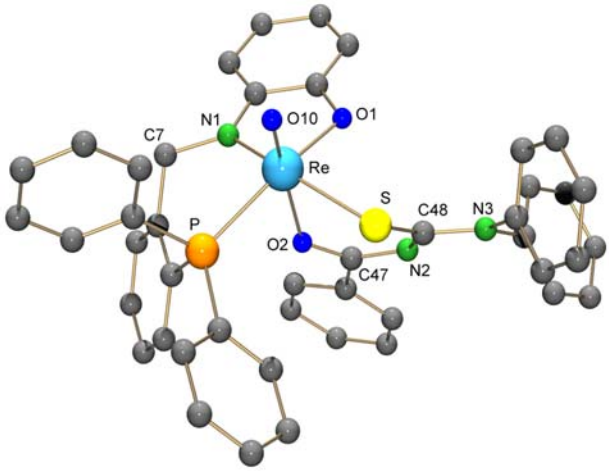

Fig. 3.2 Molecular structure of *mer*-[ReO(L^{51})(Ph_2btu)] (**10**). The hydrogen atoms were omitted for clarity.

Table 3.2 Selected bond lengths and angles of *mer*-[ReO(L^{51})(Ph_2btu)] (**10**)

Bond lengths [Å]:					
Re-O(10)	1.681(4)	Re-O(1)	1.972(4)	Re-N(1)	1.952(6)
Re-S	2.478(2)	Re-O(2)	2.146(4)	N(1)-C(7)	1.469(8)
N(2)-C(47)	1.327(8)	O(2)-C(47)	1.282(7)	N(2)-C(48)	1.329(8)
Angles [°]:					
P-Re-O(1)	161.4(1)	O(10)-Re-S	91.2(2)	O(10)-Re-O(1)	102.7(2)
Re-N(1)-C(7)	126.3(4)	O(2)-C(47)-N(2)	127.7(6)	S-C(48)-N(2)	128.6(5)

The resonance of the phosphorus atom in the ^{31}P-{^{1}H} NMR spectrum is detected at −1.8 ppm, which does not show a dramatic shift compared to that of *fac*-[$ReOCl_2(HL^{51})$] (**9**). The methylene protons of the tridentate ligand were detected as two doublets with the *HH* geminal coupling constants of J_{HH} = 15.7 Hz in the ^{1}H NMR spectrum of **10**. The infrared spectrum does not show any absorption associated with NH or OH vibrations[1].

Oxotechnetium(V) complexes with multidentate [P,P'] donor ligands are restricted to such containing the *trans*-$[TcO_2]^+$ core [6]. Moreover, oxo complexes with mixed donor chelating phosphine ligands are only known just with ligand systems, which can form five-membered chelate ring [7].

H_2L^{51} reacts with $(NBu_4)[TcOCl_4]$ under the expected reduction of Tc(V) to Tc(III) by oxygen abstraction. This is done by a reaction with the phosphine [8]. The signal of the oxidized ligand appears in the ^{31}P-{^{1}H} NMR spectrum at 28 ppm, which is in the range of the triarylphosphines oxides [9].

[1] The pure crystalline compound **10** was ground and dried under reduced pressure for 3 days before taking the IR spectrum to remove the co-crystallized methanol molecule.

In order to avoid oxygen abstraction by the phosphine group, the terminal oxo-ligand of $[Tc=O]^{3+}$ core can be protonated by a strong acid to give $[Tc\text{-}OH]^{4+}$ [10]. Thus, the oxygen abstraction reaction will be possibly hindered and the resulting $(OH)^-$ ligand can be exchanged easier than the terminal oxo ligand due to the metal-oxygen single bond.

Consequently, $(NBu_4)[TcOCl_4]$ was reacted with one equivalent of *p*-toluenesulfonic acid, *p*-TSOH, in acetonitril for 10 min. After addition of H_2L^{51}, the reaction mixture became immediately a clear dark solution. After slow evaporation of the solvent, dark green blocks of $[TcCl_3(L^{51}P)]$ (**11**) were obtained in a moderate yield, Scheme 3.5.

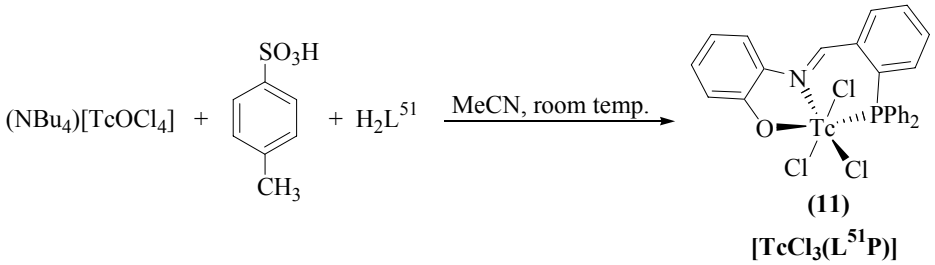

Scheme 3.5 The reaction of $(NBu_4)[TcOCl_4]$ with H_2L^{51} in the presence of *p*-toluenesulfonic acid. H_2L^{51} was added after 5 min.

Fig. 3.3 presents the molecular structure of **11** and Table 3.4 contains selected bond lengths and angles. $[TcCl_3(L^{51}P)]$ (**11**) is a neutral complex of technetium(IV). The three chloro ligands and the monoanionic tridentate ligand $(L^{51}P)^-$ compensate the positive charges of the metal ion. The environment of the technetium atom is a distorted octahedral. The bond length between C(7)-N(1) of 1.292(3) Å is clearly in the range of a C-N double bond [11]. The phenolic oxygen atom is located 0.22Å above the mean least-square plane formed by the atoms Tc, C(7), N(1) and C(11). The Tc-N(1) bond length of 2.116(2) Å is similar to that of the known technetium complex with Schiff bases derived from 2-aminophenol [12].

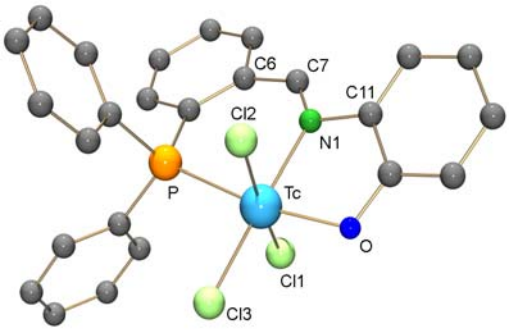

Fig. 3.3 Molecular structure of $[TcCl_3(L^{51}P)]$ (**11**). The hydrogen atoms were omitted for clarity.

Table 3.3. Selected bond lengths and angles of $[TcCl_3(L^{51}P)]$ (**11**)

Bond lengths [Å]:					
Tc-N(1)	2.116(2)	Tc-Cl(1)	2.3421(7)	Tc-P	2.4712(7)
Tc-O	1.997(2)	N(1)-C(11)	1.441(4)	N(1)-C(7)	1.292(3)
Angles [°]:					
N(1)-Tc-Cl(3)	176.58(7)	P-Tc-O	169.01(6)	Cl(1)-Tc-N(1)	88.48(6)
C(7)-N(1)-C(11)	119.3(2)	C(7)-N(1)-Tc	131.7(2)	C(6)-C(7)-N(1)	129.8(3)

The molecular structure of $[TcCl_3(L^{51}P)]$ (**11**) reveals that the secondary amine H_2L^{51} is oxidized to the related imine $H_2L^{51}P$. It is supposed that *p*-toluenesulfonic acid plays a crucial role in the oxidation of H_2L^{51}. R. Kluge *et al.* [13] showed that the oxidation of the *p*-toluenesulfonic acid gives an unstable peracid intermediate **VIII** which can selectively oxidize secondary amines to the related imines. All attempts to synthesize **11** in the absence of the *p*-toluenesulfonic acid resulted in the isolation of viscose residues. The ^{31}P-$\{^1H\}$ NMR spectra of these residues gave only a low intense signal at 29 ppm, which is associated with the oxidized H_2L^{51}. It is suggested that $[Tc^{(V)}O]^{+3}$ is reduced to $[Tc^{(IV)}]$ by oxidation of *p*-toluenesulfonic acid to the related peracid species, Scheme 3.6.

$$4\text{-}CH_3C_6H_4SO_2(OH) \rightleftharpoons 4\text{-}CH_3C_6H_4SO_2(OOH) + e^-$$

$$[Tc^{(V)}O]^{3+} + e^- \rightleftharpoons [Tc^{(IV)}]$$

$$[Tc^{(V)}O]^{3+} + [4\text{-}CH_3C_6H_4SO_2(OH)] \rightleftharpoons [Tc^{(IV)}] + [4\text{-}CH_3C_6H_4SO_2(OOH)]$$

Scheme 3.6 Supposed redox reaction between Tc(V) and *p*-toluenesulfonic acid.

The *in situ* synthesized *p*-toluenesulfonic peracid can the oxidize the 2-(benzylamino)-phosphine, H_2L^{51}, to the related 2-(benzylimino)phosphine, $H_2L^{51}P$, Scheme 3.7. Due to instability of the intermediates, the reaction mechanism can not be proven experimentally, but the suggested pathway is not without precedent [14].

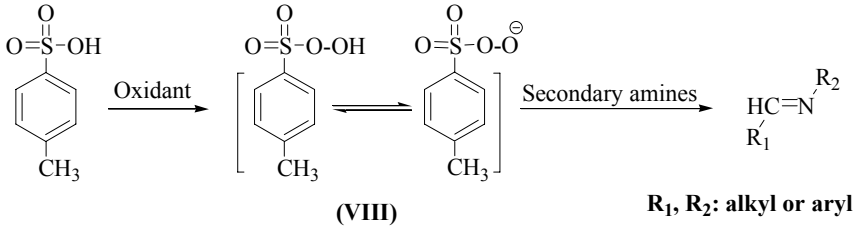

(VIII) **R_1, R_2: alkyl or aryl**

Scheme 3.7 Oxidation of the secondary amines by *p*-toluenesulfonic peracid (**VIII**)

The ^{31}P-{^{1}H} NMR spectrum shows no signal and ^{1}H NMR spectrum presents extremely broad signals which are consistent with the d^3 paramagnetism of the d^3 technetium metal ion. The IR spectrum exhibits a medium intense absorption at 1551 cm^{-1}, which is assigned to the stretching vibration of the C=N bond. It corresponds to a 30 cm^{-1} bathochromic shift compared to the value in uncoordinated $HL^{51}P$. The absence of the Tc=O band in the range of 900 to 100 cm^{-1} is consistent with the molecular structure. The experimentally determined technetium amount of 16.65% fits to the molecular formula of $[TcCl_3(L^{51}P)]$ ($C_{25}H_{19}Cl_3NOPTc$).

3.1.2.2 Reactions of H_4L^{52}

The number of structurally characterized technetium and rhenium complexes with pentadentate ligands is extremely rare. The hitherto structurally known complexes are restricted to ligand systems derived from 2-(2-aminoethylamino)ethylamine [15] and 2,6-diformylpyridine [16]. The arrangement of the donor atoms around the metal atom depends on the ligand architecture and the oxidation state of the metal ion. The flexible ligand derived from 2-(2-aminoethylamino) ethylamine forms an octahedron around the oxorhenium(V) core and the planar pentadentate ligand derived from 2,6-diformylpyridine induces a pentagonal bipyramidal geometry around the metal atom (Re^{3+}), Fig. 3.4.

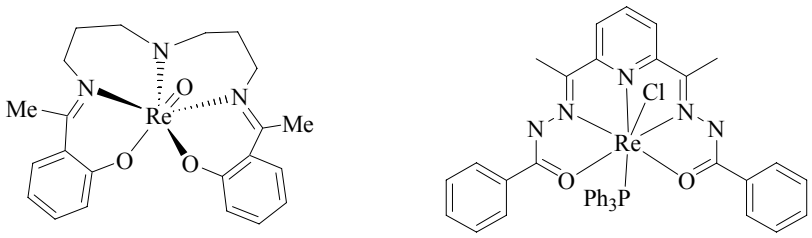

Fig. 3.4 Rhenium complexes of the pentadentate ligands derived from 2-(2-aminoethylamino)ethylamine (left) and 2,6-diformylpyridine (right).

H_4L^{52} is a potentially pentadentate [P,N,O] ligand. Due to the similar structure of H_2L^{51} and H_4L^{52}, it is assumed that the H_4L^{51} shows a favorable flexibility, which may allow coordination in both *mer*- and *fac*- modes, Fig. 3.5.

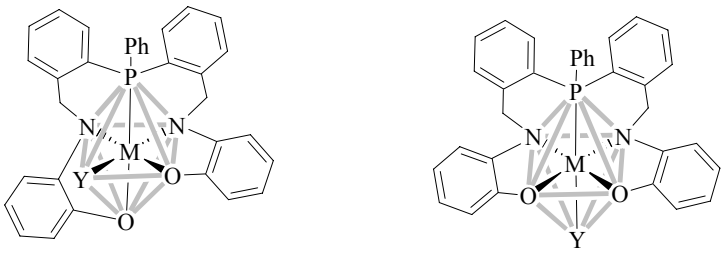

Fig. 3.5 Possible coordination modes of H_4L^{52}, *mer-* , *fac-* (left), *fac-*, *fac-* (right). M = Re, Tc; Y = any monodentate ligand

H_4L^{52} reacts with $(NBu_4)[ReOCl_4]$ in boiling MeOH under formation of a deep red solid, the recrystallization of which from a CH_2Cl_2/MeOH mixture gives red crystals of $[ReCl(L^{52})]$ (**12**). The same product was also isolated from the reaction of H_4L^{52} with $[ReOCl_3(PPh_3)_2]$ and $[Re(NPh)Cl_3(PPh_3)_2]$, Scheme 3.8.

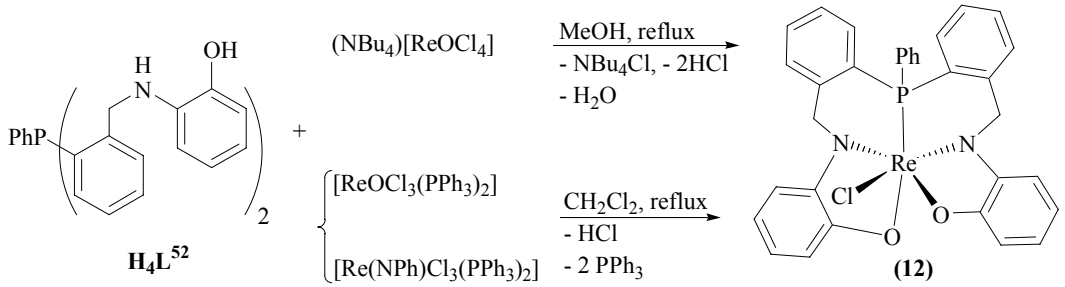

Scheme 3.8 Reactions of H_4L^{52} with oxo- and imidorhenium(V) complexes

$[ReCl(L^{52})]$ (**12**) is an uncommon rhenium(V) complex in the sense that it does not contain one of the common cores (MO^{3+}, MN^{2+}, $MNPh^{2+}$) of the rhenium(V) and technetium(V) coordination chemistry. Other examples such as $[ReCl_5]$ and $[Re(HNC_6H_4S)_3]^-$ were synthesized by either reduction of Re(VI) and Re(VII) or by oxidation of Re(III) and Re(IV) species under extreme conditions [17]. Only two examples, $[ReCl(PPh_3)(NHC_6H_4S)_2]$ and $[ReCl(PPh_3)(L)_2]$ (L = 3-nitro-1,2-diaminobenzene), were prepared by ligand substitution reactions between *trans*-$[ReOCl_3(PPh_3)_2]$ and the related bidentate ligands [18-19].

Surprisingly, H_4L^{52} reacts also with the imidorhenium(V) complex $[Re(NPh)Cl_3(PPh_3)_2]$ and the oxorhenium(V) complex $[ReOCl_3(PPh_3)_2]$ under formation of the remarkable complex **12** with high yields. The reaction was done in the absence of a supporting base. The ligand is fully deprotonated $(L^{52})^{4-}$ and coordinates to the metal ion in a pentadentate mode.

The molecular structure of **12**, Fig. 3.6, shows a distorted octahedral coordination sphere around the rhenium atom. $(L^{52})^{4-}$ coordinates in a pentadentate mode and a chloro ligand occupies the sixth position of the octahedron around the rhenium atom. Selected bond lengths and angles of **12** are presented in Table 3.4.

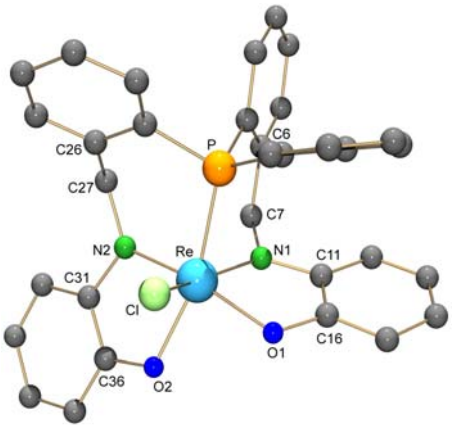

Fig. 3.6 Molecular structure of [ReCl(L^{52})] (**12**). The hydrogen atoms were omitted for clarity.

Table 3.4. Selected bond lengths and angles of [ReCl(L^{52})] (**12**)

Bond lengths [Å]:					
Re-P	2.354(3)	Re-N(1)	1.96(1)	Re-O(1)	2.018(9)
Re-N(2)	1.93(1)	Re-O(2)	2.048(8)	Re-Cl	2.379(3)
N(1)-C(7)	1.47(1)	N(1)-C(11)	1.38(1)	N(2)-C(27)	1.49(2)
N(2)-C(31)	1.42(1)				
Angles [°]:					
P-Re-O(1)	103.0(2)	P-Re-O(2)	163.9(3)	N(1)-Re-N(2)	101.8(4)
C(7)-N(1)-C(11)	117.1(9)	C(27)-N(2)-C(31)	118.8(8)	C(7)-N(1)-Re	122.9(7)
C(11)-N(1)-Re	119.1(8)	C(27)-N(2)-Re	127.5(6)	C(31)-N(2)-Re	113.6(8)

The bond lengths between N(1)-C(11) of 1.38(1) Å and Re-N(1) of 1.96(1) Å are shorter than typical single bonds (e.g. observed for [$ReOCl_2(HL^{51})$] (**9**)). This implies a partial double bound characteristic resulting from the conjugation of the electron pair of N(1) with the π-electrons of the adjacent phenyl ring [C(11) to C(16)] and free orbitals of the metal. The presence of some double bond character in these bonds is confirmed by the almost planar bonding mode of N(1) defined by the C(11)-N(1)-C(7) and C(11)-N(1)-Re angles of 117.1(9)° and 119.1(8)°. The second nitrogen atom N(2) shows a similar planar environment. The N(2)-C(27) and N(2)-C(31) bond lengths of 1.49(2) Å and 1.42(1) Å are in the range of a carbon-nitrogen single bond [20]. Thus, the planarity around N(2) is assumed as a result of the resonance of the free electron pair of N(2) and unoccupied orbitals of the rhenium atom, which is confirmed by the relatively short Re-N(2) bond length of 1.93(1) Å.

The fact that [ReCl(L^{52})] (**12**) shows well-resolved NMR spectra, which indicate diamagnetism, confirms the multiple bond characteristics of the Re-N bonds concluded from the X-ray analysis. In an octahedral geometry a noticeably short M-D multiple bond (M = metal ion, D = donor atom), induces a so called "*z-in*" Jahn-Teller distortion [21]. Due to this

distortion, the orbitals in x and y directions drop in energy. Re^{5+} is a d^2-electron system which can have a diamagnetic electronic configuration by "*z-in*" Jahn-Teller distortion, Fig. 3.7.

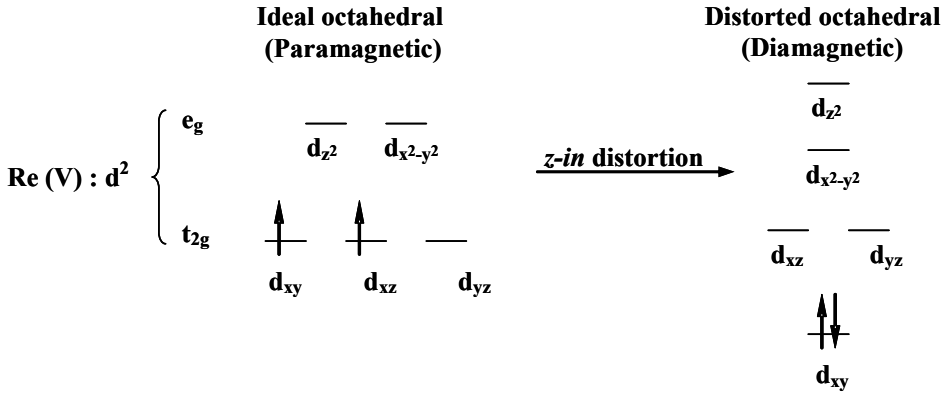

Fig. 3.7 Electronic configuration of Re(V), d^2-electron system, due to "*z-in*" Jahn-Teller distortion

The ^{31}P-{^1H} NMR spectrum of [ReCl(L^{52})] (**12**) shows a single resonance of the coordinated phosphorus atom at −11.1 ppm. The ^1H NMR spectrum of the compound is a proof for the deprotonation and consequently the oxidation state of the rhenium atom in [ReCl(L^{52})] (**12**). The ^1H NMR spectrum presents four doublets with the typical *HH* geminal coupling constant of J_{HH} = 15.2 Hz suggesting four protons of the methylene group, and signals of the aromatic hydrogen atoms, Fig. 3.8.

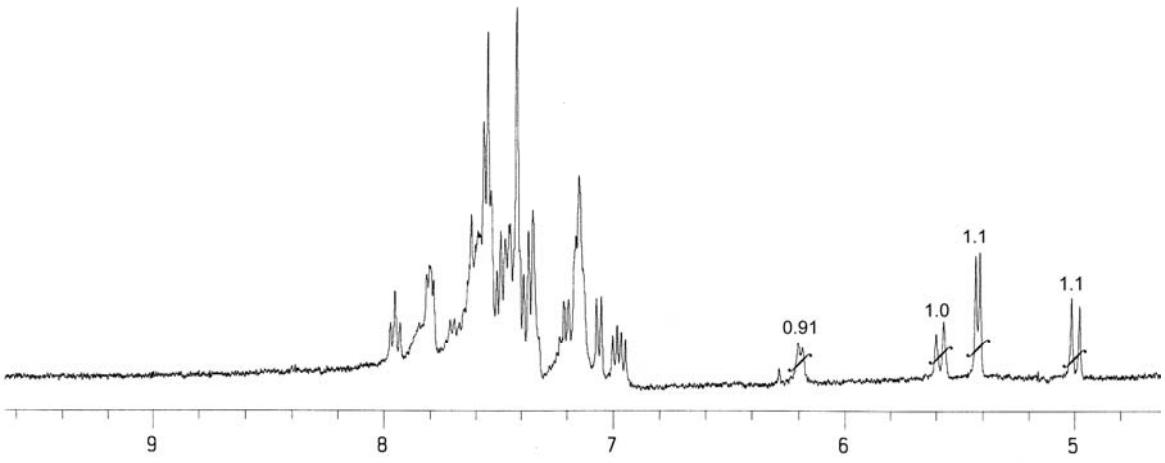

Fig. 3.8 The ^1H NMR spectrum of [ReCl(L^{52})] (**12**)

The absence of the NH signals which are expected to appear at the chemical shift values higher than 8.0 ppm (as it was observed for **9**) supports the full deprotonation of the ligand H_4L^{52} and the supposed oxidation state (+5). The infrared spectrum supports the deprotonation situation of $(L^{52})^{4-}$ by the absence of the NH stretching vibrations at the wave numbers higher than 3100 cm^{-1}. Additionally, the absence of the Re=O band in the range of 900 to 1000 cm^{-1} is consistent with the molecular structure of **12**. The MS(FAB^+) spectrum supports the

molecular structure by a peak at *m/z* = 683 amu, which can be assigned to the $[M\text{-}Cl]^+$ fragment.

The electrochemical behavior of $[ReCl(L^{52})]$ (**12**) was studied by a cyclic voltammetry measurement at a platinum electrode, Fig. 3.9. $[ReCl(L^{52})]$ (**12**) undergoes an one-electron reduction for the Re(V)/Re(IV) couple with the formal potential of $E^{\circ\prime}_{Re(V)\,/\,Re(IV)} = -0.89$ mV. The Re(V)/Re(IV) process is chemically and electrochemically reversible. This is confirmed by the ΔE_p = 72.4 mV and $I_{p(reverse)} / I_{p(forward)} = 0.93$, which are similar to the values of the nearly ideal reversible $[Fe^{(III)}(C_5H_5)_2] / [Fe^{(II)}(C_5H_5)_2]^+$ couple of ΔE_p = 69 mV, I_{pr}/I_{pf} = 0.94.

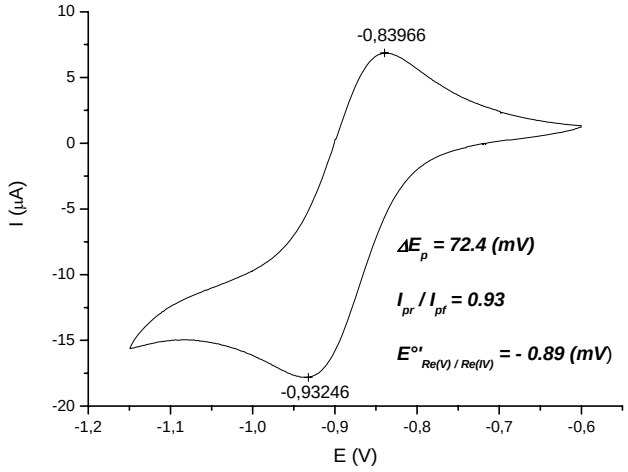

Fig. 3.9 Cyclic voltammogram recorded at a platinum electrode in a MeCN solution of $[ReCl(L^{52})]$ (**12**). Supporting electrolyte $[NBu_4][PF_6]$ (0.1 M).

Addition of a supporting base to the reaction solution of H_4L^{52} and $(NBu_4)[ReOCl_4]$ gives the oxorhenium(V) complex $[ReO(HL^{52})]$ (**13**) as a brown solid in high a yield, Scheme 3.9.

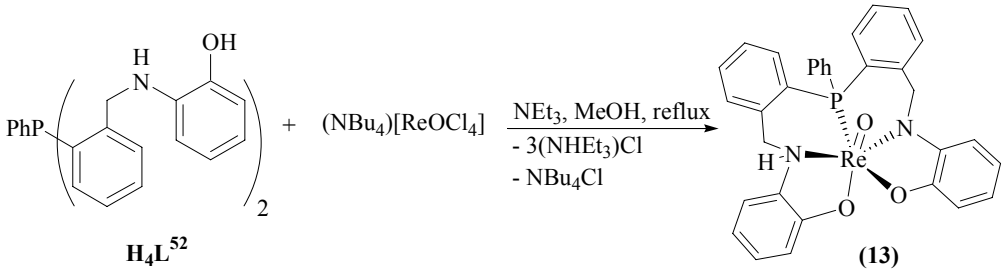

H_4L^{52} **(13)**

Scheme 3.9 The reaction between H_4L^{52} and $(NBu_4)[ReOCl_4]$ in the presence of a supporting base

Fig. 3.10 presents the molecular structure of **13** and Table 3.5 selected bond lengths and angles. $[ReO(HL^{52})]$ (**13**) is a neutral oxorhenium(V) complex. The Re-O(10) bond length of 1.688(6) Å is in the range of the metal-oxo double bond. The different environments of the two nitrogen atoms reflect the different protonation/deprotonation situation. The Re-N(1) bond length of 2.264(8) Å and the C(11)-N(1)-C(7) angle of 112.0(1)° are similar to those in $[ReOCl_2(HL^{51})]$ (**9**) suggesting a neutral amine component N(1)-H(1). In contrast, the Re-

N(2) bond length of 1.942(8) Å and the C(31)-N(2)-C(27) angle of 118.4(1)° are similar to those in the complexes **10** and **11**, which is consistent with the amido coordination mode. Additionally, N(1) establishes a hydrogen bond via H(1) to the atom O(2) in the adjacent molecule generated by the symmetry element (-x+1/2, -y+3/2, -z+2).

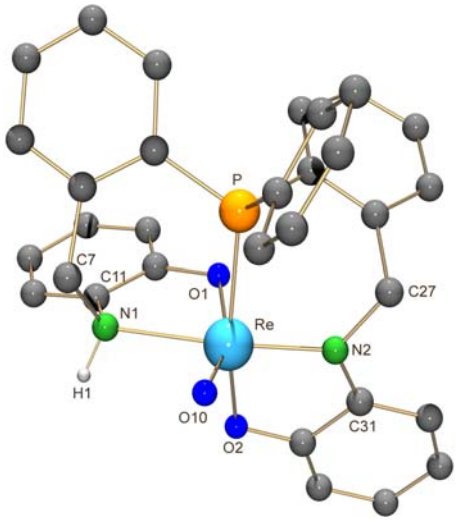

Fig. 3.10 Molecular structure of [ReO(HL^{52})] (**13**). The hydrogen atoms bonded to carbon atoms were omitted for clarity.

Table 3.5 Selected bond lengths and angles of [ReO(HL^{52})] (**13**)

Bond lengths [Å]:					
Re-O(10)	1.688(6)	Re-N(1)	2.264(8)	Re-O(1)	2.035(6)
Re-N(2)	1.942(8)	Re-O(2)	2.014(7)	N(1)-C(7)	1.46(1)
N(1)-C(11)	1.45(1)	N(2)-C(27)	1.49(1)	N(2)-C(31)	1.40(2)
Angles [°]:					
P-Re-O(10)	97.2(4)	P-Re-O(2)	157.8(3)	N(1)-Re-N(2)	168.0(5)
C(7)-N(1)-C(11)	112.0(1)	C(27)-N(2)-C(31)	118.4(1)	C(7)-N(1)-Re	1.39(1)
Hydrogen bond:					
D-H...A	d(D-H)	d(H...A)	d(D...A)	<(DHA)	
N(1)-H(1)...O(3)#1[a]	0.91	2.06	2.95(1)	166.0	

(a) Symmetry transformations used to generate equivalent atoms: #1 -x+1/2, -y+3/2, -z+2

The ^{31}P-{^{1}H} NMR spectrum of [ReO(HL^{52})] (**13**) presents a single resonance at −4.8 ppm. The ^{1}H NMR spectrum shows four doublets in the range of 5.3 to 6.0 ppm, which are associated with the two methylene groups. The broad singlet at 8.9 ppm (1H) is assigned to the NH proton, Fig. 3.11. The IR spectrum confirms the presence of terminal oxo ligand as well as the NH function by a strong absorption at 918 cm^{-1} ($\nu_{Re=O}$) and a medium intense broad band at 3178 cm^{-1} (ν_{NH}). The broadening of the NH band is consistent with the

hydrogen bond found in the X-ray analysis. The mass spectrum presents the $[M+H]^+$ peak at *m/z* = 704 amu as the base peak with the expected isotopic pattern.

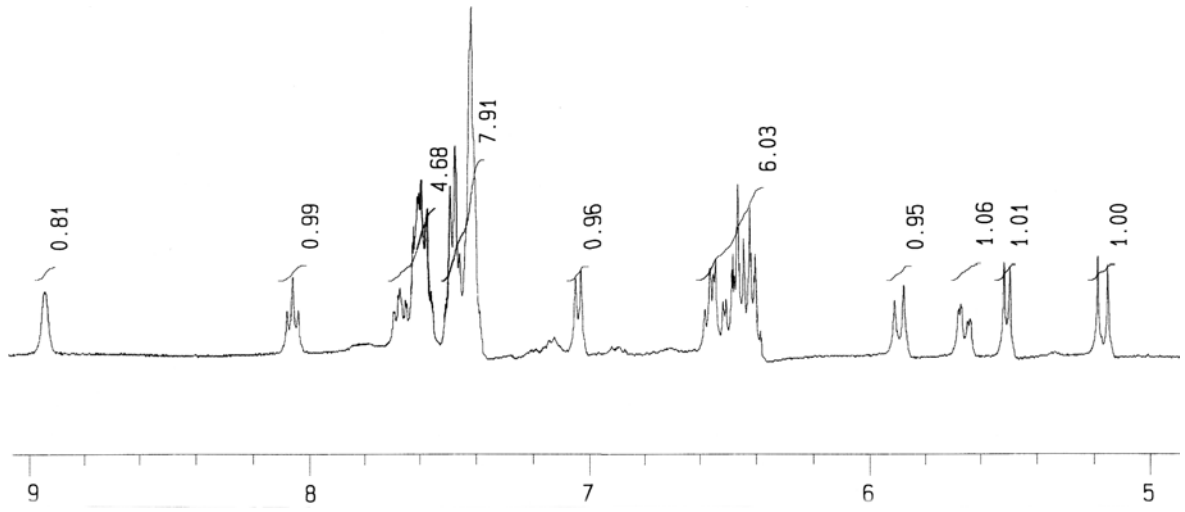

Fig. 3.11 The ^{1}H NMR spectrum of [ReO(HL^{25})] (**13**)

3.1.2.3 Reactions of H_6L^{53} with $(NBu_4)[ReOCl_4]$

Polydentate ligand systems with more than six donor atoms are extremely rare [22]. As explained previously, H_6L^{53} can be synthesized in a high yield without any purification techniques such as chromatography.

H_6L^{53} reacts with $(NBu_4)[ReOCl_4]$ in MeOH under formation of a cherry-red solution. In the absence of a supporting base, this red solution turns to green within 3 days and green hexagonal plates of [Re(L^{53}P)] (**14**) are obtained. Addition of the supporting base NEt_3 to the reaction solution causes immediately a color change of the reaction solution to green and a microcrystalline green product precipitates in an almost quantitative yield. The IR spectra of the products confirm an identical molecular structure for both compounds, Scheme 3.10.

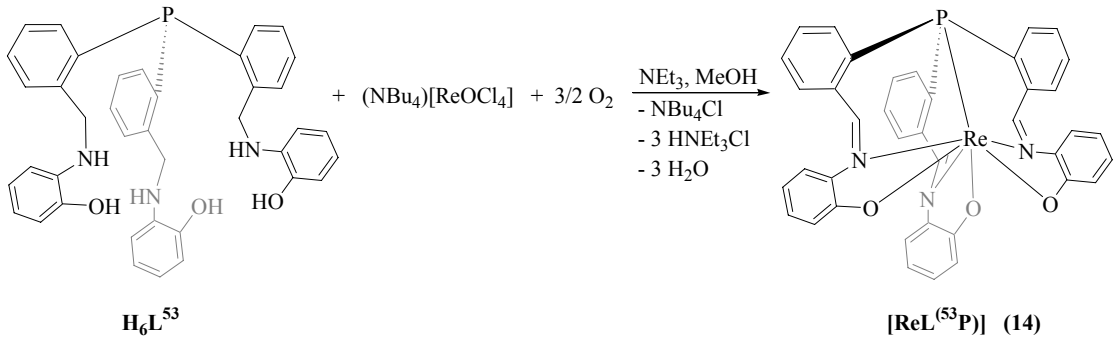

Scheme 3.10 The reaction of H_6L^{53} with $(NBu_4)[ReOCl_4]$

The molecular structure of **14** is presented in Fig. 3.12 and the selected bond lengths and angles are given in Table 3.6. [Re(L^{53}P)] (**14**) is a unique rhenium complex. The rhenium atom is encapsulated by the heptadentate ligand $(L^{53}P)^{3-}$. The coordinationenvironment of the rhenium atom is a distorted caped trigonal antiprism with the P atom as the cap. This is confirmed by a threefold rotation axis, C_3, which passes through the P and Re atoms. The polyhedron around the rhenium atom is presented in Fig 3.12. The bond lengths Re-N(1) of 2.16(1) Å and C(7)-N(1) of 1.31(1) Å are similar to the corresponding values in a rhenium complex with salicylidene-2-aminophenol [23]. The C(7)-N(1)-C(11) angle of 118.3(1)° is similar to the corresponding bond in **11** and near the ideal value of 120° for an imine component. C(7) is located 0.125 Å out of the mean leat-square plane formed by the atoms C(6), N(1), Re, and C(11).

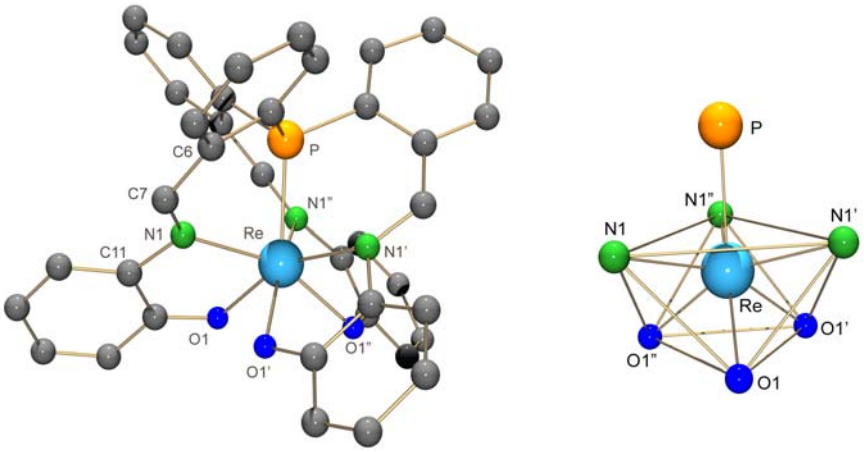

Fig. 3.12 Molecular structure of [Re(L^{53}P)] (**14**) (left) and coordination polyhedron (right). Hydrogen atoms were omitted for clarity.

Table 3.6. Selected bond lengths and angles of [Re(L^{53}P)] (**14**)

Bond lengths [Å]:					
Re-N(1)	2.16(1)	Re-O(1)	2.049(8)	Re-P	2.298(5)
N(1)-C(7)	1.31(1)	N(1)-C(11)	1.44(1)		
Angles [°]:					
P-Re-N(1)	74.7(2)	N(1)-Re-O(1)	77.8(4)	C(7)-N(1)-Re	128.7(9)
C(7)-N(1)-C(11)	118.3(1)				

Oxidative dehydrogenation of secondary amines under aerobic conditions is an important process encountered in biochemistry. A search in the literature reveals that most of the related published work involves Ni, Ru, Os, Cu and Fe complexes [24]. No similar reaction could be found for rhenium compounds. In all cases, however, it could not be found any direct evidence that molecular dioxygen is involved during these desaturation process, although O_2 is postulated as one of the key reagents in biologically occurring processes [25]. In the course of this investigation, an attempted reaction under an inert atmosphere did not result in the formation of **14** even after 2 weeks, which asserts necessitate of the presence of molecular dioxygen. The ^{31}P-{^{1}H} NMR spectrum of this reaction mixture showed a single resonance at −10.4 ppm, which confirms the coordination of the phosphorus atom with a low field shift of 20 ppm compared to the uncoordinated H_6L^{53}. Despite several attempts, no well defined compound could be isolated from such a reaction.

The ^{31}P-{^{1}H} and ^{1}H NMR spectra of **14** do not present any signal which implies paramagnetism of the rhenium ion. Because of the low solubility, the recorded EPR spectrum gives less intense and unreliable signals. The MS(ESI) shows a base peak at *m/z* = 804 amu associating with the mass of the $[M+H]^+$ ion. Absence of the ν_{NH} and ν_{OH} absorptions and presence of two bands at 1628 and 1566 cm^{-1} confirm the imine function defined by X-ray analysis.

3.2 2-(Benzylamino)phosphines derived from 3-amino-4-hydroxylbenzoic acid and their complexes with rhenium and technetium

3.2.1 Synthesis of the 2-(benzylamino)phosphines derived from 3-amino-4-hydroxylbenzoic acid

One of the most challenging tasks in the development of functional radiopharmaceuticals is the design of a suitable bifunctional chelators [26]. In this case, the exogenous chelator is to be conjugated to the native biomolecule and is therefore referred as a bifunctional chelator. Phosphine ligands have been successfully used to produce radiolabeled chelates for application in nuclear medicine for two decades [27]. However, their use in bioconjugating chemistry is limited, primarily due to the oxidative instability of alkyl phosphines and the bulky size of ligands with multi arylphosphines.

2-(Benzylamino)phosphines derived from 2-aminophenol, $H_{2n}L^{5n}$ (n = 1 - 3), show a high complex formation potential as has been demonstrated in the previous subchapter. In order to provide a conjugation-active site on the ligand skeleton, a carboxylic linker was introduced on the ligand backbone. Therefore, 3-amino-4-hydroxylbenzoic acid was chosen as a primary amine component in the synthesis of a new 2-(benzylamino)phosphine, which provides the same donor set as $H_{2n}L^{5n}$ (n = 1 - 3) and supplies an additional carboxylic component for biocoupling aims, Scheme 3.11.

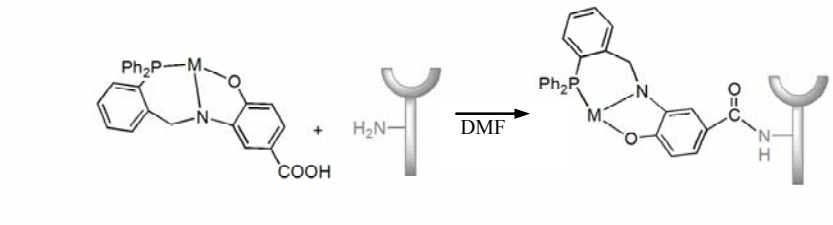

Scheme 3.11 Role of a '*bifunctional*' tridentate ligand in labeling a biomolecule

The carboxylic oxygen atom is potentially a suitable donor, which can compete with the other donors and may cause problems during the complex formation. In order to prevent the undesirable side reactions, 3-amino-4-hydroxybenzoic acid (**IX**) was reacted with $SOCl_2$ in alcohol (MeOH, EtOH) under reflux to give the corresponding esters **X** and **XI** as brown solids in high yields, Scheme 3.12.

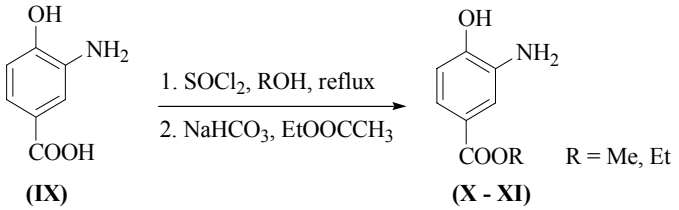

(IX) **(X - XI)**

Scheme 3.12 Esterification of 3-amino-4-hydroxybenzoic acid

The ^{1}H NMR spectrum of **X** shows a singlet at 3.2 ppm, while that of **XI** shows a triplet at 1.4 ppm confirming the presence of the methyl groups. The methylene groups of **XI** are observed as a quartet at 4.3 ppm. The elemental analyses are consistent with the molecular formulae of the products.

2-(Benzylamino)phosphines derived from the 3-amino-4-hydroxybenzoic acid derivatives were synthesized by a similar procedure, as was applied for the preparation of the phosphines $H_nL^{5n}P$ (see. 4. 2.). 2-(Formylphenyl)phosphines react with (n × 1 eq.) of **X - XI** in boiling EtOH under formation of $HL^{51}PCOOR$ (R = H, Me, Et) as orange-yellow solids in good yields, Scheme 3.13.

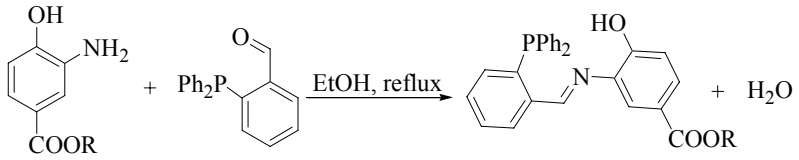

(IX-XI) **R = H (IX), Me (X), Et (XI)** **$HL^{51}PCOOR$**

Scheme 3.13 Synthesis of the Schiff' bases of 3-amino-4-hydroxybenzoic acid derivatives

The ^{31}P-{^{1}H} NMR spectra of $HL^{51}PCOOR$ (R = H, Me, Et) show single resonances between −10.0 and −20.0 ppm. The ^{1}H NMR spectra confirm the presence of the imine components by doublets at 9.1 ppm with the typical *PH* coupling constants of J_{PH} = 5.4 Hz for 2-(benzylimino)phosphines (Chapter 2). The infrared spectra show intense bands between 1650 and 1680 cm^{-1} due to the stretching vibrations of the carbonyl groups (ν_{CO}). Strong absorptions between 1550 and 1590 cm^{-1} support the presence of the imine functions.

The isolated Schiff bases $HL^{51}PCOOR$ were reduced by excess amounts of $NaBH_4$ in boiling EtOH. The crude products, which were obtained from the reduction of $HL^{51}PCOOR$ were worked up with an aqueous solution of HCl (pH ≈2). This facilitates the extraction of the product by organic solvents, Scheme 3.14.

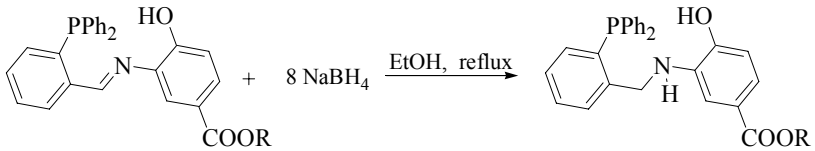

HL[51]PCOOR **R = H, Me, Et** **H_2L^{51}COOR**

Sheme 3.14 Synthesis of the potentially '*bifunctional*' ligands H_2L^{51}COOR (R= H, Me, Et).

The ^{31}P-{^{1}H} NMR spectra of H_2L^{51}COOR (R= H, Me, Et) present single resonances between −10.7 and −12.6 ppm. The ^{1}H NMR spectra confirm the supposed molecular structures by the resonances at 4.2 ppm related to the methylene protons. The ^{1}H NMR spectra prove that during the reduction of the imines HL[51]PCOOR the ester components remain intact as is indicated by a triplet at 1.3 ppm and a quartet at 4.3 ppm. Similar spectroscopic evidence confirms the stability of the methyl ester through the reduction reaction. Fig. 3.13 presents the ^{1}H NMR spectrum of H_2L^{51}COOEt.

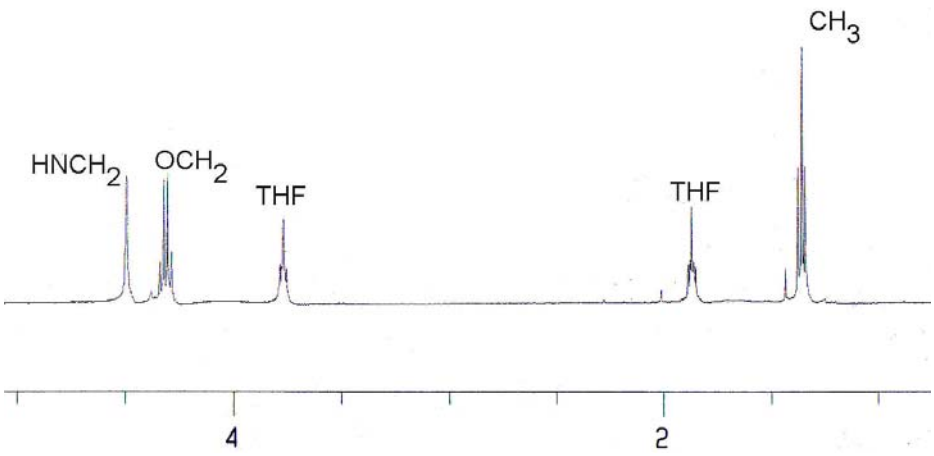

Fig 3.13 Part of the ^{1}H NMR spectrum of H_2L^{51}COOEt.

3.2.2 Rhenium and technetium-99m complexes of H_2L^{51}COOR (R = H, Me, Et)

H_2L^{51}COOEt reacts with $(NBu_4)[ReOCl_4]$ in MeOH at ambient temperatures. The product was isolated as a green solid directly from the reaction solution and was recrystallized from a CH_2Cl_2/MeOH mixture, Scheme 3.15.

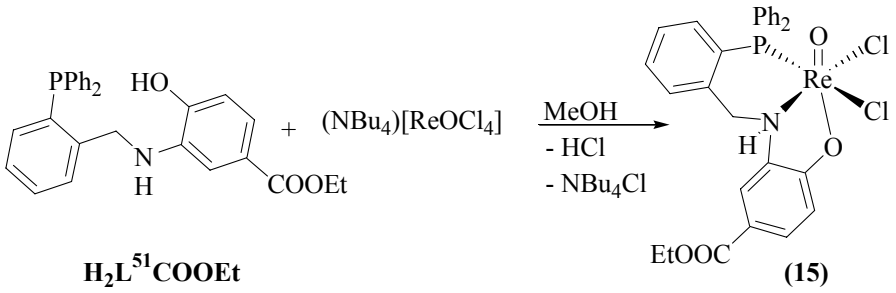

$H_2L^{51}COOEt$ **(15)**

Scheme 3.15 Synthesis of *fac*-[$ReOCl_2(HL^{51}Et)$] (**15**)

Fig. 3.14 presents the molecular structure of **15** and selected bond lengths and angles are listed in Table 3.7. The compound is a distorted octahedral oxorhenium(V) complex. The C(11)-N(1)-C(7), C(7)-N(1)-Re, and C(11)-N(1)-Re angles of 110.9(1)°, 115.4(9)°, and 109.3(9)° confirm a tetrahedral environment of N(1). The hydrogen atom H(1) establishes an intermolecular hydrogen bond with the Cl(2) ligand of the adjacent molecule generated by the symmetry element (-x+2,-y+2,-z+1).

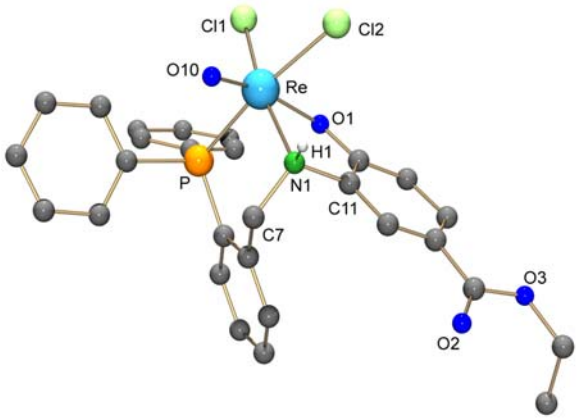

Fig. 3.14 Molecular structure of *fac*-[$ReOCl_2(HL^{51}COOEt)$] (**15**). The hydrogen atoms bonded to carbon atoms were omitted for clarity.

Table 3.7 Selected bond lengths and angles of [$ReOCl_2(HL^{51}Et)$] (**15**)

Bond lengths [Å]:					
Re-O(10)	1.64(1)	Re-N(1)	2.18(1)	Re-P	2.453(5)
Re-Cl(1)	2.341(4)	C(7)-N(1)	1.51(1)	N(1)-C(11)	1.47(2)
Angles [°]:					
O(10)-Re-O(1)	164.3(5)	Cl(1)-Re-N(1)	167.3(3)	P-Re-Cl(2)	172.1(2)
Re-N(1)-C(11)	109.3(9)	C(7)-N(1)-C(11)	110.9(1)		
Hydrogen bond:					
D-H...A	d(D-H)	d(H...A)	d(D...A)	<(DHA)	
N(1)-H(1)...Cl(2)#1[a]	0.91	2.32	3.18(1)	157.4	

(a) Symmetry transformations used to generate equivalent atoms: #1 -x+2,-y+2,-z+1

The ^{31}P-{^{1}H} NMR spectrum of *fac*-[ReOCl$_2$(HL^{51}COOEt)] (**15**) exhibits a single resonance at −16.2 ppm assigned to the coordinated phosphine. The ^{1}H NMR spectrum presents two doublets of the protons of the methylene group at 5.4 and 5.5 ppm. The NH signal is detected as a broad resonance at 9.9 ppm. The IR spectrum presents a broad band at 3425 cm^{-1}, which is characteristic for stretching vibrations of the secondary amines. A weak absorption at 1605 cm^{-1} is consistent with the bending vibrations of the NH group. The base peak of the MS(ESI) spectrum of **15** appears at *m/z* = 656.1 amu and can be associated with the [M-2Cl-H]$^{+}$ fragment.

The molecular structure of **15** shows that the modified tridentate ligand H$_2$L^{51}COOEt coordinates to the metal ion under formation of the facial isomer in the absence of a supporting base. The bis-chelating mononegative coordination mode of H$_2$L^{51}COOEt makes it a good candidate for the stabilization of the "*fac*-[Re(CO)$_3$]$^{+}$" synthon. Therefore H$_2$L^{51}COOEt was reacted with (NEt$_4$)$_2$[ReBr$_3$(CO)$_3$] in MeOH. The reaction progress was tracked by means of ^{31}P-{^{1}H} NMR spectroscopy. The ^{31}P-{^{1}H} NMR spectrum taken from the reaction mixture shows two single resonances at 4.9 and 8.1 ppm with nearly equal intensities. The chemical shift values of both signals show low-field shifts compared to that of the uncoordinated H$_2$L^{51}COOEt. This implies that the two species should belong to the metal complexes wherein H$_2$L^{51}COOEt is possibly coordinated in κ^2-(P,N) for **16** and κ^3-(P,N,O) for **16a**. The tridentate [P,N,O] ligand (H$_2$CH$_2$PNO = Ph$_2$P(*o*-C$_6$H$_4$NH(CH$_2$)$_2$OH)) shows similar modes of coordination during reactions with (NEt$_3$)$_2$[ReBr$_3$(CO)$_3$] [28], Scheme 3.16.

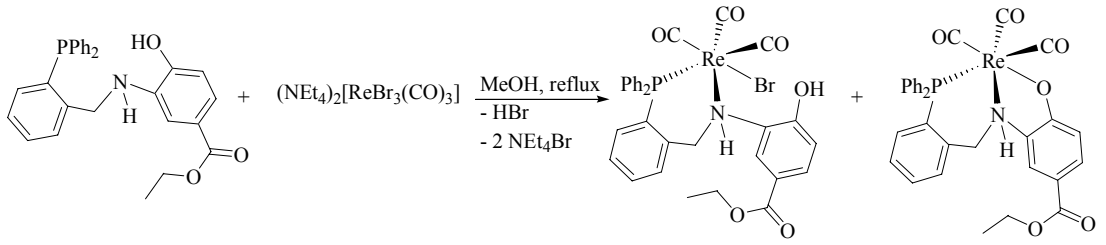

(16) **(16a)**

Scheme 3.16 The reaction between H$_2$L^{51}COOEt and [ReBr$_3$(CO)$_3$]$^{2-}$ in the absence of a supporting base

After heating the reaction mixture for 2 h, the ratio of the signals did not change dramatically. Therefore, the volume of the reaction solution was reduced to half and cooled down to −10°C to possibly isolate both compounds. By keeping the reaction solution at this temperature for 2 days, pale yellow crystals of [ReBr(CO)$_3$(H$_2$L^{51}COOEt)] (**16**) were obtained. The molecular structure of **16** is presented in Fig. 3.15.

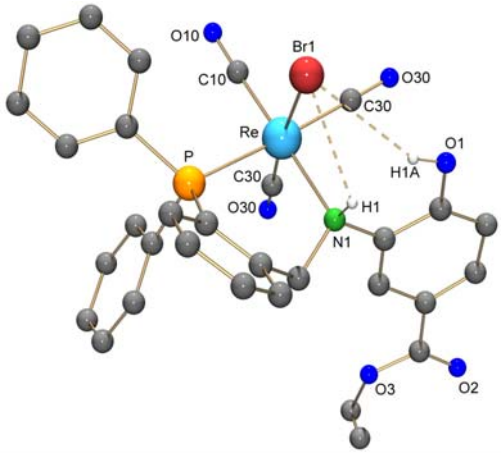

Fig. 3.15 Molecular structure of [ReBr(CO)$_3$(H$_2$L^{51}COOEt)] (**16**). The hydrogen atoms bonded to carbons were omitted for clarity.

Selected bond lengths and angles of **16** are summarized in Table 3.8. The molecular structure of [ReBr(CO)$_3$(H$_2$L^{51}COOEt)] (**16**) depicts that the compound is a neutral Re(I) complex. The coordination environment of the rhenium atom is distorted octahedral. The Re-N(1) bond length of 2.28(1) Å is longer than those observed in the similar structures **9** and **12**. This can be explained by the strong *trans* influence of the carbonyl ligands. The ligand coordinates in a neutral bidentate mode, which is supported by hydrogen bonds between N(1)-H(1)...Br(1) O(1)-H(1A)...Br(1).

Table 3.8 Selected bond lengths [Å] and angles [°] of [ReBr(CO)$_3$(H$_2$L^{51}COOEt)].NEt$_4$Br (**16**).

Bond lengths [Å]:					
Re-C(10)	1.90(2)	Re-C(20)	1.95(2)	Re-C(30)	1.95(1)
Re-Br(1)	2.637(1)	Re-N(1)	2.28(1)	C(10)-O(10)	1.15(2)
Angles [°]:					
N(1)-Re-Br(1)	82.8(3)	N(1)-Re-C(10)	176.8(4)	Br(1)-Re-C(20)	174.3(4)
Re-N(1)-C(7)	116.4(7)	Re-N(1)-C(11)	112.6(8)	C(11)-N(1)-C(7)	111.2(9)
Hydrogen bonds:					
D-H...A	d(D-H)	d(H...A)	d(D...A)	<(DHA)	
N(1)-H(1)...Br(1)	0.91	2.81	3.26(1)	112.5	
O(1)-H(1A)...Br(1)	0.82	2.92	3.65(1)	149.4	

The single resonance at 7.7 ppm[2] in the ^{31}P-{^{1}H} NMR spectrum of **16** is assigned to the coordinated phosphine. The resonance is shifted by +25 ppm compared to the uncoordinated ligand due to the coordination of the phosphorus atom.

[2] The difference between the reported chemical shift values for the reaction mixture and the isolated complexes is due to the solvent influence.

The ^{1}H NMR spectrum presents two doublets at 4.4 and 5.8 ppm. The three intense bands at 2029, 1936 and 1902 cm^{-1} in the infrared spectrum of **16** are associated with the stretching vibrations of the carbonyl ligands. The medium intense band at 1716 cm^{-1} is assigned to the stretching vibrations of the ester group. The NH bending vibrations are observed as a weak band at 1608 cm^{-1}. The base peak in the MS(ESI) spectrum of **16** at *m/z* = 726 amu belongs to the [M - Br-2CO]$^{+}$ fragment. This fragmentation implies the favourable stability of [Re(κ^2-H_2L^{51})]$^{+}$ building block, which is an essential factor for applying the complexes of H_2L^{51}COOR for pharmaceutical purposes.

In order to isolate [Re(CO)$_3$(κ^3-HL^{51}COOEt)] (**16a**), the reaction was carried out at room temperature in the presence of a supporting base NEt$_3$. The ^{31}P-{^{1}H} NMR spectrum of the reaction solution presents only one single resonance at 4.3 ppm. The bromide anion can be precipitated by the addition of Ag^{+} in the form of AgBr. This promotes the formation of the κ^3-(P,N,O) chelating type. The isolated product showed a high solubility in organic solvents which hinders the isolation of the X-ray quality crystals. The lower solubility of the methyl-substituted 2-(benzylamino)phosphine H_2L^{51}COOMe in alcohols was applied to increase the crystallization chance. H_2L^{51}COOMe reacts with $(NEt_4)_2[ReBr_3(CO)_3]$ in boiling MeOH to give a light yellow clear solution, the ^{31}P-{^{1}H} NMR spectrum of which gives two single resonances at 5.1 and 8.3 ppm. Thereafter, the reaction solution was treated with a methanolic solution of $AgNO_3$ (3 eq.). After working up the reaction mixture, the isolated solid was recrystallized from a mixture of CH_2Cl_2/MeOH to give plates of [Re(CO)$_3$(κ^3-HL^{51}COOMe)] (**17**), Scheme 3.17.

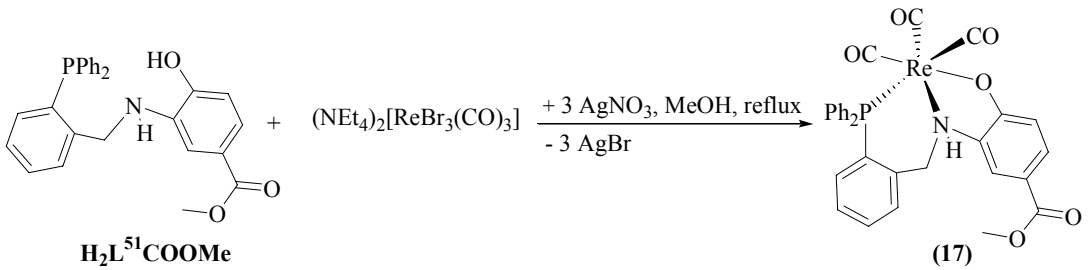

H_2L^{51}COOMe **(17)**

Scheme 3.17 Synthesis of [Re(CO)$_3$(κ^3-HL^{51}Me)] (**17**)

The molecular structure of *fac*-[Re(CO)$_3$(κ^3-HL^{51}COOMe)].3MeOH (**17**) is presented in Fig 3.16. The mononegative (HL^{51}COOMe)$^{-}$ ligand and three carbonyl ligands surround the rhenium atom under formation of a neutral complex. The bond distances Re-O(1) of 2.155(3) Å and Re-N(1) of 2.217(3) Å are in the range of the metal-donor atom (O/N) single bonds, Table 3.9. There are slight differences in the Re-C bond lengths, which reflect the *trans* influences of the respective phosphine, amine and phenolic donor sites. The hydrogen

bond between N(1) and the oxygen atom of methanol (solvent) N(1)-H(1)...O(4) of 2.812(6) Å is established.

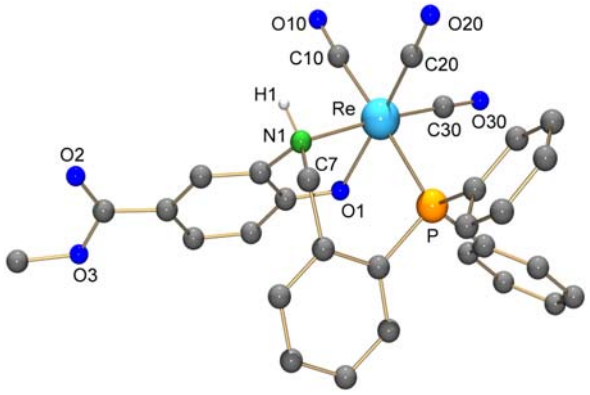

Fig. 3.16 Molecular structure of $[Re(CO)_3(\kappa^3\text{-}HL^{51}COOMe)]\cdot 3MeOH$ (**17·3MeOH**). The solvent molecules and hydrogen atoms bonded to carbon atoms were omitted for clarity.

Table 3.9 Selected bond lengths and angles of $[Re(CO)_3(HL^{51}COOMe)]\cdot 3MeOH$ (**17**)

Bond lengths [Å]:							
Re-N(1)	2.217(3)	Re-P	2.462(1)	Re-O(1)	2.155(3)		
Re-C(10)	1.951(5)	Re-C(20)	1.916(5)	Re-C(30)	1.965(5)		
Angles [°]:							
P-Re-N(1)	88.1(1)	N(1)-Re-O(1)	76.7(1)	O(1)-Re-C(10)	92.2(2)		
P-Re-O(1)	84.64(9)	C(10)-Re-C(20)	89.4(2)	C(10)-Re-C(30)	89.4(2)		
Hydrogen bond:							
D-H...A	d(D-H)	d(H...A)	d(D...A)	<(DHA)			
O(5)-H(5A)...O(6)#1[a]	0.82	1.79	2.602(7)	172.4			
N(1)-H(1)...O(4)	0.91	1.92	2.812(6)	166.1			
O(4)-H(4A)...O(5)	0.82	1.86	2.680(8)	178.5			

(a) Symmetry transformations used to generate equivalent atoms: #1 -x+1,-y+1,-z+1

The $^{31}P\text{-}\{^1H\}$ NMR spectrum of **17** presents the expected single resonance at 5.8 ppm of the coordinated phosphine. The ^1H NMR spectrum supports the molecular structure by the appearance of two doublets at 4.3 an 4.7 ppm suggesting the formation of a chelate ring due to the coordination of the [P,N] donor set. The less resolved triplet at 10.9 ppm is assigned to the NH group. The strong downfield shift of the signal compared to that of the uncoordinated $H_2L^{51}COOMe$, which appears at 5.3 ppm, indicates the coordination of the NH component. The medium intense absorption at 3186 cm^{-1} in the IR spectrum of **17** is assigned to the ν_{NH} stretching vibration, which shows a 259 cm^{-1} bathochromic shift compared to the spectrum of the uncoordinated $H_2L^{51}COOMe$. The band associated with the bending vibrations of the NH group appears at 1500 cm^{-1}, which is shifted by 27 cm^{-1} in contrast to that of $H_2L^{51}COOMe$.

The stretching vibrations of the carbonyl ligands give intense absorptions at 2021, 1925 and 1886 cm^{-1}, the stretching vibration of the methylester group is detected at 1682 cm^{-1}. The MS(ESI) spectrum of the compound exhibits peaks associated with $[M+Na]^+$ at *m/z* = 734.1 amu and $[M+Na-CO]^+$ at m/z = 706.1 amu.

The synthetic pathway and molecular structure of **17** clearly shows that $H_2L^{51}COOR$ (R = Me,Et) react with $(NEt_4)[ReBr_3(CO)_3]$ in the presence of 3 equivalents of Ag^+ to give $[Re(CO)_3(\kappa^3\text{-}HL^{51}COOR)]$ in high yields. The ester group can then be hydrolyzed by heating $[Re(CO)_3(\kappa^3\text{-}HL^{51}COOR)]$ (R = Me, Et) in an alcoholic solution of NaOH for 18 h. This reaction time of the ester hydrolysis, however, is by far too long to be applicable in the formulation of technetium-based radiopharmaceuticals, bearing in mind the physical half-life of ^{99m}Tc of approximately 6 h. Therefore, $H_2L^{51}COOH$ was reacted with $(NEt_4)_2[ReBr_3(CO)_3]$ in MeOH at 50°C for 10 min. Subsequently, 3 eq. of $AgNO_3$ were added to the reaction solution and heated for 20 min. After working up the reaction mixture, a colourless solid was obtained, the crystallization of which from warm methanol gave colourless plates of $[Re(CO)_3(\kappa^3\text{-}HL^{51}COOH)]$ (**18**), Scheme 3.18. The same product was isolated from the reaction between $H_2L^{51}COOH$ and $(NEt_4)_2[ReBr_3(CO)_3]$ in the presence of the supporting base NEt_3 but the yield of the reaction was slightly lower.

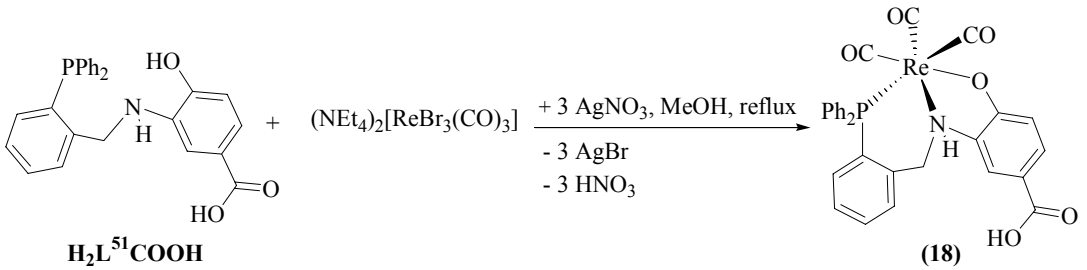

$H_2L^{51}COOH$ **(18)**

Scheme 3.18 Synthesis of $[Re(CO)_3(\kappa^3\text{-}HL^{51}COOH)]$ (**18**)

The molecular structure of $[Re(CO)_3(HL^{51}COOH)]$ (**18**) is presented in Fig. 3.17, and selected bond lengths and anglesare given in Table 3.10. The uninegative tridentate ligand $(HL^{51}COOH)^-$coordinates in the chelating κ^3-(P,N,O) mode. The Re-N(1) bond length of 2.217(7) Å is consistent with the previously mentioned complexes **16** and **17**. The bond distances C(17)-O(2) and C(17)-O(3) of 1.26(1) Å and 1.30(1) Å indicate that the π-electrons are mostly localized between C(17) and O(2). The uncoordinated carboxylic function is located in an ideal position to be used for biocoupling purposes.

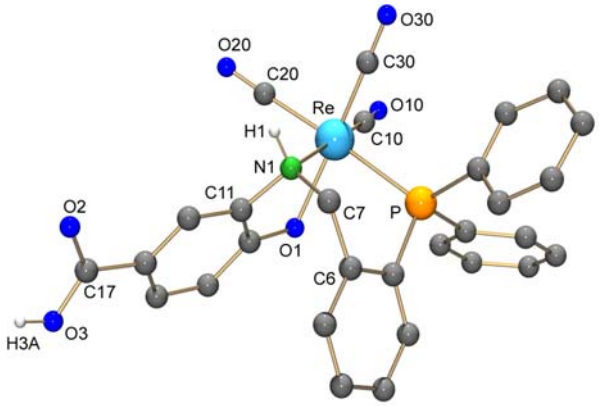

Fig. 3.17 Molecular structure of $[Re(CO)_3(HL^{51}COOH)]$ (**18**). The hydrogen atoms bonded to carbon atoms were omitted for clarity.

Table 3.10 Selected bond lengths and angles of $[Re(CO)_3(HL^{51}COOH)]$ (**18**)

Bond lengths [Å]:					
Re-N(1)	2.217(7)	Re-P	2.469(2)	Re-O(1)	2.180(6)
Re-C(10)	1.92(1)	Re-C(20)	1.97(1)	Re-C(30)	1.90(1)
C(17)-O(2)	1.26(1)	C(17)-O(3)	1.30(1)		
Angles [°]:					
P-Re-N(1)	87.3(2)	N(1)-Re-O(1)	76.1(3)	O(1)-Re-C(10)	98.4(4)
P-Re-O(1)	84.8(2)	C(10)-ReC(20)	87.9(4)	O(2)-C(17)-O(3)	124.5(8)

Hydrogen bonds:				
D-H...A	d(D-H)	d(H...A)	d(D...A)	<(DHA)
N(1)-H(1)...O(4)[a]#1	0.91	1.99	2.87(1)	163.3
O(3)-H(3A)...O(2)[a]#2	0.82	1.79	2.601(9)	172.2

(a) Symmetry transformations used to generate equivalent atoms: #1 -x,y-1/2,-z+3/2 #2 -x-1,-y,-z+1

The $^{31}P-\{^1H\}$ NMR spectrum of **18** shows a single resonance at 5.8 ppm, which has expectedly a similar chemical shift value like in **17**. Two broad signals at 12.1 and 10.2 ppm in the ^1H NMR spectrum of **18** are associated with the COOH and NH protons. The infrared spectrum of **18** shows two medium absorptions at 3217 and 1608 cm^{-1} of the stretching and bending vibrations of the NH group. The carbonyl ligands of $[Re(CO)_3(\kappa^3\text{-}HL^{51}COOH)]$ (**18**) are detected as three strong absorptions at 2033, 1944 and 1894 cm^{-1} confirming their facial arrangement and a medium band at 1686 cm^{-1} is assigned to the stretching vibrations of the carboxylic group. The base peak in the (+)MS(ESI) spectrum of **18** at *m/z* = 720.0 amu belongs to the $[M+Na]^+$ species. The $[M-H]^-$ fragment was detected in the (-)MS(ESI) spectrum of **18** at *m/z* = 696.1 amu.

The technetium(I) complex $[^{99m}Tc(OH_2)_3(CO)_3]^+$ [29] has attracted much interest as a precursor for ^{99m}Tc radiopharmaceuticals [30-32]. A number of biologically interesting

molecules, for example, peptides, scFv, or CNS receptor ligands, have already been labelled with technetium by this approach, demonstrating the potential of $[^{99m}Tc(OH_2)_3(CO)_3]^+$ for radiopharmaceutical applications [33-35]. There exist an extremely vast number of ligands and complexes, which were applied for basic studies with the aim of developing new functionalized radiopharmaceuticals. The most challenging points in radioactively labelling of the biologically active molecules can be mentioned as:

- Comprehensive knowledge about the molecular structure of the radioactive complex
- Stability of this complex during biocoupling reactions
- Selective labelling of the biologically interesting molecule, through which the molecular structure of the labelled biomolecule can be predicted.

The molecular structures of the aforementioned complexes **16 - 18** declare the ideal conditions for the synthesis of the $[^{99m}Tc(CO)_3(\kappa^3\text{-}HL^{51}COOH)]$ complex.

Thus, $H_2L^{51}COOH$ was reacted with $[^{99m}Tc(H_2O)_3(CO)_3]^+$ in a mixture of $EtOH/H_2O$ in the presence of the supporting base NEt_3 under formation of $[^{99m}Tc(CO)_3(HL^{51}COOH)]$ (**19**) in an almost quantitative yield with respect to the initial ^{99m}Tc complex, Scheme 3.19.

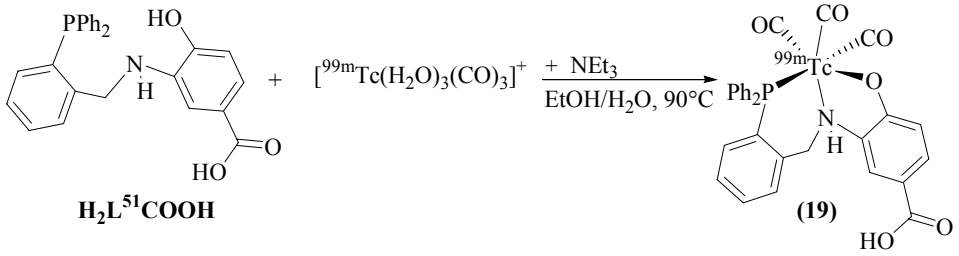

Scheme 3.19 The reaction of $[^{99m}Tc(H_2O)_3(CO)_3]^+$ with $H_2L^{51}COOH$

The reaction progress was detected by high performance liquid chromatography (HPLC). Fig. 3.18 shows the related chromatograms of the complexes $[^{99m}Tc(H_2O)_3(CO)_3]^+$ (t_R = 6.7 min) and $[^{99m}Tc(CO)_3$ $(HL^{51}COOH)]$ (**19**) (t_R = 27.2 min) recorded by a radiation detector.

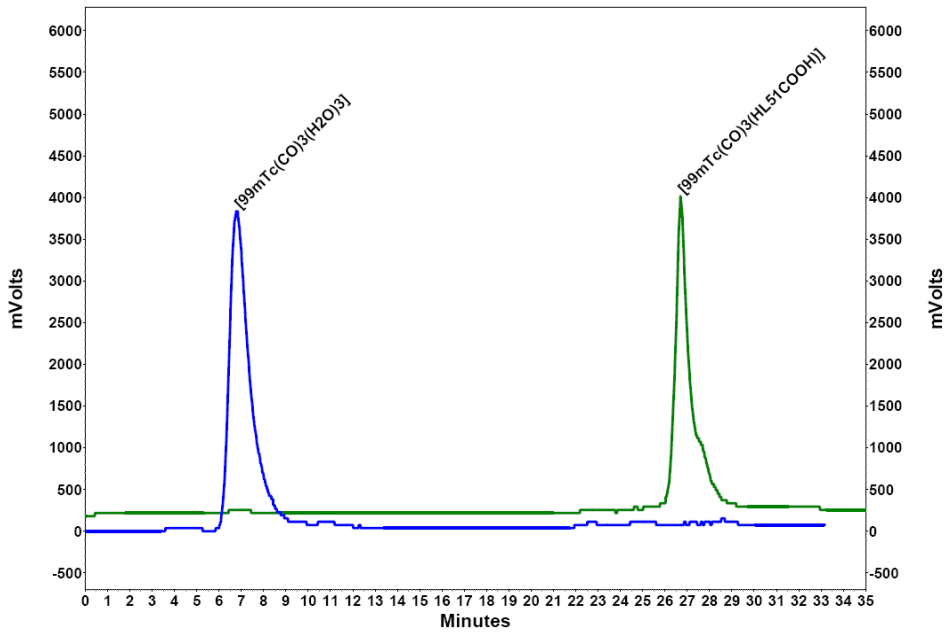

Fig. 3.18 The chromatograms of $[^{99m}Tc(H_2O)_3(CO)_3]^+$ (blue) and $[^{99m}Tc(CO)_3(HL^{51}COOH)]$ (green).

3.2.2.1. Coupling of $[Re(CO)_3(HL^{51}COOH)]$ with triglycine and substance P

The analytical data of $[Re(CO)_3(\kappa^3\text{-}HL^{51}COOH)]$ (**18**) confirm the expected coordination mode of $H_2L^{51}COOH$ to rhenium in a tridentate bis-chelating pattern and provides a free carboxylic component for bioconjugation means. In order to study these coupling possibilities, $[Re(CO)_3(\kappa^3\text{-}HL^{51}COOH)]$ (**18**) was reacted with a mixture of N-hydroxybenzotriazole (HOBt) and dicyclohexylcarbodiimide (DCC) to give the active ester (**18a**), Scheme 3.20. After pre-activation of the carboxylic group, triglycine ethylester was added to the reaction solution in solid form. After working up the reaction mixture $[Re(CO)_3(\kappa^3\text{-}HL^{51}COOH)]$-TEG (**20**) was isolated as a pale yellow solid.

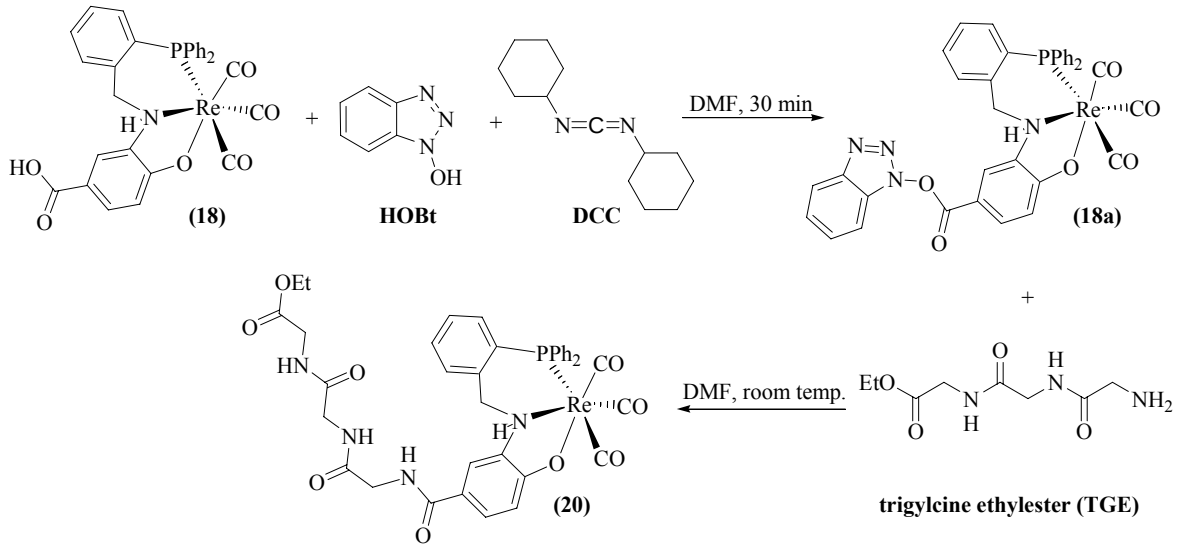

Scheme 3.20 "*Bifunctional*" coupling of $[Re(CO)_3(\kappa^3\text{-}HL^{51}COOH)]$ (**18**) and triglycine ethylester

The $^{31}P\text{-}\{^1H\}$ NMR spectrum of **20** shows the single resonance of the coordinated phosphine at 6.3 ppm. The mass of $[M+H]^+$ was detected at *m/z* = 897 amu in the MS(ESI) spectrum of **20**.

$[Re(CO)_3(\kappa^3\text{-}HL^{51}COOH)]$-TGE (**20**) confirms the biocoupling potential of $[Re(CO)_3(\kappa^3\text{-}HL^{51}COOH)]$ (**18**) and the stability of this complex during liquid-phase peptide synthesis reactions. However, selective labelling of a natural peptide with several free carboxylic groups or amines in liquid-phase is a more difficult challenge and isolation of the intended product requires special separation and purification techniques.

Solid phase peptide synthesis (SPPS), developed by R. B. Merrifield [36], was a major breakthrough for the chemical synthesis of peptides and small proteins. The first stage of the technique consists of peptide chain assembly with protected amino acid derivatives on a polymeric support. The second stage of the technique is the cleavage of the peptide from the resin support with the concurrent cleavage of all side chain protecting groups to give the crude peptide.

The general principle of SPPS bases on repeated cycles of coupling-deprotection. The free N-terminal amine of a solid-phase attached peptide is coupled to a single N-protected amino acid unit. This unit is then deprotected, revealing a new N-terminal amine to which a further amino acid or any other compound with a free carboxylic group may be attached.

According to study the solid-phase labelling (coupling of a radioactive complex with a biologically interesting molecule, which is attached to a resin) of a natural polypeptide, substance P was chosen. Substance P (SP) is a neuropeptide: an undecapeptide that functions as a neurotransmitter. These are chemicals that are used to relay, amplify and modulate

signals between a neuron and another cell. The sensory function of substance P is thought to be related to the transmission of pain information into the central nervous system.

Accordingly a part of the substance P with the sequence of (LGFFQQ), attached to the Wang resin, was synthesized. The free carboxylic function of the complex $[Re(CO)_3(\kappa^3\text{-}HL^{51}COOH)]$ (**18**) was preactivated by a mixture of (1,2,3)triazolo-(4,5-b)pyridin-3-ol (HOAT) and *N,N'*-diisopropylcarbodiimide (DIC) for 30 min and added to the polypeptide. This step was repeated twice to achieve a higher yield. Thereafter the resins were washed by DMF and CH_2Cl_2 in order to remove the unreacted starting materials and urea derivatives. This can be mentioned as one of the most important advantageous of solid-phase technique, Scheme 3.21.

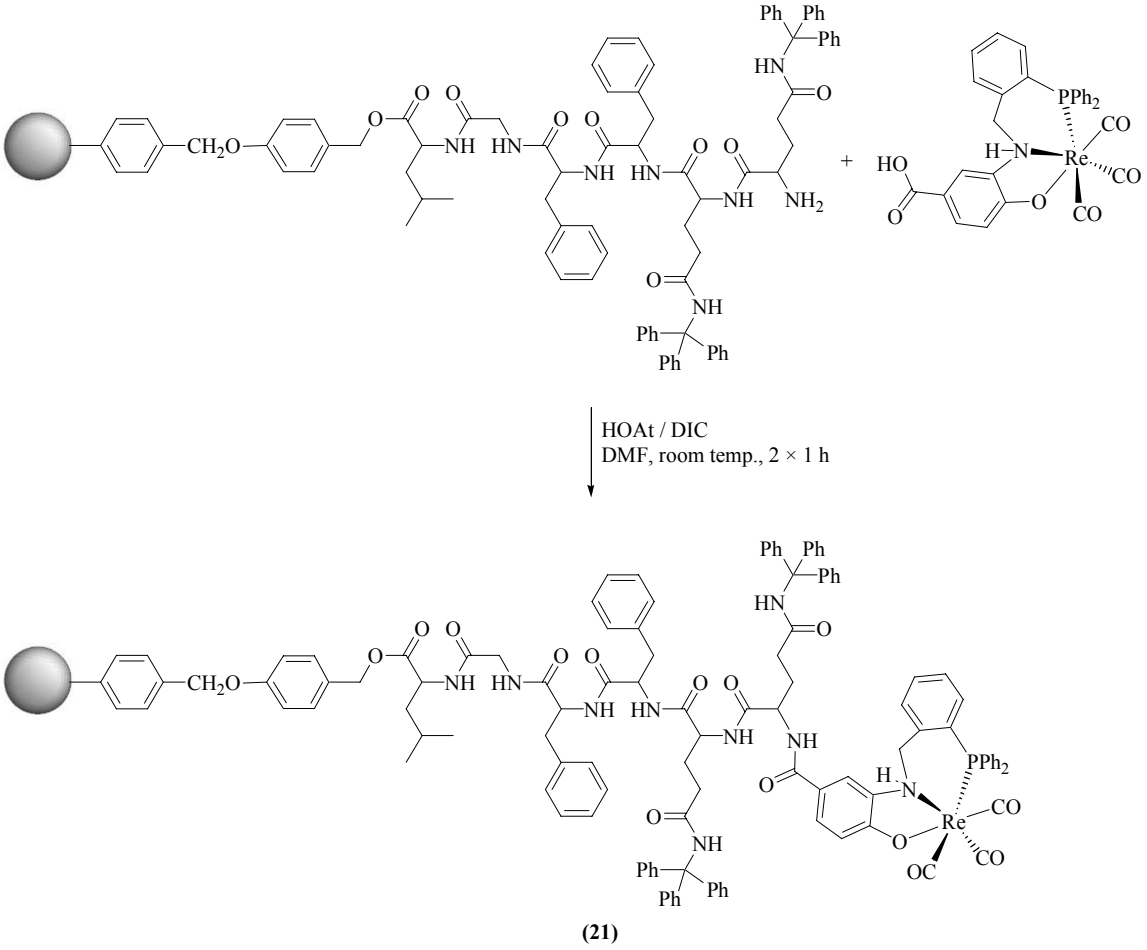

(21)

Scheme 3.21 Solid-phase labelling of Substance P (active site) with $[Re(CO)_3(\kappa^3\text{-}HL^{51}COOH)]$ (**18**)

The solid-phase attached [Re(CO)$_3$(κ^3-HL^{51}COOH)]-SP (**21**) was treated with a mixture of trifluoroacetic acid (TFA), triisopropylsilan (TIS), and water with the ratio of (9.5:0.5:0.1) in order to deprotect the protected groups and release the labelled peptide from the resin, and to obtain free [Re(CO)$_3$(κ^3-HL^{51}COOH)]-SP (**21**), Scheme 3.22.

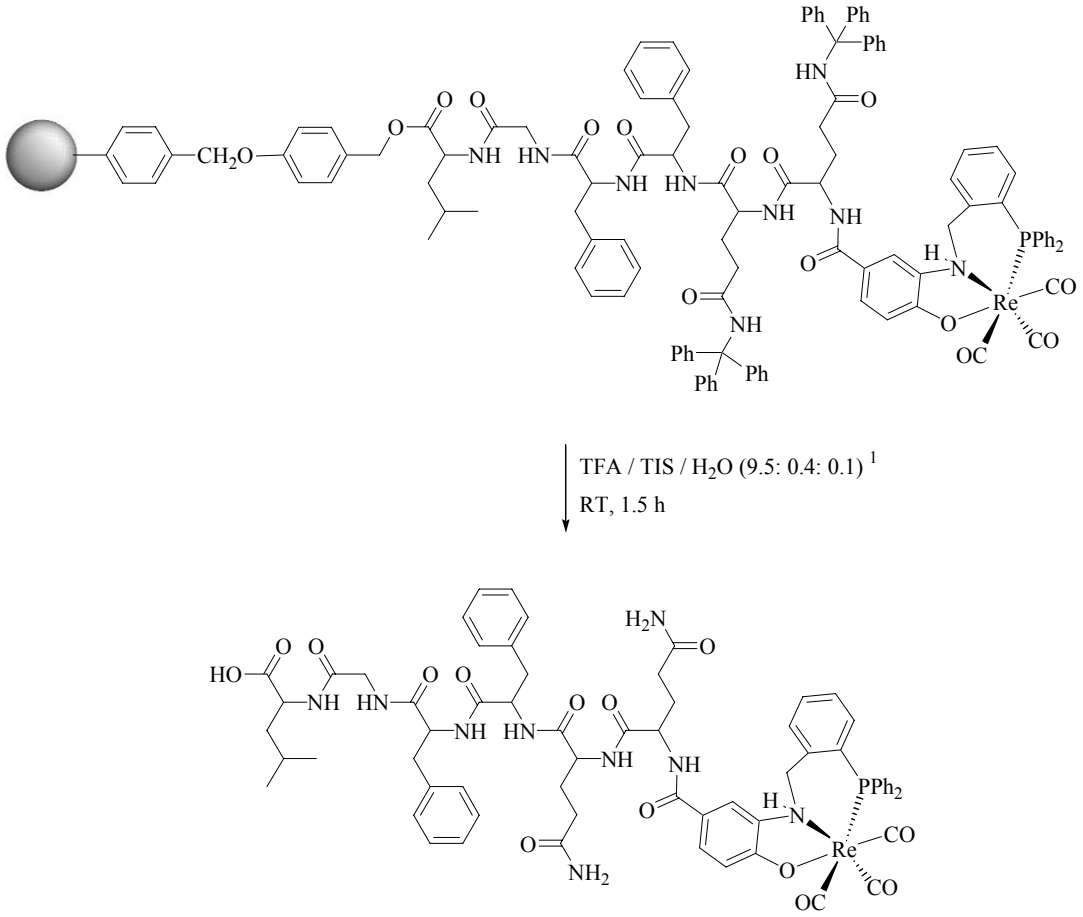

{[Re(CO)$_3$(κ^3-HL^{51}COOH)]-SP} (**21**)

Scheme 3.22 Synthesis of the free [Re(CO)$_3$(κ^3-HL^{51}COOH)]-SP (**21**)

The isolated crude product was analyzed by high performance liquid chromatography (HPLC) and ESI(TOF) mass spectrometry. The chromatogram of the crude product shows a single peak at t_R = 30.5 min. The mass spectrum of the collected fraction from HPLC presents the base peak at *m/z* = 1418.4 amu representing $[M+H]^+$ (M = molar mass of **21**) species, Fig. 3.19. This elucidates that the complex **18** remains stable under different strong acidic or basic conditions.

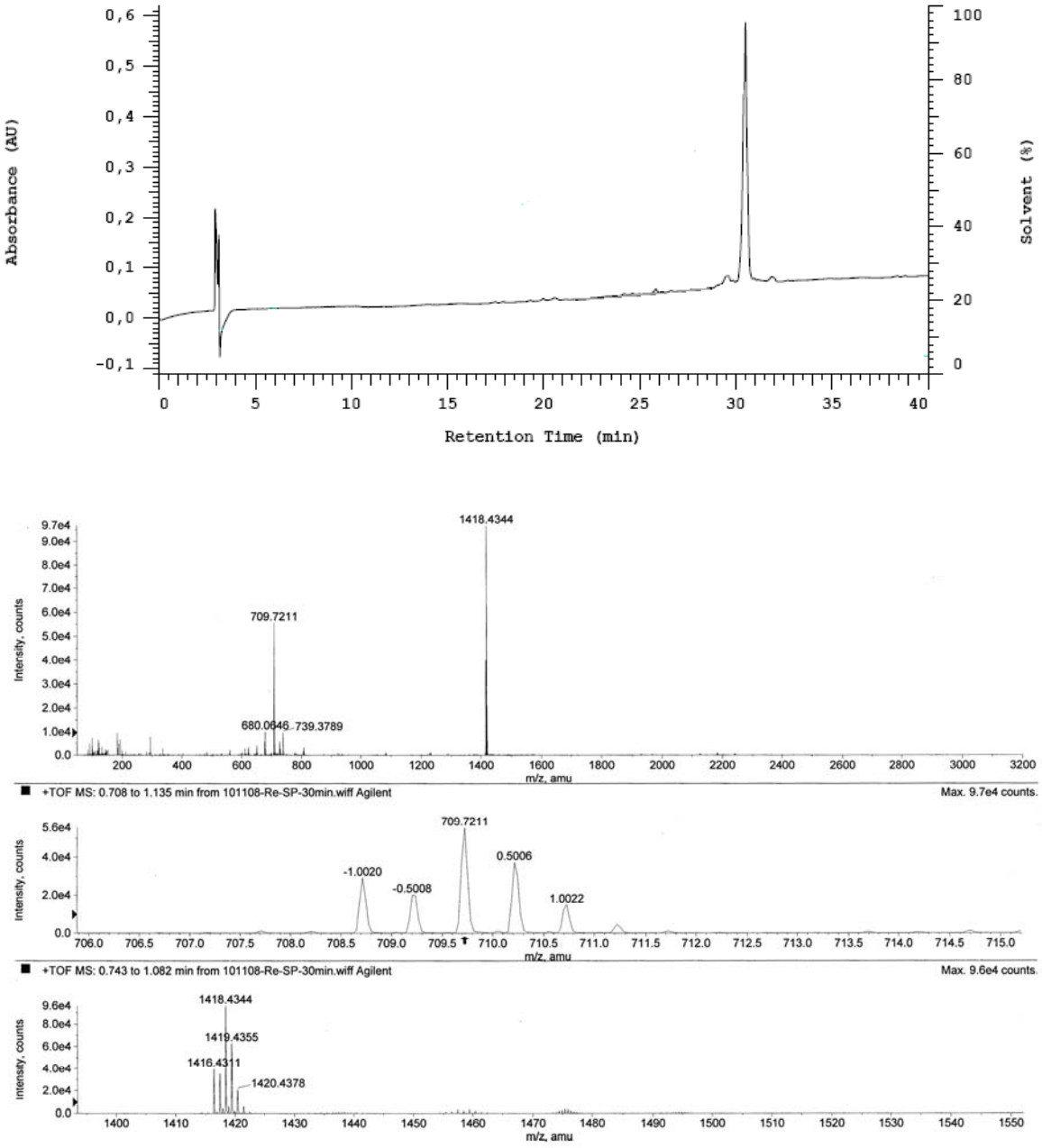

Fig. 3.19 The chromatogram (top) and mass spectrum (bottom) of $[Re(CO)_3(\kappa^3\text{-}HL^{51}H)]$-SP (**21**)

Accordingly, these studies prove that $H_2L^{51}COOH$ is a remarkable candidate for the formulation of new functionalized radiopharmaceuticals. However, it necessitates more chemical and biological studies to take an advantage of these novel ligand system and its complexes in nuclear medicine.

3.3. Summary and Conclusions

The 2-(benzylamino)phosphines $H_{2n}L^{5n}$ (n = 1 - 3) are very suitable compounds for the stabilization of rhenium and technetium metal ions in different oxidation states. The potentially pentadentate phosphine H_4L^{52} reacts with oxorhenium(V) complexes under formation of various compositions depending on the pH value of the reaction solution. Addition of a supporting base gives the oxorhenium(V) complex **13** while absence of a supporting base results in the formation of the remarkable oxo-free rhenium(V) complex **12**. The tripodal tris{2-(benzylamino)}phosphine H_6L^{53} reacts with $[ReOCl_4]^-$ to give a 1:1 complex with a completely wrapped metal ion in an almost quantitative yield, which is an unique example in coordination chemistry of rhenium.

Moreover, 2-(benzylamino)phosphines can be modified by the use of 3-amino-4-hydroxybenzoic acid, which gives a bifunctional ligand system. The bifunctional ligand $H_2L^{51}COOH$ reacts with $[M(CO)_3]^+$ (M = Re, ^{99m}Tc) under formation of complexes of the composition $[M(CO)_3(\kappa^3\text{-}HL^{51}COOH)]$ (M = Re ,**18**; ^{99m}Tc, **19**) in high yields. $[Re(CO)_3(\kappa^3\text{-}HL^{51}COOH)]$ could be successfully utilized for the labelling of small peptides (triglycine) as well as longer natural peptides such as the active site of Substance P under liquid- and solid-phase techniques.

3.4. References

[1 Palma, E.; Correia, G. D. J.; Domingos, A.; Santos, I.; Alberto, R.; Spies, H. *J. Organomet. Chem.,* **2004**, *689*, 4811.

[2] Enny, P. D.; Green, J. L.; Engelbrecht, H. P.; Barnes, C. L.; Jurisson, S. S. *Inorg. Chem.*, **2005**, *44*, 2381.

[3] Stoop, R. M.; Bachmann, S.; Valentini, M.; Mezzetti, A. *Organometallics*, **2000**, *19*, 4117.

[4] Basak, S.; Rajak, K. K. *Inorg. Chem.*, **2008**, *47*, 8813.

[5] Nguyen, H. H.; Abram, U. *Z. Anorg. Allg. Chem.*, **2008**, *634*, 1560.

[6] Oudreau, R. J.; Mertz, J. E. *Nucl. Med. Biol.*, **1997**, *24*, 395.

[7] Luo, H.; Setyawati, I.; Rettig, S. J.; Orvig, C. *Inorg. Chem.*, **1995**, *34*, 2287.

[8] Archer, C. M.; Dilworth, J. R.; Thompson, R. M.; McPartlin, M.; Povey, D. C.; Kelly, J. D. *J. Chem. Soc., Dalton Trans.,* **1993**, 461.

[9] Mikolajczyk, M. *Pure Appl. Chem.*, 1987, *59*, 983.

[10] Braband, H.; Abram, U. *Inorg. Chem.,* **2006**, *45*, 6589.

[11] Bayly, S. R.; Cowley, A. R.; Dilworth, J. R.; Ward, C. V. *J. Chem. Soc., Dalton Trans.*, **2008**, *16*, 2190.

[12] Bandoli, G.; Mazzi, U.; Clemente, D. A.; Roncari, E. *J. Chem. Soc., Dalton Trans.*, **1982**, 2455.

[13] Kluge, R.; Schulz, M.; Liebsch, S. *Tetrahedron,* **1996**, *52*, 2957.

[14] Kluge, R.; Schulz, M.; Liebsch, S. *Tetrahedron*, **1996**, *52*, 5773.

[15] Abrahams, A.; Gerber, T. I. A.; Luzipo, D. R.; Mayer, P. *J. Coord. Chem.*, **2007**, *60*, 2215.

[16] Al-Shihri, A. S. M.; Dilworth, J. R.; Howe, S. D.; Silver, J.; Thompson, R. M. *Polyhedron*, **1993**, *12*, 2297.

[17] Gardner, J. K.; Pariyadath, N.; Corbin, J. L.; Stiefel, E. I. *Inorg. Chem.,* **1978**, *17*, 897.

[18] Gerber, T. I. A.; Luzipo, D.; Mayer, P. *J. Coord. Chem.*, **2004**, *57*, 1393.

[19] Bandoli, G.; Dolmella, A.; Gerber, T. I. A.; Perils, J.; Preez, J. G. H. *Inorg. Chim. Acta*, **2000**, *303*, 24.

[20] Basak, S.; Rajak, K. K. *Inorg. Chem.*, **2008**, *47*, 8813.

[21] Shriver. D. F.; Atkins, P. W. *Inorganic Chemistry*, Oxford University Press, **2001**.

[22] Xu, L.; Setyawati, I. A.; Pierreroy, J.; Pink, M.; Young, V. G., J.; Patrick, B. O.; Rettig, S. J.; Orvig, C. *Inorg. Chem.*, **2000**, *39*, 5958.

[23] Bolzati, C.; Porchia, M.; Bandoli, G.; Boschi, A.; Malago, E.; Uccelli, L. *Inorg. Chim. Acta*, **2001**, *315*, 205.

[24] a) Machkour, A.; Mandon, D.; Lachkar, M.; Welter, R. *Eur. J. Inorg. Chem.* **2005**, 1, 158.; b) Zhu, B; Angelici, R. J. *Chem. Commun.*, **2007**, *21*, 2157.

[25] Stadtman, E. R.; *Science*, **1992**, *257*, 1220.

[26] Alberto, R.; Schibli, R.; Egli, A.; Schubiger, A. P.; Abram, U.; Kaden, T. A. *J. Amer.*

Chem. Soc., **1998**, *120*, 7987.

[27] Deutsch, E. *Radiochim. Acta*, **1993**, *63*, 195.

[28] Kniess, T.; Correia, J. D. G.; Domingos, A.; Palma, E.; Santos, I. *Inorg.Chem.*, **2003**, *42*, 6130.

[29] Alberto, R.; Ortner, K.; Wheatley, N.; Schibli, R.; Schubiger, A. P. *J. Am. Chem. Soc.*, **2001**, *123*, 3135.

[30] Waibel, R.; Alberto, R.; Willuda, J.; Finnern, R.; Schibli, R.; Stichelberger, P. A.; Egli, A.; Abram, U.; Mach, J. P.; Plueckthun, A.; Schubiger, P. A. *Nature Biotechnol.,* **1999***, 17*, 897.

[31] Alberto, R.; Schibli, R.; Abram, U.; Johannsen, B.; Pietzsch, H. J.; Schubiger, P. A. *J. Am. Chem. Soc*., **1999**, *25*, 6076.

[32] Hoepping, A.; Reisgys, M.; Brust, P.; Seifert, S.; Spies, H.; Alberto, R.; Johannsen, B. *J. Med. Chem.*, **1998**, *41*, 4429.

[33] Alberto, R.; Schibli, R.; Waibel, R.; Abram, U.; Schubiger, P. A. *Coord. Chem. Re*v., **1999**, *190*, 901.

[34] Schibli, R.; Katti, K. V.; Higginbotham, C.; Volkert, W. A.; Alberto, R. *Nucl. Med. Biol.,* **1999**, *26,* 711.

[35] Egli, A.; Alberto, R.; Tannahill, L.; Schibli, R.; Abram, U.; Schaffland, A.; Waibel, R.; Tourwe, D.; Jeannin, L.; Iterbeke, K.; Schubiger, P. A. *J. Nucl. Med*., **1999**, *40*, 1913.

[36] Merrifield, R. B. *J. Am. Chem. Soc.*, **1963**, *85*, 2149.

Chapter 4

2-(Aminophenyl)phosphines and their reactions with rhenium and technetium complexes

---

4.1 Synthesis of the potentially multidentate ligands derived from 2-(aminophenyl) phosphines

4.1.1 Synthesis of 2-(aminophenyl)phosphines

Phosphines bearing 2-aminophenyl moieties are versatile compounds in the coordination chemistry of transition metals. They can be applied directly as chelating ligands [1] or modified under formation of hemilabile polydentate ligands [2,3]. Despite their potential in coordination chemistry, applications of 2-(aminophenyl)phosphines are restricted by the fact, that they must be synthesized by complicated multistage synthetic procedures. The pathways given by Cooper *et al.* [4] and Stelzer *et al.* [5] are still applied for the synthesis of compounds of the composition $Ph_{3-n}P(2\text{-}C_6H_4NH_2)_n$ (n = 1, 2, 3).

(*tert*-Butoxycarbonylamino)benzene (**XII**) was synthesized according to a standard procedure [6] and isolated as a colorless crystalline solid. **XII** reacts with 2 equivalents of *tert*-BuLi under formation of the dilithium salt (**XIIa**) [7]. In this case, ortho-metallation is favoured due to the formation of a six-membered ring system. The dilithium salt **XIIa** reacts with the related chlorophosphines $Ph_{(3-n)}PCl_n$ (n = 1, 2, 3) under formation of the (*N*-BOC-2-aminophenyl)phosphines (**XIII-XV**) in moderate yields, Scheme 4.1.

The $^{31}P\text{-}\{^1H\}$ NMR spectra of (*N*-BOC-2-aminophenyl)phosphines present single resonances at −23.3 ppm for **XIII**, −35.5 ppm for **XIV**, −44.6 ppm for **XV**. The presence of the protecting group (BOC) is confirmed by ^1H NMR spectroscopy. The ^1H NMR spectra of **XII – XV** show single resonances of the methyl group at 1.4 ppm with the expected integrations.

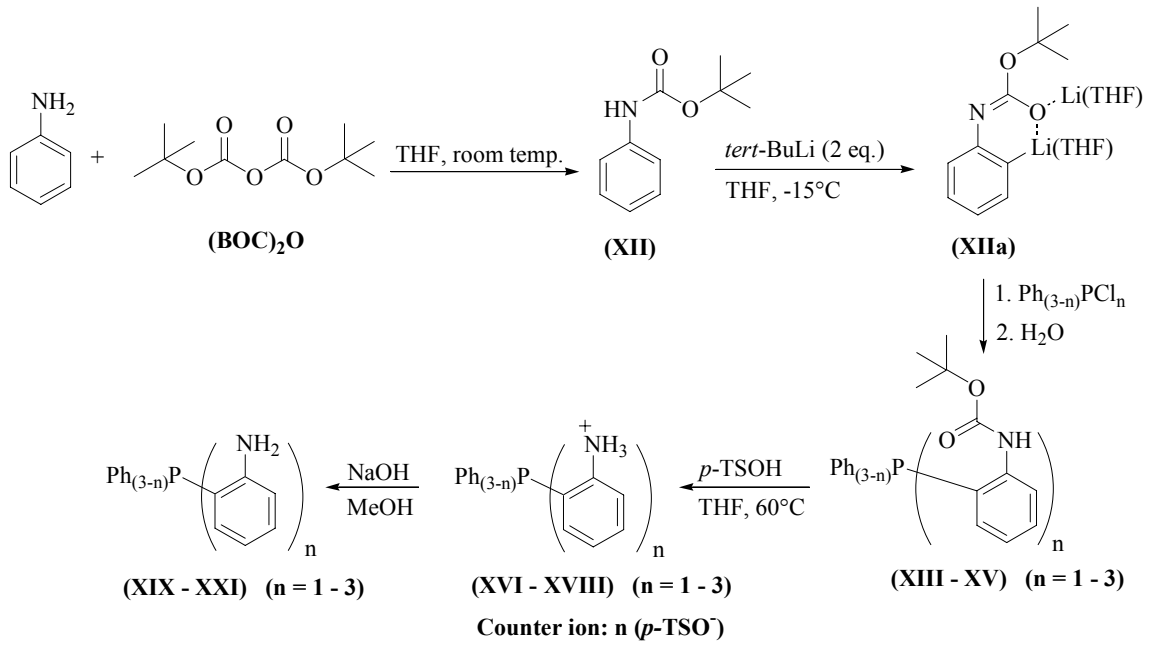

Scheme 4.1 Synthetic pathway for the preparation of 2-(aminophenyl)phosphines (**XIX - XXI**)

The compounds **XIII - XV** were treated by 2n equivalents (n = 1 - 3) of *p*-toluenesulfonic acid [8] in order to obtain the related ammonium salts **XVI - XVIII**. The salts were neutralized by equimolar amounts of NaOH in MeOH, which gives 2-(aminophenyl) phosphines (**XIX - XXI**) as colourless solids.

The ^{31}P-{^{1}H} NMR spectra of the compounds **XIX - XXI** exhibit single resonances of the phosphines at −21.0 ppm for **XIX**, −33.5 ppm for **XX** and −41.2 ppm for **XXI**. The absence of the methyl resonances at about 1.3 ppm in ^{1}H NMR spectra of **XIX - XXI** confirms the supposed molecular structure of the 2-(aminophenyl)phosphines. The molecular ion peaks of all three compounds **XXI - XXI** were detected in their mass spectra.

4.1.2 Synthesis of the potentially tri-, penta-, and heptadentate ligands derived from 2-(aminophenyl)phosphine

2-(Aminophenyl)phosphines are suitable starting materials for the synthesis of different ligand systems such as imines, amines and amids [9-10]. The hitherto known ligands are limited to the derivatives of (2-aminophenyl)diphenylphosphine $Ph_2P(2\text{-}C_6H_4NH_2)$ (**XIX**). In this work, syntheses and characterizations of the polydentate ligands derived from all three 2-(aminophenyl)phosphines (**XIX - XXI**) and salicylaldehyde are reported.

2-(Aminophenyl)phosphines (**XIX - XXI**) react with n equivalents (n = 1 - 3) of salicylaldehyde under formation of 2-(phenylimino)phosphines ($H_nL^{7n}P$). In order to achieve

a higher yield, the imine condensation reaction was catalyzed by the addition of one drop of formic acid [11] to the reaction mixture, Scheme 4.2.

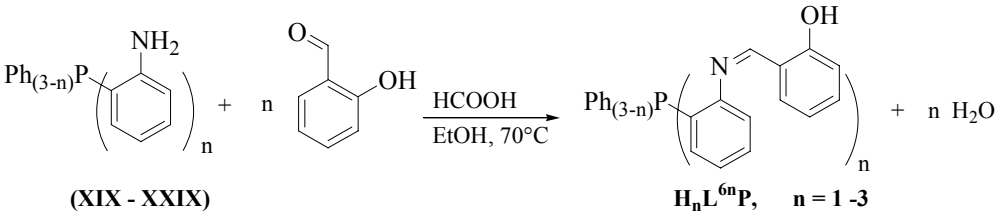

(XIX - XXIX) **$H_nL^{6n}P$, n = 1 -3**

Scheme 4.2 Synthesis of the substituted 2-(phenylimino)phosphines $H_nL^{7n}P$, n = 1 - 3

The 2-(phenylimino)phosphines $H_nL^{6n}P$ (n = 1 - 3) were isolated as pale yellow solids. The ^{31}P-{^1H} NMR spectra of $H_nL^{6n}P$ (n = 1 - 3) present single resonances at −15.4 ppm for $HL^{61}P$, −26.8 ppm for $H_2L^{62}P$ and −32.8 ppm for $H_3L^{63}P$. The ^1H NMR spectra present singlets of the imine groups at 8.5 ppm. The IR spectra of $H_nL^{6n}P$ (n = 1 - 3) exhibit the stretching vibrations of the imine functions at 1658 cm^{-1}. ESI(TOF) mass spectra of the all three 2-(phenylimino)phosphines $H_nL^{6n}P$ (n = 1 - 3) support the supposed molecular structures by the molecular ion peaks as the base peak. The elemental analyses are consistent with the molecular formulae of 2-(phenylimino)phosphines.

The resulting 2-(phenylimino)phosphines $H_nL^{6n}P$ (n = 1 - 3) were reduced to increase the stability and flexibility of the ligand systems as was discussed in Chapter 3. They react with excess amounts of $NaBH_4$ in boiling EtOH under formation of the potentially multidentate [P,N,O] phosphines $H_{2n}L^{6n}$ (n = 1 - 3), Scheme 4.3.

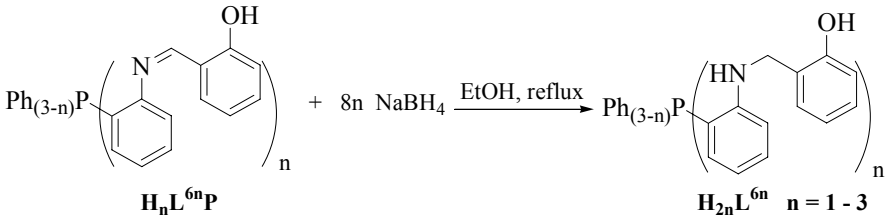

$H_nL^{6n}P$ **$H_{2n}L^{6n}$ n = 1 - 3**

Scheme 4.3 Synthesis of the 2-(aminophenyl)phosphines $H_{2n}L^{6n}$ (n = 1 - 3)

The compounds $H_{2n}L^{6n}$ (n = 1 - 3) were obtained as colourless solids in high yields. The ^{31}P-{^1H} NMR spectra of $H_{2n}L^{6n}$ (n = 1 - 3) show the phosphines signals at lower chemical shift values compared to the related 2-(phenylimino)phosphine $H_nL^{6n}P$ (n = 1 - 3). Moreover, by increasing the number of substituted phenyl rings the phosphorus resonance shifts to the higher field values −22.3 ppm for H_2L^{61}, −37.4 ppm for $H_2L^{62}P$, −55.9 ppm for $H_3L^{63}P$. This can be explained by an increasing steric hindrance about the phosphorus atom with the addition of each *ortho*-substituted phenyl group [12]. The ^1H NMR spectra confirm the reduction of the imine groups by the absence of imine signals at about 8.5 ppm and the

presence of methylene signals at 4.3 ppm. The NH signals appear as not well resolved multiplets at 5.5 ppm in the ^{1}H NMR spectra of the 2-(aminophenyl)phosphines $H_{2n}L^{6n}$ (n = 1 - 3). The IR spectra of the compounds present medium intense absorptions in the range of 3100 to 3450 cm^{-1}, which are assigned to the NH and OH vibrations. The molecular ion peaks were detected in the mass spectra at m/z = 384.1 for $[H_2L^{61}]^+$, 505.5 for $[H_4L^{62}]^+$, 616.9 for $[H_6L^{73}]^+$.

All the synthesized ligands were dried under reduced pressure for 1 day before they were used in any complex formation reactions.

4.2 Reactions of 2-(aminophenyl)phosphines $H_{2n}L^{6n}$ with oxorhenium(V) and oxotechnetium(V) complexes

4.2.1 Reactions of H_2L^{61}

Reaction patterns between phosphine-containing ligands and oxorhenium(V) and oxotechnetium(V) complexes highly depend on the chelate formation potential of the ligand applied. Monodentate phosphines such as PPh_3, Me_2PhP react with oxotechnetium(V) compounds under oxygen abstraction and consequently reduction of the metal atom [13]. Similar reactions with oxorhenium(V) are possible by prolonged heating of the reaction mixtures [14]. The size of the chelate rings in multidentate phosphine-containing ligands play a key role in the reaction of oxotechnetium(V) complexes with such ligands. Formation of six-membered chelate rings is kinetically not favoured. Therefore, the competing reaction (oxygen abstraction) will happen first, which was observed in the case of the 2-(benzylamino)phosphine (Chapter 3). In contrast, formation of a five-membered chelate ring is kinetically preferred with respect to oxygen abstraction at room temperature. $[TcO(OMe)(PN)_2]$ (PN = $Ph_2P(o\text{-}C_6H_4NH_2)$) [15] is a remarkable example of oxotechnetium(V) complexes with heterofunctionalized phosphines.

$(NBu_4)[MOCl_4]$ (M = Re, Tc) react with H_2L^{61} in MeOH at ambient temperature under formation of the isotypic complexes $[MOCl_2(HL^{61})]$ (M = Re (**22**), Tc (**23**)). Heating of the reaction mixture of H_2L^{61} and $(NBu_4)[TcOCl_4]$ leads to a dramatic increase of the phosphine oxide signal at 28.6 ppm in the $^{31}P-\{^1H\}$ NMR spectrum of the reaction mixture, which was not observed in the case of the rhenium reaction. The products were isolated as green solids, which were soluble in CH_2Cl_2 or $CHCl_3$. Recrystallization of the products from a mixture of CH_2Cl_2/MeOH (for the Re complex (**22**)) and CH_2Cl_2/Me_2CO (for the Tc complex (**23**)) gave green X-ray quality crystals of $[MOCl_2(HL^{61})]$ (M = Re (**22**), Tc (**23**)), Scheme 4.4.

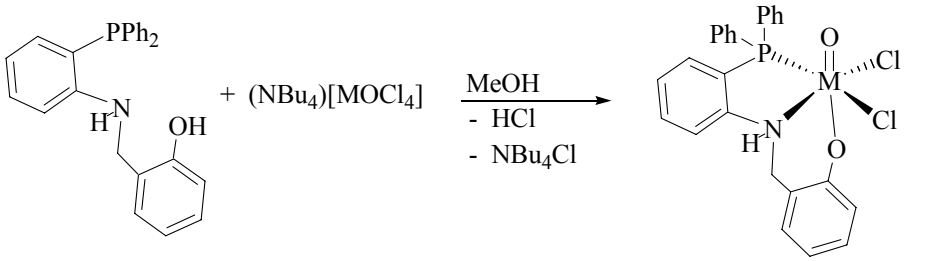

H_2L^{61} **M = Re (22), Tc (23)**

Scheme 4.4 Synthesis of the isotypic complexes $[MOCl_2(HL^{61})]$ (M = Re (**22**), Tc (**23**))

Fig. 4.2 presents the molecular structure of $[ReOCl_2(HL^{61})]$ (**22**) and selected bond lengths and angles are summarized in Table 4.1. The rhenium atom has adopted a distorted octahedral coordination sphere. The Re-O(10) bond length of 1.694(4) Å and the Re-Cl(2) bond of 2.263(1) Å confirm the distortion of the octahedron about the rhenium atom. The amine component N-H(1) makes an intermolecular hydrogen bond with Cl(1) in the adjacent molecule generated by the symmetry operation (-x+1,-y+2,-z). The bond lengths N-C(6) of 1.483(5) Å and N-C(17) of 1.511(6) Å are in the range of the C-N single bonds. The Re-N-C(6) and C(17)-N-C(6) angles of 116.0(3)° and 111.5(3)° confirm a tetrahedral geometry about the N atom. The longer Re-Cl(1) bond of 2.437(1) Å compared to Re-Cl(2) of 2.363(1) Å is explained by a higher *trans* influence of the phosphine ligand compared with Cl(2). The Re-N bond length of 2.198(4) Å is near the higher limit of the Re-N single bond range (1.90 – 2.20 Å) [16].

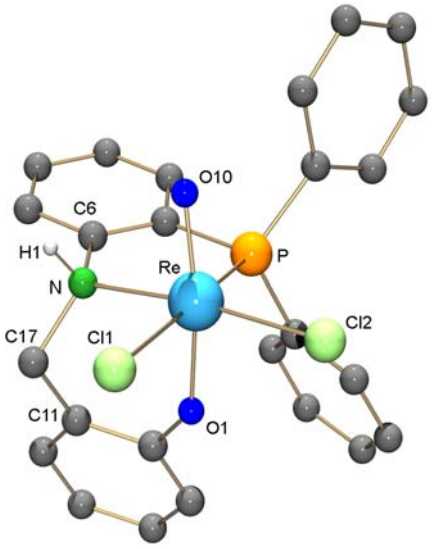

Fig. 4.2 Molecular structure of [$ReOCl_2(HL^{61})$] (**22**). The hydrogen atoms bonded to carbon atoms were omitted for clarity.

Table 4.1 Selected bond lengths (Å) and angles (°) of *fac*-[$ReOCl_2(HL^{61})$] (**22**)

Bond lengths [Å]:					
Re-O(10)	1.694(4)	Re-O(1)	1.927(3)	Re-N	2.198(4)
Re-P	2.409(1)	Re-Cl(1)	2.437(1)	Re-Cl(2)	2.363(1)
C(6)-N	1.483(5)	N-C(17)	1.511(6)		
Angles [°]:					
O(10)-Re-O(1)	166.0(1)	Cl(1)-Re-N	90.2(1)	P-Re-Cl(2)	98.76(4)
Re-N-C(6)	116.0(3)	C(17)-N-C(6)	111.5(3)		
Hydrogen bond:					
D-H...A	d(D-H)	d(H...A)	d(D...A)	<(DHA)	
N-H(1)...Cl(1)[a]#1	0.91	2.44	3.282(4)	154.7	

a) Symmetry transformations used to generate equivalent atoms: #1 -x+1,-y+2,-z

fac-[$TcOCl_2(HL^{61})$] (**23**) presents a similar molecular structure. Fig. 4.3 shows the molecular structure of this compound. It is a neutral oxotechnetium(V) complex, where the uninegative tridentate 2-(aminophenyl)phosphine ligand $(HL^{61})^-$ coordinates facially. The terminal oxo ligand together with two chloro ligands, complete the coordination sphere. Table 4.2 presents selected bond lengths and angles of **23**. The Tc-O(10) distance of 1.649(6) Å is slightly shorter than that of the rhenium analogue **22** and the Tc-O(1) bond length of 1.933(6) Å is longer than the Re-O(1) of 1.927(3) Å in **22**. The P-Tc-N angle of 81.9(2)° is bigger than the bite angle of the similar bidentate ligand 2-aminophenol [17], which results from the bigger atomic radius of the phosphorus atom compared to that of the oxygen atom. The amine group N-H(1) establishes an intermolecular hydrogen bond with the oxygen atom of the co-crystallized solvent acetone O(2).

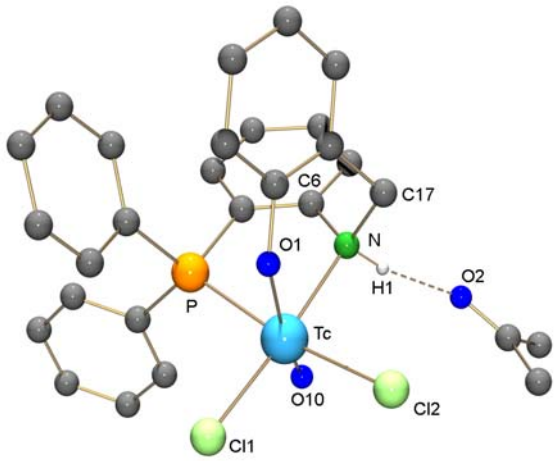

Fig. 4.3 Molecular structure of $[TcOCl_2(HL^{61})]\cdot Me_2CO$ (**23**). Hydrogen atoms bonded to carbon atoms were omitted for clarity.

Table 4.2 Selected bond lengths (Å) and angles (°) of *fac*-$[TcOCl_2(HL^{61})].Me_2CO$ (**23**)

Bond lengths [Å]:					
Tc-O(10)	1.649(6)	Tc-O(1)	1.933(6)	Tc-N	2.208(7)
Tc-P	2.410(2)	Tc-Cl(1)	2.357(3)	Tc-Cl(2)	2.436(2)
C(6)-N	1.48(1)	N-C(17)	1.51(1)		
Angles [°]:					
O(10)-Tc-O(1)	163.8(3)	O(1)-Tc-N	82.0(2)	P-Tc-O(1)	84.0(2)
P-Tc-N	81.9(2)	Tc-N-C(6)	116.1(5)	C(17)-N-C(6)	111.7(7)
Hydrogen bond:					
D-H...A	d(D-H)	d(H...A)	d(D...A)	<(DHA)	
N-H(1)...O(2)	0.91	1.99	2.89(1)	167.9	

The $^{31}P-\{^1H\}$ NMR spectra of **22** and **23** present single resonances of the coordinated phosphines at 2.5 and 2.7 ppm. The chemical shift values are higher than that of the uncoordinated H_2L^{61}. The ^1H NMR spectra of both complexes show doublets at 4.4 and 5.5 ppm with a coupling constant of 14.4 Hz, which is consistent with a (*HH*) geminal coupling. This implies the formation of the chelate ring, which hinders free rotation of the methylene group and results in two nonequivalent hydrogen atoms. The IR spectra of **22** and **23** confirm the presence of NH groups by medium absorption at 3109 cm^{-1} for **22** and 3111 cm^{-1} for **23**. The mass spectrum of $[ReOCl_2(HL^{61})]$ shows a peak at *m/z* = 621 amu with the expected isotopic pattern for the $[M-Cl]^+$ fragment. The measured technetium content of **23** is 17.2%, which fits with the theoretical value of 17.4%.

4.2.2 Reactions of H_4L^{62}

The bis(2-aminophenyl)phenylphosphine can act as a bidentate [P,N] [18] or tridentate [P,N,N] [19] ligand. Moreoveor, it can be applied for the synthesis of ligand systems with higher denticity such as H_4L^{62}, which is the first pentadentate ligand derived from bis-{2-(aminophenyl)}phenylphosphine.

$(NBu_4)[MOCl_4]$ (M = Re, Tc) react with H_4L^{62} at ambient temperature in MeOH under formation of dark solids in good yields. The recrystallization of these solids from $MeOH/CH_2Cl_2$ mixtures gave red crystals of the composition $[MOCl(H_2L^{62})]$ (M = Re (**24**), Tc (**25**)), Scheme 4.5.

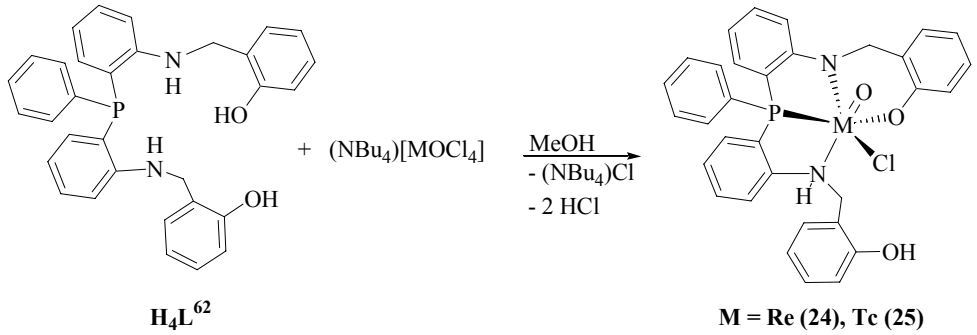

Scheme 4.5 Reaction of H_4L^{62} with $(NBu_4)[MOCl_4]$ (M = Re, Tc)

The molecular structure of **24** is presented in Fig. 4.4 and selected bond lengths and angles are given in Table 4.3. $[ReOCl(H_2L^{62})]$ (**22**) is a neutral oxorhenium(V) complex. The coordination sphere of the rhenium atom is a distorted octahedron. The Re-O(10) and Re-Cl bond lengths of 1.679(6) Å and 2.461(2) Å describe distortions of the polyhedron about the rhenium atom. The rhenium atom is located 0.328 Å above the mean least-squares plane defined by the atoms P, N(1), Cl and O(1). The Re-O(10) distance is in the range of the reported values for Re=O bonds [20]. The Re-N(2) bond length of 2.4286(6) Å is 0.4 Å longer than the rhenium-nitrogen bond in $[ReOCl\{Ph_2P(o\text{-}C_6H_4NH_2)\}_2]$ [21]. The rigid planar five-membered chelate ring formed by P, C(1), C(6), N(1), Re and the nearly ideal tetrahedral geometry around the phosphorus atom are suggested as the reasons of the lengthening of the Re-N(2) bond. The Re-N(1) and N(1)-C(6) bond lengths of 1.964(7) Å and 1.394(10) Å are slightly shorter than typical single bonds, which implies delocalization of the lone pair of N(1) between these atoms. The oxygen atom of the non-coordinated phenolic group O(2) establishes a weak hydrogen bond via H(2B) with the chloro ligand of an adjacent molecule generated by the symmetry element (-x+1,-y+2,-z).

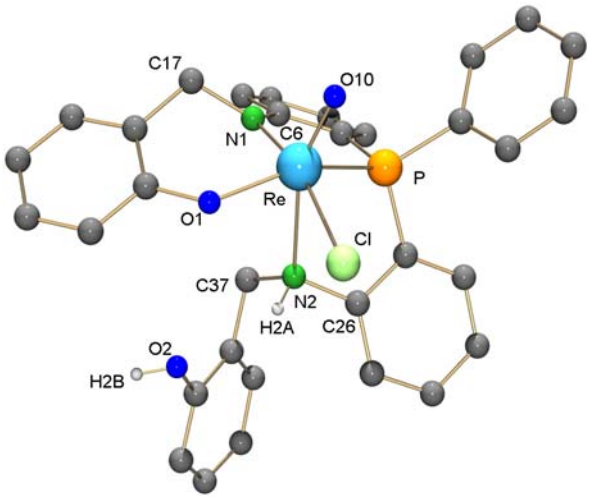

Fig. 4.4 Molecular structure of [ReOCl(H_2L^{62})] (**24**). Hydrogen atoms bonded to carbon atoms were omitted for clarity.

Table 4.3 Selected bond lengths (Å) and angles (°) of *fac*-[$ReOCl_2(H_2L^{62})$] (**24**)

Bond lengths [Å]:					
Re-O(10)	1.679(6)	Re-O(1)	1.976(6)	Re-N(1)	1.964(7)
Re-N(2)	2.428(6)	Re-Cl	2.461(2)	C(6)-N(1)	1.39(1)
C(17)-N(1)	1.47(1)	C(26)-N(2)	1.44(1)	C(37)-N(2)	1.51(1)
Angles [°]:					
O(10)-Re-N(1)	101.7(3)	O(10)-Re-O(1)	116.0(3)	O(10)-Re-N(2)	158.4(3)
O(1)-Re-N(2)	81.3(2)	O(1)-Re-Cl	81.6(2)	C(6)-N(1)-C(17)	120.8(7)
C(6)-N(1)-Re	123.3(5)	C(26)-N(2)-C(37)	111.9(6)	C(26)-N(2)-Re	113.4(5)

Hydrogen bond:

D-H...A	d(D-H)	d(H...A)	d(D...A)	<(DHA)
O(2)-H(2B)...Cl#1[a]	0.82	2.40	3.217(7)	173.6

a) Symmetry transformations used to generate equivalent atoms: #1 -x+1,-y+2,-z

The ^{31}P-{^1H} NMR spectrum of **24** shows the single resonance of the coordinated phosphine at a chemical shift of 13.3 ppm. The observed coupling pattern in the ^1H NMR spectrum of **24** is consistent with its molecular structure. The multiplet signal at 4.5 ppm with the integration of two hydrogen atoms is associated with H_2C-N(2), where the uncoordinated phenolic group allows free rotation around the C-N bond and consequently causes magnetically equivalent hydrogen atoms of the methylene group. The two doublet resonances at 5.1 and 5.3 ppm with the typical *HH* geminal coupling constant of 15 Hz are assigned to the H_2C-N(1) methylene hydrogen atoms. Coordination of the hydroxyl group O(1) prevents the free rotation of the methylene component and results in two non-equivalent hydrogen atoms. Moreover, this splitting pattern with the geminal coupling constant confirms the deprotonation of N(1), where for the uncoordinated H_4L^{62} the methylene hydrogen atoms present a doublet with the

typical *HH* spin-spin coupling constant of 5.8 Hz (H_2C-NH). The hydroxyl proton H(2B) shows a single resonance at 10.9 ppm, where the signal moves to the lower field compared to the uncoordinated ligand. The proton of N(2) appears as a broad signal at 8.4 ppm. The IR spectrum presents a broad band at 3367 cm^{-1} and a weak absorption at 3236 cm^{-1} due to the OH and NH stretching vibrations. The broadening of the OH absorption band at 3367 cm^{-1} is due to the hydrogen bond. The Re=O stretching vibration appears at 960 cm^{-1} as a medium band.

All attempts to isolate crystals of [TcOCl(H_2L^{62})] (**25**) suitable for X-ray analysis failed. However, other analytical methods are consistent with the supposed molecular structure. The ^{31}P-{^1H} NMR spectrum shows the signal of the coordinated phosphorus atom at 12.6 ppm. The ^1H NMR spectrum has a similar pattern as observed for [ReOCl(H_2L^{72})] (**24**). The resonances of the methylene groups appear as one doublet at 4.8 ppm with the spin-spin coupling constant of J_{HH} = 4.8 Hz and two doublets at 5.6 and 5.7 ppm. The proton of the free hydroxyl function exhibits a single resonance at 10.6 ppm. The triplet at 9.1 ppm is assigned to the NH group. The IR spectrum confirms the presence of the terminal oxo ligand by a medium absorption at 964 cm^{-1}, which is indicative for the Tc=O stretching vibration [22]. The technetium content, after drying the compound under reduced pressure for 2 days, is 13.1%, which is consistent with the theoretical technetium value of 12.8%.

Attempts to replace the remaining chloro ligand of **24** by the free hydroxyl group of the ligand failed. Although the reaction between H_4L^{62} and (NBu_4)[$ReOCl_4$] was repeated under prolonged heating, the same product **24** was finally isolated. Addition of the supporting base NEt_3 to the reaction mixture in MeOH or stirring a solution of **24** and the supporting base NEt_3 a mixture of CH_2Cl_2/MeOH resulted in precipitation of a dark solid. The ^{31}P-{^1H} NMR spectrum of this compound shows a singlet at +4.5 ppm, which is associated with a coordinated phosphine. The ^1H NMR spectrum of the product exhibits a single resonance at 3.4 ppm (3H), which suggests the presence of a methoxo ligand. The medium intense absorption at 3273 cm^{-1} in the IR spectrum confirms a free hydroxyl group. Since the phosphorus atom of H_4L^{62} admits a tetrahedral environment, coordination of the ligand via the [P,N,N] donor as the *fac*-[ReO(H_2L^{62})] isomer is preferred, as was observed for other heterofunctionalized [P,O/S] phosphines [23]. Thus, it is supposed that the methoxo anion coordinated *cis* to the terminal oxo ligand, which is a rare type of coordination for a methoxo ligand in oxorhenium(V) coordination chemistry [24].

Heating of a [ReOCl(H_2L^{62})] (**24**) solution in CH_2Cl_2 and the addition of NEt_3 resulted in the precipitation of a dark solid, which was not soluble in any organic solvents or water. This can

be explained by the formation of a polymeric complex due to an exchange reaction of the free hydroxyl group with the chloro anion of the neighbouring complex, Scheme 4.6.

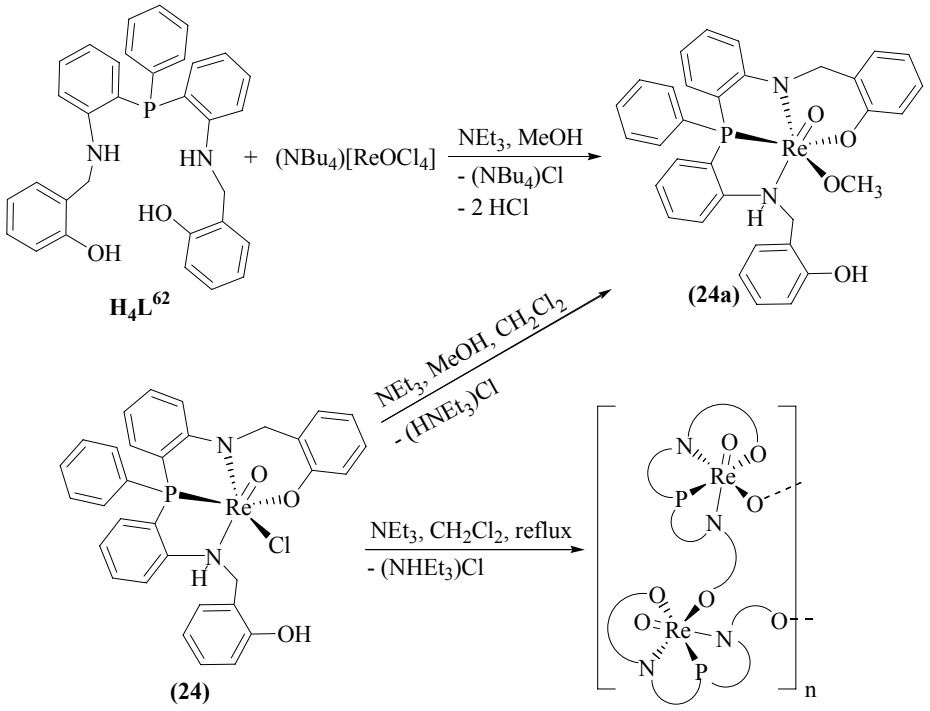

Scheme 4.6 The reactions between H_4L^{62} and $(NBu_4)[ReOCl_4]$ in the presence of a supporting base.

The reaction between $(NBu_4)[TcOCl_4]$ and H_4L^{62} in the presence of the supporting base NEt_3 led to the formation of a dark solid, which was not soluble in any organic solvent and water.

4.2.3 Reactions of H_6L^{63}

Tripodal ligand systems such as $N(C_6H_4NH_2)_3$ have been widely employed in many areas of inorganic chemistry [25]. The derivatives of these amines can form unusual arrangements around the metal ions [26].

Despite the fact that the tris(2-aminophenyl)phosphines are known since 1965 [27], less is known about the coordination chemistry of this class of compounds.Tris(2-aminophenyl)phosphine $P(2\text{-}C_6H_4NH_2)_3$ reacts with metal ions such as Co^{2+} and Ni^{2+} under formation of complexes of the composition $[MBr_2(L)]$ (L = $P(2\text{-}C_6H_4NMe_2)_3$ [27], Fig. 4.5.

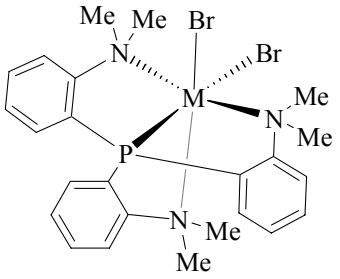

M = Co, Ni

Fig. 4.5 Complexes of the phosphine $P(2\text{-}C_6H_4NMe_2)_3$ with Co and Ni

The novel, potentially heptadentate ligand H_6L^{63} reacts with $(NBu_4)[ReOCl_4]$ in CH_2Cl_2 at ambient temperature. By slow evaporation of the solvent, orange blocks of $[ReOCl_2(H_5L^{73})]$ (**26**) were obtained, Scheme 4.7.

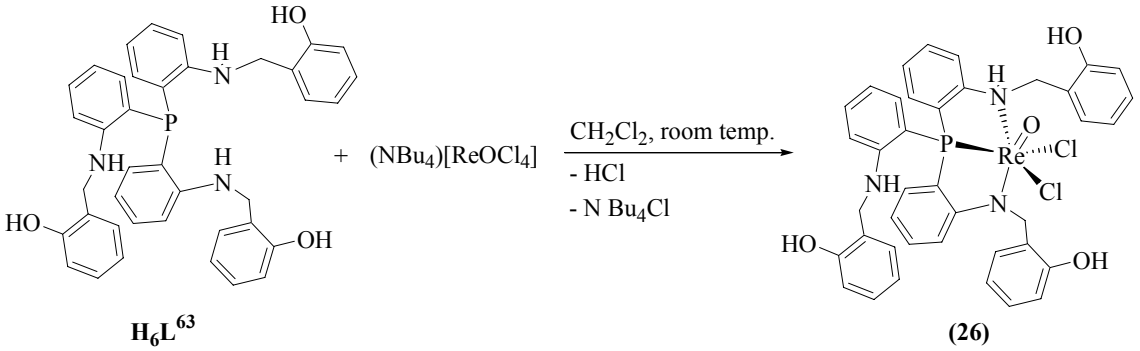

H_6L^{63} **(26)**

Scheme 4.7 Synthesis of $[ReOCl_2(H_5L^{63})]$ (**26**)

Fig 4.6 presents the molecular structure of **26** and Table 4.4 contains selected bond lengths and angles. $[ReOCl_2(H_5L^{63})]$ (**26**) is a neutral oxorhenium(V) complex. H_6L^{63} coordinates as a tridentate [P,N,N'] ligand and the rest of the coordination sphere is occupied by two chloro ligands and a terminal oxo ligand. The coordination environment about the rhenium atom is a distorted octahedron. The rhenium atom is located 0.309 Å above the equatorial plane fomed by the atoms P, Cl(1), Cl(2), N(1). The Re-O(10) distance of 1.635(7) Å is at the lower limit of the rhenium-oxygen double bond range (1.6 to 1.75 Å). The nitrogen atom N(1) is deprotonated and adopts a planar arrangement, which results from the weakly double bond characteristic between Re-N(1) with a bond length of 1.961(9) Å. The N(1)-C(2) distance of 1.44(2) Å and N(1)-C(17) of 1.47(1) Å are consistent with the bond characteristics, which denies a possible conjugation between N(1),C(2) and N(1),C(17). Moreover, the Re-Cl(1) distance of 2.471(3) Å is longer than the Re-Cl(2) of 2.374(3) Å, which implies partially double bond characteristic between Re-N(1). Another unusual feature of this structure is the planar arrangement around the non-coordinated nitrogen atom N(3). A comparison between the N(3)-C(46) bond length of 1.36(1) Å and that of N(3)-C(57) of 1.48(1) Å suggests that the

lone pair of N(3) is conjugated with the π-electrons of the adjacent phenyl ring. A strong hydrogen bond between H(3A) and Cl(1) with a distance of 2.54 Å is suggested as the driving force for the planarity about N(3). The oxygen atom of the uncoordinated hydroxyl group O(1) establishes an intermolecular hydrogen bond with Cl(3), the counter ion of co-crystallized $(NBu_4)^+$, generated by the symmetry element -x+2,-y+1,-z+1 (H(1)...Cl(3) of 2.26 Å). The hydrogen atoms at O(2) and O(3) establish hydrogen bonds with the neighboring chloro ligand Cl(3) generated by the symmetry elements -x+1,-y+1,-z+1 and -x+1,-y+2,-z+1 respectively.

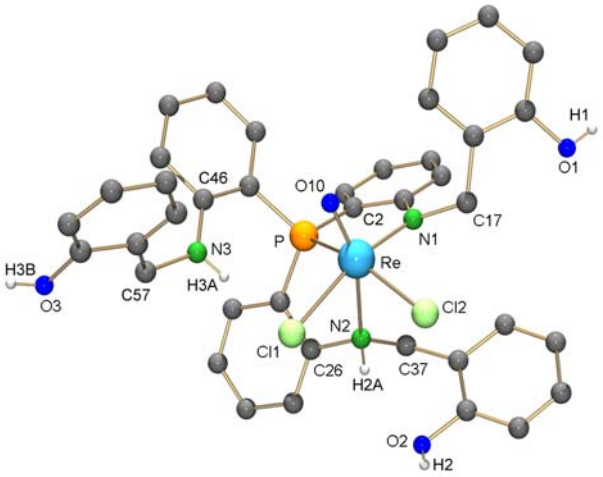

Fig. 4.6 The molecular structure of $[ReOCl_2(H_5L^{63})]$ (**26**). Hydrogen atoms bonded to the carbon atoms were omitted for clarity.

Table 4.4 Selected bond lengths (Å) and angles (°) of *fac*-$[ReOCl_2(H_5L^{63})]\cdot NBu_4Cl\cdot CH_2Cl_2$ (**26**)

Bond lengths [Å]:					
Re-O(10)	1.635(7)	Re-P	2.369(3)	Re-N(1)	1.961(9)
Re-N(2)	2.364(9)	Re-Cl(1)	2.471(3)	C(2)-N(1)	1.44(2)
N(1)-C(17)	1.47(1)	N(3)-C(46)	1.36(1)	N(3)-C(57)	1.48(1)
Angles [°]:					
O(10)-Re-N(1)	99.9(4)	O(10)-Re-P	92.0(3)	O(10)-Re-N(2)	160.4(3)
C(2)-N(1)-C(17)	114.0(1)	C(26)-N(2)-C(37)	1109.3(9))	C(46)-N(3)-C(57)	124.7(1)
Hydrogen bonds:					
D-H...A	d(D-H)	d(H...A)	d(D...A)	<(DHA)	
O(1)-H(1)...Cl(3)#1	0.82	2.26	3.073(9)	172.2	
O(2)-H(2)...Cl(3)#2	0.82	2.38	3.077(8)	143.8	
O(3)-H(3B)...Cl(3)#3	0.82	2.25	3.027(9)	159.1	
N(2)-H(2A)...O(2)	0.91	2.24	2.922(1)	131.6	
N(3)-H(3A)...Cl(1)	0.86	2.54	3.25(1)	140.6	

a) Symmetry transformations used to generate equivalent atoms: #1 -x+2,-y+1,-z+1 #2 -x+1,-y+1,-z+1 #3 -x+1,-y+2,-z+1

The ^{31}P-{^{1}H} NMR spectrum of **26** presents a single resonance at -10 ppm, which shows the expected higher chemical shift value than the uncoordinated H_6L^{63}. The ^{1}H NMR spectrum presents three sets of single resonances between 4.2 to 4.6 ppm. The co-crystallized tetrabutylammonium cation presents four multiplets in the range of the 1.3 to 3.4 ppm. The strong absorptions in the IR spectrum of **26** between 2900 and 3000 cm^{-1} are consistent with the stretching vibrations of the aliphatic CH groups of tetrabutylammonium chloride. The broadened bands from 3100 to 3450 cm^{-1} are related to the NH and OH stretching vibrations and the broadening originates from the hydrogen bonds. The medium absorption at 962 cm^{-1} confirms the presence of a terminal oxo ligand. The MS(ESI) spectrum supports the molecular structure by the base peak at *m/z* = 862.3 amu, which is assigned to the $[M\text{-}Cl]^+$ fragment.

The molecular structure of **26** shows a tridentate [P,N,N'] coordination mode of the ligand. A comparison between the molecular structures of **24** and **26** elucidates that the ligand first bite is via the formation of a [P,N] five-membered chelate ring and continues with the coordination of hydroxyl group. The molecular structure of **26** clarifies that the tetradentate [P,N,N',N"] coordination of H_6L^{63} is achieved by the rotation of the P-C(41) bond, which brings N(3) to the appropriate coordination position. The coordination of the nitrogen atom N(3) to rhenium requires the replacement of the terminal oxo ligand, which would go along with the reduction of the metal centre. This type of coordination was observed for the similar ligand system tris(2-mercaptophenyl)phosphine in $[Re(PS_3)(i\text{-}PrNC)]$ (PS = $P(2\text{-}C_6H_4SH)_3$) [29], wherein the metal centre carries no multiple bond to a donor atom (N/O) and the trigonal bipyramidal geometry about the metal atom allows the coordination of the fourth donor atom, Fig. 4.7.

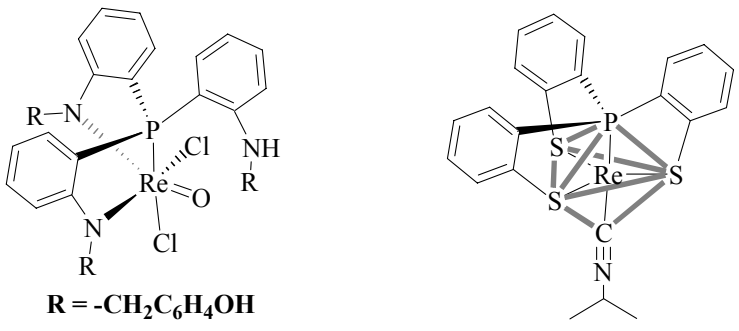

Fig. 4.7 Comparison between the molecular structures of **26** and $[Re(PS_3)(i\text{-}PrNC)]$

The reaction between $(NBu_4)[ReOCl_4]$ and H_6L^{73} in CH_2Cl_2 at ambient temperature results in the formation of the kinetically inert complex $[ReOCl_2(H_5L^{63})]$ (**26**). The reaction was repeated with heating the reaction mixture in EtOH in order to obtain the thermodynamically stable product. A brick-red precipitate was obtained directly from the reaction mixture.

Recrystallization of the product from CH_2Cl_2 gave orange plates of [ReOCl(H_4L^{63})] (**27**). Another pathway for the synthesis of **27** is to heat a solution of [$ReOCl_2(H_5L^{63})$] (**26**) in CH_2Cl_2. Slow evaporation of the solvent at room temperature gave red plates of **27**. Scheme 4.8 presents both synthetic pathways for the preparation of [ReOCl(H_4L^{63})] (**27**).

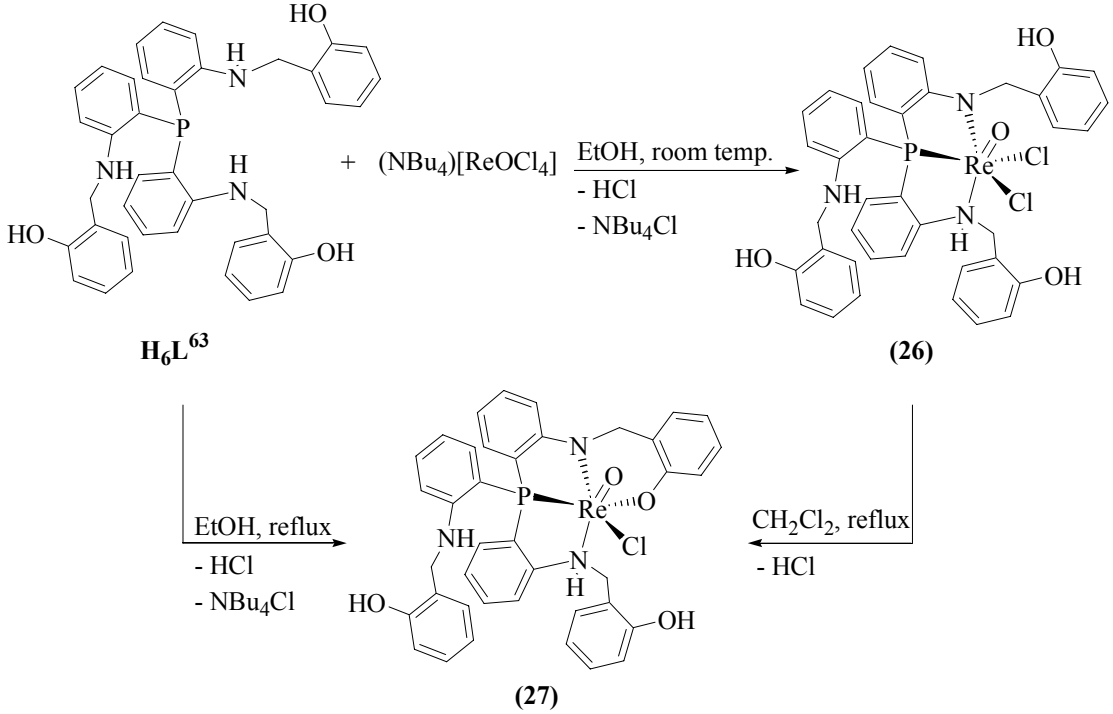

Scheme 4.8 Synthetic pathways of [ReOCl(H_4L^{63})] (**27**)

The exchange of the remaining chloro ligand by the uncoordinated hydroxyl group was attempted by heating a solution of **27** in toluene. However, the isolated product was lastly characterized as [ReOCl(H_4L^{63})] (**27**). Addition of a supporting base to a solution of **27** in CH_2Cl_2 resulted in the isolation of a dark solid, which was not soluble in any organic solvents or water.

The ^{31}P-{^1H} NMR spectrum of [ReOCl(H_4L^{63})] (**27**) shows a single resonance at −3.4 ppm. The observed low field shift compared to the uncoordinated ligand confirms the coordination of the phosphine. The ^1H NMR spectrum exhibits a doublet with a typical geminal coupling constant of 14 Hz at 4.7 ppm, which is related to the fully coordinated arm of H_6L^{63}. The two other methylene groups are characterized as poorly resolved doublet resonances at 4.2 and 4.4 ppm. The broad absorptions in the IR spectrum in the range of 3100 to 3450 cm^{-1} are assigned to the stretching vibrations of NH and OH groups, which were not characterized separately due to the broadness of the bands. The Re=O band was detected at 967 cm^{-1} as a medium intense absorption. The mass spectrum supports the molecular structure by a peak at

m/z = 826 amu, which is assigned to the $[M\text{-}Cl]^+$ fragment. The molecular structure of **27** is presented in Fig. 4.8. Table 4.5 shows selected bond lengths and bond angles of **27**.

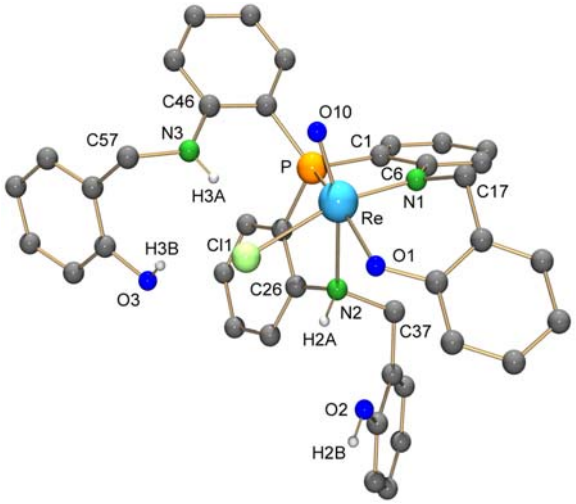

Fig. 4.8 Molecular structure of $[ReOCl(H_4L^{63})]$ (**27**). The hydrogen atoms bonded to carbon atom were omitted for clarity.

Table 4.5 Selected bond lengths (Å) and angles (°) of $[ReOCl(H_4L^{63})]$ (**27**)

Bond lengths [Å]:					
Re-O(10)	1.685(5)	Re-P	2.372(2)	Re-N(1)	1.956(6)
Re-N(2)	2.397(6)	Re-Cl(1)	2.470(2)	Re-O(1)	1.999(5)
C(6)-N(1)	1.40(1)	N(1)-C(17)	1.47(1)	N(3)-C(46)	1.37(1)
N(3)-C(57)	1.48(9)				
Angles [°]:					
O(10)-Re-N(1)	100.7(3)	O(10)-Re-P	91.8(2)	O(10)-Re-N(2)	159.8(2)
Cl(1)-Re-N(2)	77.6(1)	C(6)-N(1)-C(17)	119.9(6)	C(26)-N(2)-C(37)	111.0(6)
C(46)-N(3)-C(57)	124.7(6)				

Hydrogen bonds:				
D-H...A	d(D-H)	d(H...A)	d(D...A)	<(DHA)
O(2)-H(2B)...O(1)#1[a]	0.82	2.09	2.881(8)	161.5
O(3)-H(3B)...Cl(1)	0.82	2.67	3.404(7)	149.3

a) Symmetry transformations used to generate equivalent atoms: #1 -x+2,-y+2,-z+2

$[ReOCl(H_4L^{63})]$ (**27**) is a neutral oxorhenium(V) complex. The environment of the rhenium atom is strongly distorted octahedral. The aminophenylphosphine coordinates as a tetradentate dinegative ligand. The lengthening of the Re-N(2) bond of 2.397(6) Å compared to the Re-N(1) bond of 1.956(6) Å implies a stronger *trans* influence of the terminal oxo ligand O(10) than that of chloro Cl(1) and double bond characteristics of the Re-N(1) bond. C(46) is located 0.013 Å above the mean least-square plane containing C(44), C(45), N(3) and C(57). The planar environment of N(3) is caused by the conjugation of its lone pair with the π-

electrons of the adjacent phenyl ring. This is confirmed by the relatively short N(3)-C(46) distance of 1.37(1) Å. A hydrogen bond is found between O(3) and Cl(1) with the O(3)-H(3B)...Cl(1) distance of 3.404(7) Å.

H_6L^{73} reacts with $(NBu_4)[TcOCl_4]$ in EtOH at the ambient temperature under formation of a dark precipitate. This was recrystallized from $CHCl_3$ to obtain $[TcOCl(H_4L^{63})]$ (**28**) as red needles, Scheme 4.9.

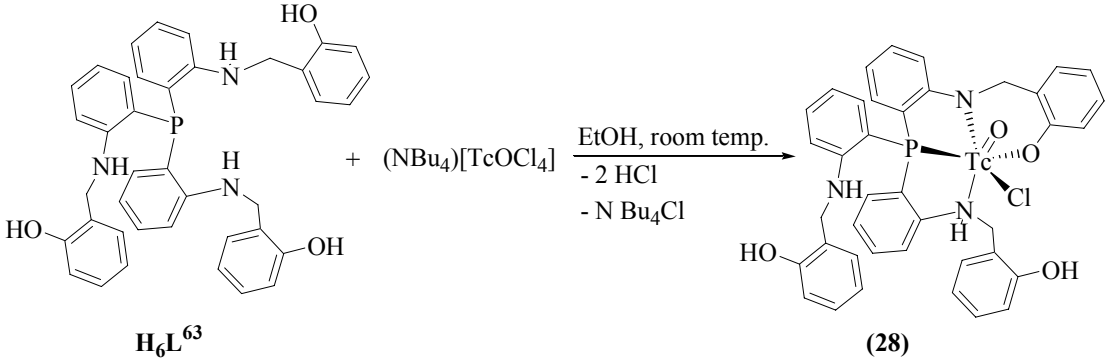

H_6L^{63} **(28)**

Scheme 4.9 The reaction of H_6L^{63} with $(NBu_4)[TcOCl_4]$

The molecular structure of (**28**) is presented in Fig 4.9 and selected bond lengths and angles are given in Table 4.6. $[TcOCl(H_4L^{63})]$ (**28**) is one of the rare examples of an oxotechnetium(V) complex with phosphine-containing ligands [30]. The donor atom arrangement about the technetium ion is a distorted octahedron. The shorter bond length of Tc-N(1) of 1.918(7) Å compared to the Tc-N(2) bond of 2.435(6) Å is consistent with the deprotonation of N(1). The planar environment about N(1) results from the delocalization of the N(1) lone pair between the d orbitals of the metal and the p orbitals of the nitrogen atom. The uncoordinated hydroxyl group establishes a hydrogen bond with O(1) in the adjacent molecule generated by the symmetry element (–x+1, -y+2, -z+1).

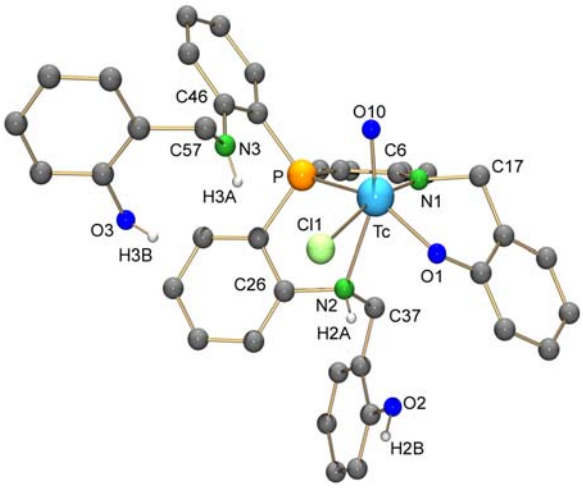

Fig. 4.9 Molecular structure of $[TcOCl(H_4L^{63})]$ (**28**). The hydrogen atoms bonded to carbon atoms were omitted for clarity.

Table 4.6 Selected bond lengths (Å) and angles (°) of [TcOCl(H_4L^{63})] (**28**)

Bond lengths [Å]:					
Tc-O(10)	1.641(6)	Tc-P	2.375(2)	Tc-N(1)	1.918(7)
Tc-N(2)	2.435(6)	Tc-Cl(1)	2.483(2)	Tc-O(1)	1.999(4)
C(6)-N(1)	1.42(1)	N(1)-C(17)	1.485(9)	N(3)-C(46)	1.387(9)
N(3)-C(57)	1.48(1)				
Angles [°]:					
O(10)-Tc-N(1)	101.4(3)	O(10)-Re-P	91.9(2)	O(10)-Tc-N(2)	158.5(2)
Cl(1)-Tc-N(2)	76.7(2)	C(6)-N(1)-C(17)	118.2(6)	C(26)-N(2)-C(37)	111.4(6)
C(46)-N(3)-C(57)	121.8(6)				
Hydrogen bond:					
D-H...A	d(D-H)	d(H...A)	d(D...A)	<(DHA)	
O(2)-H(2B)...O(1)[a]#1	0.82	2.31	3.128(8)	174.7	

a) Symmetry transformations used to generate equivalent atoms: #1 -x+1,-y+2,-z+1

The ^{31}P-{^{1}H} NMR spectrum of **28** shows a single resonance at –4.6 ppm. The low field shift of the phosphorus resonance compared to the uncoordinated H_6L^{63} is about 50 ppm. The ^{1}H NMR spectrum exhibits the resonances of the free hydroxyl groups at 9.5 and 9.9 ppm as two singlets. The signal of the methylene groups is split into six doublets, which appear in the range of 4.1 to 5.9 ppm. Two doublets show geminal coupling constants of 15 Hz and four others are not well resolved. The weak IR absorption at 945 cm^{-1} is related to the Tc=O stretching vibration. The broad band between 3100 and 3500 cm^{-1} belongs to the stretching vibrations of NH and OH groups and the broadening results from the hydrogen bonds. The technetium content of the compound after drying the crystals for 3 days under high vacuum was measured to be 12.6%, which is consistent with the theoretical value of 12.8%.

4.3 Summary and Conclusions

The multidentate phosphine-containing ligands derived from (2-aminophenyl)phosphines ($Ph_{3-n}P(2\text{-}C_6H_4NH_2)_n$; n = 1 - 3) are remarkable ligand systems for the synthesis of oxotechnetium(V) complexes. The compounds **23** and **28** are rare examples of oxotechnetium(V) complexes with phosphine-containing ligands. Although the geometric restriction around the phosphorus atom and the planar arrangement of five-membered chelate rings restrict ligand flexibility, the change of the donor set of the ligand could give novel ligand systems for the encapsulation of metal ions such as rhenium and technetium. Preferably the coordination sphere of the metal atom should not contain any multiple bond with a donor atom, which is observed for the metal ions at their lower oxidation states.

4.4 References

[1] Reddy, K. R.; Tsai, W.; Surekha, K.; Lee, G.; Peng, S.; Liu, S. *J. Chem. Soc., Dalton Trans.*, **2002**, 1776.

[2] Doherty, S.; Knight, J. G.; Scanlan, T. H.; Elsegood, M. R. J.; Clegg, W. *J. Organomet. Chem.*, **2002**, *650*, 231.

[3] Hedden, D.; Roundhill, D. M. *Inorg. Synth.*, **1990**, *27*, 322.

[4] Cooper, M. K.; Downes, J. M. *Inorg. Chem.*, **1978**, 17, *880.*

[5] Hessler, A.; Kottsieper, K. W.; Schenk, S.; Tepper, M.; Stelzer, O. *Z. Naturforsch., B: Chem. Sci.*, **2001**, *56*, 347.

[6] Burke, B. J.; Overman, L. E. *J. Amer. Chem. Soc.*, **2004**, *126*, 16820.

[7] Cho, I. S.; Gong, L.; Muchowski, J. M. *J. Org. Chem.*, **1991**, *56*, 7288.

[8] Babu, V.; Patil, B.; Vasanthakumar, G. R. *Synth. Commun.,* **2005**, *35*, 1795.

[9] Han, F. B., Yu-Liang; S. X.; Li, B. ; Guo, Y.; Tang, Y. *Organometallics*, **2008**, *27*, 1924.

[10] Atapie, L.; Le Gal, J.; Hamaoui, B.; Jaud, G. M.; Benoist, E. *Polyhedron*, **2007**, *26*, 5185.

[11] Doherty, S.; Knight, J. G.; Scanlan, T. H.; Elsegood, M. R. J.; Clegg, W. *J. Organomet. Chem.*, **2002**, *650*, 231.

[12] Elmer, C.; Song, A.; Song, S. *Inorg. Chem.*, **1995**, *34*, 3864.

[13] Tisato, F.; Refosco, F.; Bandoli, G.; Bolzati, C.; Moresco, A. *J. Chem. Soc., Dalton Trans.*, **1994**, 1453

[14] Michael G. B.; Tisley, D. G.; Walton, R. A. *Chem. Commun.*, **1970**, *10*, 600.

[15] Refosco, F.; Tisato, F.; Giuliano, B.; Cristina, B.; Dolmella, A.; Moresco, A.; Nicolini, M. *J. Chem. Soc., Dalton Trans.*, **1993**, *4*, 605.

[16] Abram, U. *Comprehensive Coordination Chemistry II*, Vol. V, Elsevier, **2004**, 271 and refs. cited therein.

[17] Refosco, F.; Mazzi, U.; Deutsch, E.; Kirchhoff, J. R.; Heineman, W. R.; Seeber, R. *Inorg. Chem.*, **1988**, *27*, 4121.

[18] Dennett, J. N. L.; Bierenstiel, M.; Ferguson, M. J.; McDonald, R.; Cowie, M. *Inorg. Chem.*, **2006**, *45*, 3705.

[19] MacLachlan, E. A.; Fryzuk, M. D. *Organometallics*, **2005**, *24*, 1112.

[20] Tisato, F.; Refosco, F.; Moresco, A.; Bandoli, G. *Inorg. Chem*., **1995**, *34*, 1779.

[21] Herrmann, W. A.; Wojtczak, W. A.; Artus, G. R. J.; Kuehn, F. E.; Mattner, M. R. *Inorg. Chem.*, **1997**, *36*, 465.

[22] Refosco, T.; Tisato, F.; Bandoli, G.; Bolzati, G.; Dolmella, A.; Moresco. A.;

Nicolini, M. *J. Chem. Soc., Dalton Trans.,* **1993**, 605.

[23] MacLachlan, E. A.; Fryzuk, M. D. *Organometallics*, **2005**, *24*, 1112.

[24] Luo, H.; Setyawati, I.; Rettig, S. J.; Orvig, C. *Inorg. Chem.*, **1995**, *34*, 2287.

[25] Abram, U.; Spies, H. *Z. Chem.*, **1984**, *24*, 74.

[26] Blackman, A. G. *Polyhedron*, **2005**, *24*, 1.

[27] Christopher, E. R.; Gordon, R. I.; Venanzi, M., L. *J. Chem. Soc., Dalton Trans.*, **1968**, 205.

[28] Jones, B. M.; Macbeth, E. C. *Inorg. Chem.*, **2007**, *46*, 8117.

[29] Shellenbarger, J. A.; Nicholson, T.; Davis, W. M.; Davison, A.; Jones, A. G. *Inorg. Chim. Acta*, **2005**, *358*, 3559.

[30] Refosco, F.; Bolzati, C.; Moresco, A.; Bandoli, G.; Dolmella, A.; Mazzi, U.; Nicoli, M. *J. Chem. Soc., Dalton Trans.*, **1991**, 3043.

Chapter 5

2-[(Hydroxymethyl)phenyl]phosphines and their reactions with rhenium and technetium complexes

---

5 Synthesis of 2-[(hydroxymethyl)phenyl]phosphines and their reactions with rhenium and technetium complexes

5.1 Synthesis of 2-[(hydroxymethyl)phenyl]phosphines

Many recent efforts have been focused on the synthesis of heterofunctionalized phosphines, which can act as reducing agents and chelating ligands [1]. (2-Hydroxyphenyl)phosphines $Ph_{3-n}P(2\text{-}C_6H_4OH)_n$ (n = 1 – 3) are remarkable examples, the coordination chemistry of which have been studied formerly [2-4]. The five-membered [P,O] chelate ring of 2-(hydroxyphenyl)diphenylphosphine can stabilize the $[M{=}O]^{+3}$ core under formation of complexes of the composition $[MOCl(PO)_2]$ (M = Re, Tc) [5-6].

The new class of [P,O] ligands, which is introduced here, is able to form six-membered chelate rings. The methylene groups give more flexibility to the ligand system but reduce the acidity of the hydroxyl group (pKa = 15) compared to that of a phenolic (pKa = 9.9) function.

(2-(Hydroxymethyl)phenyl)phosphines H_nL^n (n = 1, 3) were synthesized by the reduction of the (2-formylphenyl)phosphines **V** and **VII** with an excess amount of $NaBH_4$ under heating the reaction mixture in EtOH. After working up the reaction mixture, HL^1 and H_3L^3 were obtained as colourless solids in good yields, Scheme 5.1.

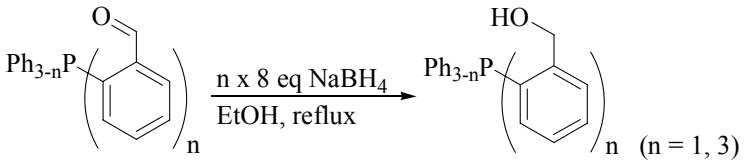

(V, VII) **H_nL^n**

Scheme 5.1 Synthesis of the (2-(Hydroxymethyl)phenyl)phosphines H_nL^n (n = 1, 3)

The $^{31}P\text{-}\{^1H\}$ NMR spectra show single resonances of the phosphorus atoms at −19.1 ppm for HL^1 and −38.3 ppm for H_3L^3. The lower chemical shift values of the phosphines in H_nL^n compared to the related aldehydes **V** and **VII** result from the electron donating characteristics of the methylene groups in contrast to the electron withdrawing properties of the carbonyl functions. The ^1H NMR spectra of both compounds show broad resonances of the OH groups at 5.1 ppm and doublets at 4.4 ppm associated with the methylene groups. Broad absorptions in the IR spectra of the compounds at 3329 cm^{-1} for HL^1 and 3440 cm^{-1} for H_3L^3 are assigned to the stretching vibrations of the hydroxyl groups with polymeric hydrogen bonds [7].

5.2 Reactions of the (2-(hydroxymethyl)phenyl)diphenylphosphine HL^1 with rhenium and technetium complexes

5.2.1 Reactions of HL^1 with oxorhenium(V) and oxotechnetium(V) complexes

The reactions of 2-(hydroxyphenyl)diphenylphosphine, $Ph_2P(2\text{-}C_6H_4OH)$, with rhenium and technetium have been investigated thoroughly with regard to their applications as radiopharmaceuticals. It is expected that the new class of [P,O] ligands, which is introduced in this chapter, establishes similar types of compounds. However, the six-member chelate ring formed by (2-(hydroxymethyl)phenyl)diphenylphosphine, HL^1, should cause differences in the coordination chemistry of HL^1 with rhenium and technetium complexes compared to that of 2-(hydroxyphenyl)phosphines.

$(NBu_4)[ReOCl_4]$ reacts with 2 eq. of HL^1 in MeOH under formation of a pale violet precipitate. The solid was recrystallized from a mixture of CH_2Cl_2/MeOH to obtain violet plates of $[ReOCl(L^1)_2]$ (**29**). A similar reaction between $(NBu_4)[TcOCl_4]$ and HL^1 resulted in the reduction of the Tc(V). This was confirmed by $^{31}P\text{-}\{^1H\}$ NMR spectroscopy, where the spectrum taken from the reaction mixture showed an intense signal at 29.3 ppm representing a phosphoryl group. Thus, the reaction was repeated by heating a mixture of $(NBu_4)[TcOCl_4]$ and 3 eq. of HL^1 in CH_2Cl_2. In this case, HL^1 acts as a reducing agent and bidentate chelating ligand. After working up the reaction mixture, an orange-red solid was obtained, which was recrystallized from a mixture of CH_2Cl_2/MeOH to give orange-red crystals of *cis*-$[TcCl_2(L^1)(HL^1)]$ (**30**), Scheme 5.2.

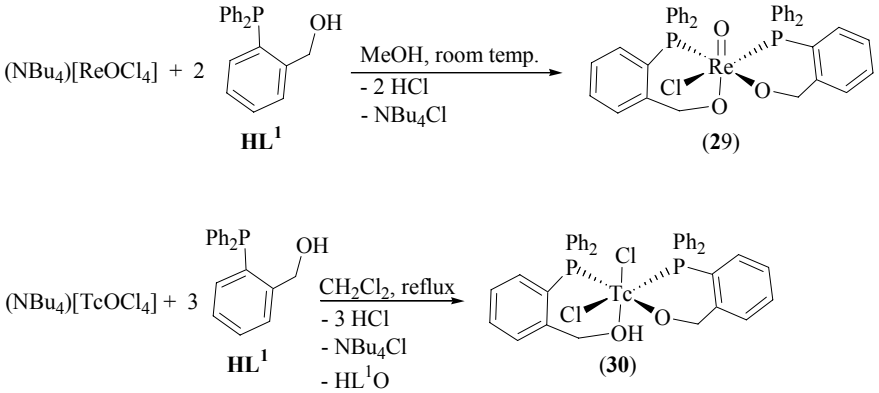

Scheme 5.2 the reactions of HL^1 with $(NBu_4)[MOCl_4]$, M = Re, Tc

The molecular structure of **29** is illustrated in Fig. 5.1 and selected bond lengths and angles are given in Table 5.1. $[ReOCl(L^1)_2]$ (**29**) is a neutral oxorhenium(V) complex. The two mononegative bidentate ligands $[L^1]^-$ together with a chloro and a terminal oxo ligand occupy the distorted octahedral coordination sphere about the metal ion. The Re-O(1) distance of 1.908(4) Å is slightly shorter than a rhenium-oxygen single bond, which implies electron transfer from the terminal oxo ligand O(10) to its *trans* position [8]. The bidentate chelating ligands coordinate mutually *cis* with a P(1)-Re-P(2) angle of 102.28(6)° and a O(1)-Re-O(2) angle of 86.7(2)°. The P(1)-Re-P(2) angle of 102.28(6)° is bigger than Cl(1)-Re-P(2) of 86.88(6)°.

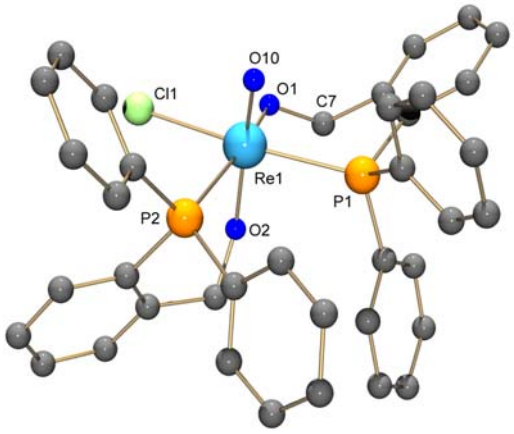

Fig. 5.1 Molecular structure of $[ReOCl(L^1)_2]$ (**29**). The hydrogen atoms were omitted for clarity.

Table 5.1 Selected bond lengths (Å) and angles (°) of $[ReOCl(L^1)_2]$ (**29**)

Bond lengths [Å]:					
Re-O(10)	1.673(4)	Re-O(1)	1.908(4)	Re-O(2)	1.981(5)
Re-P(1)	2.477(2)	Re-P(2)	2.489 (2)	Re-Cl	2.447(1)
Angles [°]:					
O(10)-Re-O(1)	167.0(2)	O(10)-Re-O(2)	105.7(2)	O(10)-Re-Cl(1)	95.6(1)
P(1)-Re-P(2)	102.28(6)	Cl(1)-Re-P(1)	170.57(6)	Cl(1)-Re-P(2)	86.88(6)

The $^{31}P-\{^1H\}$ NMR spectrum of **29** shows two resonances at 1.35 and 3.67 ppm. The ^1H NMR spectrum presents the methylene protons between 4.4 to 5.2 ppm and the protons of the aromatic rings from 6.9 to 7.7 ppm. A medium intense absorption band at 949 cm^{-1} in the IR spectrum of **29** is assigned to the Re=O stretching vibration. The absence of any absorption between 3100 and 3500 cm^{-1} confirms the deprotonation of both bidentate ligands. The MS(ESI) spectrum supports the molecular structure by the base peak at *m/z* = 785.13 amu, which is associated with the $[M-Cl]^+$ fragment.

Fig. 5.2 presents the molecular structure of $[TcCl_2(L^1)(HL^1)]$ (**30**). Selected bond lengths and angles are given in Table 5.2. The complex shows a distorted octahedral arrangement about the technetium atom. The bond distances Tc-O(1) of 1.950(4) Å and Tc-O(2) of 1.920(4) Å are in the range of Tc-O single bonds [9]. The bite angles of the both bidentate ligands P(1)-Tc-O(1) of 78.6(1)° Å and P(2)-Tc-O(2) of 83.8(1)° are in the expected range for six-membered chelate ring [10].

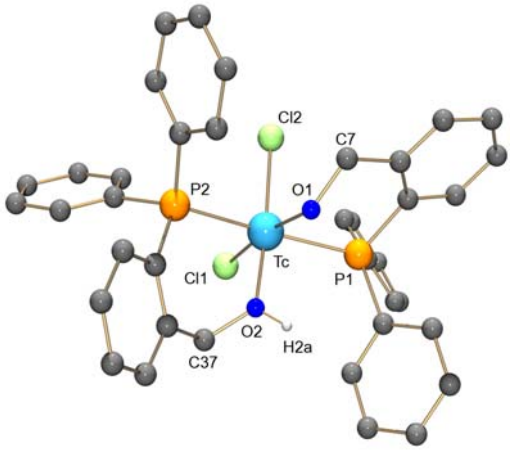

Fig. 5 2 Molecular structure of $[TcCl_2(L^1)(HL^1)]$ (**30**). Hydrogen atoms were omitted for clarity.

Table 5.2 Selected bond lengths (Å) and angles (°) of $[TcCl_2(L^1)(HL^1)]$ (**30**)

Bond lengths [Å]:					
Tc-O(1)	1.950(4)	Tc-O(2)	1.920(4)	Tc-Cl(1)	2.357(1)
Tc-Cl(2)	2.364(1)	Tc-P(1)	2.476(2)	Tc-P(2)	2.523(2)
Angles [°]:					
O(1)-Tc-O(2)	86.1(2)	O(1)-Tc-P(1)	78.6(1)	O(2)-Tc-P(2)	83.8(1)
P(1)-Tc-P(2)	169.83(5)	Cl(1)-Tc-P(1)	93.31(5)	Cl(1)-Tc-P(2)	96.55(5)

The IR spectrum of **30** supports the molecular structure by the absence of a Tc=O stretching vibration in the range of 900 to 1000 cm^{-1}. A broad band at 3409 cm^{-1} is assigned to the stretching vibration of OH component, which was observed even after drying **30** under high vacuum at 50°C for 2 days. The experimental technetium content of the isolated product of 12.9% is consistent with the theoretical value. The $^{31}P-\{^1H\}$ NMR spectrum, taken from the reaction mixture, shows an intense single resonance at 29.7 ppm, which is assigned to the resonances of the phosphoryl group. This confirms the reduction of the oxotechnetium(V) by the oxygen abstraction of the phosphine group to technetium(III).

5.2.2 Reactions of HL^1 with $[Re(NPh)Cl_3(PPh_3)_2]$

HL^1 reacts with the phenylimido complex $[Re(NPh)Cl_3(PPh_3)_2]$ under exchange of triphenylphosphine and chloro ligands by a bidentate mononegative $(L^1)^-$. After working up the reaction mixture, the obtained solid was recrystallized from a mixture of CH_2Cl_2/MeOH to give green crystals of $[Re(NPh)Cl_2(PPh_3)(L^1)]$ (**31**). In the presence of a supporting base and a four fold excess of HL^1, the second triphenylphosphine and chloro ligands are exchanged by another bidentate $(L^1)^-$ under formation of the complex $[Re(NPh)Cl(L^1)_2]$ (**32**). Moreover, **32** can be synthesized by the reaction of $[Re(NPh)Cl_2(PPh_3)(L^1)]$ (**31**) with a slight excess of HL^1 in boiling CH_2Cl_2 for 2 h, Scheme 5.3.

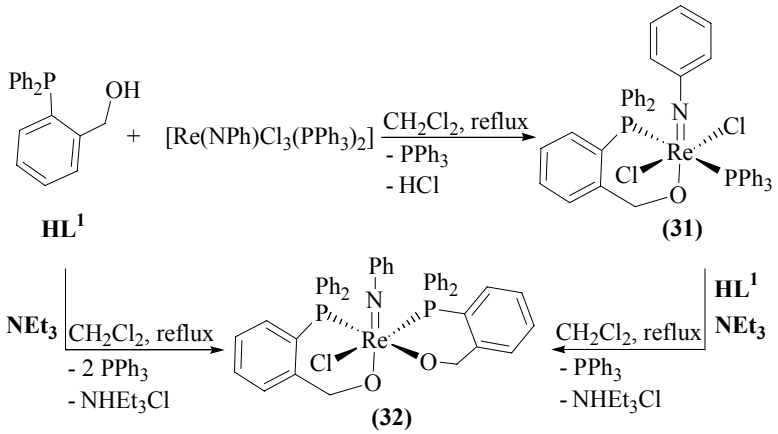

Scheme 5.3 The reactions of HL^1 with phenylimidorhenium(V) complexes

The molecular structure of $[Re(NPh)Cl_2(PPh_3)(L^1)]$ (**31**), Fig. 5.3, depicts that the compound is a neutral phenylimidorhenium(V) complex with the phosphorus atoms *trans* to each other. Selected bond lengths and angles are presented in Table 5.3. The rhenium atom has a distorted octahedral environment. The Re-N(10) bond distance of 1.740(4) Å is in the expected range of a Re=N double bond [11] .The Re-N(10)-C(31) angle of 177.7(8)°. The bond distance between N(10)-C(31) is 1.367(7) Å is between the ideal values of N-C single and double bond.

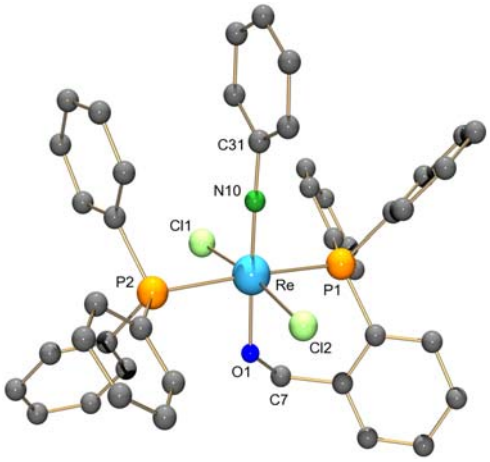

Fig. 5.3 Molecular structure of [Re(NPh)Cl_2(PPh_3)(L^1)] (**31**). The hydrogen atoms were omitted for clarity.

Table 5.3 Selected bond distances and angles of [Re(NPh)Cl_2(PPh_3)(L^1)] (**31**).

Bond lengths [Å]:					
Re-N(10)	1.740(4)	Re-O(1)	1.936(4)	Re-P(1)	2.468(2)
Re-P(2)	2.494(2)	Re-Cl(1)	2.420(2)	N(10)-C(31)	1.367(7)
Angles [°]:					
Re-N(10)-C(31)	177.7(8)	Cl(1)-Re-Cl(2)	171.27(6)	P(1)-Re-P(2)	173.77(5)
O(1)-Re-N(10)	177.8(3)				

The ^{31}P-{^1H} NMR spectrum of *trans*-[Re(NPh)Cl_2(L^1)(PPh_3)] (**31**) shows two doublets with coupling constants of J_{pp} = 843 Hz, which is in the range of mutually *trans* coordinated phosphine ligands [12], Fig 5.4.

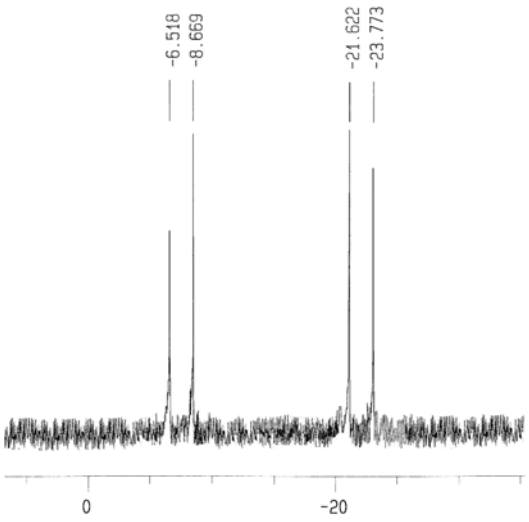

Fig. 5.4 The ^{31}P-{^1H} NMR spectrum of *cis*-[Re(NPh)Cl_2 (L^1)(PPh_3)] (**31**).

The ^{1}H NMR spectrum of **31** shows a singlet at 4.9 ppm, integrated as two protons, which are associated with the methylene protons of $(L^1)^-$. The infrared spectrum supports the deprotonation of the bidentate ligand by the absence of the OH stretching vibration in the range of 3100 to 3500 cm^{-1}. The Re=N stretching vibration appears as a medium band at 1091.6 cm^{-1}, which is typical for arylimidorhenium(V) complexes [13].

Fig. 5.5 presents the molecular structure of [Re(NPh)Cl(L^1)$_2$] (**32**) and selected bond lengths and angles are listed in Table 5.4. Compound **32** is a neutral phenylimidorhenium(V) complex with two bidenetate mononegative $(L^1)^-$ ligands. The environment of the rhenium atom is a distorted octahedron. The bond length between Re and O(2) of 1.97(1) Å is shorter than the Re-O(1) distance of 2.01(1) Å, which implies a stronger *trans* influence of the π-donor phenylimido ligand compared to that of the phosphine. The Re-N(10)-C(31) angle of 169.0(1)° shows an approximately linear bonding situation about N(10). The P(1)-Re-P(2) angle of 107.0(1)° is bigger than the ideal value 90°, which is due to the repulsion between π-electrons of the phenylimido ligand and the arylphosphines.

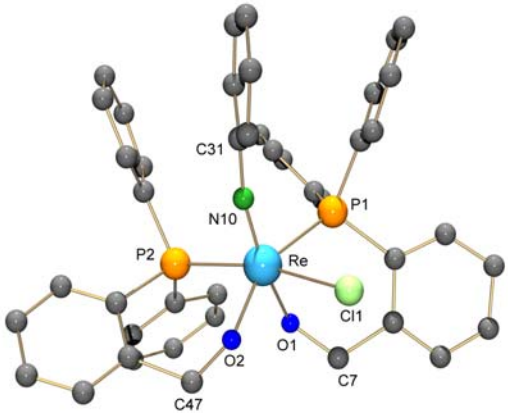

Fig. 5.5 Molecular structure of [Re(NPh)Cl(L^1)$_2$] (**32**). The hydrogen atoms were omitted for clarity.

Table 5.4 Selected bond distances and angles of [Re(NPh)Cl(L^1)$_2$] (**32**).

Bond lengths [Å]:					
Re-N(10)	1.73(1)	Re-P(1)	2.448(4)	Re-P(2)	2.434(4)
Re-O(1)	2.01(1)	Re-O(2)	1.97(1)	Re-Cl(1)	2.454(4)
N(10)-C(31)	1.42(2)				
Angles [°]:					
Re-N(10)-C(31)	169.0(1)	O(1)-Re-N(10)	165.2(5)	P(1)-Re-P(2)	107.0(1)
O(2)-Re-P(2)	87.5(3)	P(1)-Re-Cl(1)	83.2(1)		

The ^{31}P-{^{1}H} NMR spectrum of [Re(NPh)Cl(L^1)$_2$] (**32**) presents a single resonances at −22.9 ppm for the coordinated $(L^1)^-$. The high field shifts in frequencies of the resonances of the phosphine ligand is comparable with that of the starting complex [Re(NPh)Cl$_3$(PPh$_3$)$_2$] (^{31}P-{^{1}H} NMR: δ = −20.4 ppm) [14]. The ^{1}H NMR spectrum of **31** presents four doublets with typical *HH* geminal coupling constants of J_{HH} = 15.2 Hz. The Re=N stretching vibration appears as a medium band at 1091.6 cm^{-1}. The deprotonation situation of the bidentate chelating ligands is confirmed by the absence of the OH stretching absorption in the range of 3100 to 3500 cm^{-1}.

5.3 Reactions of tris(2-(hydroxymethyl)phenyl)phosphine H_3L^3 with rhenium and technetium complexes

The coordination chemistry of tris(2-phenolato)phosphine, P{O}$_3$, was explored initially by McDonald *et al.* at the end of 90's [15] Despite many attempts with reaction pathways, the isolation of rhenium complexes with tetradentate "umbrella" type chelating ligands was not successful. In all cases P{O}$_3$ coordinates as a tridentate κ^3-(P,O,O´) ligand. In order to increase the flexibility of the ligand system, H_3L^3 was synthesized, which has an extra methylene group compared to P{O}$_3$. This can induce higher flexibility and electron donating properties to the ligand system.

5.3.1 Reactions of tris(2-(hydroxymethyl)phenyl)phosphine H_3L^3 with oxorhenium(V) and oxotechnetium(V) complexes

H_3L^3 reacts with (NBu$_4$)[ReOCl$_4$] in MeOH at ambient temperature under ürecipitation of a violet solid directly from the reaction mixture. Recrystallization of this solid from a mixture of CH_2Cl_2/MeOH gave violet plates of [ReOCl$_2$(H_2L^3)]·MeOH (**33·MeOH**), Scheme 5.4.

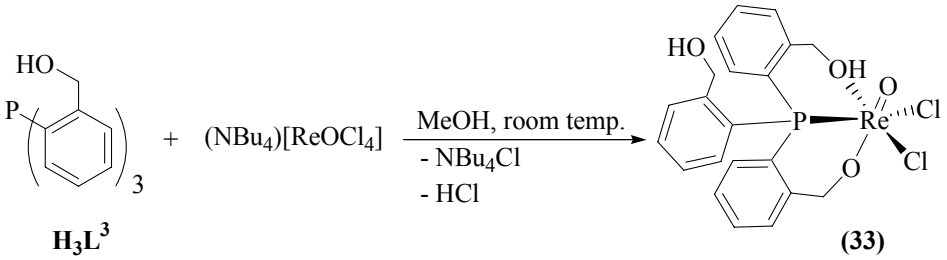

H_3L^3 **(33)**

Scheme 5.4 The reaction between H_3L^3 and (NBu$_4$)[ReOCl$_4$]

The molecular structure of $[ReOCl_2(H_2L^3)]$ (**33**), Fig 5.6, suggests that the isolated complex should be the kinetically favoured product, wherein the phosphine ligand coordinates in a tridentate κ^3-(P,O,O´) mode. In order to obtain a tetradentate "umbrella" type chelating mode, the aforementioned reaction was repeated under heating the reaction solution in a mixture of $CH_2Cl_2/PhCH_3$. After working up the reaction mixture, the product was characterized by infrared spectroscopy also as **33**.

The molecular structure of $[ReOCl_2(H_2L^3)]$ (**33**) elucidates that this compound is a neutral oxorhenium(V) complex. The mononegative chelating ligand $(H_2L^3)^-$ is bonded to the rhenium atom in a "*fac*-$[ReO(\kappa^3\text{-}H_2L^3)]$" mode. The clear difference in the "bite" angles O(1)-Re-P of 75.8(2)° and O(2)-Re-P of 89.1(2)° shows the flexibility of the ligand for adopting the values either near to that of tris(2-phenolato)phosphine , $P\{O\}_3$, (74.2° – 75.91°) [16] or tris-(2-thiophenolato)phosphine, $P\{S\}_3$, (83.07° - 85.66°) [17].

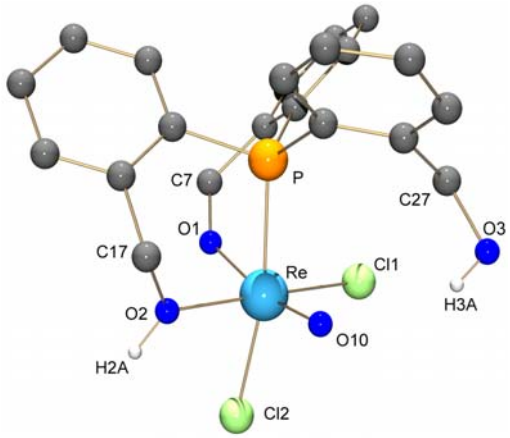

Fig. 5.6 Molecular structure of $[ReOCl_2(H_2L^3)]\cdot MeOH$ (**33·MeOH**). The solvent molecule and hydrogen atoms bonded to carbon atoms were omitted for clarity

Table 5.5 Selected bond lengths (Å) and angles (°) of *fac*-$[ReOCl_2(H_2L^3)]\cdot MeOH$ (**33·MeOH**)

Bond lengths [Å]:					
Re-O(10)	1.671(7)	Re-O(1)	1.927(6)	Re-O(2)	2.074(5)
Re-P	2.405(2)	Re-Cl(1)	2.399(2)	Re-Cl(2)	2.430(2)
Angles [°]:					
O(10)-Re-O(1)	167.3(3)	O(1)-Re-P	75.8(2)	O(2)-Re-P	89.1(2)
Cl(1)-Re-Cl(2)	89.03(8)	Cl(1)-Re-O(10)	92.8(2)		

Hydrogen bonds:

D-H...A	d(D-H)	d(H...A)	d(D...A)	<(DHA)
O(2)-H(2A)...O(4)#1[a]	0.93	1.73	2.47(1)	133.9
O(3)-H(3A)...O(5)#2[a]	0.82	2.11	2.77(1)	137.1

a) Symmetry transformations used to generate equivalent atoms: #1 -x+y+1,-x+1,z; #2 -x+y,-x,z

The bond lengths Re-O(1) of 1.927(6) Å and Re-O(2) of 2.074(5) Å imply an electron transfer from the terminal oxo O(10) to its *trans* position, which results in a shortening of the Re-O(1) bond. This difference implies the deprotonation situation of the hydroxyl groups. The oxo ligand O(2) establishes a hydrogen bond with the co-crystallized solvent methanol.

The ^{31}P-{^{1}H} NMR spectrum of [$ReOCl_2(H_2L^3)$] (**33**) shows a single resonance of the coordinated phosphine at −28.3 ppm. The ^{1}H NMR spectroscopy confirms the molecular structure by four doublets between 4.8 ppm and 6.3 ppm associated with the methylene groups of the coordinated arms and a singlet at 4.1 ppm (2H) for that of the uncoordinated arm of the ligand. The infrared spectrum presents a broad intense band at 3381 cm^{-1} representative for the stretching vibrations of the hydroxyl groups.

H_3L^3 reacts with $(NBu_4)[TcOCl_4]$ at ambient temperature in EtOH. The reaction progress was tracked by ^{31}P-{^{1}H} NMR spectroscopy. The signal of the uncoordinated H_3L^3 at −38.2 ppm disappeared during 2 h and a new signal at −13.1 ppm was observed. Additionally, a resonance at 35.5 ppm (with 5 % intensity compared to that of the product) suggests the reduction of the metal ion as a side reaction. By slow evaporation of the solvent, dark-green blocks of $[(TcOCl)_2(\mu\text{-}HL^3)_2]$ (**34**) were obtained, Scheme 5.5.

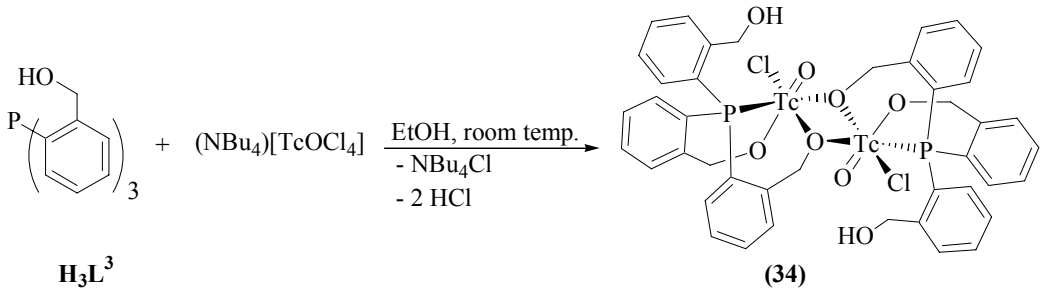

H_3L^3 **(34)**

Scheme 5.5 The reaction between H_3L^3 and $(NBu_4)[TcOCl_4]$

The dinegative ligand $(HL^3)^{2-}$ coordinates in an expected tridentate κ^3-(P,O,O′) mode. One of the coordinated oxygen atom occupies the *trans* position to the terminal oxo ligand and the other one establishes a bridge between the two technetium atoms.

The molecular structure of **34** is presented in Fig. 5.7 and the selected bond distances and angles are given in Table 5.6. $[(TcOCl)_2(\mu\text{-}HL^3)_2]$ (**34**) is a neutral dinucleartechnetium(V) complex. The bond lengths Tc=O(10) of 1.644(9) Å and Tc-O(1) of 1.904(8) Å are similar to those of the oxotechnetium(V) complex with (2-phenolato) phosphine [18].

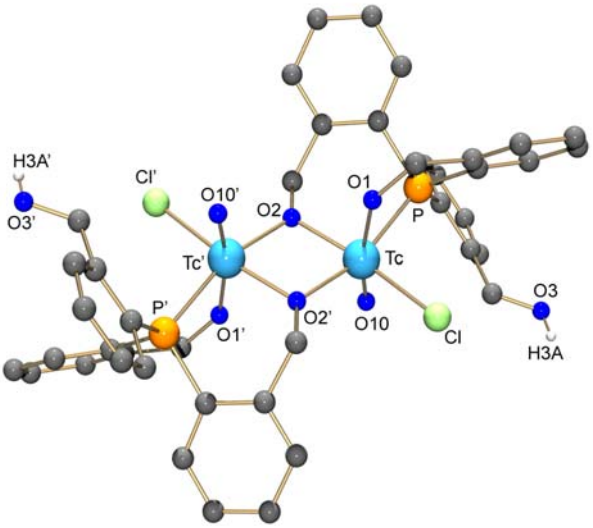

Fig. 5.7 Molecular structure of $[(TcOCl)_2(\mu\text{-}HL^3)_2]\cdot 1/2EtOH$ (**34·1/2EtOH**). The solvent molecule and the hydrogen atoms bonded to carbon atoms were omitted for clarity.

Table 5.5 Selected bond lengths (Å) and angles (°) of $[(TcOCl)_2(\mu\text{-}HL^3)_2]\cdot 1/2EtOH$ (**34·1/2EtOH**)

Bond lengths [Å]:					
Tc-O(10)	1.644(9)	Tc-O(1)	1.904(8)	Tc-O(2)	2.023(8)
O(2)-Tc'#1[a]	2.094(9)	Tc-P	2.380(3)	Tc-Cl	2.430(3)
Angles [°]:					
O(10)-Tc-O(1)	167.7(5)	Tc-O(2)-Tc'#1[a]	102.9(3)	O(2)-Tc-P	91.0(2)
O(10)-Tc-O(2)	94.2(4)	Cl(1)-Tc-O(10)	90.9(3)		

Hydrogen bond:				
D-H...A	d(D-H)	d(H...A)	d(D...A)	<(DHA)
O(3)-H(4A)...O(5)#2[a]	0.82	2.30	2.86(4)	126.6

a) Symmetry transformations used to generate equivalent atoms: #1 -x+1,-y+2,-z+1; #2 -x+1,-y+1,-z+1,

The terminal oxo ligand O(10) is oriented *cis* to the oxygen bridge defined by the O(10)-Tc-O(2) angle of 94.2(4)°. The uncoordinated hydroxyl group O(3) establishes a hydrogen bond with a co-crystallized ethanol molecule.

The IR spectrum of $[(TcOCl)_2(\mu\text{-}HL^3)_2]\cdot 1/2EtOH$ supports the molecular structure by a strong absorption at 3391 cm^{-1} associated with the stretching vibrations of a hydroxyl group as it was observed in the IR spectrum of H_3L^3. The Tc=O vibration appears as an intense band at 933 cm^{-1}.

5.3.2 Reactions of tris(2-(hydroxymethyl)phenyl)phosphine H_3L^3 with $TcCl_4$

So far, the coordination chemistry of {(2-hydroxymethyl)phenyl}phosphines H_nL^n (n = 1 - 3) has been described with the rhenium and technetium complexes, which have a multiple bond to a donor atom such as $[M{=}NPh]^{3+}$ or $[M{=}O]^{3+}$ (M = Re, Tc). This means, one of the potentially coordination positions is blocked by the oxo or phenylimido ligands. Since these ligands induce an intense *trans* influence, the phosphine group is bonded *cis* to $[M{=}O/NPh]^{3+}$ (M = Re, Tc) cores.

The neutral technetium tetrachloride (**XXII**) is a polymeric compound with Cl^- bridges between the metal atoms. The longest Tc-Cl bonds of 2.49 Å are associated with the bridging chlorine atoms perpendicular to the polymeric chain. These bonds can be easily cleaved by donor solvents such as THF to give *cis*-$[TcCl_4(L)_2]$ (L = solvent molecule; **XXIII** : L = THF) complexes [19], Scheme 5.6.

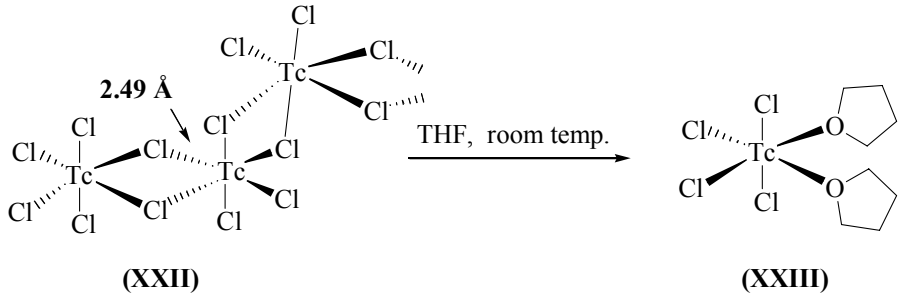

Scheme 5.6 Synthesis of *cis*-$[TcCl_4(THF)_2]$ (**XXIII**) as a suitable starting material [19].

cis-$[TcCl_4(THF)_2]$ (**XXIII**) was synthesized *in situ* and reacted with an equimolar amount of H_3L^3 in dry THF. After reducing the volume of the solvent to half, the solution was cooled to -10°C and kept at this temperature overnight. $[TcCl_3(H_2L^3)]$ (**35**) was obtained as orange plates in a good yield. The singly deprotonated ligand $(H_2L^3)^-$ coordinates in a κ^3-(P,O,O´) mode, Scheme 5.7.

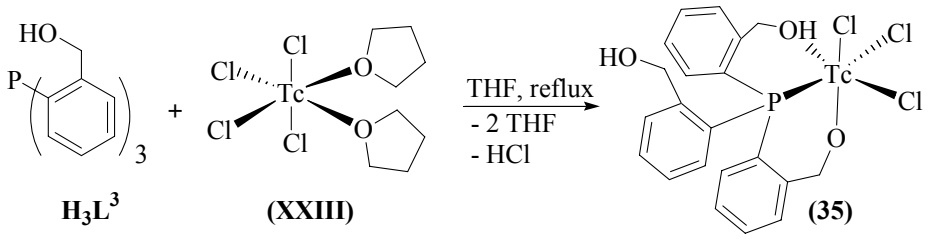

Scheme 5.7 Reaction between H_3L^3 and *in situ* synthesized $[TcCl_4(THF)_2]$

The molecular structure of $[TcCl_3(H_2L^3)]$ (**35**) is presented in Fig. 5.8 and selected bond lengths and angles are listed in Table 5.6. $[TcCl_3(H_2L^3)]$ (**35**) is a neutral technetium(IV) complex. The mononegative $(H_2L^3)^-$ and three chloro ligands compensate the positive charges of the octahedrally coordinated metal ion. The difference in the bond lengths Tc-O(1) of 1.931(8) Å and Tc-O(2) of 2.112(6) Å imply the deprotonation of the ligand on oxygen atom O(1). Moreover, O(2) establishes a hydrogen bond with O(3) in the molecule generated by the symmetry element x,-y+3/2,z-1/2.

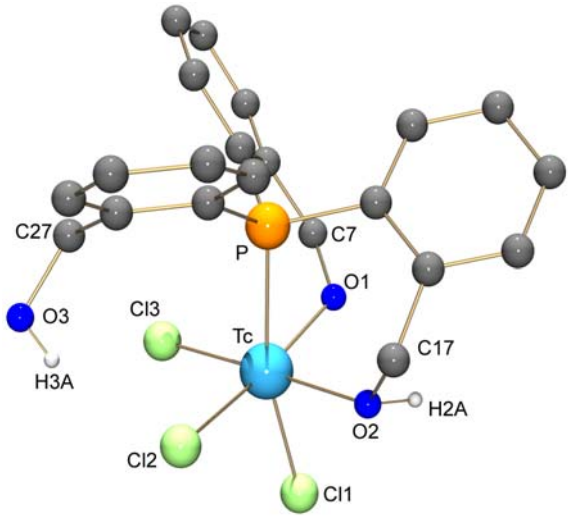

Fig. 5.8 Molecular structure of $[TcCl_3(H_2L^3)]$ (**35**). The hydrogen atoms bonded to carbon atoms were omitted for clarity.

Table 5.6 Selected bond lengths (Å) and angles (°) of $[TcCl_3(H_2L^3)]$ (**35**)

Bond lengths [Å]:					
Tc-O(1)	1.931(8)	Tc-O(2)	2.112(6)	Tc-P	2.516(3)
Tc-Cl(1)	2.361(3)	Tc-Cl(2)	2.368(3)	Tc-Cl(3)	2.284(3)
Angles [°]:					
O(1)-Tc-P	73.3(2)	O(2)-Tc-P	84.8(2)	O(1)-Tc-Cl(1)	96.6(2)
P-Tc-Cl(1)	165.6(1)	P-Tc-Cl(2)	94.68(9)	P-Tc-Cl(3)	96.1(1)
Hydrogen bonds:					
D-H...A	d(D-H)	d(H...A)	d(D...A)	<(DHA)	
O(2)-H(2B)...O(3)#1[a]	0.97	1.629(6)	2.559(9)	158.1	
O(3)-H(3A)...Cl(2)	0.82	2.41	3.174(7)	154.9	

a) Symmetry transformations used to generate equivalent atoms: #1 x,-y+3/2,z-1/2

The tridentate ligand establishes two different "bite" angles defined by P-Tc-O(1) of 73.3(2)° and P-Tc-O(2) of 84.8(2)°. The oxygen atom of the uncoordinated hydroxyl group O(3) interacts with Cl(2) through a hydrogen bond with a donor-acceptor distance of 3.174(7) Å.
The infrared spectrum shows no absorption in the range of 900 cm^{-1} to 1000 cm^{-1}, which is consistent with the absence of the technetium-oxygen multiple bond. The broad medium band at 3425 cm^{-1} is assigned to the stretching vibration of OH. The broadening of the band supports the hydrogen bonds detected by X-ray analysis. The Tc content of the crystalline product (Tc, 17.9%) is in agreement with the theoretical amount calculated for $C_{21}H_{20}O_3PTc$ as the molecular formula of $[TcCl_3(H_2L^3)]$ (**35**).

5.3.3 Reactions of H_3L^3 with $(NEt_4)_2[Re(CO)_3Br_3]$

Carbonyl complexes of rhenium and technetium attracted much interest in bioorganometallic and radiopharmaceutical chemistry. Since the direct synthesis of $[M(OH_2)_3(CO)_3]^+$ (M = Re, ^{99,99m}Tc) in water was reported [20], the $[M(CO)_3]^+$ core is one of the most intensively investigated cores of Re and Tc chemistry and represents a comparatively simple way of labelling of bimolecules [21-22]. For the *in situ* generation of the "*fac*-$\{Re(CO)_3\}^+$" unit, $(NEt_4)_2[Re(CO)_3Br_3]$ [23] is a convenient starting material. The three bromide ligands are highly labilized by the strong *trans* influence of the carbonyl ligands and are, thus, expected to undergo at least partial substitution with solvent molecules. Precipitation of halides with Ag^+ ions results in an activated "*fac*-$\{Re(CO)_3(solvent)_3\}^+$," complex moiety, which readily reacts with tridentate chelating ligands under formation of stable complexes [24]. The possible facial coordination mode of H_3L^3, which was repeatedly observed during reactions with the different rhenium and technetium starting materials, makes it a promising candidate for stabilization of the "*fac*-$\{Re(CO)_3\}^+$" core. Consequently, H_3L^3 was reacted with $(NEt_4)_2[ReBr_3(CO)_3]$ in MeOH. Heating of the reaction mixture gave a yellow solution. The $^{31}P-\{^1H\}$ NMR spectrum, directly taken from the reaction solution, presents two resonances at -7.1 ppm and -12.5 ppm. The signals were assigned to complexes of the compositions $[ReBr(CO)_3(\kappa^2\text{-}H_2L^3)]$ and $[Re(CO)_3(\kappa^3\text{-}H_2L^3)]$, Scheme 5.8. During subsequent addition of the supporting base NEt_3 the signal at -12.5 ppm disappeared and the singlet at −7.1 ppm remained. After the reaction mixture was cooled down to ambient temperature a colourless precipitate was obtained.

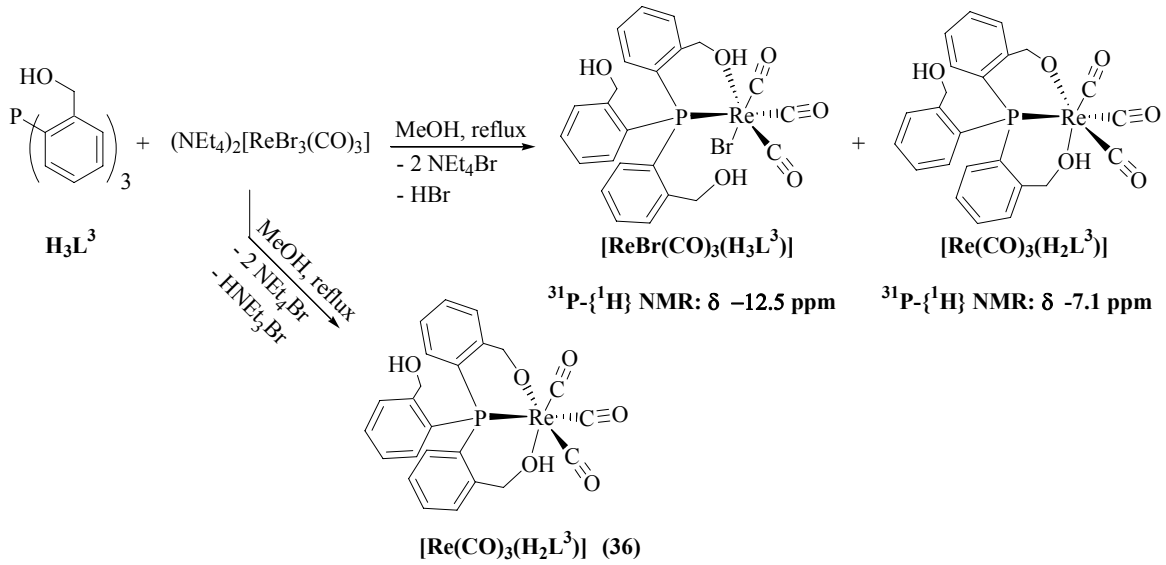

Scheme 5.8 Reaction between H_3L^3 and $[ReBr_3(CO)_3]^{2-}$ in the presence and absence of a supporting base.

The molecular structure of *fac*-$[Re(CO)_3(H_2L^3)]$ (**36**) is shown in Fig. 5.9 and selected bond lengths and angles are given in Table 5.7. The chelating ligand coordinates in a mononegative tridentate mode. The rest of the octahedral rhenium coordination sphere is occupied by three carbonyl ligands. The lengthening in the bond distances Re-C(30) of 1.98(1) Å is due to the stronger *trans* influence of the phosphine ligand to the oxygen donors.

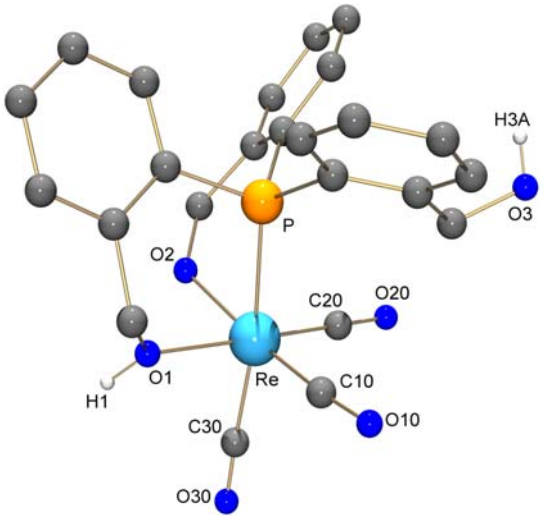

Fig. 5.9 Molecular structure of $[Re(CO)_3(H_2L^3)]$ (**36**). The hydrogen atoms bonded to carbon atoms were was omitted for clarity

Table 5.7 Selected bond lengths (Å) and angles (°) of $[Re(CO)_3(H_2L^3)]\cdot MeOH$ (**36·MeOH**)

Bond lengths [Å]:					
Re-O(1)	2.143(6)	Re-O(2)	2.141(8)	Re-P	2.439(3)
Re-C(10)	1.87(1)	Re-C(20)	1.89(1)	Re-C(30)	1.98(1)
Angles [°]:					
O(1)-Re-P	85.0(2)	O(2)-Re-P	78.8(2)	C(10)-Re-O(2)	173.7(4)
P-Re-C(10)	94.9(3)	C(10)-Re-C(20)	88.5(4)	C(20)-Re-O(1)	174.9(4)

Hydrogen bonds:				
D-H...A	d(D-H)	d(H...A)	d(D...A)	<(DHA)
O(1)-H(1)...O(2)#1[a]	0.93	1.53	2.45(1)	172.3
O(3)-H(3A)...O(4)#2[a]	0.82	1.91	2.71(2)	162.5

a) Symmetry transformations used to generate equivalent atoms: #1 -x+2,-y,-z ; #2 -x+1,-y,-z

The insignificant difference between the bond lengths of Re-O(1) of 2.14(6) Å and Re-O(2) of 2.141(8) Å do not prove the deprotonation position unambiguously. However, a comparison of the bite angles of H_3L^3 of the hitherto studied molecular structures **32-36** provides a guide to understand the deprotonation position. In all the previous structures, the smaller P-M-O (M = Re, Tc) angle are associated with the mononegative hydroxyl group. The bond angle P-Re-O(2) of 78.8(2)° is clearly smaller than P-Re-O(1) of 85.0(2)°, which implies the deprotonation position on O(2). The oxygen atom O(1) establishes a hydrogen bond with O(2) in the adjacent molecule, generated by the symmetry element -x+2,-y,-z , with a donor-acceptor distance of 2.45(1) Å.

The $^{31}P-\{^1H\}$ NMR spectrum of **36** shows a singlet at −7.7 ppm associated with the coordinated phosphine. The ^1H NMR spectrum supports the molecular structure by presenting the methylene protons between 4.5 and 5.0 ppm. The triplet at 6.2 ppm is assigned to the uncoordinated hydroxyl group, which appears at the chemical shift values of the uncoordinated H_3L^3. The multiplet at 7.8 ppm is assigned to the coordinated hydroxyl group. The presence of the "*fac*-$\{Re(CO)_3\}^+$" core is proved by three strong absorptions at 1882, 1913 and 2021 cm^{-1} in the infrared spectrum of **36**. The MS(FAB^+) spectrum presents the $[M+H]^+$ species at *m/z* = 623.1 amu.

5.3.4. Tris(2-(hydroxymethyl)phenyl)phosphine H_3L^3: A bifunctional tridentate ligand

The space filling representation of the molecular structure of $[Re(CO)_3(H_2L^3)]$ (**36**) elucidates that the chelating ligand and three tightly bonded carbonyls surround the metal ion and hinder the direct interactions between the rhenium atom and its surrounding medium, Fig. 5.10.

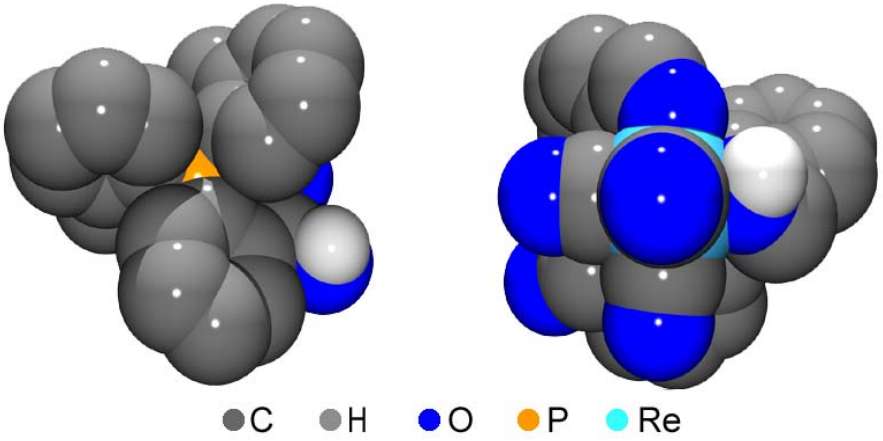

Fig. 5.10 Space filling representation of the molecular structure of **36**. Top view (left), bottom view (right)

The molecular structure of **36** elucidates that the free hydroxyl group of H_3L^3 O(3) grants a "*bifunctional*" attribute to H_3L^3. This hydroxyl group can react with a carboxylic function of a protein or a peptide to form a benzyl ester.

In order to prove the stability of $[Re(CO)_3(H_2L^3)]$ (**36**) during the coupling reaction, the complex **36** was reacted with 1.1 eq. of pre-activated *N*-BOC-diglycine (**XXIV**). After working up the reaction mixture a colorless solid of the conjugate (**37**) was obtained in a moderate yield, Scheme 5.9.

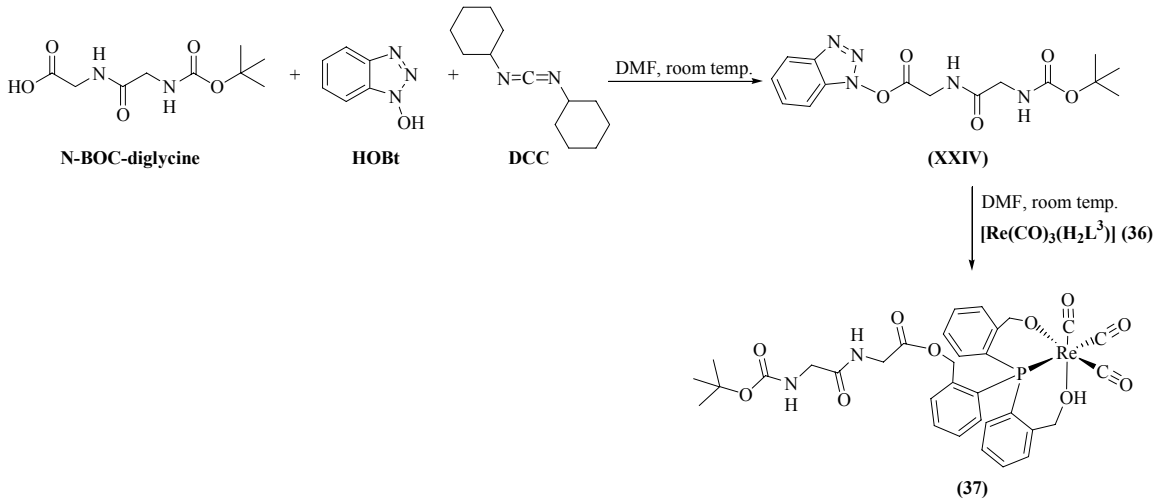

Scheme 5.9 "Bifunctional" coupling of $[Re(CO)_3(H_2L^3)]$ (**36**) with *N*-BOC-diglycine

The ^{31}P-{^{1}H} NMR spectrum of **37** shows a single resonance at −3.4 ppm, which is similar to the chemical shift value of **36**. The MS(ESI) spectrum supports the supposed molecular structure of the product **37** by a peak at m/z = 837.1 amu, which is associated with the $[M+H]^+$ species.

The analytical evidences of **37** elucidates that H_3L^3 can act as a bifunctional ligand and can successfully be coupled with a biologically interesting molecule. However, further chemical and biological studies are required to get the benefit of this interesting ligand system.

5.4 Summary and Conclusions

The {(2-hydroxymethyl)phenyl}phosphines H_nL^n (n = 1 - 3) are a new class of hetero-functionalized phosphines, which can readily be synthesized by reduction of the related aldehydes. HL^1 reacts with the $[Re= O/NPh]^{3+}$ cores under simple ligand exchange reactions. The reaction between HL^1 and the technetium congener $[Tc=O]^{3+}$ resulted in the reduction of the metal core and subsequent ligand substitution to give a complex of the composition *cis*-$[TcCl_2(L^1)(HL^1)]$ (**30**). The potentially tetradentate ligand H_3L^3 reacts with different complexes of rhenium and technetium under facial coordination. The molecular structures of all isolated compounds elucidate that H_3L^3 coordinates in a tridentate bis-chelating κ^3-(P,O,O´) mode with one uncoordinated hydroxyl group. The potential "*bifunctional*" coordination mode of H_3L^3 was employed for the coupling of $[Re(CO)_3(H_2L^3)]$ (**36**) with pre-activated diglycine. The analytical data elucidate that the dipeptide (*N*-BOC-diglycine) can be successfully conjugated with the complex **36**.

5.5 References

[1] Bolzati, C.; Uccelli, L.; Refosco, F.; Tisato, F.; Duatti, A.; Giganti, M.; Piffanelli, A. *Nuc. Med. Biol.*, **1998**, *25*, 71.

[2] Luo, H.; Setyawati, I.; Rettig, S. J.; Orvig, C. *Inorg. Chem.*, **1995**, *34*, 2287.

[3] Fan, W.; Zhang., R.; Leong, W. K.; Chu, C. K.; Yan, Y. K. *J. Organomet. Chem.*, **2005**, *690*, 3765.

[4] Dilsky, S.; Schenk, W. A. *Eur. J. Inorg. Chem.,* **2004**, *24*, 485.

[5] Couillens, X.; Gressier, M.; Coulais, Y.; Dartiguenave, M. *Inorg. Chim. Acta*, **2004**, *357*, 195.

[6] Bolzati, C.; Tisato, F.; Refosco, F.; Bandoli, G. *Inorg. Chim. Acta*, **1996**, *247*, 125.

[7] Brisdon K. A. Inorganic spectroscopic methods, *oxford chemistry primers*, **1998**.

[8] Bandoli, G.; Dolmella, A.; Gerber, T. I. A.; Mpinda, D.; Perils, J.; Du Preez, J. G. H. *J. Coord. Chem.*, **2002**, 55, 823.

[9] Münze, R.; Abram, U.; Stach, J.; Hiller, W. *Inorg. Chim. Acta*, **1991**, *186*, 151.

[10] Zhang, H.; Li, B.; Dai, M. *J. Pharm. Pharmacol.*, **2003**, *55*, 505.

[11] Hecht, M.; Saucedo, A. S.; Hagenbach, A.; Abram, U. *Inorg. Chem.*, **2005**, *44*, 3172.

[12] Palmer, R. A.; Whitcomb, D. R. *J. Magn. Reson.*, **1980**, *39*, 371.

[13] Booysen, I.; Gerber, T. I. A.; Hosten, E.; Mayer, P. *J. Coord. Chem.*, **2007**, *60*, 1749.

[14] Bereau, V. M.; Khan, S. I.; Abu-Omar, M. M. *Inorg. Chem.*, **2001**, *40*, 6767.

[15] Cavell, R. G.; Hilts, R. W.; Luo, H.; McDonald, R. *Inorg. Chem.*, **1999**, *38*, 897.

[16] Yamamoto, Y.; Sugawara, K.; Kakeya, M. *Inorg. Chim. Acta,* **2002**, *340*, 21.

[17] Lee, C. M.; Chuang, Y. L.; Chiang, C. Y.; Lee, G. H.; Liaw, W. F. *Inorg. Chem.*, **2006**, *45*, 10895.

[18] Luo, H.; Setyawati, I.; Rettig, S. J.; Orvig, C. *Inorg. Chem.*, **1995**, *34*, 2287.

[19] Hagenbach, A.; Yegen, E.; Abram, U. *Inorg. Chem.*, **2006**, *45*, 7331.

[20] Alberto, R.; Schibli, R.; Egli, A.; Schubiger, A. P.; Abram, U.; Kaden, T. A. *J. Amer. Chem. Soc.*; **1998**, *120*, 7987.

[21] Mundwiler, S.; Waibel, R.; Spingler, B.; Kunze, S.; Alberto, R. *Nucl. Med. Biol.*; **2005**, *32*, 473.

[22] Haefliger, P.; Agorastos, N.; Renard, A.; Giambonini-Brugnoli, G.; Marty, C.; Alberto, R. *Bioconjugate Chem.*; **2005**, *16*, 582.

[23] Hinrichs, M.; Hofbauer, F. R.; Kluefers, P. *Chem. Eur. J.*, **2006**, *12*, 4675.

[24] Burzlaff, N.; Hegelmann, I.; Weibert, B. *J. Organomet. Chem.,* **2001**, *626*, 16.

Chapter 6

Experimental Section

6.1 Starting materials

All chemicals and reagents were purchased from commercial sources (Acros Organics, Fluka, Sigma-Aldrich, Alfa Aesar, Merck).

All solvent were used as received (pure for synthesis) unless otherwise stated. THF and diethylether were dried intensively by heating over sodium metal.

The technetium and rhenium precursors were synthesized with respect to the cited references:

$(NBu_4)[ReOCl_4]$, $(NEt_4)_2[ReBr_3(CO)_3]$ [1]

$[ReOCl_3(PPh_3)_2]$ [2]

$[Re(NPh)Cl_3(PPh_3)_2]$ [3]

$[ReCl_3(PPh_3)_2(NCMe)]$ [4]

$(NBu_4)[TcOCl_4]$ [5]

$[TcCl_4]$ [6]

6.2 Analytical methods

- All IR spectra were measured from KBr pellets on a *Shimadzu-FTIR 8300* spectrometer.
- The ^{1}H, ^{31}P, ^{13}C NMR spectra were recorded on a *JEOL-400MHz* nuclear magnetic resonance spectrometer (*Lambda*- software).
- Cyclic voltammetric studies were performed in acetonitrile solutions, containing tetra-n-butylammonium hexafluorophosphate (0.1 $molL^{-1}$) as supporting electrolyte, using a *Gamry PCI4-300* potentiostat board and *PHE200* software.
- The technetium content was measured by a *Beckman* LS6500 liquid scintillation counter.
- Carbon, hydrogen, nitrogen and sulfur contents were measured by a *Heraeus* (Vario EL) elemental analyzer.
- The ESI-TOF mass spectra were measured on an Agilent 6210 ESI-TOF, Agilent Technologies, Santa Clara, CA, USA. Solvent flow rate was adjusted to 4 µL/min, spray voltage set to 4 kV. Drying gas flow rate was set to 15 psi (1 bar). All other parameters were adjusted for a maximum abundance of the relative $[M+H]^+$.
- The FAB mass spectra were measured on a CH-5, Varian MAT, Bremen. Glycol (Metanitrotoluene, etc.) was used as matrix.
- Analytical HPLC was carried out on a LaChrom-HPLC L-7000 interface (**Merck**) equipped with two HPLC pumps L-7100, a diode array continuous flow detector L-7450 and an

autosampler L-7200 with 100µl sample loop. The following columns were used: *LUNATM C8(2)* column (10µm particle size ,300A° pore size 250×4.60 mm inner diameter, phenomenex®, USA) and Capcell C8(2) column (5µm particle size, 300 A° pore size, 250×460mm inner diameter, shiseido, Japan).

6.3 Syntheses

6.3.1 Ligands

6.3.1.1 [2-(1,3-Dioxolan-2-yl)benzene-1-yl]phosphines, II – IV

2-Phenyl-1,3-dioxolane (20 g, 87 mmol) was dissolved in 30 mL of THF and cooled to -70°C. To this solution, 65 mL of a 1.6 M solution of *n*-butyllithium (104 mmol) in *n*-hexane was added and stirred for 4 h. Thereafter, a solution of the related phosphine (chlorodiphenylphosphine (19 g, 87 mmol), dichlorophenylphosphine (7.8 g, 43.5 mmol), or phosphorus trichloride (3.9 g, 29 mmol)), in 50 mL of THF was added and the reaction mixture warmed up slowly to room temperature. After stirring for 14 h at room temperature, a saturated solution of NaCl in 40 mL of distilled water was added. The organic phase was separated and dried over $MgSO_4$. The residue obtained after removal of all volatiles under vacuum was recrystallized from 30 mL of ethanol. Yield: 18.4 g (63%) for **II**; 6.7 g (59%) for **III**; 9.3 g (67%) for **IV**.

[2-(1,3-Dioxolan-2-yl)benzene-1-yl]diphenylphosphine, **II**

^{1}H NMR (25° C, $CDCl_3$, ppm): δ 3.46 (m, 4H, CH_2), 6.12 (d, 1H, J_{PH} = 5.84 Hz), 6.9 – 7.76 (m, 14H, aromatic).

^{31}P NMR (25° C, $CDCl_3$, ppm): δ −20.1 (s).

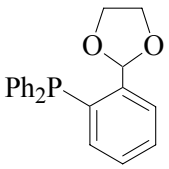

Bis[2-(1,3-dioxolan-2-yl)benzene-1-yl]phenylphosphine, **III**

^{1}H NMR (25° C, DMSO-d_6, ppm): δ 3.8 (m, 4H, CH_2), 4.0 (m, 4H, CH_2), 6.26 (d, 2H, CH, J_{PH} = 5.4 Hz), 6.5 – 7.6 (m, 13H, aromatic).

^{31}P-{^{1}H} NMR (25° C, DMSO-d_6, ppm): δ −27 (s).

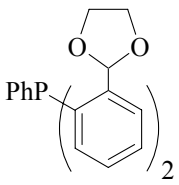

Tris[2-(1,3-dioxolan-2-yl)benzene-1-yl]phosphine, **IV**

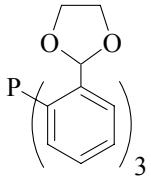

^{1}H NMR (25° C, DMSO-d_6, ppm): δ 3.7 – 3.8 (m, 6H, CH_2), 3.9 – 4.0 (m, 6H, CH_2), 6.16 (d, 3H, CH, J_{PH} = 5.4 Hz), 6.7 – 7.57 (m, 12H, aromatic).

^{31}P-{^{1}H} NMR (25° C, DMSO-d_6, ppm): δ −36.4 (s).

6.3.1.2 (2-Formylphenyl)phosphines, V – VII

[2-(1,3-Dioxolan-2-yl)benzene-1-yl]phosphines, (**II** (15 g, 45 mmol) or **IV** (15 g, 31 mmol)) and *p*-toluenesulfonic acid monohydrate (1 g, 0.5 mmol) were dissolved in 250 mL of acetone and heated for 3 h. After addition of 15 mL distilled water, the organic solvent (acetone) was removed under vacuum. During removal of acetonet pure crystalline product was obtained, which was filtered off and washed twice with distilled water. Yield: 12.4 g (95%) for **V**; 10.3 (95%) for **VII**.

(2-Formylphenyl)diphenylphosphine, **V**

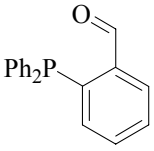

Elemental analysis:

Calcd. for $C_{19}H_{15}OP$ (290.3): C, 77.78; H, 5.21%.

Found: C, 78.6; H, 5.11%.

^{1}H NMR (25° C, DMSO-d_6, ppm): δ 6.8 – 8.0 (m, 14H, aromatic), 10.3 (d, 1H, CHO, J_{PH} = 4.4 Hz).

^{13}C NMR (25° C, DMSO-d_6, ppm): δ 129 – 134 (aromatic), 192.0 (CHO).

^{31}P-{^{1}H} NMR (25° C, DMSO-d_6, ppm): δ −9.3 (s).

IR (KBr, cm^{-1}): 3055 (m), 2827 (m), 1678 (st), 1581 (m), 1558 (m), 1458(m), 1431(m), 1396(m), 1292 (m), 1195 (m), 1122 (m), 1068 (w), 1022 (w), 844 (st), 752 (st), 698 (st), 671 (m), 505 (st).

MS (EI): m/z 290.1 ($[M]^+$, 49%), 261.1 ($[M\text{-}CHO]^+$, 97%).

Tris-(2-formylphenyl)phosphine, **VII**

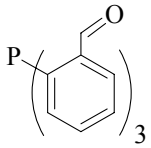

Elemental analysis:

Calcd. for $C_{21}H_{15}O_3P$ (346.3): C, 72.83; H, 4.37%.

Found: C, 70.06; H, 4.36%.

^{1}H NMR (25° C, DMSO-d_6, ppm): δ 6.8 – 8.1 (m, 12H, aromatic), 10.4 (d, 3H, CHO, J_{PH} = 4.9 Hz).
^{13}C NMR (25° C, DMSO-d_6, ppm): δ 129.4 – 139.5 (aromatic), 192.6 (d, J_{PC} = 57.6 Hz).
^{31}P-{^{1}H} NMR (25° C, DMSO-d_6, ppm): δ −19.9 (s).
MS (EI): *m/z* 346.1 ([M]$^{+}$, 36%), 317.1 ([M-CHO]$^{+}$, 66%).

Bis(2-formylphenyl)phenylphosphine, **VI**
III (10 g, 25 mmol) and p-toluenesulfonic acid monohydrate (0.5 g, 2.6 mmol) were dissolved in 250 mL of acetone and stirred at room temperature for 6 h. Then, 15 mL of distilled water was added and acetonewas removed by rotary evaporator at room temperature during which time a crystalline product precipitated, which was filtered off and washed twice with distilled water. Yield 10.5 g (59%).

Elemental analysis:
Calcd. for $C_{20}H_{15}O_2P$ (318.31): C, 75.47; H, 4.75%.
Found: C, 76.13; H, 4.66%.

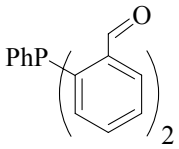

^{1}H NMR (25° C, DMSO-d_6, ppm): δ 6.8 – 8.5 (m, 13H, aromatic), 10.4 (d, 2H, CHO, J_{PH} = 4.88 Hz).
^{31}P-{^{1}H} NMR (25° C, DMSO-d_6, ppm): δ −15.2 (s).
IR (KBr, cm^{-1}): 3051 (w), 2820 (w), 2739 (w), 1693 (st), 1578 (m), 1558 (m), 1458 (w), 1435 (w), 1389 (w), 1292 (w), 1196 (st), 1126 (w), 1111 (w), 999 (w), 841 (w), 756 (st), 698 (m), 547 (w).

6.3.1.3 L^{11}

(1R,2R)-Cyclohexane-1,2-diamine (0.19 g, 1.7 mmol) and (2-formylphenyl)diphenyl phosphine (1g, 3.4 mmol) were dissolved in 5 mL of toluene and stirred at room temperature for 5 h. Then, the reaction solution was heated under reflux for 1 h. After removal of the solvent, the orange-red residue was recrystallized from MeOH to give a colourless solid. Yield 0.9 g (86%).

Elemental analysis:

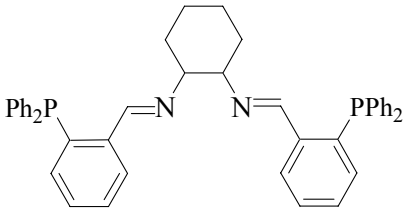

Calcd. for $C_{44}H_{40}N_2P_2$ (658.75): C, 80.22; H, 6.12; N, 4.25%.

Found: C, 80.18; H, 6.38; N, 4.27%.

^{1}H NMR (25° C, $CDCl_3$, ppm): δ 1.2-1.7 (m, 8H, CH_2), 3.1 (m, 2H, N-CH), 6.8-7.7 (m, 28H, aromatic), 8.68 (d, 2H, HC=N, J_{PH} = 4.28 Hz).

^{31}P-{^{1}H} NMR (25° C, $CDCl_3$, ppm): δ −13.15 (s).

IR (KBr, cm^{-1}): 3047 (m), 3004 (w), 2927 (st), 2854 (st), 1635 (st), 1581 (w), 1447 (w), 1431 (st), 1369 (m), 1342 (w), 1265 (w), 1203 (w), 1088 (m), 1026 (m), 933 (w), 748 (st), 698 (st), 501 (st).

MS (FAB$^+$): *m/z* 659 ([M+H]$^+$, 2%), 581 ([M-Ph]$^+$, 42%), 288 ([M-PPh$_2$]$^+$, 100%) .

6.3.1.4 L^{21}

(2-Formylphenyl)diphenylphosphine (1g, 3.4 mmol) was dissolved in 20 mL of EtOH and a solution of 1,2-ethylenediamine (0.1 g, 1.7 mmol) in 10 mL of EtOH added dropwise. The reaction mixture was stirred at room temperature for 1 h and subsequently heated for 3 h. After cooling down the reaction mixture, the product was filtered off and washed with EtOH. Yield 0.85 g (85%).

Elemental analysis:

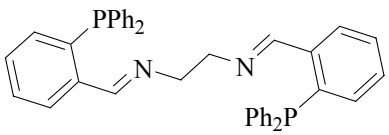

Calcd. for $C_{40}H_{34}N_2P_2$ (604.66): C, 79.45; H, 5.67; N, 4.63%.

Found: C, 77.31; H, 5.46; N, 4.6%.

^{1}H NMR (25° C, acetone-d_6, ppm): δ 3.5 (s, 4H, CH_2), 6.9 – 7.9 (m, 28H, aromatic), 8.7 (d, 2H, HC=N, J_{PH} = 4.52 Hz).

^{31}P-{^{1}H} NMR (25° C, acetone-d_6, ppm): δ −13 (s).

^{13}C NMR (25° C, acetone-d_6, ppm): δ 61.9 (CH_2), 129.0 – 140.5 (aromatic), 161.1 (d, C=N, J_{PC} = 75 Hz).

IR (KBr, cm^{-1}): 3051 (m), 3004 (w), 2920 (m), 2835 (m), 1632 (st), 1581 (w), 1477 (m), 1435 (st), 1365 (w), 1277 (w), 1184 (w), 1092 (w), 1064 (w), 1022 (w), 964 (w), 748 (st), 698 (st), 501 (st), 482 (st), 424 (w).

6.3.1.5 HL[31]

(2-Formylphenyl)diphenylphosphine (1 g, 3.45 mmol) and benzhydrazide (0.52 g, 3.48 mmol) were heated in 10 mL of EtOH for 2 h. The product was filtered off and washed twice with 3 mL of EtOH. Yield 1.2 g (86%).

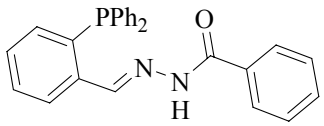

Elemental analysis:

Calcd. for $C_{26}H_{21}N_2OP$ (408.43): C, 76.46; H, 5.18; N, 6.86%.

Found: C, 75.28; H, 4.77; N, 7.1%.

^{1}H NMR (25° C, DMSO-d_6, ppm): δ 7.16 - 8.8 (m, 19H, aromatic), 9.18 (d, 1H, HC=N, J_{PH} = 4.86 Hz), 12.02 (s, 1H, NH).

^{13}C NMR (25° C, DMSO-d_6, ppm): δ 145.19 (d, HC=N, J_{PC} = 27 Hz), 163.05 (s, C=O).

^{31}P-{^{1}H} NMR (25° C, DMSO-d_6, ppm): δ −16.52 (s).

IR (KBr, cm^{-1}): 3209 (w), 3058 (w), 2923 (w), 1651 (st), 1554 (m), 139 (w), 1369 (w), 1284 (m), 1149 (w), 1080 (w), 748 (w), 694 (m).

MS (FAB$^+$): *m/z* 431 ([$PPh_2C_{14}H_{11}ON_2$+Na]$^+$, 14%), 409 ([$PPh_2C_{14}H_{11}ON_2$+ H]$^+$, 18%).

6.3.1.6 HL[41]

(2-Formylphenyl)diphenylphosphine (0.3 g, 1 mmol) and 4-phenylsemicarbazide (0.15 g, 1 mmol) were dissolved in 5 mL of EtOH and heated under reflux for 2 h. Upon cooling, a colourless solid precipitated, which was filtered off and washed with cold EtOH. Yield 0.4 g (90%).

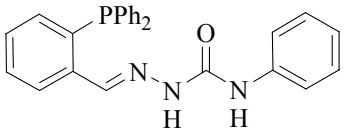

Elemental analysis:

Calcd. for $C_{26}H_{22}N_3OP$ (423.4): C, 73.75; H, 5.24; N, 9.92%.

Found: C, 73.52; H, 5.19; N, 9.90%.

^{1}H NMR (25° C, DMSO-d_6, ppm): δ = 6.79–7.28 (m, 19H, Ph), 8.56 (d, 1H, HC=N, J_{PH} = 4.58 Hz), 8.80 (s, 1H, NH), 10.86 (s, 1H, HN-N) ppm.

^{13}C NMR (25° C, DMSO-d_6, ppm): δ = 138.79 (C=O), 152.67 (C=N) ppm.

^{31}P-{^{1}H} NMR (25° C, DMSO-d_6, ppm): δ −14.04 (s).

IR (KBr): 3344 (w), 3317 (w), 3058 (w), 2916 (w), 2866 (w), 1681 (st), 1596 (m), 1535 (st), 1438 (m), 1157 (w), 1126 (1126), 752 (m), 694 (m).

6.3.1.7 $HL^{51}P$

A mixture of (2-formylphenyl)diphenylphosphine (1.5 g, 5.2 mmol) and 2-aminophenol (0.57 g, 5.2 mmol) was dissolved in 10 mL of ethanol and heated under reflux for 1.5 h. The product precipitated as a yellow powder, which was filtered off and washed with cold ethanol. Yield 1.6 g (82%).

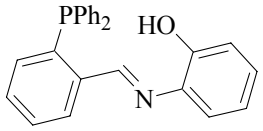

Elemental analysis:
Calcd. for $C_{25}H_{20}NOP$ (381.13): C, 78.73; H, 5.29; N, 3.67%.
Found: C, 78.92; H, 5.29; N, 3.51%.
^{1}H NMR (25° C, DMSO-d_6, ppm): δ 6.72 - 8.30 (m, 18H, aromatic), 8.78 (s, 1H, OH), 9.14 (d, 1H, HC=N, J_{PH} = 4.88 Hz).
^{13}C NMR (25° C, DMSO-d_6, ppm): δ 115 - 136 (aromatic), 156 (HC=N).
^{31}P-{^{1}H} NMR (25° C, DMSO-d_6, ppm): δ −12.9 (s).
IR (KBr, cm^{-1}): 3283 (st), 3043 (m), 3013 (w), 2881 (w), 1632 (st), 1581 (m), 1481 (st), 1431 (m), 1369 (w), 1281 (w), 1250 (st), 1270 (m), 1122 (w), 1026 (w), 968 (w), 883 (w), 856 (w), 744 (st), 698 (st), 602 (w), 509 (m), 482 (m).
MS (EI): *m/z* 381 ($[M]^+$, 83%), 304 ($[M\text{-}Ph]^+$, 100%).

6.3.1.8 $HL^{51}PO$

$HL^{51}P$ (1 g, 2.6 mmol) was dissolved in 5 mL of THF and H_2O_2 (0.3 mL, 30% wt) was added. After stirring the reaction mixture for 10 min, 10 mL of a saturated aqueous NaCl solution was added and the organic phase separated. The organic phase was dried over $MgSO_4$ and after removal of the solvent, $HL^{51}PO$ isolated as a yellow powder. Yield 0.98 g (95%).

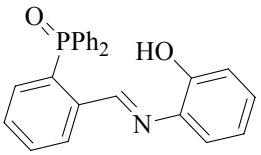

Elemental analysis:
Calcd. for $C_{25}H_{20}NO_2P$ (397.41): C, 75.56; H, 5.07; N, 3.52%.
Found: C, 75.68; H, 5.05; N, 3.61%.
^{1}H NMR (25° C, DMSO.d_6, ppm): δ 6.55 - 8.30 (m, 18H, aromatic), 8.9 (s, 1H, HC=N), 10.05 (s, 1H, OH).
^{31}P-{^{1}H} NMR (25° C, DMSO.d_6, ppm): δ 31.6 (s).
^{13}C NMR (25° C, DMSO.d_6, ppm): δ 156.20 (s, $C_{aromatic}$-OH), 164.1 (s, HC=N).

IR (KBr, cm^{-1}): 3420 (w), 3058 (m), 3024 (m), 1632 (m), 1578 (m), 1485 (s), 1435 (m), 1377 (w), 1354 (w), 1292 (m), 1223 (m), 1257 (s), 1157 (m), 1130 (m), 1111 (m), 1072 (m), 1029 (w), 968 (w), 767 (m), 748 (s), 702 (s), 578 (m), 540 (s).

6.3.1.9 H_2L^{51}

$HL^{51}P$ (1.4 g, 3.6 mmol) and $NaBH_4$ (0.91 g, 24 mmol) were suspended in 20 mL of EtOH and heated for 10 min. After the reaction solution became colorless, the solvent was removed under high vacuum and the product extracted with 50 mL of diethylether. The organic phase was washed with water and dried over $MgSO_4$. The colorless solid was obtained after removal of the solvent under vacuum. Yield 1.2 (88%).

Elemental analysis:
Calcd. for $C_{25}H_{22}NOP$ (383.4): C, 78.31; H, 5.78; N, 3.65%.
Found: C, 77.05; H, 5.42; N, 3.14%.

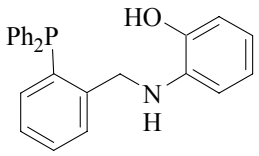

^1H NMR (25°C, DMSO-d_6, ppm): δ 4.36 (d, 2H, CH_2, J_{HH} = 5.24 Hz), 5.4 (t, 1H, NH J_{HH} = 5.84 Hz), 6.05 – 7.6 (m, 18H, aromatic), 9.2 (s, 1H, OH).
^{31}P-{^1H} NMR (25°C, DMSO-d_6, ppm): δ −16.6 (s).
IR (KBr, cm^{-1}): 3514 (w), 3425 (m), 3055(m), 2866 (w), 1604 (st), 1515 (st), 1438 (m), 1242 (m), 1192 (m), 1041 (w), 737 (st), 698 (m).

6.3.1.10 $H_2L^{52}P$

Bis(2-formylphenyl)phenylphosphine (1 g, 3.1 mmol) and 2-aminophenol (0.7 g, 6.2 mmol) were suspended in 10 mL of ethanol and heated under reflux for 1.5 h. The product precipitated as a yellow powder, which was filtered off and washed with cold ethanol. Yield 1.3 g (82%).

Elemental analysis:
Calcd. for $C_{32}H_{25}N_2O_2P$ (500.53): C, 76.79; H, 5.03; N, 5.60%.
Found: C, 77.31; H, 4.91; N, 5.62%.

^{1}H NMR (25° C, DMSO-d_6, ppm): δ 6.7 – 8.3 (m, 21H aromatic), 8.8 (s, 2H, OH), 9.1 (d, 2H, HCN, J_{PH} = 4.9 Hz).

^{31}P-{^{1}H} NMR (25° C, DMSO-d_6, ppm): δ −18.8 (s).

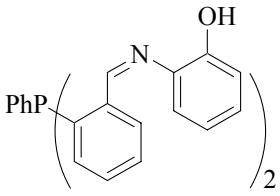

IR (KBr,cm^{-1}): 3441 (w), 3313 (w), 3051 (w), 2897 (w), 1624 (m), 1585 (m), 1485 (st), 1462 (w), 1435 (w), 1373 (w),1284 (w), 1254 (m), 1234 (m), 1207 (w), 1176 (w), 1149 (w), 1030 (w), 887 (w), 764 (st), 744 (m), 698 (we), 575 (w), 494 (m).

6.3.1.11 H_4L^{52}

$H_2L^{52}P$ (1.5 g, 3 mmol) and $NaBH_4$ (1.7 g, 48 mmol) were suspended in 20 mL of EtOH and heated. The reaction mixture turned to colorless within 10 min. Subsequently, the solvent was evaporated to dryness under vacuum and the product extracted by 50 mL of a THF/toluene mixture. The organic phase was washed with water and dried over $MgSO_4$. H_4L^{52} was isolated as a colorless solid after removal of the solvent under vacuum. Yield 1.3 g (86%).

Elemental analysis:

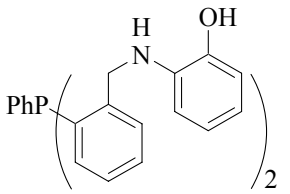

Calcd. for $C_{32}H_{29}N_2O_2P$ (504.56): C, 76.17; H, 5.79; N, 5.55%.

Found: C, 75.67; H, 5.93; N, 5.69%.

^{1}H NMR (25° C, DMSO-d_6, ppm): δ 4.4 (dd, 4H, CH_2), 5.4 (br, 2H, NH), 6.1 – 7.4 (m, 21H, aromatic), 9.2 (br, 2H, OH).

^{31}P-{^{1}H} NMR (25° C, DMSO-d_6, ppm): δ −27.4 (s).

IR (KBr, cm^{-1}): 3514 (w), 3425 (m), 3055 (w), 2866 (w), 1605 (m), 1516 (st), 1439 (m), 1354 (w), 1242 (m), 1192 (m), 1107 (m), 1041 (w), 832 (w), 736 (st), 698 (m).

6.3.1.12 $H_3L^{53}P$

Tris(2-formylphenyl)phosphine (1.5 g, 4.3 mmol) and 2-aminophenol (1.47 g, 13.5 mmol) were suspended in 4 mL of EtOH and heated for 2 h. The product was filtered off and washed with EtOH. Yield 2.2 g (83%).

Elemental analysis:

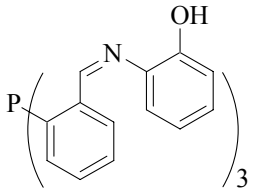

Calcd. for $C_{39}H_{30}N_3O_3P$ (619,65): C, 75.95; H, 4.88; N, 6.78%.

Found: C, 77.12; H, 4.78; N, 6.41%.

^{1}H NMR (25° C, DMSO-d_6, ppm): δ 6.6 – 8.3 (m, 24H, aromatic), 9.18 (d, 3H, CH=N, J_{PH} = 5.12 Hz).

^{31}P-{^{1}H} NMR (25° C, DMSO-d_6, ppm): δ −25.5 (s).

IR (KBr, cm^{-1}): 3556 (w), 3120 (st), 1635 (st), 1581 (st), 1485 (st), 1435 (m), 1380 (st), 1284 (st), 1257 (st), 1211 (st), 1173 (st), 1149 (st), 1088 (st), 1029 (m), 975 (w), 887 (st), 856 (m), 790(m), 752 (st), 686 (m), 582 (st), 540 (st), 516 (st), 428 (m).

6.3.1.13 H_6L^{53}

$H_3L^{53}P$ (1.5 g, 4.3 mmol) and $NaBH_4$ (1.8 g, 50 mmol) were suspended in 20 mL of EtOH and heated for 10 min. After removal of all volatiles, the product was extracted with 100 mL of a mixture of THF/toluene (10:1). The organic phase was washed twice with water and dried over $MgSO_4$. H_6L^{53} was obtained after removal of the solvent under high vacuum as a colorless solid. Yield 1.8 g (67%).

Elemental analysis:

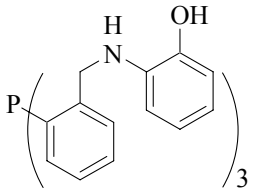

Calcd. for $C_{39}H_{36}N_3O_3P$ (625.70): C, 74.86; H, 5.80; N, 6.72%.

Found: C, 76.21; H, 5.67; N, 6.83%.

^{1}H NMR (25° C, DMSO-d_6, ppm): δ 4.3 (br, 6H, CH_2), 5.6 (br, 3H, NH), 6.1 – 7.5 (m, 24H, aromatic).

^{31}P-{^{1}H} NMR (25° C, DMSO-d_6, ppm): δ −37.05 (s).

IR (KBr, cm^{-1}): 3502 (st), 3433 (st), 3333 (st), 3058 (st), 2835 (st), 1601 (st), 1512 (st), 1443 (st), 1362 (st), 1250 (st), 1184 (st), 1111(st), 1041 (m), 987 (m), 953 (w), 914 (w), 814 (w), 741 (st), 625 (w), 548 (w), 474 (w).

6.3.1.14 (3-Amino-4-hydroxy)alcoholates, X-XI

(3-Amino-4-hydroxy)benzoic acid, **IX**, (2.5 g, 16.3 mmol) was dissolved in 200 mL of abs. alcohols (MeOH for **X** and EtOH for **XI**) and cooled to −10°C. To this solution,

thionylchloride (1.2 mL, 16.3 mmol) was added dropwise under stirring within 20 min. The resulting red-brown solution was heated under reflux for 5 h. All volatiles were removed under reduced pressure and the residue was dissolved in 200 mL of ethylacetate and washed twice with 100 mL of aqueous $NaHCO_3$ solution. After drying the organic phase over $MgSO_4$, the solvent was removed by rotary evaporation and the residue dried under vacuum for 3 h. Yields: 2.43 g (82%) for **X**; 2.3 g (84%) for **XI**.

(3-Amino-4-hydroxy)methylbenzoate, **X**

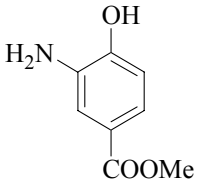

Elemental analysis:

Calcd. for $C_8H_9NO_3$ (167.16): C, 57.48; H, 5.43; N, 8.38%.

Found: C, 59.10; H, 5.33; N, 8.20%.

^{1}H NMR (25° C, $CDCl_3$, ppm): δ 2.16 (s, 3 H, CH_3), 7.45 – 6.75 (m, 3H, aromatic).

IR (KBr, cm^{-1}): 3406 (st), 3344 (st), 3283 (st), 2978 (st), 2673 (st), 2561 (s), 1720 (st), 1697 (st), 1609 (st), 1520 (st), 1474 (st), 1366 (st), 1292 (st), 1204 (st), 1107 (st), 899 (st), 814 (st), 764 (st), 718 (st), 640 (m), 598 (w), 451 (w).

(3-Amino-4-hydroxy)ethylbenzoate, **XI**

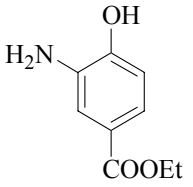

Elemental analysis:

Calcd. for $C_9H_{11}NO_3$ (181.1): C, 59.66; H, 6.12; N, 7.73%.

Found: C, 59.51; H, 6.03; N, 7.20%.

^{1}H NMR (25° C, $CDCl_3$, ppm): δ 1.36 (t, 3 H, CH3), 4.3 (q, 2 H, OCH2), 7.45 – 6.75 (m, 3H, aromatic)

IR (KBr, cm^{-1}): 3406 (st), 3344 (st), 3283 (st), 2978 (st), 2673 (st), 2561 (s), 1720 (st), 1697 (st), 1609 (st), 1520 (st), 1474 (st), 1366 (st), 1292 (st), 1204 (st), 1107 (st), 899 (st), 814 (st), 764 (st), 718 (st), 640 (m), 598 (w), 451 (w).

6.3.1.15 $HL^{51}PCOOR$ (R = H, Me, Et)

$HL^{51}PCOOR$ (R = H, Me, Et) were synthesized following the procedure applied for $HL^{51}P$. Yields: 1.12 g (86 %) for $HL^{51}Pet$ and 1.06 g (85%). $HL^{51}PCOOR$ (R = H, Me) were used directly for the synthesis of the next compounds.

$HL^{51}PCOOEt$.

Elemental analysis:

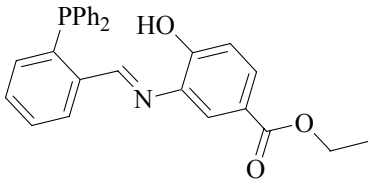

Calcd. for $C_{28}H_{24}NO_3P$ (453.5): C, 74.16; H, 5.33; N, 3.09%.

Found: C, 74.10; H, 3.30; N, 3.00%.

^1H NMR (25° C, $CDCl_3$, ppm): δ 1.36 (t, 3 H, CH_3), 4.3 (q, 2 H, OCH_2), 7.9 – 6.9 (m, 17 H, aromatic), 8.9 (d, 1 H, HC=N, J_{PH} = 4.5Hz.).

^{31}P-{^1H} NMR (25° C, $CDCl_3$, ppm): δ −10.7 (s).

IR (KBr, cm^{-1}): 3255 (m), 3051 (w), 2978 (w), 1705 (st), 1632 (m), 1589 (st), 1497 (m), 1435 (m), 1366 (m), 1285 (st), 1219 (st), 1200 (s), 1092 (st), 1018 (m), 756 (st), 702 (st), 498 (m).

$HL^{51}COOMe$.

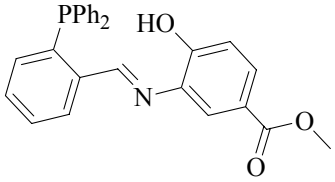

^{31}P-{^1H} NMR (25° C, $CDCl_3$, ppm): δ −11.4 (s).

6.3.1.16 $H_2L^{51}COOR$ (R = H, Me, Et)

The compound was synthesized following the procedure applied for H_2L^{51}. Yields: 0.43 g (86 %) for $H_2L^{51}COOEt$, 0.37 g (85%) for $H_2L^{51}COOMe$ and 0.35 g (81%) for$H_2L^{51}COOH$.

$H_2L^{51}COOEt$.

Elemental analysis:

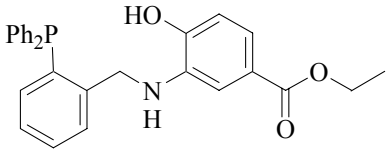

Calcd. for $C_{28}H_{26}NO_3P$ (453.5): C, 73.83; H, 5.75; N, 3.08%.

Found: C, 72.43; H, 5.62; N, 2.80%.

^1H NMR (25° C, $CDCl_3$, ppm): δ 1.36 (t, 3 H, CH_3), 4.3 (q, 2 H, OCH_2), 4.5 (d, 2 H, CH_2), 7.4 – 6.7 (m, 17 H,aromatic).

^{31}P-{^1H} NMR (25° C, $CDCl_3$, ppm): δ −18.8 (s).

IR (KBr, cm^{-1}): 3290 (m), 3051 (m), 2978 (m), 1709 (st), 1674 (st), 1601 (st), 1524 (st), 1435 (st), 1366 (m), 1265 (st), 1200 (st), 1107 (st), 1022 (m), 868 (w), 745 (st), 694 (st), 502 (w).

$H_2L^{51}COOMe$.

Elemental analysis:

Calcd. for $C_{27}H_{24}NO_3P$ (441.5): C, 73.46; H, 5.48; N, 3.17%.

Found: C, 74.10; H, 5.41; N, 3.02 %.

^{1}H NMR (25° C, DMSO-d_6, ppm): δ 4.5 (s, 3H, OMe), 4.6 (s, 2H, CH_2), 5.3 (m, 1H, NH), 6.4 – 7.7 (m, 17H, aromatic), 8.9 (s, 1H, OH).

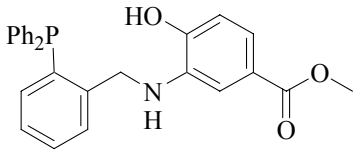

^{31}P-{^{1}H} NMR (25° C, DMSO-d_6, ppm): δ −17.1 (s).

IR (KBr, cm^{-1}): 3445 (m), 3236 (m), 3055 (w), 2962 (m), 1674 (st), 1572 (st), 1431 (st), 1481 (st), 1400 (st), 1354 (w), 1288 (st), 1257 (st), 1211 (st), 1026 (st), 1103 (st), 972 (w), 860 (w), 802 (st), 764 (st), 744 (st), 698 (st).

$H_2L^{51}COOH$.

Elemental analysis:

Calcd. for $C_{26}H_{22}NO_3P$ (427.4): C, 73,06; H, 5,19; N, 3,28%.

Found: C, 74.10; H, 5.01; N, 3.37 %.

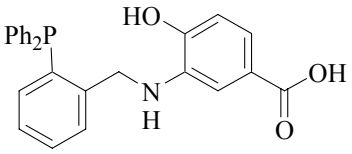

^{1}H NMR (25° C, DMSO-d_6, ppm): δ 4.2 (s, 2H, CH_2), 5.6 (m, 1H, NH), 6.5 – 7.6 (m, 17H, aromatic), 10.2 (br, 1H, OH), 12.1 (br, 1H, COOH)

^{31}P-{^{1}H} NMR (25° C, DMSO-d_6, ppm): δ −20.1 (s).

IR (KBr, cm^{-1}): 3433 (w), 3205 (m), 3055 (m), 2978 (w), 1697 (st), 1674 (st), 1601 (st), a527 (m), 1454 (m), 1435 (m), 1358 (m), 1292 (st), 1257 (st), 1207 (m), 1119 (w), 1065 (w), 744 (m), 698 (m).

6.3.1.17 (2-(N-BOC-Aminophenyl))phosphines, XIII-XV

tert-Butyl-N-phenylcarbamate (10 g, 52 mmol) was suspended in 80 mL of diethylether and cooled to -20°C. 60 mL of a 1.7 N tert-butyllithum in *n*-pentane were added and stirred for 3 h. The reaction mixture was cooled to -70°C and a solution of the phosphine (chlorodiphenylphosphine (11.4 g, 52 mmol), dichlorophenylphosphine (4.6 g, 26 mmol) or phosphorus trichloride (2.3 g, 17 mmol)) in 40 mL of diethylether was added dropwise. The reaction mixture was warmed to room temperature and stirred for 7 h. Subsequently, 50 mL of a saturated aqueous NaCl solution was added. The organic phase was separated and dried over $MgSO_4$. After removal of the solvent, the residue was crystallized from 30 mL of a mixture of *n*-hexane/ethanol (2:1). Yield: 16.2 g (83%) for **XIII**; 17.3 g (68%) for **XIV**; 15 g (71%) for **XV**.

(2-(N-BOC-Aminophenyl))diphenylphosphine, **XIII**

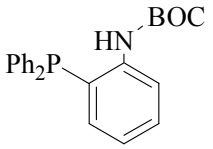

Elemental analysis:

Calcd. for $C_{23}H_{24}NO_2P$ (377.42): C, 77.96; H, 5.82; N, 5.05%.

Found: C, 79.10; H, 5.82; N, 4.91%

^{1}H NMR (25° C, $CDCl_3$, ppm): δ 1.5 (s, 9H, CH_3), 7.1- 7.4 (m, 14H, aromatic).

^{31}P-{^{1}H} NMR (25° C, $CDCl_3$, ppm): δ −22.1 (s).

Bis(2-(N-BOC-aminophenyl))phenylphosphine, **XIV**

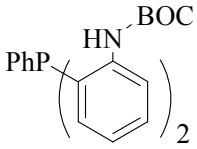

Elemental analysis:

Calcd. for $C_{28}H_{33}N_2O4P$ (492.5): C, 68.28; H, 6.75; N, 5.69%.

Found: C, 70.21 ; H, 6.55; N, 5.83%.

^{31}P-{^{1}H} NMR (25° C, $CDCl_3$, ppm): δ −25.6 (s).

Tris(2- (N-BOC-aminophenyl))phosphine, **XV**

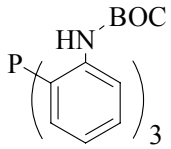

Elemental analysis:

Calcd. for $C_{33}H_{42}N_3O_3P$ (607.7): C, 65.22; H, 6.97; N, 6.91%.

Found: C, 66.51; H, 6.56; N, 7.22%.

^{31}P-{^{1}H} NMR (25° C, DMSO-d_6, ppm): δ. −33.3 (s).

6.3.1.18 (2-Aminophenyl)phosphines, XVI-XVIII

(2-(N-BOC-Aminophenyl))phosphines, **(XIII** (15 g, 50 mmol), **XIV** (12 g, 25 mmol) or **XV** (10 g, 17 mmol)) and *p*-toluenesulfonic acid monohydrate (19 g, 0.1 mol) were dissolved in 200 mL of THF, warmed up to 40°C and stirred for 5 h. After cooling the reaction mixture to ambient temperature, the precipitated product was filtered off and washed twice with cold THF. The remaining colorless solid was dissolved in 100 mL methanolic solution of sodium hydroxide (2 g, 50 mmol). After stirring the reaction mixture for 2 h, the resulting colorless precipitate was filtered off and washed with 10 mL of cold MeOH. Yield: 8.8 g (95%) for **XIX**, 4.3 g (73%) for **XX**, 5.3 g (71%) for **XXI**.

(2-Aminophenyl)diphenylphosphine, **XIX**

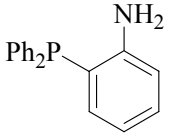

Elemental analysis:

Calcd. for $C_{18}H_{16}NP$ (277.3): C, 77.96; H, 5.82; N, 5.05%.

Found: C, 77.69; H, 5.91; N, 5.14%.

^{1}H NMR (25° C, acetone-d_6, ppm): δ 5.6 (br, 2H, NH_2), 6.5 – 7.4 (m, 14H, aromatic).

^{31}P-{^{1}H} NMR (25° C, acetone-d_6, ppm): δ −23.4 (s).

IR (KBr): 3418 (m), 3325 (m), 3198 (w), 3059 (m), 3009 (w), 1616 (st), 1585 (st), 1562 (m), 1473 (st), 1435 (st), 1296 (m), 1250 (w), 1176 (w), 1088 (w), 1026 (w), 1065 (w), 995 (w), 748 (st), 698 (st), 478 (m), 451 (w).

Bis(2-aminophenyl)phenylphosphine, **XX**

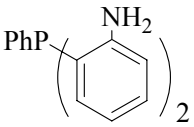

Elemental analysis:

Calcd. for $C_{18}H_{17}N_2P$ (292.3): C, 73.96; H, 5.86; N, 9.58%.

Found: C, 74.1; H, 5.65; N,.9.83%

^{1}H NMR (25° C, acetone-d_6, ppm): δ 4.6 (s, 4H, NH), 6.4 – 7.2 (m, 13H, aromatic).

^{31}P-{^{1}H} NMR (25° C, acetone-d_6, ppm): δ −35.3 (s).

IR (KBr, cm^{-1}): 3445 (m), 3356 (m), 3313 (m), 3059 (w), 3009 (w), 1612 (st), 1585 (m), 1562 (m), 1473 (st), 1439 (st), 1299 (m), 1250 (w), 1157 (w), 1142 (w), 1088 (w), 1022 (w), 752 (st), 698 (m), 482 (m).

Tris(2-aminophenyl)phosphine, **XXI**

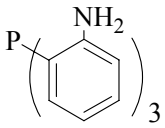

Elemental analysis:

Calcd. for $C_{18}H_{18}N_3P$ (307.3): C, 70.35; H, 5.90; N, 13.67%.

Found: C, 71.56; H, 5.78; N, 13.33%.

^{1}H NMR (25° C, acetone-d_6, ppm): δ 4.7 (br, 6H, NH), 6.5 – 7.2 (m, 12H, aromatic).

^{31}P-{^{1}H} NMR (25° C, acetone-d_6, ppm): δ −52.8 (s).

IR (KBr, cm^{-1}): 3441 (m), 3348 (m), 3213 (w), 3055 (w), 1616 (st), 1562 (m), 1473 (st), 1443 (st), 1304 (m), 1250 (w), 1157 (w), 752 (m), 694 (w), 575 (w), 521 (w).

6.3.1.19 $HL^{61}P$

(2-Aminophenyl)diphenylphosphine (1.5 g, 5.4 mmol) and salicylaldehyde (0.65 g, 5.4 mmol) were dissolved in 5 mL of EtOH. After addition of 0.1 mL formic acid, the reaction solution was heated for 1.5 h. The yellow microcrystalline compound $HL^{61}P$ was isolated by slow evaporation of the solvent at room temperature. Yield 1.5 g (71%).

Elemental analysis:

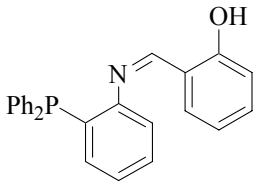

Calc. for $C_{25}H_{20}NOP$ (381.4): C, 78.73; H, 5.29; N, 3.67%.

Found: C, 77.72; H, 5.10; N, 3.77%.

^{1}H NMR (25° C, DMSO-d_6, ppm): δ 6.7 – 7.5 (m, 18H, aromatic), 8.8 (s, 1H, CH=N), 12.4 (br, 1H, OH).

^{31}P-{^{1}H} NMR (25° C, DMSO-d_6, ppm): δ −15.4 (s).

6.3.1.20 H_2L^{61}

A suspension of $HL^{61}P$ (1.5 g, 3.9 mmol) and $NaBH_4$ (1.1 g, 31 mmol) in 15 mL of EtOH was heated for 10 min under reflux. After removal of the solvent under high vacuum, the product was extracted by 50 mL of diethylether. The organic phase was washed twice with an aqueous solution of NH_4Cl and dried over $MgSO_4$. After removal of the solvent under vacuum, a colorless solid was obtained. Yield 1.3 g (88%).

Elemental analysis:

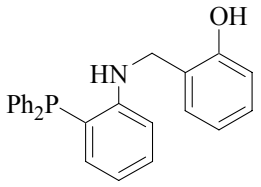

Calcd. for $C_{25}H_{22}NOP$ (383.42): C, 78.31; H, 5.78; N, 3.65%.

Found: C, 77.31; H, 5.64; N, 3.82%.

^{1}H NMR (25° C, DMSO-d_6, ppm): δ 4.3 (d, 2H, CH_2, J_{HH} = 5.8 Hz), 5.7 (m, 1H, NH), 6.4 – 7.5 (m, 18H, aromatic), 9.6 (s, 1H, OH).

^{13}C NMR (25° C, DMSO-d_6, ppm): δ 42.1 (CH_2), 114.9 – 155.1 (aromatic).

^{31}P-{^{1}H} NMR (25° C, DMSO-d_6, ppm): δ −22.3 (s).

IR (KBr, cm^{-1}): 3371 (m), 3278 (m), 2854 (w), 1581 (st), 1489 (st), 1442 (st), 1242 (m), 1165 (m), 1095 (m), 1034 (w), 748 (st), 694 (m), 478 (w).

6.3.1.21 $H_2L^{62}P$

Bis(2-aminophenyl)phenylphosphine (1.5 g, 5.1 mmol) and salicylaldehyde (0.62 g, 5.1 mmol) were dissolved in 5 mL of EtOH. After addition of 0.1 mL formic acid, the reaction solution was heated for 1.5 h under reflux. The product precipitated as a yellow solid, which was filtered off and washed with EtOH. Yield 2.1 g (82%).

Elemental analysis:

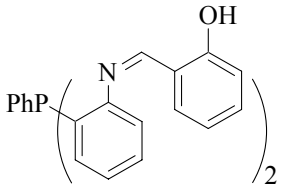

Calcd. for $C_{32}H_{25}N_2O_2P$ (500.53): C, 76.79; H, 5.03; N, 5.60%.

Found: C, 78.11; H, 4.94; N, 5.27%.

^{1}H NMR (25° C, acetone-d_6, ppm): δ 6.8 – 7.5 (m, 21H, aromatic), 8.6 (s, 2H, HC=N), 12.4 (s, 2H, OH).

^{31}P-{^{1}H} NMR (25° C, acetone-d_6, ppm): δ −26.8 (s).

IR (KBr, cm^{-1}): 3051 (m), 1608 (st), 1554 (st), 1489 (st), 1458 (st), 1435 (st), 1365 (st), 1273 (w), 1223 (m), 1180 (st), 1149 (m), 1119 (w), 1092(w), 1030 (w), 976 (w), 906 (w), 845 (m), 787 (st), 756 (st), 698 (st), 644 (w), 493 (m).

6.3.1.22 H_4L^{62}

$H_2L^{62}P$ (1.5 g, 3 mmol) and $NaBH_4$ (1.7 g, 48 mmol) were suspended in 20 mL of EtOH and heated for 10 min under reflux. After the reaction solution became colorless, the solvent was removed under high vacuum and the product extracted with 30 mL of a THF/diethylether mixture. The organic phase was washed with water and dried over $MgSO_4$. After removal of the solvent, H_4L^{62} was isolated as a colorless powder. Yield 1.2 g (82%).

Elemental analysis:

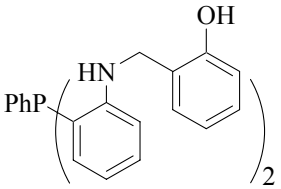

Calcd. for $C_{32}H_{29}N_2O_2P$ (504.56): C, 76.17; H, 5.79; N, 5.55%.

Found: C, 75.56; H, 5.66; N, 5.78%.

^{1}H NMR (25° C, acetone-d_6, ppm): δ 4.4 (d, 4H, CH_2, J_{HH} = 5.84 Hz), 5.4 (m, 2H, NH), 6.6 – 7.6 (m, 21H, aromatic), 8.6 (s, 2H, OH).

^{31}P-{^{1}H} NMR (25° C, acetone-d_6, ppm): δ −37.4 (s).

IR (KBr, cm^{-1}): 3371 (m), 3290 (m), 3067 (m), 2858 (m), 2384 (m), 1589 (st), 1570 (st), 1493 (st), 1450 (st), 1354 (m), 1319 (m), 1242 (st), 1165 (m), 1103 (m), 1072 (m), 1038 (m), 841 (w), 748 (st), 694 (m), 605 (w), 486 (m).

6.3.1.23 $H_3L^{63}P$

Tris(2-aminophenyl)phosphine (1.5 g, 4.8 mmol) and salicylaldehyde (1.7 g, 14.4 mmol) were dissolved in 5 mL of EtOH. After addition of 0.1 mL formic acid, the reaction solution was heated for 1.5 h under reflux. The product precipitated as a yellow solid, which was filtered off and washed with EtOH. Yield 2.4 g (82%).

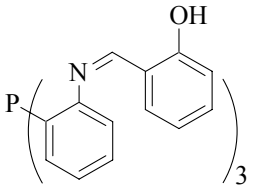

Elemental analysis:
Calcd. for $C_{39}H_{30}N_3O_3P$ (619.6): C, 75.59; H, 4.88; N, 6.78%.
Found: C, 74.84; H, 4.88; N, 7.12%.
^{1}H NMR (25° C, $CDCl_3$, ppm): δ 6.7 – 7.3 (m, 24H, aromatic), 8.3 (s, 3H, HC=N), 12.0 (s, 3H, OH)
^{31}P-{^{1}H} NMR (25° C, $CDCl_3$, ppm): δ −32.8 (s).
IR (KBr, cm^{-1}): 3545 (w), 3344 (w), 3051 (w), 2827 (w), 1651 (m), 1612 (st), 1566 (st), 1462 (st), 1434 (st), 1369 (m), 1272 (st), 1184 (m), 1153 (m), 1118 (w), 1060 (w), 1033 (w), 975 (st) (w), 906 (m), 844 (m), 760 (st), 648 (w), 486 (m).

6.3.1.24 H_6L^{63}

$H_3L^{63}P$ (1.5 g, 2.4 mmol) and $NaBH_4$ (2.2 g, 57 mmol) were suspended in 30 mL of EtOH and heated for 10 min under reflux. After the reaction solution became colorless, the solvent was removed under high vacuum and the product was extracted with 15 mL of a THF/toluene mixture (10: 1). The organic phase was washed with water and dried over $MgSO_4$. After removal of the solvent, H_6L^{63} was isolated as a colorless powder. Yield 1.15 g (76%).

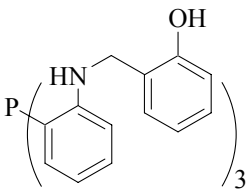

Elemental analysis:
Calcd. for $C_{39}H_{36}N_3O_3P$ (625.7): C, 74.86; H, 5.80; N, 6.72%.
Found: C, 75.25; H, 5.66; N, 7.31%.
^{1}H NMR (25° C, acetone-d_6, ppm): δ 4.3 (d, 6H, CH_2, J_{HH} = 5.6 Hz), 5.3 (m, 3H, NH), 6.6 – 7.2 (m, 24H, aromatic), 8.6 (s, 3H, OH)
^{31}P-{^{1}H} NMR (25° C, acetone-d_6, ppm): δ −55.9 (s).

IR (KBr, cm^{-1}): 3545 (w), 3344 (w), 3051 (w), 2827 (m), 1612 (st), 1566 (st), 1462 (st), 1435 (m), 1369 (m), 1272 (w), 1184 (m), 1153 (m), 1118 (w), 1060 (w), 975 (w), 906 (w), 844 (w), 760 (st), 648 (w), 486 (w).

6.3.1.25 HL^1

(2-Formylphenyl)diphenylphosphine (2.9 g, 10 mmol) and NBH_4 (3.0 g, 80 mmol) were suspended in 10 mL of EtOH and heated for 10 min under reflux. After removal of all volatiles, the residue was suspended in 5 mL of distilled water and extracted with 30 mL of diethylether. The organic phase was dried over $MgSO_4$ and a colorless solid was isolated after removal of the solvent under high vacuum. Yield 2.3 g (70%).

Elemental analysis:
Calcd. for $C_{19}H_{17}OP$ (292.3): C, 78.07; H, 5.86%.
Found: C, 78.07; H, 5.86%.

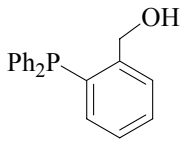

^{1}H NMR (25° C, acetone-d_6, ppm): δ 4.3 (br, 1H, OH), 4.78 (d, 2H, CH_2, J_{PH} = 4.8 Hz), 6.8 – 7.7 (m, 14H, aromatic).
^{31}P-{^{1}H} NMR (25° C, acetone-d_6, ppm): δ –19.3 (s).
IR (KBr, cm^{-1}): 3329 (st), 3024 (st), 2923 (st), 2866 (st), 1963 (w), 1894 (w), 1821 (w), 1716 (m), 1589 (m), 1566 (w), 1473 (m), 1435 (m), 1335 (m), 1269 (w), 1161 (m), 1119 (m), 1022 (m), 953 (w), 744(w), 694 (w), 544 (w).

6.3.1.26 H_3L^3

Tris(2-formylphenyl)phosphine (2.9 g, 10 mmol) and $NaBH_4$ (3.0 g, 80 mmol) were suspended in 10 mL of EtOH and heated for 10 min under reflux. After the reaction mixture turned to a colorless solution, the solvent was removed under vacuum. The residue was suspended in 5 mL of water and extracted with THF. The organic phase was dried over $MgSO_4$ and a colorless solid was isolated after removal of the solvent under high vacuum. Yield 2.6 g (74%).

Elemental analysis:

Calcd. for $C_{21}H_{21}O_3P$ (352.36): C, 71.58; H, 6.01%.

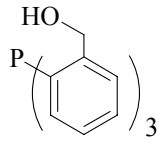

Found: C, 71.55; H, 6.03%.

^{1}H NMR (25° C, DMSO-d_6, ppm): δ 4.5 (d, 6H, CH_2, J_{PH} = 4.8 Hz), 5.2 (t, 3H, OH), 6.6 – 7.6 (m, 12H, aromatic).

^{13}C NMR (25° C, DMSO-d_6, ppm): δ 60.9 (CH_2), 126.2 – 132.3 (aromatic).

^{31}P-{^{1}H} NMR (25° C, DMSO-d_6, ppm): δ −38.3 (s).

IR (KBr, cm^{-1}): 3448 (m), 3190 (m), 3047 (m), 2927 (m), 2870 (m), 1462 (m), 1434 (m), 1354 (w), 1200 (m), 1126 (w), 1068 (w), 1038 (m), 995 (st), 952 (w), 879 (w), 822 (w), 756 (st), 671 (w), 601 (m), 505 (m), 471 (w).

6.3.2 Complexes of rhenium and technetium

6.3.2.1 [ReOCl(L^{11a})](μ-O)[$ReOCl_2$(L^{11b})], [ReOCl(L^{11b})$_2$]

(NBu_4)[$ReOCl_4$] (58 mg, 0.1 mmol) and L^{11} (66 mg, 0.1 mmol) were dissolved at ambient temperature in 4 mL of MeOH. After 30 min, a gelatine like solid was formed, which redissolved in MeOH after a few minutes. After stirring the reaction mixture for 2 h at room temperature, a dark brown precipitate was obtained, which was filtered off and washed with MeOH. Recrystallization of the obtained solid from a CH_2Cl_2/MeOH mixture gave **1** as the main product and **2** as few crystals. The crystals were separated mechanically. Yield 40 mg (46%) for **1**.

[ReOCl(L^{11b})$_2$], (**1**)

Elemental analysis:

Calcd. for $C_{40}H_{36}ClO_5P_2Re$ (880.32): C, 54.57; H, 4.12%.

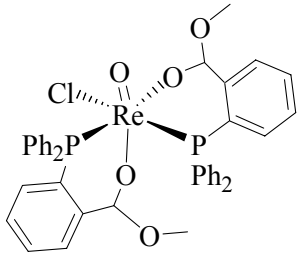

Found: C, 56.38; H, 4.10%.

^{1}H NMR (25° C, DMSO - d_6, ppm): δ 1.7 (s, 6H, CH_3), 7.2 – 8.0 (m, 28H, aromatic), 10.6 (s, 2H, CH).

^{31}P-{^{1}H} NMR (25° C, DMSO-d_6, ppm): δ 29.9 (s).

IR (KBr, cm^{-1}): 3059 (w), 2826 (w), 1481 (w), 1435 (m), 1308 (st), 1242 (st), 1120 (st), 1130 (st), 1099 (st), 1061 (m), 984 (st), 933 (m), 748 (m), 698 (m), 517 (m), 440 (w).

MS (ESI): *m/z* 881 ([M+H]$^+$, 100%).

[$ReOCl(L^{11a})$](μ-O)[$ReOCl_2(L^{11b})$], (**2**)

Since just a few crystals of this compound were obtained from the recrystallization of the product, analysis of the complex was just done by X-ray diffraction.

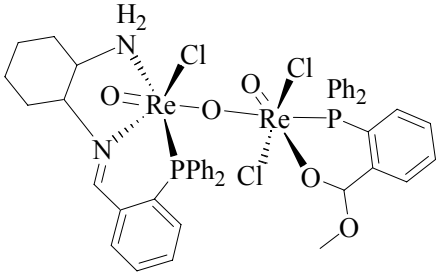

6.3.2.2 [{$ReOCl_2(OMe)$}$_2$(μ-L^{21})], (3)

(NBu_4)[$ReOCl_4$] (58 mg, 0.1 mol) was dissolved in 5 mL of MeOH. L^{21} (30 mg, 0.05 mmol) was added. The color of the solution turned from green to brownish red. The obtained solid was filtered off and washed with MeOH. Red crystals of [{$ReOCl_2(OMe)$}$_2$(μ-L^{21})] (**3**) were isolated by recrystalization of the product from nitromethane. Yield 40 mg (65%).

Elemental analysis:

Calcd. for $C_{42}H_{40}C_{l4}N_2O4P_2Re_2$ (1212.9): C, 41.59; H, 3.32; N, 2.31%.

Found: C, 40.23; H, 3.16; N, 2.56%.

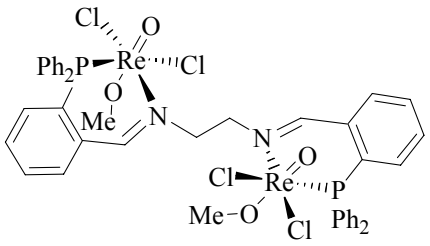

^{1}H NMR (25° C, DMSO-d_6, ppm): δ 3.6 (s, 4H, CH_2), 7.1 – 8.2 (m, 28H, aromatic), 8.9 (s, 2H, HC=N).

^{31}P-{^{1}H} NMR (25° C, DMSO-d_6, ppm): δ −1.3 (s).

IR (KBr, cm^{-1}): 3055 (m), 2959 (st), 2874 (m), 1616 (st), 1562 (w), 1481 (m), 1435 (st), 1308 (w), 1192 (w), 1099 (st), 948 (st), 945 (st), 748 (st), 694 (st), 536 (st), 509 (m).

6.3.2.3 [ReOCl(OMe)(L^{31})], (4)

(NBu_4)[$ReOCl_4$] (58 mg, 0.1 mmol) and HL^{31} (47 mg, 0.1 mmol) were dissolved in 5 mL of MeOH and stirred at room temperature for 2 h. During this time, a green solid precipitated from the reaction solution. The green product was filtered off and washed with MeOH. By recrystallization of the product from THF, a green crystalline compound, [ReOCl(OMe)(L^{31})], was obtained. (Caution: The reaction should not be heated in any step). Yield 47 mg (71%).

Elemental analysis:

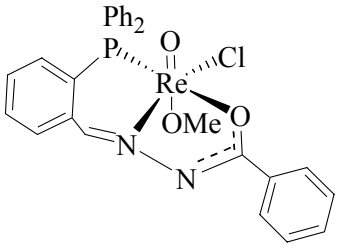

Calcd. for $C_{27}H_{23}ClN_2O_3PRe$ (676.12): C, 47.96; H, 3.43; N, 4.14%.

Found: C, 50.33; H, 3.37; N, 4.04%.

^{1}H NMR (25° C, $CDCl_3$, ppm): δ 2.3 (s, 3H, CH_3), 7.2 – 8.4 (m, 19H, aromatic), 9.0 (s, 1H, HC=N).

^{31}P-{^{1}H} NMR (25° C, $CDCl_3$, ppm): δ 6.5 (s).

IR (KBr, cm^{-1}): 3058 (w), 2912 (w), 2812 (w), 1612 (w), 1493 (st), 1435 (st), 1392 (m), 1350 (st), 1103 (st), 933 (st), 995 (w), 698 (m), 490 (w).

MS (ESI): *m/z* 641 ([M-Cl]$^+$, 100%), 699 ([M+Na]$^+$, 50%).

6.3.2.4 [ReO(L^{31a})(Et$_2$btu)], (5)

HEt_2bu (24 mg, 0.1 mmol) was added as a solid to a solution of [ReOCl(OMe)(L^{31})] in 5 mL of CH_2Cl_2 and the mixture was stirred for 5 min. NEt_3 (0.1 mL) was added and the resulting red-brown solution stirred at room temperature for 1 h. The solvent was removed under reduced pressure and the red brown residue was dissolved in 3 mL of MeOH. This solution was stirred at ambient temperature for 10 min, whereupon a red microcrystalline solid precipitated. Single crystals suitable for X-ray crystallography were obtained by recrystallization of the product from Me_2CO/CH_2Cl_2. Yield 46 mg (48%).

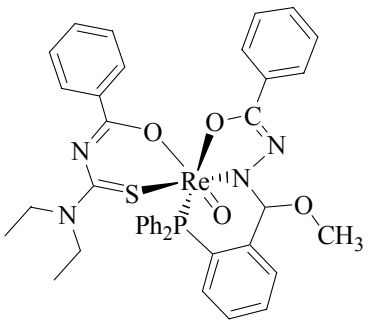

Elemental analysis:

Calcd. for $C_{48}H_{39}N_3O_4PReS$ (971.1): C, 59.37; H, 4.05; N, 4.33; S, 3.30 %.

Found: C, 61.30; H, 3.96; N, 4.28; S, 3.28 %.

^{1}H NMR (25° C, $CDCl_3$, ppm): δ 1.2 (t, 3H, CH_3), 1.4 (t, 3H, CH_3), 2.8 (s, 3H, OCH_3), 3.7 – 4.2 (m, 4H, CH_2), 6.4 (s, 1H, CH), 6.8 – 7.8 (m, 24H, aromatic)

^{31}P-{^{1}H} NMR (25° C, $CDCl_3$, ppm): δ 18.2 (s).

IR (KBr, cm^{-1}): 3051 (w), 2945 (w), 2324 (w), 2881 (w), 1497 (st), 1416 (st), 1358 (m), 1311 (w), 1257 (w), 1203 (w), 1122 (w), 1095 (m), 1065 (m), 999 (w), 933 (m), 748 (w), 710 (m), 690 (m), 532 (m), 517 (m).

6.3.2.5 [ReOCl(OMe)(L^{41})], (6)

$(NBu_4)[ReOCl_4]$ (58 mg, 0.1 mmol) was dissolved in 3 ml MeOH and HL^{41} (42 mg, 0.1 mmol) was added to this solution. After stirring for 1 h at room temperature, a microcrystalline, red-purple precipitate was filtered off and washed with methanol. Recrystallization from a CH_2Cl_2/methanol mixture gave red blocks of pure $[ReOCl(OMe)(L^{41})]$ (**6**). (Caution: The reaction should not be heated in any step). Yield 47 mg (68%).

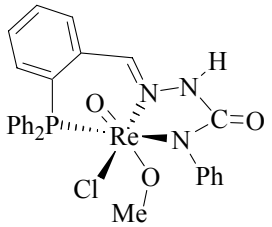

Elemental analysis:

Calcd. for $C_{27}H_{24}N_3O_3PReCl$ (691.1): C, 46.91; H, 3.52; N, 6.11%.

Found: C, 47.82; H, 3.61; N, 6.14%.

^{1}H NMR (25° C, DMSO-d_6, ppm): δ 2.5 (s, 3H, CH_3), 7.2-8.0 (s, 19H, aromatic.) 8.65 (s, 1H, HC=N) , 12.1 (s, 1H, N-NH) ppm.

^{13}C NMR (25° C, DMSO-d_6, ppm): δ 175.15 (C=O), 164.8 (C=N.) ppm.

^{31}P-{^{1}H} NMR (25° C, DMSO-d_6, ppm): δ 0.67 (s).

IR (KBr, cm^{-1}): 3425 (w), 3055 (w), 2904 (w), 2808 (w), 1635 (st), 1596 (m), 1531 (w), 1488 (m), 1435 (m), 1354 (st), 1215 (w), 1153 (w), 1122 (m), 937 (st), 756 (m), 698 (m), 509 (m).

6.3.2.6 [$ReOCl(PPh_3)(L^{51}PO)$], (7); [$ReCl_3(NC_6H_4OH)(PPh_3)_2$], (8)

$[ReOCl_3(PPh_3)_2]$ (0.17 g, 0.2 mmol) and $HL^{51}PO$ (79 mg, 0.2 mmol) were dissolved in 20 mL of THF and heated for 2 h under reflux. Then the volume of the solution was reduced to 3 mL. By cooling the reaction solution to −10°C, two different types of crystalline products, red $[ReOCl(PPh_3)(L^{51}PO)]$ (**7**) and green $[ReCl_3(NC_6H_4OH)(PPh_3)_2]$ (**8**) were isolated and separated mechanically.

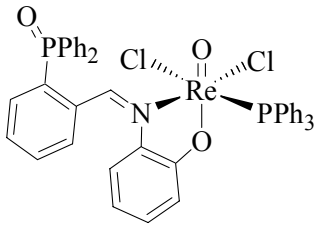

$[ReOCl(PPh_3)(L^{51}PO)]$, (**7**).

Elemental analysis:

Calcd. for $C_{43}H_{34}Cl_2NO_3P_2Re$ (931.7): C, 55.43; H, 3.68; N, 1.50%.

Found: C, 53.87; H, 3.66; N, 1.62%.

^{1}H NMR (25° C, DMSO-d_6, ppm): δ 6.85 - 8.04 (m, 33H, aromatic), 10.58 (s, 1H, HC=N).

^{31}P-{^{1}H} NMR (25° C, DMSO-d_6, ppm): δ 26.08 (s, PPh_3), 29.44 (s, $OPPh_2$).

IR (KBr, cm^{-1}): 3055 (m), 2851 (w), 1697 (w), 1589 (w), 1566 (w), 1477 (m), 1431 (st), 1194 (m), 1161 (m), 1095 (m), 1068 (w), 1026 (w), 941 (w), 748 (st), 694 (st), 517 (st).
MS (FAB^+): *m/z* 896 ($[M\text{-}Cl]^+$, 1%), 635 ($[M\text{-}C_{18}H_{14}PCl]^+$, 3%).

$[ReCl_3(NC_6H_4OH)(PPh_3)_2]$, (**8**)
Elemental analysis:
Calcd. for $C_{42}H_{35}Cl_3NOP_2Re$ (924.2): C, 54.58; H, 3.82; N, 1.52%.
Found: C, 55.18; H, 4.19; N, 1.27%.
^1H NMR (25° C, $CDCl_3$, ppm): δ 6.17 - 7.87 (m, 34H, aromatic).
^{13}C NMR (25° C, $CDCl_3$, ppm): δ 127.8 - 138.7 (aromatic).
$^{31}P\text{-}\{^1H\}$ NMR (25° C, $CDCl_3$, ppm): δ −20.68 (s).

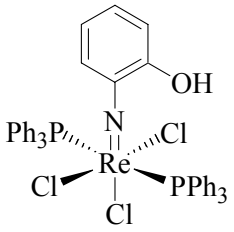

IR (KBr, cm^{-1}): 3132 (w), 3055 (w), 2970 (w), 2851 (w), 1593 (w), 1473 (m), 1431 (m), 1342 (w), 1238 (w), 1200 (m), 1153 (w), 1092 (m), 1061 (w), 1030 (w), 999 (w), 744 (m), 694 (st), 652 (w), 517 (st).
MS (FAB^+): *m/z* 663 ($[M\text{-}PPh_3]^+$, 2%), 400.9 ($[M\text{-}2PPh_3]^+$, 25%).

6.3.2.7 $[ReOCl_2(HL^{51})]$, (9)

$(NBu_4)[ReOCl_4]$ (58 mg, 0.1 mmol) was added to a suspension of H_2L^{51} (38 mg, 0.1 mmol) in 5 mL of MeOH. The mixture became immediately olive green, and the resulting solution was heated under reflux for 30 min. The product precipitated as a green solid, which was filtered through a Celite pad and washed twice with MeOH. The product was recrystallized from a CH_2Cl_2/MeOH mixture. Yield 46 mg (71%).

Elemental analysis:
Calcd. for $C_{25}H_{21}NO_2Cl_2PRe$ (656.5): C, 45.74; H, 3.38; N, 2.13%.
Found: C, 45.91; H, 3.34; N, 1.91%.
^1H NMR (25° C, DMSO-d_6, ppm): δ 5.0 (d, 1H, CH_2, J_{HH} = 11 Hz), 5.6 (d, 1H, CH2, J_{HH} = 11 Hz), 6.0 (t, 1H, NH), 6.3 – 7.8 (m, 18H, aromatic).
$^{31}P\text{-}\{^1H\}$ NMR (25° C, DMSO-d_6, ppm): δ −4.6 (s).

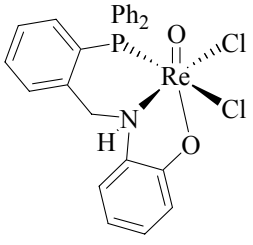

IR (KBr, cm^{-1}): 3452 (m), 3058 (m), 2943 (w), 2846 (w), 1485 (st), 1435 (m), 1257 (m), 188 (w), 1099 (w), 968 (m), 771 (m), 752 (m), 694 (m), 633 (m), 517 (m).
MS (FAB^+): *m/z* 654.4 ($[M-H]^+$, 7%), 620 ($[M-HCl]^+$, 48%).

6.3.2.8 [ReO(L^{51})(Ph_2btu)], (10)

$(NBu_4)[ReOCl_4]$ (58 mg, 0.1 mmol) and H_2L^{51} (38 mg, 0.1 mmol) were dissolved in 4 mL of CH_2Cl_2 and was stirred at room temperature for 10 min. HPh_2btu (33 mg, 0.1 mmol) and 0.15 mL of NEt_3 were added to the reaction solution. After heating the reaction for 30 min under reflux, the solvent was removed under vacuum and the residue suspended in 2 mL of MeOH. The resulting solid was filtered off and washed with MeOH. Red-brown crystals of [ReO(L^{51})(Ph_2btu)] were obtained by recrystallization of the product from a MeOH/CH_2Cl_2 mixture. Yield 52 mg (58%).

Elemental analysis:
Calcd. for $C_{45}H_{35}N_3O_3PReS$ (915.0): C, 59.07; H, 3.86; N, 4.59; S, 3.50%.
Found: C, 60.45; H, 3.97; N, 4.61; S, 3.51%.

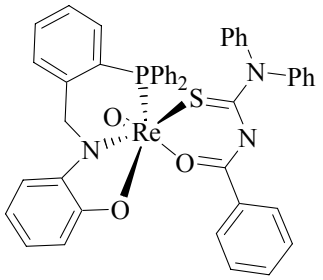

^1H NMR (25° C, DMSO-d_6, ppm): δ 4.5 - 5.8 (m, 2H, CH_2), 6.7 – 7.6 (m, 33H, aromatic).
^{31}P-{^1H} NMR (25° C, $CDCl_3$, ppm): δ −1.8 (s).
IR (KBr, cm^{-1}): 3058 (w), 2981 (w), 1589 (w), 1485 (st), 1435 (st), 1385 (st), 1261 (m), 1230 (w), 1115 (w), 1095 (w), 941 (w), 806 (w), 698 (m), 528 (w).

6.3.2.9 [$TcCl_3$(L^{51}P)], (11)

$(NBu_4)[TcOCl_4]$ (50 mg, 0.1 mmol) was dissolved in 5 mL of MeCN and *p*-toluenesulfonic acid monohydrate (19 mg, 0.1 mmol) was added as a solid. The resulting clear solution was stirred at room temperature for 10 min, and H_2L^{51} (38 mg, 0.1 mmol) was added. The reaction mixture was stirred at ambient temperature for 1.5 h, during which time the color of the solution became red. Red crystals were obtained by slow evaporation of the solvent. Yield 27 mg (47%).

Elemental analysis:

Calcd. for $C_{25}H_{19}Cl_3NOPTc$ (585.7): Tc, 16.89%.

Found: Tc, 16.65%.

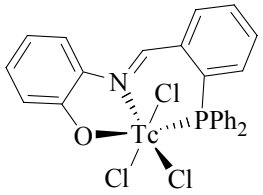

IR (KBr, cm^{-1}): 3058 (m), 1585 (m), 1551 (w), 1466 (st), 1435 (m), 1408 (m), 1254 (st), 1223 (w), 1134 (w), 1088 (w), 1030 (w), 864 (w), 748 (st), 694 (st), 633 (m), 555 (m), 494 (m).

6.3.2.10 [ReCl(L^{52})], (12)

H_4L^{52} (50 mg, 0.1 mmol) was added to a solution of $(NBu_4)[ReOCl_4]$ (58 mg, 0.1 mmol) in 5 mL of MeOH. The color of the solution turned immediately to cherry red and after stirring the reaction solution at 50°C for 2 h, a microcrystalline solid was obtained. The solid was filtered off and washed with MeOH. The product was recrystallized from a CH_2Cl_2/MeOH mixture. Yield 50 mg (68%).

Elemental analysis:

Calcd. for $C_{32}H_{25}ClN_2O_2PRe$ (722.19): C, 53.22; H, 3.49; N, 3.88%.

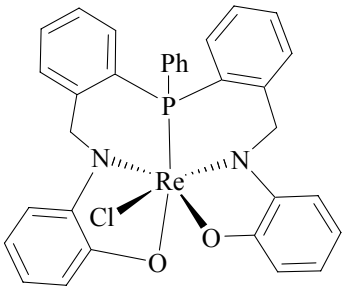

Found: C, 52.41; H, 3.44; N, 3.75%.

^{1}H NMR (25° C, DMSO-d_6, ppm): δ 5.0 (d, 1H, CH_2, J_{HH} = 15 Hz), 5.4 (d, 1H, CH_2, J_{HH} = 12 Hz), 5.6 (d, 1H, CH_2, J_{HH} = 14.3 Hz), 5.0 (d, 1H, CH_2, J_{HH} = 11.2 Hz), 6.7 – 8.0 (m, 21H, aromatic),

^{31}P-{^{1}H} NMR (25° C, acetone-d_6, ppm): δ −11.1 (s).

IR (KBr, cm^{-1}): 3055 (m), 2981 (w), 1570 (m), 1462 (m), 1335 (m), 1261 (w), 1153 (w), 1122 (w), 1065 (w), 741 (st), 694 (w), 621 (w), 548 (m), 525 (m).

MS (FAB^+): *m/z* 683 ($[M\text{-}Cl]^+$, 9.3%), 719 ($[M+H]^+$, 8.3%)

6.3.2.11 [ReO(HL^{52})], (13)

$(NBu_4)[ReOCl_4]$ (58 mg, 0.1 mmol) and H_4L^{52} (50 mg, 0.1 mmol) were suspended in 10 mL of MeOH and stirred for 30 min. NEt_3 (0.3 mL) was added and the reaction mixture was stirred at ambient temperature for 1 h. The product, which precipitated directly from the

reaction mixture was filtered off and washed with MeOH. Recrystallization from THF gave red crystals of [ReO(HL[52])]. Yield 62 mg (81%).

Elemental analysis:
Calcd. for $C_{32}H_{26}N_2O_3PRe$ (702.7): C, 54.69; H, 3.59; N, 3.99%.
Found: C, 53.37; H, 3.50; N, 3.81%.

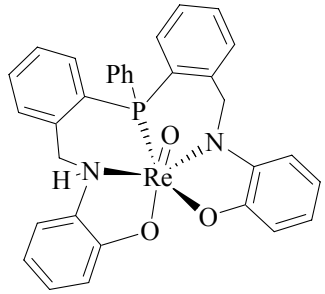

^{1}H NMR (25° C, $CDCl_3$, ppm): δ 5.3 (d, 1H, CH_2, J_{HH} = 13.5 Hz), 5.4 (d, 1H, CH_2, J_{HH} = 9.6 Hz), 5.7 (d, 1H, CH_2, J_{HH} = 9.7 Hz), 6.0 (d, 1H, CH_2, J_{HH} = 13.5 Hz), 6.4 – 7.9 (m, 21H, aromatic).
^{31}P-{^{1}H} NMR (25° C, $CDCl_3$, ppm): δ −4.8 (s).
IR (KBr, cm^{-1}): 3178 (m), 3055 (m), 2931 (w), 1593 (m), 1469 (st), 1439 (m), 1288 (st), 1261 (st), 1230 (st), 1191 (w), 1115 (m), 918 (st), 860 (w), 748 (st), 694 (w), 617 (m), 532 (m).
MS (ESI): *m/z* 704 ([M+H]$^+$, 100%).

6.3.2.12 [Re(L[53]P)], (14)

Method a. $(NBu_4)[ReOCl_4]$ (58 mg, 0.1 mmol) was dissolved in 5 mL of MeOH and H_6L^{53} (62 mg, 0.1 mmol) was added as a solid. The color of the reaction mixture became immediately purple. After stirring the reaction mixture for 1 h, the solvent was removed under reduced pressure and the residue was suspended in 2 mL of MeCN. The suspension was filtered through a Celite pad and the filtrate was left for crystallization. Green crystals of [Re(L[53]P)] were obtained by slow evaporation of the solvent overnight. Yield 22 mg (28%).
Method b. $(NBu_4)[ReOCl_4]$ (58 mg, 0.1 mmol) was dissolved in 5 mL of MeOH and H_6L^{53} (62 mg, 0.1 mmol) was added as a solid. The color of the reaction mixture became immediately purple. After stirring the reaction mixture for 30 min, NEt_3 (0.2 mL) was added. The color of the solution changed within 1 min to green, which followed by the precipitation of a green microcrystalline solid. Yield 76 mg (95%).

Elemental analysis:

Calcd. for $C_{39}H_{27}N_3O_3PRe$ (802.8): C, 58.35; H, 3.39; N, 5.23%.

Found: C, 56.22; H, 3.48; N, 5.05%.

IR (KBr, cm^{-1}): 3186 (w), 3059 (m), 2940 (m), 2793 (w), 2692 (w), 1628 (w), 1566 (m), 1470 (st), 1346 (w), 1296 (st), 1138 (w), 748 (st), 563 (w).

MS (ESI): *m/z* 804 ($[M+H]^+$, 100%).

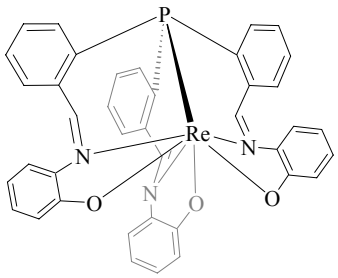

6.3.2.13 [$ReOCl_2(HL^{51}Et)$], (15)

The complex was synthesized by the reaction of $(NBu_4)[ReOCl_4]$ (58 mg, 0.1 mmol) with $H_2L^{51}COOEt$ (45 mg, 0.1 mmol) by the same procedure described in **6.3.2.7**. Yield 59 mg (82 %).

Elemental analysis:

Calcd. for $C_{28}H_{25}Cl_2NO_4PRe$ (727.6): C, 46.22; H, 3.46; N, 1.93%.

Found: C, 45.23; H, 2.84; N, 1.85%.

^1H NMR (25° C, $CDCl_3$, ppm): δ 1.40 (t, 3 H, CH_3), 4.35 (q, 2 H, OCH_2), 5.5 (dd, 2H, CH_2), 6.4 – 8.2 (m, 17 H, aromatic), 9.9 (br, 1 H, NH).

^{31}P-{^1H} NMR (25° C, $CDCl_3$, ppm): δ −16.2 .

MS (ESI): *m/z* 656.1 ($[M-2Cl-H]^+$, 100%).

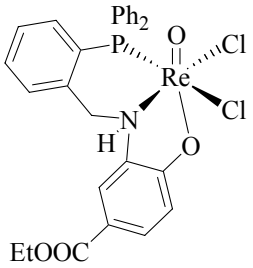

6.3.2.14 [$ReBr(CO)_3(H_2L^{51}COOEt)$], (16)

$(NEt_4)_2[ReBr_3(CO)_3]$ (77 mg, 0.1 mmol) was dissolved in 5 mL of MeOH and $H_2L^{51}COOEt$ (45 mg, 0.1 mmol) was added as solid. The reaction solution was heated under reflux for 30 min. The solvent was evaporated under reduced pressure and the residue suspended in 10 mL of distilled water. The product was extracted from the aqueous phase by 10 mL of CH_2Cl_2, and after drying the organic phase over $MgSO_4$, the solvent was removed under vacuum. The resulting pale yellow solid was recrystallized from a CH_2Cl_2/MeOH mixture. Yield 67 mg (93 %).

Elemental analysis:

Calcd. for $C_{31}H_{26}BrNO_6PRe$ (1015.9): C, 46.11; H, 4.56; N, 2.76%.

Found: C, 46.38; H, 4.38; N, 2.82%.

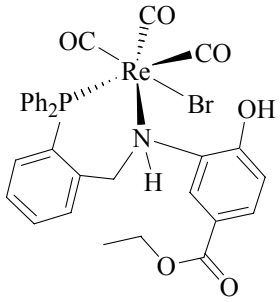

^{1}H-NMR (25° C, $CDCl_3$, ppm): δ 1.20 (t, 3H, CH_3), 1.3 (t, 12H, CH_3), 3.3 (q, 8H, NCH_2), 4.2 (q, 2H, OCH_2), 4.5, 5.8 (m, 2H, CH_2), 6.7 – 7.6 (m, 17H, aromatic).

^{31}P-{^{1}H}NMR (25° C, $CDCl_3$, ppm): δ 7.7 (s).

IR (KBr, cm^{-1}) : 3194 (w), 3051 (w), 2978 (m), 2681 (w), 2565 (w), 2029 (st), 1936 (st), 1902 (st), 1855 (m), 1717 (m), 1609 (w), 1439 (m), 1396 (w), 1366 (w), 1285 (m), 1261 (m), 1173 (w), 1115 (m), 1022 (w), 999 (w), 748 (w), 698 (m), 637 (w), 621 (w), 529 (m)

MS (ESI): *m/z* 726 ([M – Br-2CO]$^+$, 100%).

6.3.2.15 [Re(CO)$_3$(HL^{51}COOMe)], (17)

$(NEt_4)_2[ReBr_3(CO)_3]$ (77 mg, 0.1 mmol) was dissolved in 5 mL of MeOH and H_2L^{51}COOMe (44 mg, 0.1 mmol) was added as solid. The reaction mixture was heated under reflux for 30 min. $AgNO_3$ (54 mg, 0.3 mmol) was dissolved in 3 mL of MeOH and added dropwise to the reaction solution. The precipitated AgBr was filtered off and the filtrate was cooled to −10°C. The complex $[Re(CO)_3(HL^{51}COOMe)]$ was obtained as a colorless solid. Yield 40 mg (56%).

Elemental analysis:

Calcd. for $C_{30}H_{23}NO_6PRe$ (710.7): C, 50.70; H, 3.26; N, 1.97 %.

Found: C, 51.7; H, 3.10; N, 2.03 %.

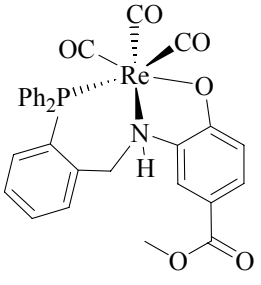

^{1}H-NMR (25° C, acetone-d_6, ppm): δ 3.7 (s, 3H, CH_3), 4.3 (d, 1H, CH_2, J_{HH} = 13 Hz), 4.7 (d, 2H, CH_2, J_{HH} = 13 Hz), 6.2 – 8.0 (m, 17H, aromatic), 10.8 (s, 1H, NH).

^{31}P-{^{1}H} NMR (25° C, $CDCl_3$, ppm): δ 4.9 (s).

IR (KBr, cm^{-1}) : 3186 (m), 3047 (w), 2947 (w), 2021 (st), 1923 (st), 1886 (st), 1682 (st), 1597 (st), 1500 (st), 1465 (st), 1319 (st), 1292 (st), 1242 (m), 1196 (w), 1165 (m), 1095 (w), 818 (w), 748 (w), 694 (w), 528 (m).

MS (ESI): *m/z* 678 ([M + Na-2CO]$^+$, 100%), 734 ([M+Na]$^+$, 81%).

6.3.2.16 [Re(CO)$_3$(HL^{51}COOH)], (18)

The synthetic procedure of [Re(CO)$_3$(HL^{51}COOMe)] was applied.

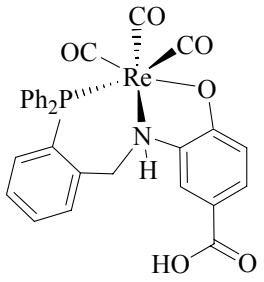

Elemental analysis:
Calcd. for $C_{29}H_{21}NO_6PRe$ (696,66): C, 50,00; H, 3,04; N, 2,01%.
Found: C, 49.3; H, 3.04; N, 1.92%.
^{1}H-NMR (25° C, acetone-d$_6$, ppm): δ 4.5 (d, 1H, CH_2), 4.7 (t, 1H, NH), 5.9 (d, 1H, CH_2) , 6.7 – 8.0 (m, 17H, aromatic), 10.8 (br, 1H, COOH).
^{31}P-{^{1}H} NMR (25° C, acetone-d$_6$, ppm): δ 6.3 (s).
IR (KBr, cm^{-1}): 3217 (m), 3055 (w), 2033 (st), 1944 (st), 1894 (st), 1685 (m), 1608 (m), 1435 (w), 1404 (w), 1288 (w), 1265 (w), 1122 (w), 1095 (w), 748 (w), 694 (w), 528 (w).
MS (ESI): *m/z* 720 ([M+Na]$^+$, 100%).

6.3.2.17 [^{99m}Tc(CO)$_3$(H$_2$O)$_3$]Cl

[^{99m}Tc(CO)$_3$(H$_2$O)$_3$]Cl was synthesized based on the procedure reported by Alberto *et al.* [7].

6.3.2.18 [^{99m}Tc(CO)$_3$(HL^{51}COOH)], (19)

A solution of H$_2$L^{51}COOH (1 mL, 10^{-3} M) in EtOH was added to a sealed vial containing an aqueous solution of [^{99m}Tc(CO)$_3$(H$_2$O)$_3$] (2.5 mL) and heated at 90°C for 10 min. Thereafter, a solution of NEt_3 (0.3, 10^{-3} M) in EtOH was added and the vial was heated in a water bath at 90°C for 20 min. HPLC analysis demonstrated the formation of a single complex **19**. The identity of this complex was established by comparative HPLC studies using a sample of the well characterized complex **18** as reference. (radiochemical yield >95%).
The gradient elution was performed with solutions A and B where A was 99.9%H2O, 0.1%TFA (v/v/v) and solvent B was MeOH.
The applied gradient for [^{99m}Tc(CO)$_3$(HL^{51}COOH] (**19**): Linear gradient from 100%A to 100%B, 40min.

T_r = 26.8 min.

6.3.2.19 [Re(CO)$_3$(κ^3-HL^{51}CO-TGE)], (20)

[Re(CO)$_3$(HL^{51}COOH)], (**18**) (0.1 g, 0.14 mmol) was reacted with N-hydroxybenzotriazole (20 mg, 0.15 mmol), and dicyclohexylcarbodiimide (32 mg, 0.15 mmol) in DMF at room temperature for 30 min. Then, triglycine ethylester (33 mg, 0.14 mmol) was added and the reaction solution was stirred at room temperature for 3 h. The solvent was removed under high vacuum and the residue suspended in 3 mL of ethylacetate. The insoluble urea derivatives were filtered off and the filtrate was washed with 10 mL of distilled water. After drying the organic phase over $MgSO_4$, the solvent was evaporated under reduced pressure during which time a colorless solid was obtained. (The separation of **20** from the not reacted triglycine ethylester requires HPLC technique).

^{31}P-{^{1}H} NMR (25° C, $CDCl_3$, ppm): δ 5.3 (s).
MS(ESI): 896.7 ([M+H]$^+$, 100%).

6.3.2.20 [Re(CO)$_3$(κ^3-HL^{51}COOH)]-SP, (21)

[Re(CO)$_3$(HL^{51}H)] (0.28 g, 0.4 mmol), *N,N'*-diisopropylcarbodiimide (26 mg, 0.21 mmol) and (1,2,3)-triazolo-(4,5-b)pyridin-3-ol (30 mg, 0.21 mmol) were dissolved in 10 mL of DMF and stirred at room temperature for 10 min. This solution was added to the natural peptide SP (61 mg, 0.05 mmol), which was pre-synthesized on a Wang resin, and stirred at room temperature for 1.5 h. Then, the resin was washed with DMF and CH_2Cl_2 several times. Thereafter, 10 mL of the cleavage cocktail trifluoroacetic acid/triisopropylsilane/water (9.5:0.5:0.1) was added and stirred for 1 h. The resulting solution was treated with 100 mL of diethylether in order to precipitate the product. The suspension was centrifuged and the product [Re(CO)$_3$(κ^3-HL^{51}COOH)]-SP (**21**) was obtained as a colorless solid. HPLC analysis demonstrated the formation of a single compound **21**.
The gradient elution was performed with solutions A and B where A was 95%H2O, 5%ACN and 0.1%TFA (v/v/v) and solvent B was 95%ACN, 5%H2O and 0.1%TFA (v/v/v).
The applied gradient for [Re(CO)$_3$(κ^3-HL^{51}COOH)]-SP (**21**): Linear gradient from 70%A, 30%B to 30%A, 70%B, 40min.

T_r = 30.5 min.

^{31}P-{^{1}H} NMR (25°C, DMSO-d_6, ppm): 4.9 (s).
MS(ESI): *m/z* 1418.4 ([M+H]$^{+}$, 100%), 709.7 ([M+2H]$^{2+}$, 60%).

6.3.2.21 [ReOCl$_2$(HL^{61})], (22)

(NBu_4)[$ReOCl_4$] (58 mg, 0.1 mmol) was added to a suspension of H_2L^{61} (38 mg, 0.1 mmol) in 5 mL of MeOH. The mixture became immediately a clear green solution, which was heated under reflux for 30 min. The product precipitated as a green solid, was filtered through a celite pad and washed twice with MeOH. The product was recrystallized from a CH_2Cl_2/MeOH mixture. Yield 52 mg (80%).

Elemental analysis:
Calcd. for $C_{25}H_{21}NO_2Cl_2PRe$ (655.5): C, 45.74; H, 3.38; N, 2.13%.
Found: C, 45.91; H, 3.34; N, 1.91%.

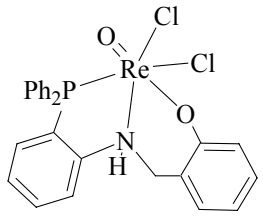

^{1}H NMR (25° C, $CDCl_3$, ppm): δ 4.6 (d, 1H, CH_2, J_{HH} = 13.4 Hz), 5.8 (d, 1H, CH_2, J_{HH} = 14.4 Hz), 6.5 – 8.3 (m, 18H, aromatic).
^{31}P-{^{1}H} NMR (25° C, $CDCl_3$, ppm): δ 2.55 (s).
IR (KBr, cm^{-1}): 3109 (m), 3078 (m), 1581 (w), 1481 (m), 1435 (m), 1250 (st), 1203 (w), 1142 (w), 1095 (w), 957 (st), 887 (m), 764 (st), 694 (m), 640 (w), 509 (st).
MS (FAB^{+}): *m/z* 654.9 ([M-H]$^{+}$, 7%), 621 ([M-Cl]$^{+}$, 48%).

6.3.2.22 [TcOCl$_2$(HL^{61})], (23)

(NBu_4)[$TcOCl_4$] (50 mg, 0.1 mmol) was dissolved in 5 mL of MeOH and H_2L^{61} (38 mg, 0.1 mmol) was added as a suspension in 2 mL of MeOH. The mixture became immediately a clear violet solution, which was stirred at room temperature for 2 h. The precipitated dark solid was filtered off and recrystallized from a CH_2Cl_2/Me_2CO mixture. Yield 30 mg (54%).

Elemental analysis:

Calcd. for $C_{25}H_{21}NO_2Cl_2PTc$ (568.23): Tc, 17.41%.

Found: Tc, 17.23%.

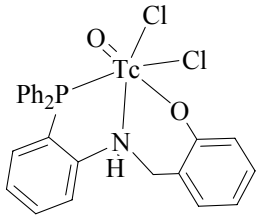

^{1}H NMR (25° C, DMSO-d_6, ppm): δ 4.6 (d, 1H, CH_2, J_{HH} = 14.8 Hz), 4.8 (d, 1H, CH_2, J_{HH} = 14 Hz), 6.4 – 8.3 (m, 18H, aromatic), 10.7 (br, 1H, NH).

^{31}P-{^{1}H} NMR (25° C, DMSO-d_6, ppm): δ 3.1 (s).

IR (KBr, cm^{-1}): 3448 (w), 3055 (m), 1581 (w), 1481 (m), 1443 (m), 1250 (m), 1095 (m), 1095 (m), 933 (st), 887 (w), 756 (m), 694 (m), 640 (w), 509 (m).

6.3.2.23 [ReOCl(H_2L^{62})], (24)

(NBu_4)[$ReOCl_4$] (58 mg, 0.1 mmol) and H_4L^{62} (50 mg, 0.1 mmol) were suspended in 5 mL of MeOH and heated under reflux for 2 h. The product precipitated as a green solid which was filtered off and recrystallized from THF. Yield 31 mg (42%).

Elemental analysis:

Calcd. for $C_{32}H_{26}ClN_2O_3PRe$ (739.2): C, 51.99; H, 3.55; N, 3.79%.

Found: C, 52.99; H, 3.55; N, 3.81%.

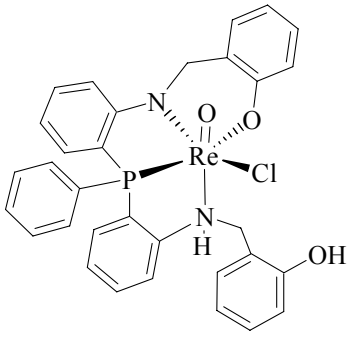

^{1}H NMR (25° C, DMSO-d_6, ppm): δ 4.5 (m, 2H, CH_2), 5.2 (d, 1H, CH_2, J_{HH} = 15.6 Hz), 5.3 (d, 1H, CH_2, J_{HH} = 16.4 Hz), 6.0 – 8.3 (m, 21H, aromatic), 8.4 (br, 1H, NH), 10.9 (s, 1H, OH).

^{31}P-{^{1}H} NMR (25° C, DMSO-d_6, ppm): δ13.3 (s).

IR (KBr, cm^{-1}): 3367 (m), 3236 (w), 3051 (w), 2819 (w), 1578 (m), 1477 (m), 1443 (st), 1269 (w), 1234 (st), 1192 (w), 1107 (w), 960 (w), 933 (w), 837 (w), 752 (st), 648 (w), 493 (m)

6.3.2.24 [$ReOCl_2(H_5L^{63})$], (26)

(NBu_4)[$ReOCl_4$] (58 mg, 0.1 mmol) and H_6L^{63} (63 mg, 0.1 mmol) were dissolved in 5 mL of CH_2Cl_2 and stirred at ambient temperature for 2 h. Orange Crystals were obtained by slow evaporation of the solvent. Yield 46 mg (38%).

Elemental analysis:

Calcd. for $C_{55}H_{71}BrCl_2N_4O4PRe$ (1220.2): C, 54.14; H, 5.87; N, 4.59%.

Found: C, 55.8; H, 5.71; N, 4.74%.

^{1}H NMR (25° C, DMSO-d_6, ppm): δ 4.2 – 4.6 (m, 6H, CH_2).

^{31}P-{^{1}H} NMR (25° C, DMSO-d_6, ppm): δ 4.03 (s).

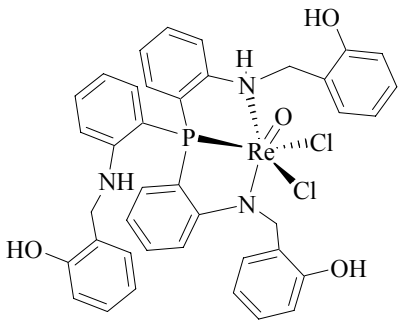

6.3.2.25 [ReOCl(H_4L^{63})], (27)

$(NBu_4)[ReOCl_4]$ (58 mg, 0.1 mmol) and H_6L^{63} were suspended in 5 mL of EtOH and heated under reflux for 2 h. The product was precipitated as an orange solid, which filtered off and recrystallized from CH_2Cl_2. Yield 57 mg (67%).

Elemental analysis:

Calcd. for $C_{39}H_{34}ClN_3O4PRe$ (861.3): C, 54.38; H, 3.98; N, 4.88%.

Found: C, 52.87; H, 3.83; N, 4.91%.

^{1}H NMR (25° C, DMSO-d_6, ppm): δ 4.2 (s, 2H, CH_2), 4.4 (s, 2H, CH_2), 4.7 (d, 2H, CH_2, J_{HH} = 14 Hz), 9.5 (s, 1H, OH), 9.9 (s, 1H, OH), 6.8 – 7.8 (m, 24H, aromatic).

^{31}P-{^{1}H} NMR (25° C, DMSO-d_6, ppm): δ 2.7 (s).

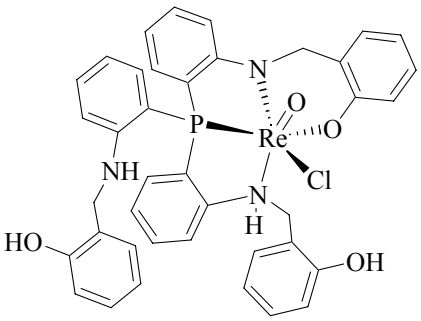

IR (KBr, cm^{-1}): 3344 (m), 3248 (w), 3059 (w), 2924 (w), 2851 (w), 1585 (m), 1512 (m), 1481 (m), 1454 (st), 1265 (w), 1234 (m), 1192 (w), 1172 (w), 1038 (w), 957 (w), 930 (w), 833 (w), 752 (st), 648 (w).

MS (ESI): *m/z* 826.1 ([M-Cl]$^+$, 100%).

6.3.2.26 [TcOCl(H_4L^{63})], (28)

$(NBu_4)[ReOCl_4]$ (58 mg, 0.1 mmol) and H_6L^{63} were suspended in 5 mL of EtOH and heated gently (~40°C) for 30 min. The product precipitated as an orange solid, which was filtered off and recrystallized from $CHCl_3$. Yield 57 mg (50%).

Elemental analysis:

Calcd. for $C_{39}H_{34}ClN_3O_4PTc$ (774.0): Tc, 12.78%.

Found: Tc, 12.66%.

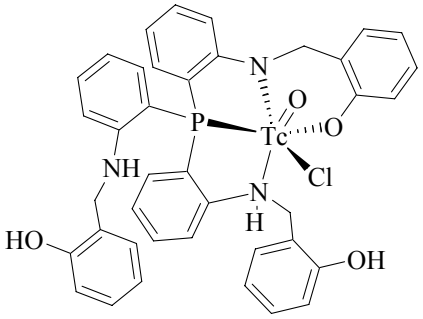

^{1}H NMR (25° C, DMSO-d_6, ppm): δ 4.18 - 4.33 (m, 3H, CH_2), 4.8 (d, 1H, CH_2, J_{HH} = 12 Hz), 5.0 (d, 1H, CH_2, J_{HH} = 13 Hz), 5.6 (d, 1H, CH_2, J_{HH} = 12 Hz), 6.0 (m, 1H, NH), 6.3 (m, 1H, NH), 6.5 – 7.9 (m, 24H, aromatic).

^{31}P-{^{1}H} NMR (25° C, DMSO-d_6, ppm): δ 5.7 (s).

IR (KBr, cm^{-1}): 3418 (m), 3186 (m), 2939 (m), 2793 (m), 2692 (m), 2611 (m), 1628 (m), 1566 (m), 1470 (st), 1346 (m), 1269 (st), 1138 (w), 876 (w), 748 (st), 640 (w), 563 (m).

6.3.2.27 [ReOCl(L^1)$_2$], (29)

(NBu_4)[$ReOCl_4$] (58 mg, 0.1 mmol) was dissolved in 3 mL of MeOH and after adding HL^1 (60 mg, 0.2 mmol) the reaction mixture was stirred at room temperature for 2 h. The resulting precipitate was filtered off and washed with MeOH. Red-brown crystals were obtained after recrystallization from a CH_2Cl_2/MeOH mixture. Yield 60 mg (75%).

Elemental analysis:

Calcd. for $C_{38}H_{32}ClO3P_2Re$ (820.3): C, 55.64; H, 3.93%.

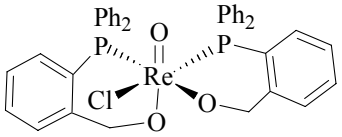

Found: C, 57.01; H, 3.81%.

^{1}H NMR ($CDCl_3$, 25° C, ppm): δ 4.4 (s, 2H, CH_2), 5.2 (s, 2H, CH_2), 6.9 – 7.7 (m, 28H, aromatic).

^{31}P-{^{1}H} NMR ($CDCl_3$, 25° C, ppm): δ 1.35 (s), 3.67 (s).

IR (KBr, cm^{-1}): 3047 (m), 2831 (w), 1473 (m), 1427 (st), 1188 (m), 1088 (st), 949 (st), 748 (st), 694 (st), 509 (st).

MS (ESI): *m/z* 785.13 ([M-Cl]$^+$, 100%).

6.3.2.28 *cis*-[$TcCl_2$(L^1)(HL^1)], (30)

Method a. (NBu_4)[$TcOCl_4$] (50 mg, 0.1 mmol) was dissolved in 3 mL of MeOH, HL^1 (60 mg, 0.2 mmol) was added and the reaction mixture was stirred at room temperature for 2

h. Red crystals of $[TcCl_2(L^1)(HL^1)]$ were obtained by cooling the reaction solution some. Yield (<10%).

Method b. $(NBu_4)[TcOCl_4]$ (50 mg, 0.1 mmol) and HL (120 mg, 0.4 mmol) were dissolved in 5 mL of CH_2Cl_2 and heated under reflux for 30 min. After removing the solvent the residue was suspended in 3 mL of MeOH and filtered off. Red crystals were obtained after recrystallization from a CH_2Cl_2/MeOH mixture. Yield 50 mg (64%).

Elemental analysis:

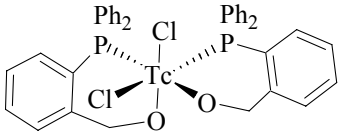

Calcd. for $C_{39}H_{36}Cl_2O_3P_2Tc$ (784.6): Tc 12.61%.

Found: Tc 12.92%.

IR (KBr, cm^{-1}): 3409 (br), 3051 (m), 2962 (m), 2923 (m), 2881(m), 1431 (m), 1161 (m), 1122 (m), 1095 (m), 895 (st), 748 (w), 694 (m), 548 (m), 501 (w).

6.3.2.29 *trans*-$[ReCl_2(NPh)(PPh_3)(L^1)]$, (31)

HL^1 (60 mg, 0.2 mmol) dissolved in 2 mL of CH_2Cl_2 was added to a suspension of $[ReCl_3(NPh)(PPh_3)_2]$ (86 mg, 0.1 mmol) in 5 mL of CH_2Cl_2. The reaction mixture was heated under reflux for 3 h, during which time the reaction mixture became a clear green solution. After removal of the solvent under reduced pressure, the residue was suspended in 3 mL of MeOH and filtered off. The isolated green solid was recrystallized from a CH_2Cl_2/MeOH mixture. Yield 40 mg (44%).

Elemental analysis:

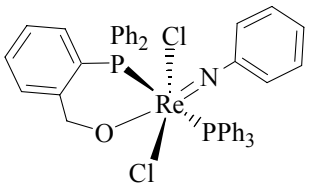

Calcd. for $C_{43}H_{36}Cl_2NOP_2Re$ (901.8): C, 57.27; H, 4.02; N, 1.55%.

Found: C, 58.63; H, 3.92; N, 1.58%.

^1H NMR (25° C, DMSO-d_6, ppm): δ 4.97 (s, 2H, CH_2), 6.8 – 7.7 (m, 34H, aromatic).

^{31}P-{^1H} NMR (25° C, DMSO-d_6, ppm): −21.6 (d, PPh_3, J_{PP} = 860 Hz), −6.5 (d, L^1, J_{PP} = 860 Hz).

IR (KBr, cm^{-1}): 3051 (m), 2881 (w), 2804 (w), 1574 (w), 1477 (m), 1431 (m), 1261 (w), 1188 (w), 1092 (st), 1061 (st), 1022 (m), 991 (m), 818 (w), 741 (m), 690 (st), 513 (st), 463 (m).

6.3.2.30 *cis*-[ReCl(NPh)(L^1)$_2$], (32)

[$ReCl_3(NPh)(PPh_3)_2$] (86 mg, 0.1 mmol) and HL^1 (90 mg, 0.3 mmol) were suspended in 10 mL of CH_2Cl_2 and heated under reflux for 1 h. Subsequently, 0.1 mL of NEt_3 was added and the reaction mixture was heated for one more hour. The solvent was removed under reduced pressure and the residue suspended in 3 mL of MeOH. The solid was isolated by filteration and crystallized from a CH_2Cl_2/MeOH mixture. Yield 41 mg (46%).

Elemental analysis:

Calcd. for $C_{44}H_{37}ClNO_2P_2Re$ (895.4): C, 59.02; H, 4.17; N, 1.56%.

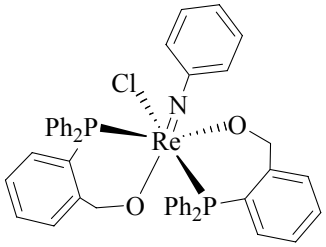

Found: C, 60.83; H, 4.02; N, 1.56%.

^{31}P-{^1H} NMR ($CDCl_3$, 25° C, ppm): δ -22.9 (s), -26.7 (s).

IR (KBr, cm^{-1}): 3051 (w), 2962 (w), 1481 (m), 1431 (st), 1261 (m), 1196 (w), 1092 (st), 1022 (st), 1061 (st), 910 (w), 802 (m), 744 (m), 690 (st), 513 (st), 463 (w).

6.3.2.31 [$ReOCl_2(H_2L^3)$], (33)

H_3L^3 (35 mg, 0.1 mmol) was added to a solution of (NBu_4)[$ReOCl_4$] (58 mg, 0.1 mmol) in 5 mL of MeOH. The reaction mixture became immediately a clear purple solution which was stirred at ambient temperature for 1 h. The obtained solid was filtered off and recrystalized from a CH_2Cl_2/MeOH mixture. Yield 48 mg (77%).

Elemental analysis:

Calcd. for $C_{21}H_{19}Cl_2O_4PRe$ (623.5): C, 40.46; H, 3.07%.

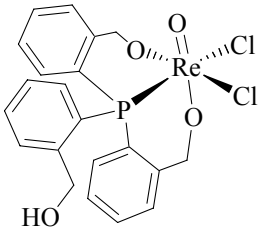

Found: C, 41.27; H, 2.91%.

^1H NMR (25° C, acetone-d_6, ppm): δ 4.1 – 6.3 (m, 6H, CH_2), 6.8 – 7.9 (m, 12H, aromatic).

^{31}P-{^1H} NMR (25° C, acetone-d_6, ppm): δ −28.3 (s).

IR (KBr, cm^{-1}): 3445 (m), 3059 (w), 2874 (w), 1470 (w), 1435 (w), 1200 (m), 1095 (m), 984 (m), 953 (st), 825 (w), 760 (st), 629 (w), 571 (m), 517 (m).

MS (FAB^+): *m/z* 553 ($[M-2Cl]^+$, 1%).

6.3.2.32 $[(TcOCl)_2(\mu\text{-}HL^3)_2]$, (34)

$(NBu_4)[TcOCl_4]$ (50 mg, 0.1 mmol) was dissolved in 5 mL of EtOH and H_3L^3 (35 mg, 0.1 mmol) was added as a solid. The solution was stirred at room temperature for 2 h, then the solvent volume was halfed under reduced pressure. By slow evaporation of the solvent, green crystals were obtained. Yield 43 mg (43%).

Elemental analysis:

Calcd. for $C_{42}H_{38}Cl_2O_8P_2Tc_2$ (1001.4): Tc, 19.75%.

Found: Tc, 19.59%.

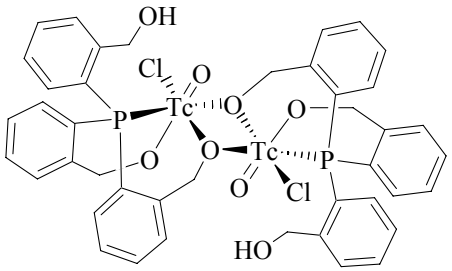

^1H NMR (25° C, $CDCl_3$, ppm): δ 4.4 (d, 2H, CH_2, J_{HH} = 17.3 Hz), 4.6 (d, 2H, CH_2, J_{HH} = 13.3), 4.8 (d, 2H, CH_2, J_{HH} = 12.4 Hz), 5.1 (d, 2H, CH_2, J_{HH} = 17.7), 5.3 (d, 2H, CH_2, J_{HH} = 14.0 Hz), 6.5 (d, 2H, CH_2, J_{HH} = 12.5 Hz), 7.1 – 7.7 (m, 24H, aromatic).

^{31}P-$\{^1H\}$ NMR (25° C, $CDCl_3$, ppm): δ -13.1 (s).

IR (KBr, cm^{-1}): 3391 (st), 2825 (w), 1384 (m), 1200 (w), 1095 (m), 1076 (m), 1018 (m), 933 (st), 760 (w), 621 (w), 563 (w), 509 (w), 463 (w).

6.3.2.33 $[TcCl_3(H_2L^3)]$, (35)

H_3L^3 (35 mg, 0.1 mmol) was added as a solid to a solution of $TcCl_4$ (0.1 mmol) in THF under an argon atmosphere. The colour of the solution became light orange during 2 h at ambient temperature. Thereafter, the reaction solution was cooled to −10°C and orange plates of $[TcCl_3(H_2L^3)]$ deposited overnight. Yield 22 mg (41%).

Elemental analysis:

Calcd. for $C_{21}H_{19}Cl_3O_3PTc$ (555.6): Tc, 17.8%.

Found: Tc, 18.5%.

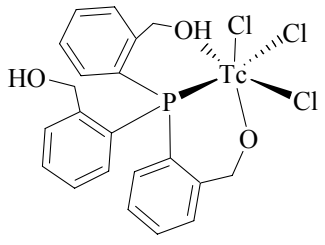

IR (KBr, cm^{-1}): 3425 (m), 3066 (w), 2951 (m), 2870 (m), 1466 (w), 1439 (m), 1203 (w), 1038 (st), 852 (w), 760 (st), 548 (w), 532 (w).

6.3.2.34 $[Re(CO)_3(H_2L^3)]$, (36)

$(NEt_4)_2[ReBr_3(CO)_3]$ (74 mg, 0.1 mmol) was added as a solid to a suspension of H_3L^3 (35 mg, 0.1 mmol) in 5 mL of MeOH. The reaction mixture was heated under reflux for 1 h and 3 drops of NEt_3 were added to the resulting pale yellow solution. A colorless solid formed during cooling to room temperature. Colorless crystals of $[Re(CO)_3(H_2L^3)]$ were obtained by recrystallization of the product from a CH_2Cl_2/MeOH mixture. Yield 40 mg (67%).

Elemental analysis:

Calcd. for $C_{24}H_{20}O_6PRe$ (621.6): C, 46.37; H, 3.24%.

Found: C, 47.14; H, 3.18%.

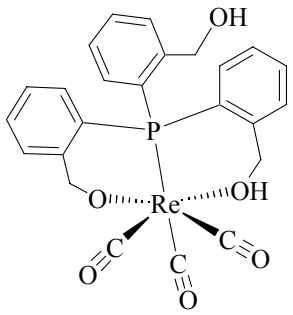

^1H NMR (25° C, acetone-d_6, ppm): δ 4.5 – 5.0 (m, 6H, CH_2), 6.8 – 7.8 (m, 12H, aromatic).

^{31}P-{^1H} NMR (25° C, acetone-d_6, ppm): δ -7.7 (s).

IR (KBr, cm^{-1}): 3055 (w), 2924 (w), 2021 (st), 1913 (st), 1882 (st), 1466 (w), 1435 (w), 1396 (w), 1203 (w), 1026 (w), 1002 (w), 964 (w), 756 (w), 532 (w)

MS (FAB^+): *m/z* 623 ($[M+H]^+$, 5.5%), 520.3 ($[M-C_7H_7O]^+$, 5.2%).

6.4 Crystal structure determination

The intensities for the X-ray determinations were collected on a *STOE* IPDS 2T or *Brucker*-Smart-CCD-100-M instruments with Mo/K_α radiation. The space groups were determined using *CHECK-HKL* [8] software. The empirical and integration absorption corrections were carried out by *SADABS* [9] and *X-RED*32 [10] programs, respectively. Structure solution and refinement were performed with *SIR 97* [11], *SHELXS 97* [12] and *SHELXS 86* [12] and *SHELXL 97* [13] programs. Hydrogen atom positions were calculated for idealized positions and treated with the 'riding model' option of *SHELXL* 97.

6.5 References

[1] Alberto, R.; Schibli, R.; Egli, A.; Schubiger, P. A.; Hermann, W. A.; Artus, G.; Abram, U.; Kaden, T. A. *J. Organomet. Chem.*, **1995**, 493, 119.

[2] Johnson, N. P.; Lock, C. J. L.; Wilkinson, G. *J. Chem. Soc.*, **1964**, 1054.

[3] Goeden, G. V.; Haymore, B. L. *Inorg. Chem.*, **1983**, *22*, 157.

[4] Archer, C. M.; Dilworth, J. R.; Thompson, R. M.; McPartlin, M.; Povey, D. C.; Kelly, J. *J Chem Soc, Dalton Trans*., **1993**, 461.

[5] Preetz, W.; Peters, G. *Z. Naturforsch.*, **1980**, *35b*, 1355.

[6] Hagenbach, A.; Yegen, E.; Abram, U. *Inorg. Chem.*, **2006**, 45, 7331.

[7] Alberto, R.; Ortner, K.; Wheatley, N.; Schibli, R., Schubiger, P. A. *J. Am. Chem. Soc.,* **2001,** *123,* 3135.

[8] *CHECK-HKL*. Kretschmar, M. Universität Tübingen, **1998**.

[9] *SADABS.* Sheldrick, G.M. Universität Gottingen.
Blessing, B. *Acta Cryst.,* **1995**, *A51*,33.

[10] *X-RED32*. STOE&Cie GmbH, Darmstadt, Germany.

[11] *SIR 92.* Altomare, A.; Cascarano, G.; Giacovazzo, C.; Guagliardi, A. *J. Appl. Crystallogr.,* **1993**, 26, 343.

[12] *SHELXS 86, 97*. Sheldrick, G.M. Universität Gottingen, **1986** and **1997**. Sheldrick, G.M., *Acta Cryst*., **1990**, *A46*, 467.

[13] *SHELXL 97*. Sheldrick, G.M. Universität Göttingen, **1997**.

Summary

This thesis contains synthesis and structural characterization of novel technetium and rhenium complexes with polydentate phosphine-containing ligand systems, which have been designed: (i) for the synthesis of metal complexes of high stability and (ii) as starting materials for bioconjugation purposes.

2-(Benzylimino)phosphines were synthesized by heating mixtures of primary amines and (2-formylphenyl)phosphines in EtOH. The products were obtained in solid forms directly from the reaction mixtures.

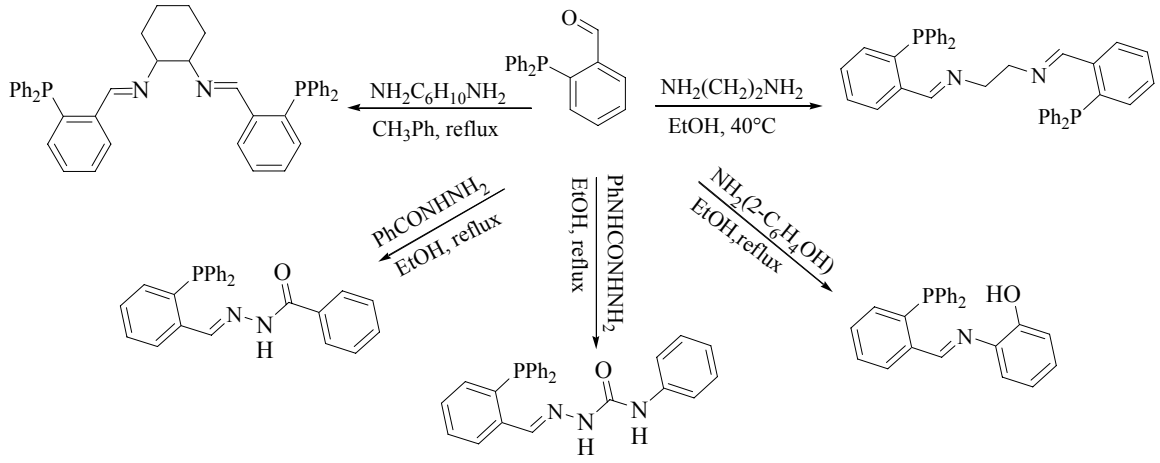

The 2-(benzylimino)phosphines show low chemical stability during the complex formation reactions with oxorhenium(V) complexes. Dissociation and/or rearrangement of the Schiff bases resulted in the formation of a number of unexpected products.

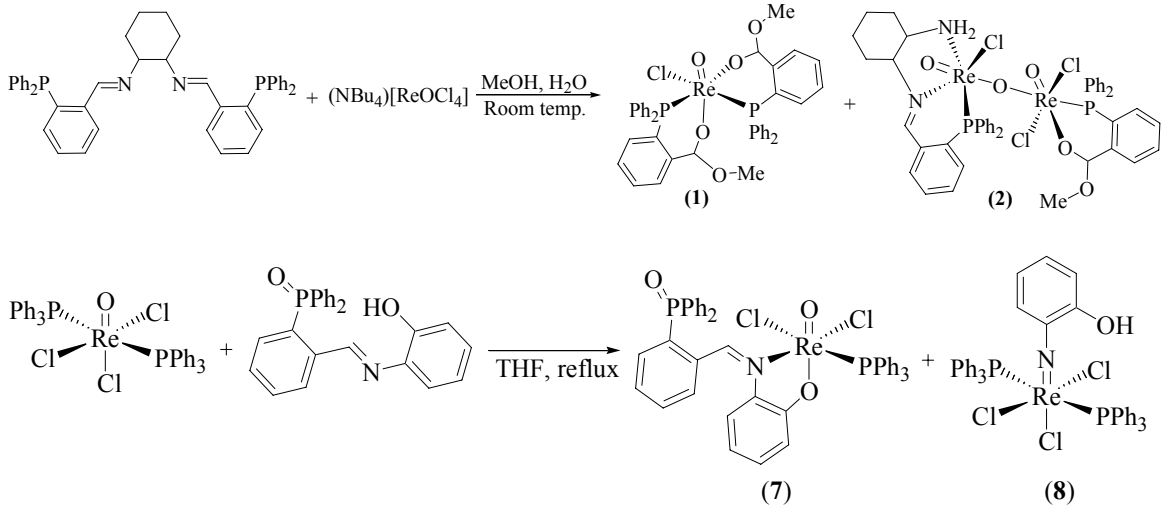

In order to benefit the mixed donor set of the 2-(benzylimino)phosphines and increase the chemical stability of these compounds, 2-(benzylamino)phosphines were synthesized by reduction of the 2-(benzylimino)phosphines by excess amounts of $NaBH_4$. The resulting

potentially multidentate ligands react with complexes of rhenium and technetium under formation of the novel complexes.

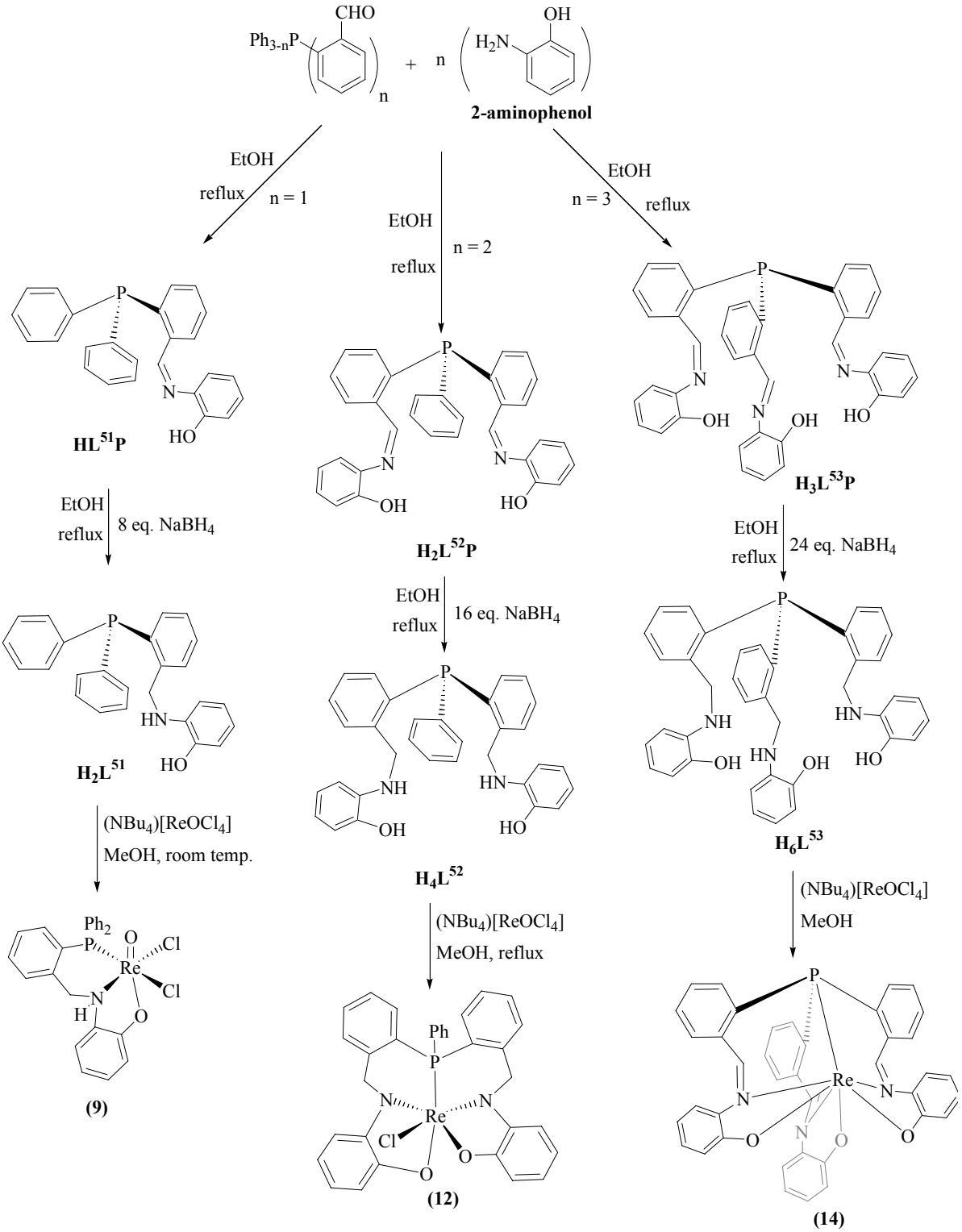

With the intention of applying the 2-(benzylamino)phosphines for biolabelling aims, the potentially bifunctional 2-(benzylamino)phosphines derived from 3-amino-4-hydroxybenzoic acid were synthesized. These compounds react with the rhenium(I) and technetium(I) complexes under formation of the predicted complexes of the composition $[M(CO)_3(\kappa^3\text{-}HL^{51}COOH]$ (M = Re, ^{99m}Tc).

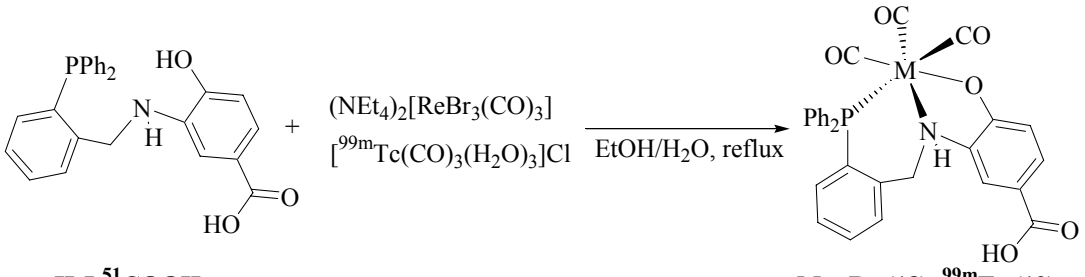

$H_2L^{51}COOH$ **M = Re (18), ^{99m}Tc (19)**

$[Re(CO)_3(\kappa^3\text{-}HL^{51}COOH)]$ (**18**) was successfully utilized for labelling small peptides (triglycine) as well as longer natural peptides such as the active site of Substance P (**21**) under liquid- and solid-phase techniques.

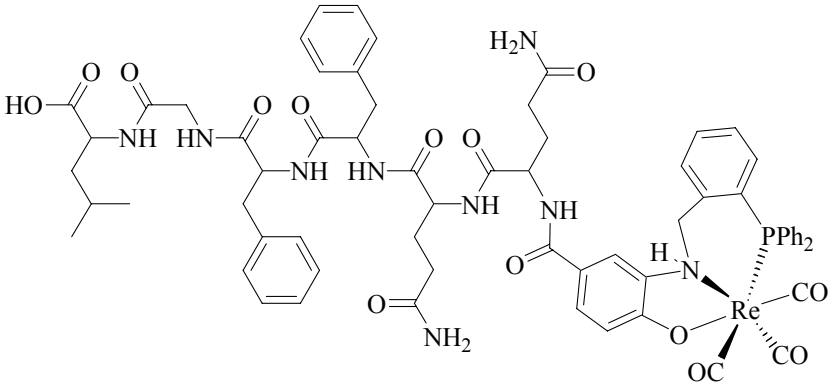

{$[Re(CO)_3(\kappa^3\text{-}HL^{51}COOH)]$-SP} (21)

The 2-(benzylamino)phosphines are remarkable ligands for stabilization of technetium complexes with the metal ion in lower oxidation states. In order to obtain stable oxotechnetium(V) complexes, 2-(aminophenyl)phosphines were synthesized.

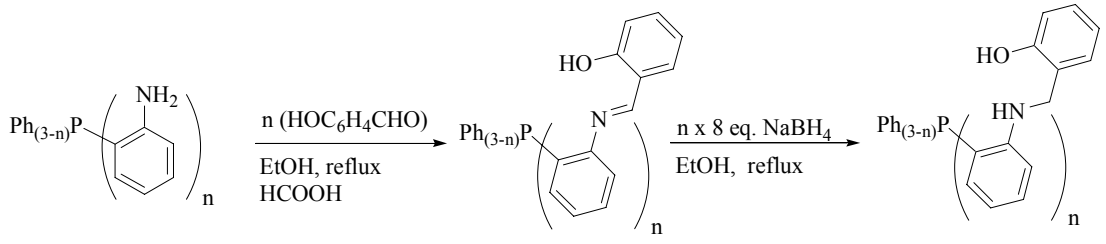

(n = 1 - 3)

The 2-(aminophenyl)phosphines react with $(NBu_4)[TcOCl_4]$ under formation of novel oxotechnetium(V) complexes.

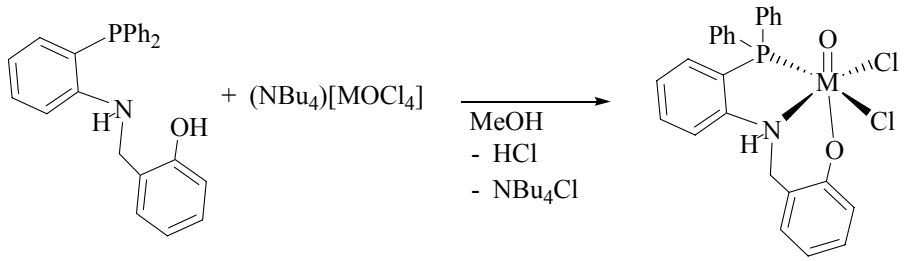

M = Re (22), Tc (23)

The {(2-hydroxymethyl)phenyl}phosphines H_nL^n (n = 1 - 3) are a new class of hetero-functionalized phosphines, which can readily be synthesized by reduction of the related aldehydes.

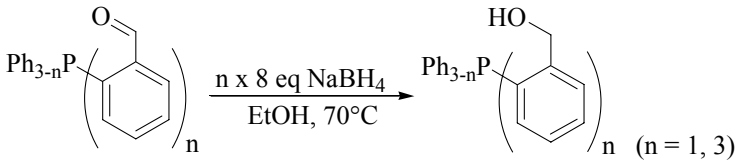

H_nL^n

The potentially tetradentate ligand H_3L^3 reacts with different complexes of rhenium and technetium under facial coordination. The molecular structures of all isolated compounds elucidate that H_3L^3 coordinates in a tridentate bis-chelating κ^3-(P,O,O´) mode with one uncoordinated hydroxyl group. The potential "*bifunctional*" coordination mode of H_3L^3 was employed for the coupling of $[Re(CO)_3(H_2L^3)]$ (**36**) with pre-activated diglycine. The analytical data elucidate that the dipeptide (*N*-BOC-diglycine) can be successfully conjugated with the complex **36**.

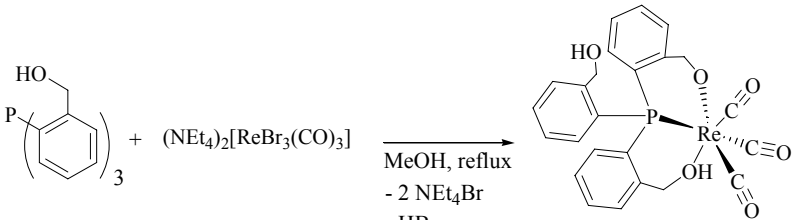

H_3L^3 **$[Re(CO)_3(H_2L^3)]$ (36)**

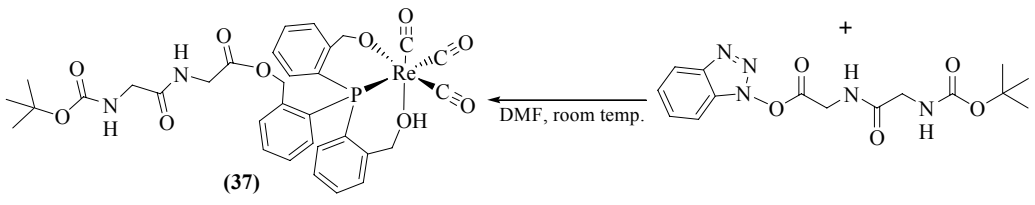

(37)

Appendix

Crystallographic Data

$[ReOCl(L^{11b})_2]$, (1)

Table 1 Crystal data and structure refinement for $[ReOCl(L^{11b})_2]$

Empirical formula	$C_{40}H_{36}ClO_5P_2Re$	
Formula weight	880.33	
Temperature	200(2) K	
Wavelength	0.71073 Å	
Crystal system	Monoclinic	
Space group	$P2_1/n$	
Unit cell dimensions	a = 9.832(1) Å	α= 90°.
	b = 18.966(2) Å	β= 96.05(1)°.
	c = 19.538(2) Å	γ = 90°.
Volume	3622.9(6) $Å^3$	
Z	4	
Density (calculated)	1.614 g/cm^3	
Absorption coefficient	3.560 mm^{-1}	
F(000)	1752	
Crystal size	0.12 x 0.07 x 0.06 mm^3	
Crystal description	Needle	
Crystal color	Brown	
Diff. measurement device type	STOE IPDS 2T	
Theta range for data collection	1.50 to 26.84°.	
Index ranges	-12<=h<=12, -21<=k<=23, -23<=l<=24	
Reflections collected	17632	
Independent reflections	7648 [R(int) = 0.1446]	
Completeness to theta = 26.84°	98.1 %	
Absorption correction	Integration	
Max. and min. transmission	0.8155 and 0.6077	
Refinement method	Full-matrix least-squares on F^2	
Data / restraints / parameters	7648 / 0 / 442	
Goodness-of-fit on F^2	0.885	
Final R indices [I>2sigma(I)]	R1 = 0.0550, wR2 = 0.1146	
R indices (all data)	R1 = 0.1861, wR2 = 0.1940	
Largest diff. peak and hole	1.174 and -2.136 $e.Å^{-3}$	

Table 2 Atomic coordinates (x 10^4) and equivalent isotropic displacement parameters ($Å^2$x 10^3) for [ReOCl(L^{11b})$_2$]. U(eq) is defined as one third of the trace of the orthogonalized U^{ij} tensor.

	x	y	z	U(eq)
Re	1650(1)	2500(1)	4362(1)	25(1)
O(10)	1055(9)	2559(9)	5138(5)	30(2)
Cl	54(4)	1624(3)	3864(2)	33(1)
P(1)	3107(6)	3552(3)	4664(3)	26(1)
C(1)	2044(14)	4343(9)	4523(8)	27(4)
C(2)	2240(17)	4907(9)	4961(10)	37(4)
C(3)	1460(20)	5522(9)	4777(14)	59(8)
C(4)	555(18)	5551(10)	4214(10)	36(4)
C(5)	343(17)	4979(8)	3771(10)	33(4)
C(6)	1078(15)	4368(8)	3900(8)	23(3)
C(7)	911(16)	3742(9)	3455(8)	29(4)
O(1)	453(10)	3145(6)	3778(6)	23(3)
O(2)	-70(12)	3895(6)	2880(6)	36(3)
C(8)	-280(20)	3344(11)	2375(11)	50(5)
C(11)	4543(15)	3694(8)	4168(8)	24(3)
C(12)	4511(17)	4265(9)	3681(11)	45(5)
C(13)	5610(20)	4363(11)	3291(13)	60(7)
C(14)	6783(18)	3924(11)	3419(12)	51(6)
C(15)	6768(17)	3350(11)	3861(9)	39(4)
C(16)	5638(16)	3231(10)	4212(8)	31(4)
C(21)	3830(15)	3641(8)	5564(7)	23(3)
C(22)	5140(20)	3864(10)	5737(14)	57(7)
C(23)	5700(20)	3888(11)	6391(10)	47(5)
C(24)	4970(20)	3717(11)	6957(13)	58(7)
C(25)	3570(20)	3476(12)	6750(9)	50(6)
C(26)	3050(20)	3459(9)	6095(11)	43(5)
P(2)	3111(6)	1506(3)	4763(3)	24(1)
C(31)	3142(16)	894(9)	4030(10)	35(4)
C(32)	2945(16)	181(8)	4121(10)	35(4)
C(33)	2948(19)	-259(9)	3574(13)	54(6)
C(34)	3112(19)	-12(11)	2913(11)	47(5)
C(35)	3330(20)	694(10)	2837(10)	42(5)
C(36)	3313(17)	1164(9)	3377(9)	31(4)
C(37)	3580(20)	1954(10)	3276(9)	43(5)

O(3)	2694(10)	2375(7)	3575(6)	34(3)
O(4)	3657(16)	2098(9)	2577(8)	56(4)
C(38)	4220(30)	2763(13)	2422(12)	62(7)
C(41)	4940(14)	1635(9)	5051(8)	24(3)
C(42)	5314(16)	2028(9)	5646(10)	35(4)
C(43)	6678(17)	2195(10)	5853(8)	35(4)
C(44)	7715(19)	1945(11)	5504(11)	49(5)
C(45)	7303(18)	1503(12)	4867(10)	48(5)
C(46)	5962(16)	1352(9)	4684(9)	31(4)
C(51)	2556(16)	948(8)	5464(8)	27(4)
C(52)	3472(18)	602(10)	5916(9)	37(4)
C(53)	3070(20)	169(11)	6416(11)	47(5)
C(54)	1670(20)	64(10)	6444(10)	45(5)
C(55)	770(30)	417(13)	6010(20)	100(13)
C(56)	1136(18)	866(11)	5480(11)	48(5)

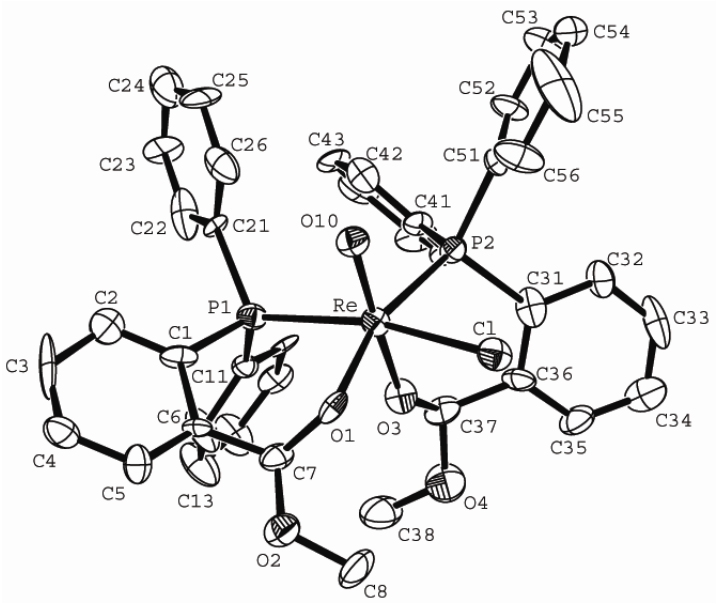

Fig. 1 Ellipsoid plot (50% probability) of [ReOCl(L^{11b})$_2$] (**1**).

[{ReOCl(L^{11a})}(μ-O)[$ReOCl_2$(L^{11b})] (2)

Table 3 Crystal data and structure refinement for [ReO(L^{11a})](μ-O)[$ReOCl_2$(L^{11b})].

Empirical formula	$C_{45}H_{45}Cl_3N_2O_5P_2Re_2$	
Formula weight	1234.52	
Temperature	200(2) K	
Wavelength	0.71069 Å	
Crystal system	Triclinic	
Space group	$P\bar{1}$	
Unit cell dimensions	a = 13.205(5) Å	α= 88.746(5)°.
	b = 14.613(5) Å	β= 75.896(5)°.
	c = 17.929(5) Å	γ = 72.059(5)°.
Volume	3187.0(2) $Å^3$	
Z	2	
Density (calculated)	1.286 g/cm^3	
Absorption coefficient	4.004 mm^{-1}	
F(000)	1200	
Crystal size	0.160 x 0.093 x 0.040 mm^3	
Crystal description	Needle	
Crystal color	Orange-red	
Diff. measurement device type	STOE IPDS 2T	
Theta range for data collection	1.82 to 29.40°.	
Index ranges	-18<=h<=18, -20<=k<=19, -20<=l<=24	
Reflections collected	33086	
Independent reflections	16982 [R(int) = 0.1911]	
Completeness to theta = 29.40°	96.5 %	
Absorption correction	Integration	
Max. and min. transmission	0.8513 and 0.6104	
Refinement method	Full-matrix least-squares on F^2	
Data / restraints / parameters	16982 / 0 / 533	
Goodness-of-fit on F^2	0.630	
Final R indices [I>2sigma(I)]	R1 = 0.0754, wR2 = 0.1702	
R indices (all data)	R1 = 0.2120, wR2 = 0.2397	
Extinction coefficient	0.0046(4)	
Largest diff. peak and hole	1.238 and -1.678 e.$Å^{-3}$	

Table 4 Atomic coordinates (x 10^4) and equivalent isotropic displacement parameters ($Å^2$x 10^3) for [ReO(L^{11a})](μ-O)[$ReOCl_2$(L^{11b})]. U(eq) is defined as one third of the trace of the orthogonalized U^{ij} tensor.

	x	y	z	U(eq)
Re(1)	8810(1)	6885(1)	10688(1)	38(1)
O(10)	8892(9)	6181(9)	9936(8)	57(3)
Cl(1)	7812(4)	6031(3)	11587(3)	58(1)
P(1)	7209(3)	8142(3)	10527(2)	41(1)
C(1)	7576(12)	9184(13)	10225(8)	42(4)
C(2)	6724(15)	10048(13)	10354(13)	62(5)
C(3)	6925(17)	10933(13)	10031(11)	55(5)
C(4)	7940(20)	10877(19)	9629(13)	82(7)
C(5)	8800(20)	10035(19)	9531(15)	84(7)
C(6)	8606(15)	9195(12)	9839(8)	45(4)
C(7)	9681(15)	8331(18)	9638(9)	62(6)
N(1)	9874(10)	7518(11)	9930(8)	49(3)
C(11)	10960(13)	6783(14)	9643(11)	57(5)
C(12)	11876(13)	7168(17)	9131(13)	70(6)
C(13)	13005(17)	6360(20)	8960(30)	143(19)
C(14)	13270(20)	5860(20)	9680(20)	116(12)
C(15)	12438(15)	5564(16)	10130(19)	106(12)
C(16)	11303(12)	6265(13)	10363(13)	67(7)
N(2)	10408(10)	5912(9)	10776(9)	48(4)
C(21)	6651(12)	7838(12)	9793(10)	43(4)
C(22)	6299(15)	7036(16)	9873(12)	65(5)
C(23)	5891(18)	6742(16)	9274(13)	72(6)
C(24)	5767(18)	7264(18)	8665(14)	78(7)
C(25)	6140(20)	8111(19)	8554(13)	82(7)
C(26)	6595(15)	8331(15)	9164(12)	62(5)
C(31)	6031(12)	8524(12)	11377(11)	47(4)
C(32)	6200(15)	8505(16)	12083(10)	64(5)
C(33)	5291(15)	8820(20)	12699(12)	92(9)
C(34)	4270(20)	9150(30)	12685(15)	115(11)
C(35)	4058(15)	9138(17)	11938(17)	93(9)
C(36)	4922(12)	8844(14)	11266(10)	56(5)
O(20)	8953(8)	7634(9)	11433(7)	50(3)
Re(2)	9469(1)	8229(1)	12216(1)	43(1)
O(30)	10736(9)	8223(8)	11725(6)	48(3)

Cl(2)	10237(4)	6603(3)	12600(3)	63(1)
Cl(3)	8513(3)	9732(3)	11788(3)	52(1)
P(2)	9753(3)	8987(3)	13323(2)	45(1)
C(41)	8439(11)	9599(14)	13988(10)	52(5)
C(42)	8226(13)	10474(16)	14374(12)	70(7)
C(43)	7275(14)	10879(17)	14900(12)	67(6)
C(44)	6463(18)	10420(20)	15066(14)	94(9)
C(45)	6643(15)	9581(15)	14714(11)	63(5)
C(46)	7605(14)	9115(15)	14177(10)	59(5)
C(47)	7815(14)	8196(14)	13780(10)	51(4)
O(1)	8179(8)	8232(9)	12976(6)	48(3)
O(2)	6866(10)	7888(11)	13978(8)	66(4)
C(48)	6900(30)	6960(30)	13729(19)	146(15)
C(51)	10500(14)	8182(15)	13939(11)	55(5)
C(52)	11579(17)	7601(19)	13539(16)	88(8)
C(53)	12230(20)	6980(20)	14047(17)	114(12)
C(54)	11812(12)	6952(13)	14822(14)	64(6)
C(55)	10700(20)	7501(19)	15150(16)	90(7)
C(56)	10061(18)	8146(17)	14724(11)	71(6)
C(61)	10459(16)	9865(11)	13185(11)	60(6)
C(62)	11099(12)	10004(14)	13625(10)	51(4)
C(63)	11690(18)	10758(17)	13478(11)	71(6)
C(64)	11534(14)	11285(16)	12875(14)	71(7)
C(65)	10890(20)	11200(20)	12416(17)	102(9)
C(66)	10390(20)	10435(16)	12538(15)	79(7)

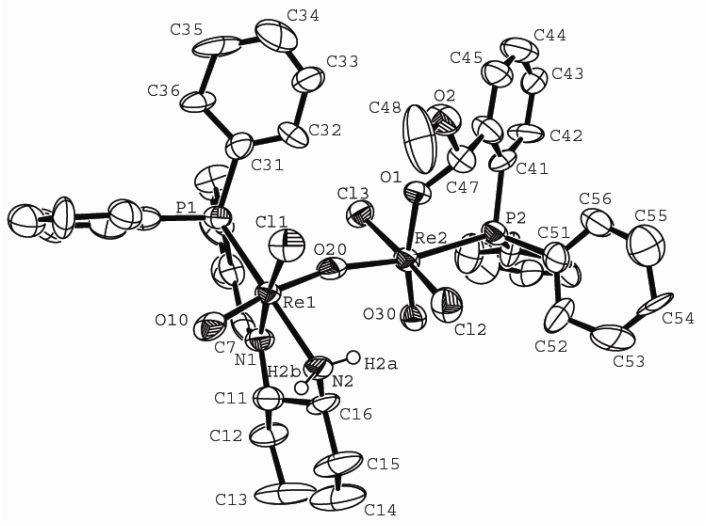

Fig. 2 Ellipsoid plot (50% probability) of [ReO(L^{11a})](μ-O)[ReOCl$_2$(L^{11b})] (**2**)

$[\{ReOCl_2(OMe)\}_2(\mu\text{-}L^{21})]$ (3)

Table 5 Crystal data and structure refinement for $[\{ReO(OMe)Cl_2\}_2(\mu\text{-}R1)]\cdot 3/2CH_3NO_2$.

Empirical formula	$C_{22.50}H_{24.50}Cl_2N_{2.50}O_5PRe$	
Formula weight	698.02	
Temperature	200(2) K	
Wavelength	0.71073 Å	
Crystal system	Triclinic	
Space group	$P\bar{1}$	
Unit cell dimensions	a = 9.78(4) Å	α= 106.01(9)°.
	b = 10.47(5) Å	β= 93.80(1)°.
	c = 14.90(7) Å	γ = 112.48(9)°.
Volume	1329.4(1) $Å^3$	
Z	2	
Density (calculated)	1.744 Mg/m^3	
Absorption coefficient	4.867 mm^{-1}	
F(000)	682	
Crystal size	0.4 x 0.1 x 0.06 mm^3	
Crystal description	Plate	
Crystal color	Red	
Diff. measurement device type	CCD AREA DETECTOR	
Theta range for data collection	1.45 to 25.15°.	
Index ranges	-11<=h<=11, -12<=k<=12, -17<=l<=16	
Reflections collected	9721	
Independent reflections	4693 [R(int) = 0.0443]	
Completeness to theta = 25.15°	98.1 %	
Absorption correction	Empirical	
Max. and min. transmission	1.00 and 0.667742	
Refinement method	Full-matrix least-squares on F^2	
Data / restraints / parameters	4693 / 21 / 294	
Goodness-of-fit on F^2	1.061	
Final R indices [I>2sigma(I)]	R1 = 0.0458, wR2 = 0.1094	
R indices (all data)	R1 = 0.0633, wR2 = 0.1190	
Largest diff. peak and hole	2.195 and -1.625 $e.Å^{-3}$	

Table 6 Atomic coordinates (x 10^4) and equivalent isotropic displacement parameters ($Å^2$x 10^3) for [{ReO(OMe)Cl_2}$_2$(μ-R1)]·3/2CH_3NO_2. U(eq) is defined as one third of the trace of the orthogonalized U^{ij} tensor.

	x	y	z	U(eq)
Re(1)	9240(1)	4758(1)	2631(1)	18(1)
O(10)	11141(8)	5882(7)	2838(4)	31(2)
Cl(1)	8454(3)	5520(2)	1417(2)	27(1)
Cl(2)	8738(3)	6632(3)	3795(2)	41(1)
O(1)	7306(7)	3371(7)	2579(4)	25(1)
C(31)	6267(15)	2643(16)	3108(11)	72(4)
P(1)	9493(3)	2798(2)	1480(2)	17(1)
C(1)	8893(10)	1204(9)	1861(6)	16(2)
C(2)	8277(10)	-168(9)	1202(6)	21(2)
C(3)	7837(11)	-1412(10)	1458(7)	27(2)
C(4)	7983(11)	-1310(10)	2410(7)	29(2)
C(5)	8625(12)	53(10)	3096(7)	32(2)
C(6)	9084(11)	1344(10)	2854(6)	26(2)
C(7)	9740(11)	2691(10)	3662(6)	28(2)
N(1)	9911(9)	4005(8)	3727(5)	26(2)
C(41)	10601(11)	5090(9)	4696(6)	23(2)
C(11)	11402(10)	3191(10)	1304(6)	23(2)
C(12)	12196(10)	4434(10)	1071(7)	26(2)
C(13)	13661(12)	4776(12)	946(8)	39(3)
C(14)	14367(12)	3871(13)	1047(7)	39(3)
C(15)	13571(12)	2619(13)	1270(8)	41(3)
C(16)	12093(10)	2282(10)	1404(6)	24(2)
C(21)	8325(9)	2159(8)	298(6)	15(2)
C(22)	8950(11)	2109(10)	-521(6)	27(2)
C(23)	8047(12)	1687(11)	-1394(7)	37(3)
C(24)	6512(12)	1309(11)	-1457(7)	35(2)
C(25)	5887(11)	1362(11)	-655(7)	35(2)
C(26)	6803(10)	1793(9)	226(7)	24(2)
N(4)	2980(20)	9370(20)	4272(14)	137(7)
C(64)	2170(20)	10270(30)	4170(15)	161(9)
O(6)	3020(30)	8750(30)	5000(20)	138(11)
O(5)	4240(30)	9330(40)	3870(30)	179(14)
N(3)	2170(20)	10270(30)	4170(15)	161(9)

C(63)	2980(20)	9370(20)	4272(14)	137(7)
O(3)	1410(40)	10840(40)	4810(20)	171(14)
O(4)	2420(30)	11130(30)	3550(20)	141(11)
O(8)	14860(90)	6690(90)	4850(40)	440(50)
O(7)	14450(40)	5380(40)	3800(30)	189(15)
N(5)	14600(40)	6980(40)	3940(30)	127(12)
C(62)	15160(40)	7840(30)	3480(20)	80(9)

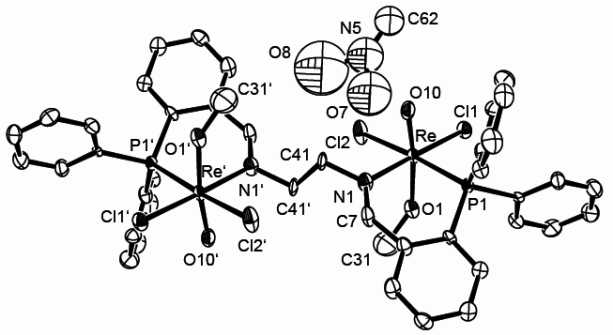

Fig. 3 Ellipsoid plot (50% probability) of $[\{ReOCl_2(OMe)\}_2(\mu\text{-}L^{21})]\cdot 3/2\ CH_3NO_2$

[ReOCl(OMe)(L^{31})], (4)

Table 7 Crystal data and structure refinement for [ReOCl(OMe)(HL^{41})]·THF

Empirical formula	$C_{31}H_{31}ClN_2O_4PRe$	
Formula weight	748.20	
Temperature	200(2) K	
Wavelength	0.71073 Å	
Crystal system	Monoclinic	
Space group	$P2_1/c$	
Unit cell dimensions	a = 11.2748(9) Å	α= 90°.
	b = 17.304(2) Å	β= 97.580(6)°.
	c = 14.914(1) Å	γ = 90°.
Volume	2884.4(4) $Å^3$	
Z	4	
Density (calculated)	1.723 g/cm^3	
Absorption coefficient	4.401 mm^{-1}	
F(000)	1480	
Crystal size	0.2 x 0.07 x 0.02 mm^3	
Crystal description	Plate	
Crystal color	Green	
Diff. measurement device type	STOE IPDS 2T	
Theta range for data collection	1.81 to 25.00°.	
Index ranges	-13<=h<=13, -20<=k<=19, -15<=l<=17	
Reflections collected	20489	
Independent reflections	5034 [R(int) = 0.1624]	
Completeness to theta = 25.00°	99.1 %	
Absorption correction	Integration	
Max. and min. transmission	0.7548 and 0.4095	
Refinement method	Full-matrix least-squares on F^2	
Data / restraints / parameters	5034 / 0 / 356	
Goodness-of-fit on F^2	1.040	
Final R indices [I>2sigma(I)]	R1 = 0.0746, wR2 = 0.1595	
R indices (all data)	R1 = 0.1296, wR2 = 0.1962	
Largest diff. peak and hole	3.363 and -2.109 e.$Å^{-3}$	

Table 8 Atomic coordinates (x 10^4) and equivalent isotropic displacement parameters ($Å^2$x 10^3) for [ReOCl(OMe)(HL^{41})]·THF. U(eq) is defined as one third of the trace of the orthogonalized U^{ij} tensor.

	x	y	z	U(eq)
Re	7267(1)	761(1)	7828(1)	46(1)
O(10)	6047(10)	310(6)	7284(7)	47(3)
C(40)	8734(19)	1953(13)	9118(19)	94(8)
Cl	8741(5)	146(3)	7060(3)	64(1)
P	6936(4)	1803(2)	6770(3)	42(1)
C(1)	8160(13)	2491(9)	6770(10)	44(4)
C(2)	8008(15)	3275(8)	6849(12)	49(4)
C(3)	8999(15)	3760(9)	6823(13)	57(5)
C(4)	10113(15)	3467(10)	6763(13)	57(4)
C(5)	10285(14)	2660(9)	6718(12)	53(4)
C(6)	9311(15)	2193(9)	6751(11)	52(4)
C(11)	6566(16)	1484(8)	5615(10)	47(4)
C(12)	5366(18)	1184(10)	5328(13)	62(5)
C(13)	5120(20)	885(11)	4478(14)	72(5)
C(14)	5920(20)	863(12)	3887(14)	78(6)
C(15)	7050(20)	1157(12)	4147(14)	77(6)
C(16)	7390(20)	1466(14)	5028(13)	76(6)
C(21)	5617(14)	2355(8)	7001(11)	44(4)
C(22)	5151(16)	2893(9)	6345(12)	55(4)
C(23)	4162(16)	3346(9)	6452(12)	54(4)
C(24)	3621(14)	3273(9)	7208(12)	51(4)
C(25)	4057(14)	2746(8)	7868(11)	48(4)
C(26)	5081(13)	2283(8)	7792(10)	41(3)
C(27)	5405(16)	1785(10)	8587(11)	54(4)
N(1)	6179(11)	1246(6)	8696(8)	40(3)
N(2)	6280(11)	877(7)	9557(8)	43(3)
C(30)	7008(15)	258(8)	9583(12)	49(4)
O(1)	7529(11)	12(6)	8924(8)	55(3)
C(31)	7211(16)	-166(9)	10459(11)	51(4)
C(32)	8189(15)	-648(10)	10622(11)	55(4)
C(33)	8461(19)	-1054(10)	11410(14)	67(5)
C(34)	7713(18)	-977(9)	12076(12)	60(4)
C(35)	6742(17)	-508(9)	11945(11)	55(4)
C(36)	6482(16)	-90(10)	11124(12)	55(4)

O(4)	2330(14)	1451(10)	5702(11)	97(5)
O(2)	8433(10)	1393(6)	8492(8)	56(3)
C(41)	1490(30)	828(14)	5402(18)	107(9)
C(43)	1500(20)	1717(16)	4224(19)	101(8)
C(42)	670(20)	1201(16)	4661(18)	98(8)
C(44)	2260(20)	2005(14)	5010(15)	91(7)

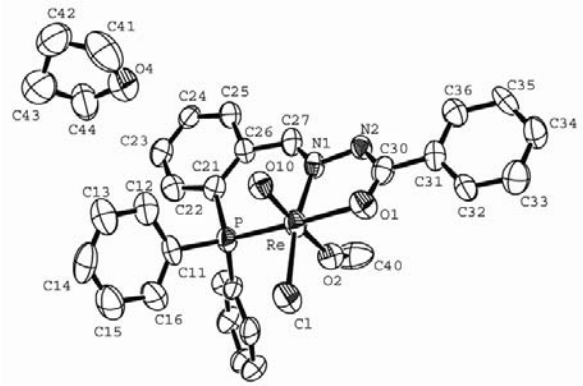

Fig. 4 Ellipsoid plot (50% probability) of [ReOCl(OMe)(HL^{41})]·THF

[ReO(L^{31a})(Et$_2$btu)], (5)

Table 9 Crystal data and structure refinement for [ReO((Ph$_2$P{(C$_6$H$_4$)CH$_2$OH})(Et$_2$btu)]·Me$_2$CO

Empirical formula	$C_{42}H_{43}N_4O_5PReS$	
Formula weight	933.03	
Temperature	200(2) K	
Wavelength	0.71073 Å	
Crystal system	Monoclinic	
Space group	$P2_1/c$	
Unit cell dimensions	a = 21.368(3) Å	α= 90°.
	b = 9.6402(8) Å	β= 91.05(1)°.
	c = 19.847(2) Å	γ = 90°.
Volume	4087.6(8) Å^3	
Z	4	
Density (calculated)	1.516 g/cm^3	
Absorption coefficient	3.111 mm^{-1}	
F(000)	1876	
Crystal size	0.34 x 0.19 x 0.02 mm^3	
Crystal description	Plate	
Crystal color	Orange	
Diff. measurement device type	STOE IPDS 2T	
Theta range for data collection	1.91 to 26.83°.	
Index ranges	-27<=h<=25, -10<=k<=12, -24<=l<=25	
Reflections collected	18802	
Independent reflections	8617 [R(int) = 0.1582]	
Completeness to theta = 26.83°	98.2 %	
Absorption correction	Integration	
Max. and min. transmission	0.8771 and 0.4216	
Refinement method	Full-matrix least-squares on F^2	
Data / restraints / parameters	8617 / 0 / 491	
Goodness-of-fit on F^2	0.801	
Final R indices [I>2sigma(I)]	R1 = 0.0613, wR2 = 0.1355	
R indices (all data)	R1 = 0.1804, wR2 = 0.2062	
Extinction coefficient	0.0100(5)	
Largest diff. peak and hole	1.502 and -1.955 e.Å^{-3}	

Table 10 Atomic coordinates (x 10^4) and equivalent isotropic displacement parameters ($Å^2$x 10^3) for[ReO((Ph$_2$P{(C$_6$H$_4$)CH$_2$OH})(Et$_2$btu)]·Me$_2$CO. U(eq) is defined as one third of the trace of the orthogonalized U^{ij} tensor.

	x	y	z	U(eq)
Re	3063(1)	-7129(1)	2064(1)	44(1)
O(10)	3558(6)	-7821(12)	2643(5)	65(3)
P	3820(2)	-7123(5)	1163(2)	49(1)
C(1)	3408(7)	-7703(16)	394(7)	44(3)
C(2)	3532(10)	-7049(19)	-219(7)	75(6)
C(3)	3186(13)	-7472(19)	-804(9)	92(8)
C(4)	2692(11)	-8440(20)	-732(9)	71(6)
C(5)	2615(9)	-9080(18)	-143(7)	59(5)
C(6)	2934(8)	-8724(16)	447(7)	50(4)
C(7)	2811(8)	-9557(17)	1081(7)	49(4)
N(1)	2606(7)	-8636(13)	1654(6)	52(3)
C(8)	3330(9)	-11090(20)	1828(8)	71(5)
O(3)	3394(6)	-10178(10)	1246(5)	60(3)
N(2)	2022(7)	-8987(14)	1869(7)	57(4)
C(17)	1850(7)	-8110(15)	2327(7)	44(4)
O(1)	2224(5)	-7043(11)	2501(4)	45(2)
C(11)	1247(8)	-8185(17)	2645(8)	53(4)
C(12)	838(8)	-9295(19)	2492(9)	64(5)
C(13)	262(10)	-9350(20)	2807(10)	76(6)
C(14)	103(10)	-8360(20)	3276(10)	77(6)
C(15)	506(10)	-7290(20)	3422(11)	80(6)
C(16)	1068(8)	-7210(20)	3113(9)	65(5)
C(21)	4533(9)	-8231(16)	1245(8)	61(5)
C(22)	4666(8)	-8860(20)	1853(8)	68(5)
C(23)	5250(12)	-9640(30)	1857(12)	103(8)
C(24)	5563(11)	-9850(20)	1316(11)	89(8)
C(25)	5456(8)	-9237(17)	705(9)	59(5)
C(26)	4836(9)	-8421(19)	716(8)	62(5)
C(31)	4133(9)	-5420(20)	966(8)	65(5)
C(32)	4743(12)	-5080(20)	1207(10)	91(7)
C(33)	4967(16)	-3720(30)	1159(12)	121(11)
C(34)	4522(18)	-2710(30)	870(11)	123(11)
C(35)	3924(12)	-3041(19)	605(10)	79(6)

C(36)	3756(10)	-4388(18)	664(10)	69(5)
S	3289(2)	-4736(4)	2463(2)	54(1)
O(2)	2599(6)	-5905(10)	1308(5)	54(3)
C(47)	2249(7)	-4823(15)	1351(7)	40(3)
C(41)	1893(8)	-4490(16)	709(7)	52(4)
C(42)	1534(7)	-3297(17)	659(8)	55(4)
C(43)	1175(9)	-3050(20)	77(10)	72(5)
C(44)	1270(12)	-3950(20)	-483(11)	94(8)
C(45)	1624(9)	-5070(20)	-448(7)	64(5)
C(46)	2004(8)	-5326(19)	121(7)	60(5)
N(3)	2197(6)	-3959(12)	1840(6)	49(3)
C(51)	2561(9)	-3960(15)	2391(8)	56(5)
N(4)	2379(6)	-3125(13)	2903(6)	47(3)
C(52)	2712(9)	-3017(19)	3552(7)	62(5)
C(53)	3130(10)	-1802(19)	3615(9)	77(6)
C(54)	1808(8)	-2319(18)	2828(9)	69(5)
C(55)	1233(8)	-3140(19)	2989(9)	67(5)
O(5)	103(8)	6170(20)	4170(9)	117(6)
C(61)	-403(12)	6730(20)	4259(10)	78(6)
C(62)	-552(11)	8090(30)	4032(14)	114(9)
C(63)	-933(14)	6000(30)	4604(17)	164(16)

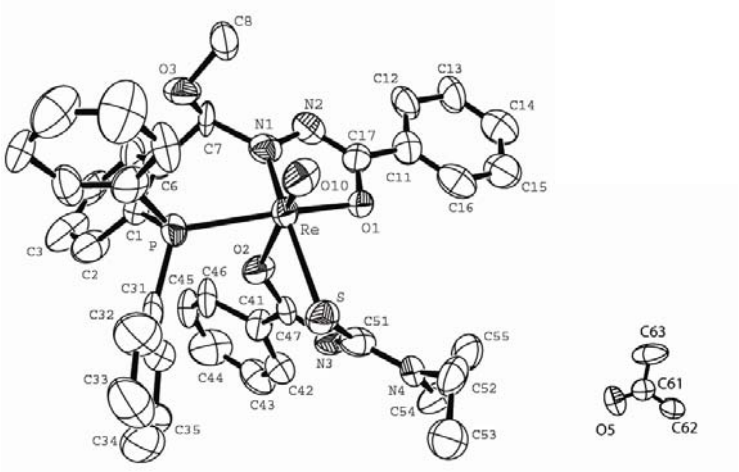

Fig. 5 Ellipsoid plot (50% probability) of [ReO((Ph$_2$P-{(C$_6$H$_4$)CH$_2$OH)})(Et$_2$btu)]·Me$_2$CO.

[ReOCl(OMe)(L^{41})], (6)

Table 11 Crystal data and structure refinement for [ReOCl(OMe)(L^{41}P)]

Empirical formula	$C_{27}H_{24}ClN_3O_3PRe$	
Formula weight	691.11	
Temperature	200(2) K	
Wavelength	0.71073 Å	
Crystal system	Monoclinic	
Space group	P 2_1/n	
Unit cell dimensions	a = 8.7907(3) Å	α= 90°.
	b = 19.6058(3) Å	β= 104.394(2)°.
	c = 15.4818(2) Å	γ = 90°.
Volume	2584.5(1) $Å^3$	
Z	4	
Density (calculated)	1.776 g/cm^3	
Absorption coefficient	4.901 mm^{-1}	
F(000)	1352	
Crystal size	0.8 x 0.6 x 0.5 mm^3	
Crystal description	Block	
Crystal color	Red	
Diff. measurement device type	STOE IPDS 2T	
Theta range for data collection	1.71 to 29.28°.	
Index ranges	-12<=h<=12, -26<=k<=26, -21<=l<=16	
Reflections collected	19316	
Independent reflections	6934 [R(int) = 0.1205]	
Completeness to theta = 29.28°	98.5 %	
Absorption correction	Integration	
Max. and min. transmission	0.5715 and 0.4666	
Refinement method	Full-matrix least-squares on F^2	
Data / restraints / parameters	6934 / 0 / 326	
Goodness-of-fit on F^2	1.008	
Final R indices [I>2sigma(I)]	R1 = 0.0657, wR2 = 0.1327	
R indices (all data)	R1 = 0.1217, wR2 = 0.1614	
Extinction coefficient	0.0036(4)	
Largest diff. peak and hole	4.522 and -1.985 $e.Å^{-3}$	

Table 12 Atomic coordinates (x 10^4) and equivalent isotropic displacement parameters ($Å^2$x 10^3) For [ReOCl(OMe)(L^{41}P)]. U(eq) is defined as one third of the trace of the orthogonalized U^{ij} tensor.

	x	y	z	U(eq)
Re	7595(1)	1004(1)	6862(1)	32(1)
O(10)	6020(9)	519(4)	6934(5)	40(2)
Cl(1)	8333(4)	1405(2)	8351(2)	50(1)
P	5768(3)	1942(1)	6345(2)	29(1)
C(1)	4423(11)	1690(5)	5311(6)	33(2)
C(2)	3013(12)	2045(6)	5024(7)	41(2)
C(3)	1918(12)	1911(6)	4215(7)	42(2)
C(4)	2251(13)	1406(5)	3678(7)	42(2)
C(5)	3652(13)	1064(6)	3905(7)	43(2)
C(6)	4761(12)	1177(5)	4712(6)	36(2)
C(7)	6143(13)	757(6)	4835(7)	41(2)
N(1)	7270(9)	652(4)	5545(5)	33(2)
N(2)	8482(11)	229(5)	5475(6)	48(2)
C(10)	9611(13)	39(6)	6238(7)	43(3)
O(1)	10733(9)	-315(4)	6119(5)	49(2)
N(3)	9326(10)	246(5)	7008(6)	37(2)
C(11)	10483(12)	54(6)	7798(7)	39(2)
C(12)	12073(14)	168(6)	7881(9)	49(3)
C(13)	13192(16)	-27(7)	8640(10)	60(3)
C(14)	12715(16)	-342(7)	9329(9)	56(3)
C(15)	11168(19)	-430(6)	9273(8)	61(4)
C(16)	9999(15)	-240(6)	8510(7)	46(3)
C(21)	4500(11)	2240(5)	7046(7)	34(2)
C(22)	4037(12)	2908(5)	7051(7)	37(2)
C(23)	3055(13)	3122(6)	7560(8)	47(3)
C(24)	2494(17)	2654(8)	8060(10)	62(3)
C(25)	2920(19)	1991(7)	8063(10)	67(4)
C(26)	3947(15)	1771(6)	7559(9)	52(3)
C(31)	6730(11)	2708(5)	6098(7)	32(2)
C(32)	7970(11)	2975(6)	6736(7)	39(2)
C(33)	8698(14)	3559(6)	6573(8)	48(3)
C(34)	8210(15)	3885(6)	5751(9)	52(3)
C(35)	6988(14)	3626(6)	5116(7)	44(3)
C(36)	6253(13)	3037(6)	5271(7)	40(2)

O(2)	9084(8)	1574(4)	6517(5)	41(2)
C(30)	9835(17)	1790(8)	5870(11)	68(4)

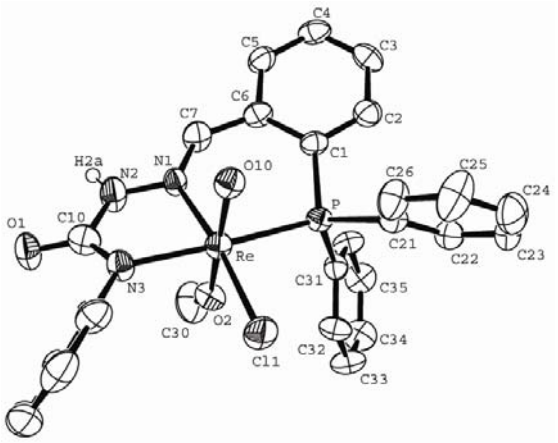

Fig. 6 Ellipsoid plot (50% probability) of [ReOCl(OMe)($L^{41}P$)]

[ReOCl(PPh$_3$)(L^{51}PO)], (7)

Table 13 Crystal data and structure refinement for [ReOCl$_2$(PPh$_3$)(HL^{51}PO)]

Empirical formula	$C_{43}H_{34}Cl_2NO_3P_2Re$	
Formula weight	931.75	
Temperature	293(2) K	
Wavelength	0.71073 Å	
Crystal system	Monoclinic	
Space group	$P2_1/c$	
Unit cell dimensions	a = 9.591(7) Å	α= 90°.
	b = 14.02(7) Å	β= 97.62(6)°.
	c = 31.38(3) Å	γ = 90°.
Volume	4181.4(5) Å^3	
Z	4	
Density (calculated)	1.480 g/cm^3	
Absorption coefficient	3.148 mm^{-1}	
F(000)	1848	
Crystal size	0.3 x 0.2 x 0.07 mm^3	
Crystal description	Plate	
Crystal color	Red	
Diff. measurement device type	STOE IPDS 2T	
Theta range for data collection	2.66 to 26.84°.	
Index ranges	-12<=h<=12, -17<=k<=15, -36<=l<=39	
Reflections collected	24050	
Independent reflections	8732 [R(int) = 0.0988]	
Completeness to theta = 26.84°	97.2 %	
Refinement method	Full-matrix least-squares on F^2	
Data / restraints / parameters	8732 / 0 / 470	
Goodness-of-fit on F^2	0.919	
Final R indices [I>2sigma(I)]	R1 = 0.0608, wR2 = 0.1200	
R indices (all data)	R1 = 0.1244, wR2 = 0.1428	
Extinction coefficient	0.0075(4)	
Largest diff. peak and hole	1.014 and -0.860 e.Å^{-3}	

Table 14 Atomic coordinates (x 10^4) and equivalent isotropic displacement parameters ($Å^2$x 10^3) for [$ReOCl_2(PPh_3)(HL^{51}PO)$]. U(eq) is defined as one third of the trace of the orthogonalized U^{ij} tensor.

	x	y	z	U(eq)
Re	6523(1)	5125(1)	8844(1)	46(1)
O(10)	5659(6)	4137(4)	8685(2)	52(2)
Cl(1)	5178(2)	6308(2)	8452(1)	56(1)
Cl(2)	5444(2)	5640(2)	9447(1)	58(1)
O(1)	9426(7)	1635(5)	9241(2)	61(2)
P(1)	8048(3)	1218(2)	9065(1)	54(1)
C(1)	6572(10)	1832(7)	9250(3)	54(2)
C(2)	5339(12)	1323(8)	9264(4)	73(3)
C(3)	4168(12)	1738(9)	9420(4)	74(3)
C(4)	4237(11)	2639(8)	9541(4)	69(3)
C(5)	5441(11)	3191(8)	9526(3)	60(3)
C(6)	6611(9)	2806(7)	9370(3)	47(2)
N(1)	8016(7)	4235(5)	9258(2)	45(2)
C(7)	7898(10)	3366(7)	9385(3)	57(2)
C(11)	9338(8)	4716(7)	9364(3)	49(2)
C(12)	10573(9)	4326(8)	9576(3)	58(3)
C(13)	11760(9)	4890(8)	9665(3)	61(3)
C(14)	11684(11)	5847(8)	9553(4)	65(3)
C(15)	10465(9)	6258(7)	9355(3)	57(2)
C(16)	9290(9)	5674(7)	9259(3)	50(2)
O(2)	8060(6)	6002(4)	9044(2)	52(2)
C(21)	7891(9)	-3(7)	9219(3)	55(2)
C(22)	8425(11)	-255(8)	9643(4)	69(3)
C(23)	8376(12)	-1206(8)	9781(4)	71(3)
C(24)	7790(11)	-1884(8)	9501(4)	63(3)
C(25)	7281(11)	-1650(7)	9084(4)	64(3)
C(26)	7347(11)	-729(7)	8947(4)	63(3)
C(31)	7761(10)	1221(7)	8487(3)	53(2)
C(32)	6521(11)	1549(8)	8245(3)	63(3)
C(33)	6364(12)	1509(10)	7812(4)	77(3)
C(34)	7428(13)	1150(9)	7594(4)	75(3)
C(35)	8656(14)	834(9)	7817(4)	75(3)
C(36)	8808(11)	877(8)	8270(4)	67(3)
P(2)	7845(2)	5005(2)	8223(1)	48(1)

C(41)	8119(10)	6151(8)	7961(3)	56(2)
C(42)	7666(11)	6264(8)	7532(3)	63(3)
C(43)	7858(12)	7130(10)	7326(4)	84(4)
C(44)	8500(11)	7886(9)	7558(4)	73(3)
C(45)	8901(12)	7767(9)	7995(4)	73(3)
C(46)	8736(11)	6913(7)	8192(3)	61(3)
C(51)	6944(10)	4294(7)	7786(3)	54(2)
C(52)	5493(10)	4380(7)	7689(3)	59(2)
C(53)	4847(12)	3973(9)	7309(4)	74(3)
C(54)	5543(13)	3504(9)	7041(4)	77(3)
C(55)	7012(15)	3413(9)	7134(4)	86(4)
C(56)	7708(12)	3804(8)	7505(4)	68(3)
C(61)	9580(9)	4476(7)	8343(3)	48(2)
C(62)	10823(9)	4996(7)	8349(3)	57(2)
C(63)	12106(10)	4562(8)	8479(4)	65(3)
C(64)	12183(10)	3629(7)	8607(3)	56(2)
C(65)	10974(10)	3124(8)	8607(3)	57(2)
C(66)	9658(10)	3529(7)	8474(3)	53(2)

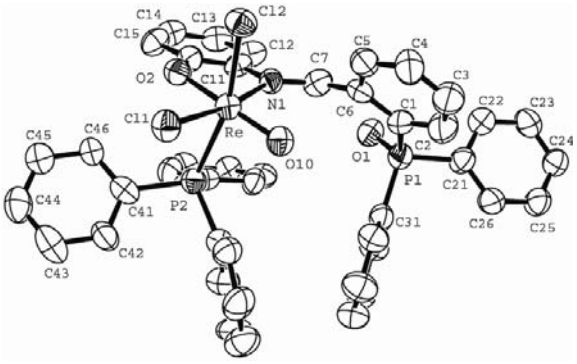

Fig. 7 Ellipsoid plot (50% probability) of $[ReOCl_2(PPh_3)(HL^{51}PO)]$

$[ReCl_3(NC_6H_4OH)(PPh_3)_2]$, (8)

Table 15 Crystal data and structure refinement for $[Re(NC_6H_4OH)Cl_3(PPh_3)_2)]\cdot THF$

Empirical formula	$C_{46}H_{43}Cl_3NO_2P_2Re$	
Formula weight	996.37	
Temperature	200(2) K	
Wavelength	0.71073 Å	
Crystal system	Triclinic	
Space group	$P\bar{1}$	
Unit cell dimensions	a = 10.8740(7) Å	α= 73.124(5)°.
	b = 12.198(1) Å	β= 75.088(5)°.
	c = 16.772(1) Å	γ = 82.032(5)°.
Volume	2052.4(2) $Å^3$	
Z	2	
Density (calculated)	1.612 g/cm^3	
Absorption coefficient	3.274 mm^{-1}	
F(000)	996	
Crystal size	0.13 x 0.09 x 0.03 mm^3	
Crystal description	Plate	
Crystal color	Green	
Diff. measurement device type	STOE IPDS 2T	
Theta range for data collection	2.61 to 29.26°.	
Index ranges	-14<=h<=14, -16<=k<=16, -22<=l<=23	
Reflections collected	20987	
Independent reflections	10926 [R(int) = 0.0700]	
Completeness to theta = 29.26°	97.8 %	
Absorption correction	Integration	
Max. and min. transmission	0.8172 and 0.6807	
Refinement method	Full-matrix least-squares on F^2	
Data / restraints / parameters	10926 / 0 / 543	
Goodness-of-fit on F^2	1.022	
Final R indices [I>2sigma(I)]	R1 = 0.0547, wR2 = 0.1203	
R indices (all data)	R1 = 0.0781, wR2 = 0.1312	
Extinction coefficient	0.0082(6)	
Largest diff. peak and hole	1.726 and -2.842 $e.Å^{-3}$	

Table 16 Atomic coordinates (x 10^4) and equivalent isotropic displacement parameters ($Å^2$x 10^3) for $[Re(NC_6H_4OH)Cl_3(PPh_3)_2)]\cdot THF$. U(eq) is defined as one third of the trace of the orthogonalized U^{ij} tensor.

	x	y	z	U(eq)
Re	1294(1)	1463(1)	2502(1)	25(1)
Cl(1)	3437(2)	2021(1)	1861(1)	36(1)
Cl(2)	984(2)	2403(1)	1074(1)	37(1)
Cl(3)	1876(2)	567(1)	3846(1)	36(1)
P(1)	1944(2)	-407(1)	2128(1)	29(1)
C(1)	609(6)	-1335(5)	2580(4)	30(1)
C(2)	120(7)	-1577(6)	3461(4)	37(1)
C(3)	-840(7)	-2330(6)	3862(5)	42(2)
C(4)	-1317(8)	-2838(6)	3379(5)	46(2)
C(5)	-855(8)	-2606(7)	2511(5)	46(2)
C(6)	125(7)	-1852(6)	2110(5)	41(2)
C(11)	3230(6)	-1325(5)	2566(4)	32(1)
C(12)	3223(7)	-2528(6)	2717(5)	40(2)
C(13)	4255(8)	-3227(6)	2973(5)	47(2)
C(14)	5251(8)	-2774(6)	3093(5)	47(2)
C(15)	5242(8)	-1603(7)	2959(6)	51(2)
C(16)	4232(7)	-879(6)	2696(5)	42(2)
C(21)	2413(7)	-383(6)	997(4)	35(1)
C(22)	1557(8)	92(7)	468(5)	44(2)
C(26)	3601(8)	-844(7)	646(5)	46(2)
C(23)	1885(11)	104(8)	-380(6)	63(3)
C(25)	3915(10)	-834(9)	-215(6)	61(2)
C(24)	3069(11)	-366(9)	-725(6)	67(3)
P(2)	879(2)	3341(1)	2864(1)	27(1)
C(41)	-735(6)	3409(5)	3526(4)	27(1)
C(42)	-976(6)	2593(6)	4324(4)	36(1)
C(43)	-2166(7)	2553(6)	4860(4)	37(1)
C(44)	-3167(7)	3296(6)	4614(4)	36(1)
C(45)	-2963(6)	4098(6)	3830(5)	37(1)
C(46)	-1737(6)	4166(5)	3290(4)	35(1)
C(51)	1792(6)	3642(5)	3538(4)	29(1)
C(52)	2965(7)	3073(6)	3636(4)	37(1)
C(53)	3642(7)	3349(6)	4137(5)	42(2)
C(54)	3167(8)	4217(6)	4538(5)	42(2)

C(55)	2007(7)	4800(6)	4439(5)	40(2)
C(56)	1329(6)	4527(5)	3942(4)	34(1)
C(61)	1043(7)	4611(5)	1957(4)	34(1)
C(62)	2065(8)	5288(6)	1760(5)	41(2)
C(63)	2222(10)	6222(7)	1046(5)	53(2)
C(64)	1386(10)	6510(7)	528(5)	57(2)
C(65)	384(9)	5835(7)	703(5)	52(2)
C(66)	210(7)	4881(6)	1411(4)	38(2)
N(10)	-292(5)	1181(4)	2870(3)	30(1)
C(31)	-1574(6)	1039(5)	3105(4)	31(1)
C(32)	-2145(7)	429(7)	3939(5)	42(2)
C(33)	-3433(7)	308(7)	4171(6)	50(2)
C(34)	-4183(7)	805(8)	3589(6)	51(2)
C(35)	-3648(7)	1402(7)	2766(6)	47(2)
C(36)	-2343(7)	1536(6)	2505(5)	39(1)
O(1)	-1864(6)	2122(6)	1694(4)	59(2)
O(2)	6850(20)	5630(40)	1705(15)	73(11)
C(71)	6080(20)	4647(17)	1811(14)	51(4)
C(74)	6560(30)	6400(30)	1000(19)	71(8)
C(73)	6450(30)	5800(30)	415(17)	62(6)
C(72)	5840(30)	4650(20)	953(15)	70(8)
O(3)	6780(40)	5660(30)	1840(30)	115(16)
C(81)	6030(40)	5320(60)	710(50)	190(40)
C(82)	6700(40)	4860(40)	1490(30)	125(16)
C(83)	6030(30)	6590(40)	630(20)	129(17)
C(84)	6830(40)	6800(30)	1144(15)	91(12)

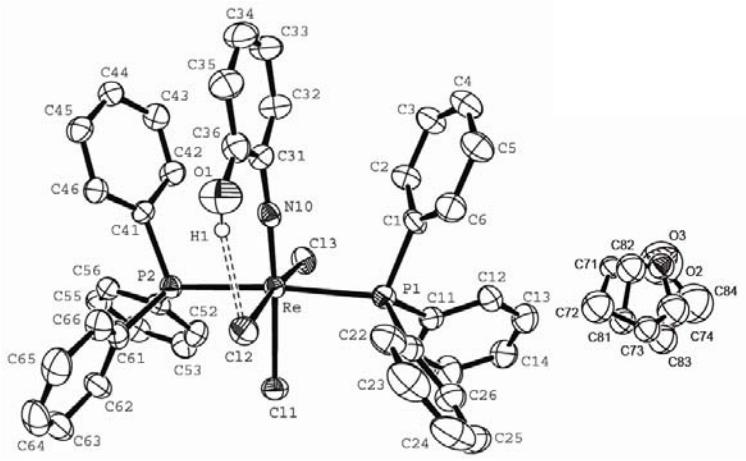

Fig. 8 Ellipsoid plot (50% probability) of [Re(NC_6H_4OH) $Cl_3(PPh_3)_2$)]·THF.

$[ReOCl_2(HL^{51})]$, (9)

Table 17 Crystal data and structure refinement for $[ReOCl_2(HL^{51})]\cdot MeOH$

Empirical formula	$C_{26}H_{25}Cl_2NO_3PRe$	
Formula weight	687.54	
Temperature	200(2) K	
Wavelength	0.71073 Å	
Crystal system	Triclinic	
Space group	$P\bar{1}$	
Unit cell dimensions	a = 9.496(1) Å	α= 81.489(8)°.
	b = 10.733(1) Å	β= 78.660(9)°.
	c = 13.209(1) Å	γ = 74.984(8)°.
Volume	1268.1(2) $Å^3$	
Z	2	
Density (calculated)	1.801 g/cm^3	
Absorption coefficient	5.094 mm^{-1}	
F(000)	672	
Crystal size	0.41 x 0.2 x 0.06 mm^3	
Crystal description	Plate	
Crystal color	Green	
Diff. measurement device type	STOE IPDS 2T	
Theta range for data collection	1.97 to 29.27°.	
Index ranges	-12<=h<=12, -14<=k<=14, -18<=l<=14	
Reflections collected	14474	
Independent reflections	6753 [R(int) = 0.0570]	
Completeness to theta = 29.27°	97.7 %	
Absorption correction	Integration	
Max. and min. transmission	0.5527 and 0.4470	
Refinement method	Full-matrix least-squares on F^2	
Data / restraints / parameters	6753 / 0 / 294	
Goodness-of-fit on F^2	1.053	
Final R indices [I>2sigma(I)]	R1 = 0.0381, wR2 = 0.0951	
R indices (all data)	R1 = 0.0458, wR2 = 0.1015	
Extinction coefficient	0.0196(10)	
Largest diff. peak and hole	2.897 and -1.281 $e.Å^{-3}$	

Table 18 Atomic coordinates (x 10^4) and equivalent isotropic displacement parameters ($Å^2$x 10^3) for $[ReOCl_2(HL^{51})]$·MeOH. U(eq) is defined as one third of the trace of the orthogonalized U^{ij} tensor.

	x	y	z	U(eq)
Re	8908(1)	9662(1)	7199(1)	25(1)
P	9316(1)	7775(1)	8448(1)	26(1)
Cl(1)	8299(2)	11032(1)	8527(1)	35(1)
Cl(2)	8157(2)	11487(1)	5938(1)	34(1)
N(1)	9033(5)	8445(4)	5972(3)	30(1)
O(10)	10733(4)	9509(4)	6813(3)	36(1)
O(1)	6870(4)	9436(3)	7389(3)	28(1)
C(16)	6443(6)	8960(5)	6627(4)	31(1)
C(1)	8923(5)	6399(4)	7996(4)	27(1)
C(21)	8219(5)	7941(4)	9736(4)	28(1)
C(6)	9245(6)	6218(5)	6944(4)	33(1)
C(11)	7530(6)	8462(5)	5835(4)	34(1)
C(12)	7195(8)	8017(6)	5006(5)	43(1)
C(2)	8303(6)	5511(5)	8710(4)	33(1)
C(32)	11855(6)	8219(5)	8892(4)	35(1)
C(7)	9969(6)	7092(5)	6112(4)	36(1)
C(31)	11226(5)	7284(5)	8640(4)	31(1)
C(4)	8331(9)	4268(6)	7340(6)	53(2)
C(15)	4952(6)	9009(5)	6609(5)	39(1)
C(3)	8010(7)	4453(5)	8384(5)	43(1)
C(14)	4628(8)	8535(7)	5790(6)	50(2)
C(13)	5720(9)	8073(7)	4979(6)	52(2)
C(25)	5830(7)	8443(6)	10796(5)	45(1)
C(26)	6687(6)	8344(6)	9838(5)	40(1)
C(22)	8852(7)	7664(7)	10621(5)	46(1)
C(36)	12074(7)	6019(6)	8548(5)	43(1)
C(35)	13511(8)	5702(7)	8749(7)	58(2)
C(24)	6471(7)	8205(7)	11679(5)	48(1)
C(5)	8942(8)	5145(6)	6635(5)	47(1)
C(34)	14141(7)	6619(7)	8980(6)	53(2)
C(33)	13310(7)	7874(7)	9076(5)	44(1)
C(23)	7992(8)	7773(9)	11591(5)	59(2)
O(3)	6451	4849	4284	53(2)
C(51)	4823	5138	4364	143(12)

O(4)	3887	4969	6098	66(3)
C(52)	5299	4686	6473	111(8)

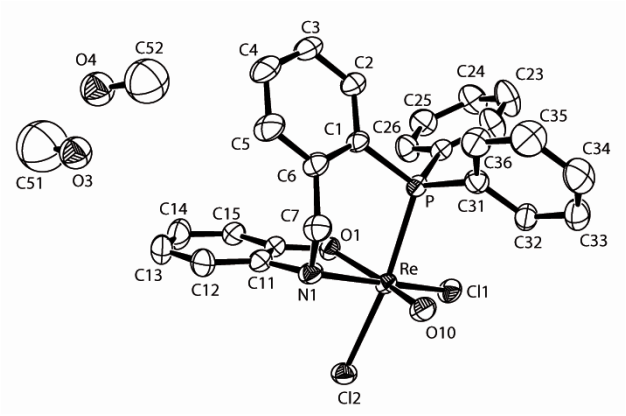

Fig. 9 Ellipsoid plot (50% probability) of [$ReOCl_2$ (HL^{51})]·MeOH

[ReO(L^{51})(Ph_2btu)], (10)

Table 19 Crystal data and structure refinement for [ReO(L^{51})(tbuPh_2)]·MeOH

Empirical formula	$C_{46}H_{39}N_3O_4PReS$	
Formula weight	947.03	
Temperature	200(2) K	
Wavelength	0.71073 Å	
Crystal system	Monoclinic	
Space group	$P2_1/c$	
Unit cell dimensions	a = 9.9411(6) Å	α= 90°.
	b = 21.283(1) Å	β= 98.585(5)°.
	c = 18.667(1) Å	γ = 90°.
Volume	3905.2(4) $Å^3$	
Z	4	
Density (calculated)	1.611 g/cm^3	
Absorption coefficient	3.256 mm^{-1}	
F(000)	1896	
Crystal size	0.3 x 0.09 x 0.04 mm^3	
Crystal description	Needle	
Crystal color	Red-brown	
Diff. measurement device type	STOE IPDS 2T	
Theta range for data collection	2.67 to 26.75°.	
Index ranges	-10<=h<=12, -26<=k<=26, -23<=l<=23	
Reflections collected	23854	
Independent reflections	8263 [R(int) = 0.0921]	
Completeness to theta = 26.75°	99.4 %	
Absorption correction	Integration	
Max. and min. transmission	0.7828 and 0.5226	
Refinement method	Full-matrix least-squares on F^2	
Data / restraints / parameters	8263 / 0 / 497	
Goodness-of-fit on F^2	0.825	
Final R indices [I>2sigma(I)]	R1 = 0.0425, wR2 = 0.0692	
R indices (all data)	R1 = 0.1030, wR2 = 0.0803	
Extinction coefficient	0.00082(7)	
Largest diff. peak and hole	1.256 and -1.271 e.$Å^{-3}$	

Table 20 Atomic coordinates (x 10^4) and equivalent isotropic displacement parameters ($Å^2$x 10^3) for [ReO(L^{51})($tbuPh_2$)]·MeOH. U(eq) is defined as one third of the trace of the orthogonalized U^{ij} tensor.

	x	y	z	U(eq)
Re	6165(1)	8748(1)	1625(1)	28(1)
O(10)	4892(4)	9272(2)	1452(3)	33(1)
P	7666(2)	9283(1)	900(1)	27(1)
C(1)	9369(6)	9154(3)	1366(4)	29(2)
C(2)	10438(6)	8947(3)	1016(4)	34(2)
C(3)	11706(7)	8839(3)	1398(4)	43(2)
C(4)	11946(8)	8934(3)	2135(5)	50(2)
C(5)	10914(7)	9149(3)	2500(4)	39(2)
C(6)	9607(7)	9255(3)	2118(4)	33(2)
C(7)	8482(7)	9476(3)	2525(4)	38(2)
N(1)	7329(5)	9040(2)	2497(3)	32(1)
C(11)	7079(6)	8755(4)	3147(3)	36(2)
C(12)	7699(7)	8885(3)	3853(4)	43(2)
C(13)	7298(9)	8570(4)	4434(4)	56(2)
C(14)	6275(10)	8119(4)	4311(5)	60(2)
C(15)	5668(9)	7987(4)	3622(4)	48(2)
C(16)	6066(7)	8291(3)	3042(4)	36(2)
O(1)	5511(5)	8182(2)	2336(3)	36(1)
C(21)	7688(7)	9092(3)	-50(4)	27(2)
C(22)	7772(7)	8467(3)	-263(4)	35(2)
C(23)	7742(7)	8304(3)	-988(4)	40(2)
C(24)	7609(7)	8784(4)	-1499(4)	45(2)
C(25)	7495(8)	9396(4)	-1308(4)	44(2)
C(26)	7551(7)	9551(3)	-582(4)	34(2)
C(31)	7475(6)	10139(3)	881(3)	29(2)
C(32)	6213(7)	10412(3)	830(4)	35(2)
C(33)	6090(7)	11058(3)	766(4)	43(2)
C(34)	7205(8)	11429(3)	752(4)	43(2)
C(35)	8477(7)	11155(3)	822(4)	37(2)
C(36)	8616(7)	10518(3)	892(4)	33(2)
C(41)	8868(7)	7088(3)	1889(4)	33(2)
C(42)	9969(8)	7403(4)	2276(4)	43(2)
C(43)	11144(8)	7077(4)	2538(5)	55(2)
C(44)	11207(9)	6439(4)	2413(5)	63(3)

C(45)	10118(9)	6123(3)	2015(5)	55(2)
C(46)	8942(8)	6453(3)	1762(4)	44(2)
C(47)	7603(7)	7434(3)	1625(4)	31(2)
O(2)	7688(4)	8035(2)	1611(2)	31(1)
N(2)	6506(6)	7082(2)	1436(3)	33(1)
C(48)	5352(7)	7297(3)	1067(4)	30(2)
S	5019(2)	8027(1)	684(1)	33(1)
N(3)	4384(6)	6845(2)	911(3)	35(1)
C(51)	3094(7)	6959(3)	450(4)	34(2)
C(52)	2913(9)	6776(4)	-257(5)	53(2)
C(53)	1658(11)	6860(4)	-680(5)	69(3)
C(54)	613(10)	7133(4)	-378(7)	69(3)
C(55)	822(9)	7302(4)	312(6)	64(3)
C(56)	2039(9)	7224(3)	754(5)	51(2)
C(61)	4625(7)	6223(4)	1211(4)	43(2)
C(62)	4502(8)	6121(4)	1915(5)	61(2)
C(63)	4691(9)	5515(5)	2200(6)	72(3)
C(64)	5031(11)	5035(4)	1780(7)	80(3)
C(65)	5198(15)	5139(4)	1091(7)	114(5)
C(66)	5001(13)	5743(4)	795(5)	92(4)
O(6)	624(8)	4956(3)	9511(4)	90(2)
C(81)	1537(9)	5129(4)	9543(5)	51(2)

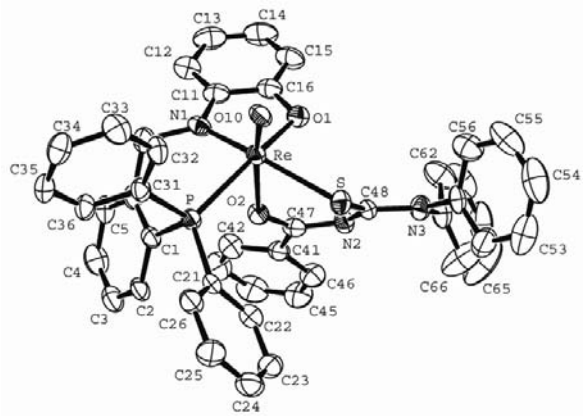

Fig. 10 Ellipsoid plot (50% probability) of [ReO(L^{51})(Ph_2tbu)]·MeOH

$[TcCl_3(L^{51}P)]$, (11)

Table 21 Crystal data and structure refinement for $[TcCl_3(L^{51}P)]\cdot MeCN$

Empirical formula	$C_{27}H_{22}Cl_3N_2OPTc$	
Formula weight	625.79	
Temperature	200(2) K	
Wavelength	0.71073 Å	
Crystal system	Orthorhombic	
Space group	Pbca	
Unit cell dimensions	a = 17.1510(6) Å	α= 90°.
	b = 12.8243(5) Å	β= 90°.
	c = 24.207(1) Å	γ = 90°.
Volume	5324.3(4) $Å^3$	
Z	8	
Density (calculated)	1.561 g/cm^3	
Absorption coefficient	0.926 mm^{-1}	
F(000)	2520	
Crystal size	0.360 x 0.340 x 0.320 mm^3	
Crystal description	Octahedron	
Crystal color	Red	
Diff. measurement device type	STOE IPDS 2T	
Theta range for data collection	2.86 to 29.29°.	
Index ranges	-23<=h<=23, -17<=k<=17, -29<=l<=33	
Reflections collected	50359	
Independent reflections	7207 [R(int) = 0.0700]	
Completeness to theta = 29.29°	99.0 %	
Absorption correction	None	
Max. and min. transmission	None and None	
Refinement method	Full-matrix least-squares on F^2	
Data / restraints / parameters	7207 / 0 / 317	
Goodness-of-fit on F^2	0.673	
Final R indices [I>2sigma(I)]	R1 = 0.0339, wR2 = 0.0887	
R indices (all data)	R1 = 0.0612, wR2 = 0.1037	
Largest diff. peak and hole	0.467 and -0.925 $e.Å^{-3}$	

Table 22 Atomic coordinates (x 10^4) and equivalent isotropic displacement parameters ($Å^2$x 10^3) for $[TcCl_3(L^{51}P)]\cdot MeCN$. U(eq) is defined as one third of the trace of the orthogonalized U^{ij} tensor.

	x	y	z	U(eq)
Tc	567(1)	2709(1)	1219(1)	24(1)
Cl(1)	645(1)	3538(1)	2079(1)	34(1)
Cl(2)	364(1)	1758(1)	417(1)	37(1)
Cl(3)	1144(1)	4071(1)	759(1)	39(1)
P	-750(1)	3480(1)	1149(1)	25(1)
O	1530(1)	1876(2)	1360(1)	30(1)
N(1)	86(1)	1394(2)	1622(1)	27(1)
C(1)	-1364(2)	2938(2)	1691(1)	31(1)
C(2)	-2034(2)	3495(3)	1819(1)	40(1)
C(3)	-2570(2)	3111(3)	2198(2)	50(1)
C(4)	-2443(2)	2171(3)	2454(2)	56(1)
C(5)	-1781(2)	1610(3)	2332(1)	45(1)
C(6)	-1221(2)	1975(2)	1951(1)	32(1)
C(7)	-565(2)	1262(2)	1882(1)	33(1)
C(11)	645(2)	555(2)	1608(1)	31(1)
C(12)	482(2)	-494(2)	1705(1)	41(1)
C(13)	1080(2)	-1209(3)	1690(2)	50(1)
C(14)	1838(2)	-890(3)	1576(2)	49(1)
C(15)	2003(2)	144(3)	1469(1)	40(1)
C(16)	1403(2)	879(2)	1475(1)	30(1)
C(21)	-1268(2)	3249(2)	507(1)	29(1)
C(22)	-2041(2)	2911(3)	493(1)	40(1)
C(23)	-2407(2)	2780(3)	-12(2)	53(1)
C(24)	-2015(2)	2959(3)	-499(2)	51(1)
C(25)	-1250(2)	3290(3)	-490(1)	43(1)
C(26)	-874(2)	3434(2)	13(1)	35(1)
C(31)	-787(2)	4890(2)	1253(1)	28(1)
C(32)	-868(2)	5558(2)	806(1)	37(1)
C(33)	-877(2)	6626(3)	889(2)	45(1)
C(34)	-812(2)	7029(3)	1415(2)	46(1)
C(35)	-737(2)	6370(3)	1859(2)	48(1)
C(36)	-721(2)	5304(3)	1782(1)	39(1)
N(2)	-1444(3)	-240(4)	1107(2)	87(1)
C(41)	-1503(3)	-4(4)	656(2)	67(1)

C(42)	-1584(4)	289(4)	82(2)	81(2)

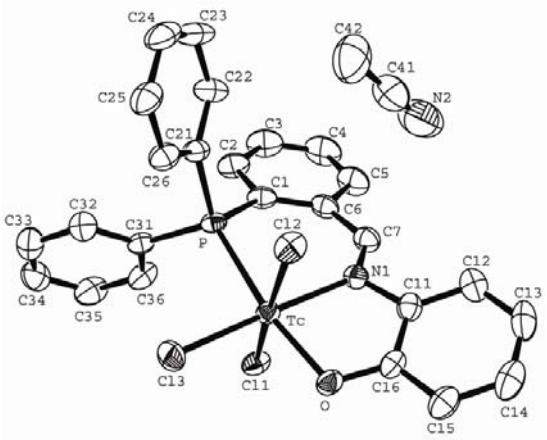

Fig. 11 Ellipsoid plot (50% probability) of $[TcCl_3(L^{51}P)]\cdot MeCN$

[ReCl(L^{52})], (12)

Table 23 Crystal data and structure refinement for [ReCl(L^{52})]·H_2O

Empirical formula	$C_{32}H_{25}ClN_2O_3PRe$	
Formula weight	738.16	
Temperature	200(2) K	
Wavelength	0.71073 Å	
Crystal system	Triclinic	
Space group	P $\bar{1}$	
Unit cell dimensions	a = 8.763(1) Å	α= 106.92(1)°.
	b = 11.019(1) Å	β= 90.90(1)°.
	c = 15.830(2) Å	γ = 108.46(1)°.
Volume	1377.2(3) $Å^3$	
Z	2	
Density (calculated)	1.780 g/cm^3	
Absorption coefficient	4.605 mm^{-1}	
F(000)	724	
Crystal size	0.2 x 0.147 x 0.1 mm^3	
Crystal description	Block	
Crystal color	Red	
Diff. measurement device type	STOE IPDS 2T	
Theta range for data collection	2.47 to 25.00°.	
Index ranges	-10<=h<=10, -13<=k<=13, -18<=l<=18	
Reflections collected	10016	
Independent reflections	4733 [R(int) = 0.1239]	
Completeness to theta = 25.00°	97.6 %	
Absorption correction	Integration	
Max. and min. transmission	0.7803 and 0.4536	
Refinement method	Full-matrix least-squares on F^2	
Data / restraints / parameters	4733 / 0 / 361	
Goodness-of-fit on F^2	1.093	
Final R indices [I>2sigma(I)]	R1 = 0.0616, wR2 = 0.1042	
R indices (all data)	R1 = 0.1040, wR2 = 0.1151	
Largest diff. peak and hole	1.580 and -2.285 e.$Å^{-3}$	

Table 24 Atomic coordinates (x 10^4) and equivalent isotropic displacement parameters ($Å^2$x 10^3) for [ReCl(L^{52})]·H_2O. U(eq) is defined as one third of the trace of the orthogonalized U^{ij} tensor.

	x	y	z	U(eq)
Re	6479(1)	7525(1)	7285(1)	46(1)
Cl	5993(3)	9208(3)	8478(2)	59(1)
P	6024(3)	6225(3)	8260(2)	46(1)
C(1)	6374(11)	4602(11)	7844(8)	48(3)
C(2)	6267(12)	3871(11)	8436(8)	49(3)
C(3)	6481(12)	2647(11)	8184(9)	53(3)
C(4)	6789(12)	2119(12)	7328(10)	57(3)
C(5)	6903(12)	2836(11)	6726(9)	51(3)
C(6)	6671(11)	4089(10)	6984(8)	45(3)
C(7)	6876(11)	4869(10)	6312(8)	45(3)
N(1)	5818(10)	5714(9)	6443(6)	50(2)
C(11)	4222(12)	5048(10)	6067(7)	44(3)
C(12)	3480(13)	3732(11)	5564(8)	51(3)
C(13)	1827(14)	3310(13)	5296(9)	57(3)
C(14)	981(15)	4189(12)	5542(8)	59(3)
C(15)	1670(13)	5520(12)	6012(8)	53(3)
C(16)	3369(12)	5949(11)	6306(7)	44(3)
O(1)	4213(9)	7214(7)	6765(5)	51(2)
C(21)	7478(12)	7112(11)	9257(8)	49(3)
C(22)	7157(15)	7305(12)	10108(9)	63(4)
C(23)	8289(15)	8082(12)	10814(9)	59(3)
C(24)	9899(15)	8679(11)	10652(9)	60(4)
C(25)	10240(14)	8493(11)	9793(10)	59(3)
C(26)	9121(12)	7704(10)	9056(8)	47(3)
C(27)	9583(12)	7428(11)	8139(8)	46(3)
N(2)	8793(10)	7919(9)	7553(6)	45(2)
C(31)	9807(12)	8877(10)	7182(8)	43(3)
C(32)	11509(12)	9211(11)	7199(8)	52(3)
C(33)	12316(14)	10132(13)	6768(10)	73(4)
C(34)	11481(16)	10671(15)	6315(11)	76(4)
C(35)	9823(14)	10365(11)	6306(9)	56(3)
C(36)	9003(13)	9429(11)	6762(9)	58(3)
O(2)	7352(8)	9024(7)	6724(6)	53(2)
C(41)	3981(12)	5712(11)	8564(8)	49(3)

C(42)	2887(12)	4509(12)	8027(9)	55(3)
C(43)	1247(15)	4138(14)	8168(11)	70(4)
C(44)	767(15)	4921(16)	8862(11)	72(4)
C(45)	1827(15)	6136(15)	9417(10)	73(4)
C(46)	3446(14)	6546(12)	9246(9)	58(3)
O(3)	4956(15)	1125(11)	4644(9)	120(4)

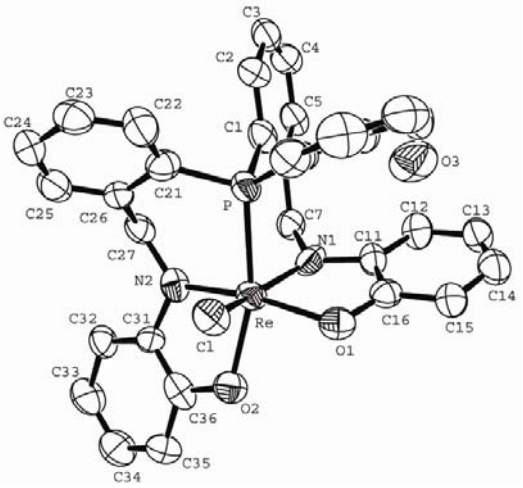

Fig. 12 Ellipsoid plot (50% probability) of $[ReCl(L^{52})]\cdot H_2O$

[ReO(HL^{52})], (13)

Table 25 Crystal data and structure refinement for [ReO(HL^{52})]·THF

Empirical formula	$C_{36}H_{34}N_2O_4PRe$	
Formula weight	775.82	
Temperature	200(2) K	
Wavelength	0.71073 Å	
Crystal system	Monoclinic	
Space group	C2/c	
Unit cell dimensions	a = 28.044(2) Å	α= 90°.
	b = 12.9448(8) Å	β= 90.422(7)°.
	c = 16.748(1) Å	γ = 90°.
Volume	6080.0(8) Å^3	
Z	8	
Density (calculated)	1.695 g/cm^3	
Absorption coefficient	4.094 mm^{-1}	
F(000)	3088	
Crystal size	0.200 x 0.150 x 0.050 mm^3	
Crystal description	Plate	
Crystal color	Yellow	
Diff. measurement device type	STOE IPDS 2T	
Theta range for data collection	2.43 to 25.00°.	
Index ranges	-32<=h<=33, -15<=k<=15, -19<=l<=19	
Reflections collected	19319	
Independent reflections	5301 [R(int) = 0.1528]	
Completeness to theta = 25.00°	98.9 %	
Absorption correction	Integration	
Max. and min. transmission	0.7833 and 0.4986	
Refinement method	Full-matrix least-squares on F^2	
Data / restraints / parameters	5301 / 0 / 387	
Goodness-of-fit on F^2	0.927	
Final R indices [I>2sigma(I)]	R1 = 0.0551, wR2 = 0.0953	
R indices (all data)	R1 = 0.1094, wR2 = 0.1088	
Largest diff. peak and hole	1.067 and -1.680 e.Å^{-3}	

Table 26 Atomic coordinates (x 10^4) and equivalent isotropic displacement parameters ($Å^2$x 10^3) for [ReO(HL^{52})]·THF. U(eq) is defined as one third of the trace of the orthogonalized U^{ij} tensor.

	x	y	z	U(eq)
Re	3342(1)	7351(1)	9361(1)	31(1)
O(1)	3115(3)	8535(4)	9175(5)	37(2)
P	3736(1)	7089(2)	8110(2)	29(1)
C(1)	3392(4)	6417(7)	7341(6)	31(2)
C(2)	3620(4)	5969(7)	6695(6)	39(3)
C(3)	3366(5)	5436(8)	6116(7)	47(3)
C(4)	2878(5)	5337(8)	6183(8)	47(3)
C(5)	2644(4)	5822(8)	6811(7)	37(3)
C(6)	2892(4)	6384(7)	7398(7)	37(3)
C(7)	2591(4)	6998(8)	7999(7)	39(3)
N(1)	2649(3)	6743(6)	8842(5)	31(2)
C(11)	2630(4)	5632(7)	8950(7)	36(3)
C(12)	2224(5)	5053(9)	8837(8)	51(3)
C(13)	2250(5)	3990(9)	8868(8)	54(4)
C(14)	2674(5)	3519(8)	9032(8)	52(3)
C(15)	3088(4)	4089(7)	9173(7)	42(3)
C(16)	3058(4)	5164(8)	9147(7)	38(3)
O(2)	3437(2)	5793(5)	9322(5)	34(2)
C(21)	4250(4)	6337(7)	8405(6)	31(2)
C(22)	4357(4)	5342(7)	8101(7)	37(3)
C(23)	4746(4)	4803(8)	8392(7)	44(3)
C(24)	5044(5)	5234(8)	8968(8)	51(3)
C(25)	4945(4)	6186(7)	9272(7)	36(3)
C(26)	4541(4)	6739(7)	9025(7)	35(3)
C(27)	4413(3)	7717(8)	9448(6)	36(2)
N(2)	3955(3)	7583(6)	9879(5)	34(2)
C(31)	3970(3)	7432(6)	10703(6)	30(2)
C(32)	4362(4)	7503(7)	11242(6)	39(2)
C(33)	4312(4)	7322(8)	12028(7)	44(3)
C(34)	3887(4)	7022(7)	12342(7)	41(3)
C(35)	3491(4)	6921(7)	11843(6)	36(3)
C(36)	3531(4)	7153(7)	11039(6)	32(2)
O(3)	3156(3)	7075(4)	10501(4)	33(2)
C(41)	3987(4)	8193(7)	7596(7)	33(2)

C(42)	3766(4)	9165(7)	7629(7)	42(3)
C(43)	3959(5)	9990(8)	7229(8)	50(3)
C(44)	4363(5)	9874(8)	6761(9)	61(4)
C(45)	4581(5)	8902(9)	6721(9)	63(4)
C(46)	4400(5)	8083(8)	7126(9)	52(3)
O(4)	562(5)	4426(9)	547(10)	114(5)
C(01)	482(4)	3386(9)	418(9)	52(3)
C(02)	892(6)	2794(11)	316(13)	103(6)
C(03)	1317(5)	3488(9)	580(12)	82(5)
C(04)	1105(5)	4516(10)	346(11)	73(5)

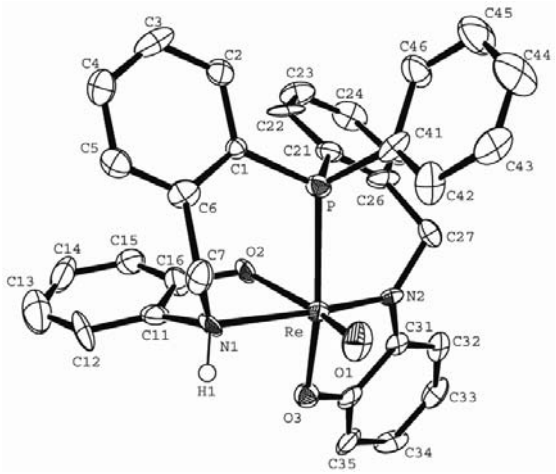

Fig. 13 Ellipsoid plot (50% probability) of [[ReO(HL^{52})]·THF

[Re(L^{53}P)], (14)

Table 27 Crystal data and structure refinement for [Re(L^{53}P)].H_2O

Empirical formula	$C_{39}H_{27}N_3O_4PRe$	
Formula weight	818.81	
Temperature	200(2) K	
Wavelength	0.71073 Å	
Crystal system	Trigonal	
Space group	$R\bar{3}$	
Unit cell dimensions	a = 14.014(1) Å	α= 90°.
	b = 14.014(1) Å	β= 90°.
	c = 30.647(3) Å	γ = 120°.
Volume	5212.4(7) $Å^3$	
Z	6	
Density (calculated)	1.565 g/cm^3	
Absorption coefficient	3.587 mm^{-1}	
F(000)	2424	
Crystal size	0.150 x 0.077 x 0.02 mm^3	
Crystal description	Plate	
Crystal color	Green	
Diff. measurement device type	STOE IPDS 2T	
Theta range for data collection	3.53 to 26.83°.	
Index ranges	-17<=h<=17, -17<=k<=17, -35<=l<=38	
Reflections collected	13756	
Independent reflections	2328 [R(int) = 0.1721]	
Completeness to theta = 26.83°	93.3 %	
Absorption correction	Integration	
Max. and min. transmission	0.6816 and 0.5113	
Refinement method	Full-matrix least-squares on F^2	
Data / restraints / parameters	2328 / 0 / 147	
Goodness-of-fit on F^2	0.929	
Final R indices [I>2sigma(I)]	R1 = 0.0566, wR2 = 0.1183	
R indices (all data)	R1 = 0.1072, wR2 = 0.1353	
Extinction coefficient	0.0028(3)	
Largest diff. peak and hole	1.249 and -0.685 $e.Å^{-3}$	

Table 28 Atomic coordinates (x 10^4) and equivalent isotropic displacement parameters ($Å^2$x 10^3) for [Re(L^{53}P)]·H_2O. U(eq) is defined as one third of the trace of the orthogonalized U^{ij} tensor.

	x	y	z	U(eq)
Re(1)	3333	6667	3423(1)	45(1)
P	3333	6667	2672(1)	45(1)
C(1)	2193(7)	5416(7)	2463(3)	48(2)
C(2)	1495(7)	5402(8)	2142(3)	51(2)
C(3)	633(9)	4411(9)	2000(3)	62(3)
C(4)	484(9)	3440(8)	2170(4)	61(3)
C(5)	1160(8)	3455(8)	2492(4)	57(2)
C(6)	2037(8)	4439(7)	2655(3)	49(2)
O(1)	4515(5)	6744(5)	3835(2)	51(2)
C(7)	2736(8)	4394(8)	2991(4)	56(2)
C(11)	4173(8)	5088(8)	3507(3)	51(2)
C(12)	4401(9)	4234(9)	3469(4)	63(3)
C(13)	5120(10)	4188(11)	3764(5)	78(3)
C(14)	5621(10)	4976(11)	4086(4)	73(3)
C(15)	5390(9)	5795(10)	4121(4)	66(3)
C(16)	4692(7)	5920(8)	3824(3)	50(2)
N(1)	3406(6)	5230(7)	3238(3)	51(2)
O(2)	4510(12)	6953(12)	5063(5)	32(3)

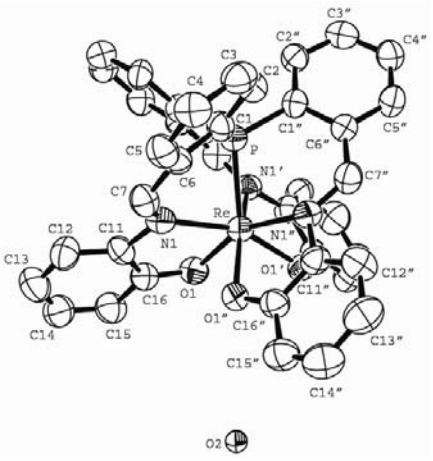

Fig. 14 Ellipsoid plot (50% probability) of [Re(L^{53}P)]·H_2O

$[ReOCl_2(HL^{51}COOEt)]$, (15)

Table 29 Crystal data and structure refinement for $[ReOCl_2(HL^{51}COOEt)]$

Empirical formula	$C_{28}H_{25}Cl_2NO_4PRe$	
Formula weight	727.56	
Temperature	200(2) K	
Wavelength	0.71073 Å	
Crystal system	Triclinic	
Space group	$P\bar{1}$	
Unit cell dimensions	a = 9.696(1) Å	α= 82.91(1)°.
	b = 10.740(1) Å	β= 78.60(1)°.
	c = 13.736(2) Å	γ = 73.76(1)°.
Volume	1342.8(3) $Å^3$	
Z	2	
Density (calculated)	1.799 g/cm^3	
Absorption coefficient	4.819 mm^{-1}	
F(000)	712	
Crystal size	0.7 x 0.04 x 0.03 mm^3	
Crystal description	Needle	
Crystal color	Green	
Diff. measurement device type	STOE IPDS 2T	
Theta range for data collection	2.58 to 29.29°.	
Index ranges	-13<=h<=13, -14<=k<=14, -16<=l<=18	
Reflections collected	13310	
Independent reflections	7046 [R(int) = 0.1990]	
Completeness to theta = 29.29°	96.0 %	
Absorption correction	Integration	
Max. and min. transmission	0.7608 and 0.6033	
Refinement method	Full-matrix least-squares on F^2	
Data / restraints / parameters	7046 / 0 / 335	
Goodness-of-fit on F^2	0.803	
Final R indices [I>2sigma(I)]	R1 = 0.0815, wR2 = 0.1123	
R indices (all data)	R1 = 0.2155, wR2 = 0.1544	
Extinction coefficient	0.00057(14)	
Largest diff. peak and hole	2.011 and -1.873 $e.Å^{-3}$	

Table 30 Atomic coordinates (x 10^4) and equivalent isotropic displacement parameters ($Å^2$x 10^3) for [$ReOCl_2(HL^{51}COOEt)$]. U(eq) is defined as one third of the trace of the orthogonalized U^{ij} tensor.

	x	y	z	U(eq)
Re	9101(1)	9622(1)	7249(1)	23(1)
Cl(2)	8454(5)	11379(4)	5961(4)	39(1)
O(1)	7137(11)	9375(10)	7320(9)	31(3)
Cl(1)	8174(5)	11103(4)	8484(3)	36(1)
P	9462(4)	7769(4)	8494(4)	24(1)
N(1)	9457(12)	8288(11)	6098(10)	24(3)
C(5)	9260(20)	5008(16)	6797(16)	36(5)
C(21)	8328(15)	8001(14)	9700(13)	22(4)
O(3)	5041(13)	7140(12)	3974(10)	47(3)
C(17)	6410(20)	6938(16)	4167(16)	42(5)
C(13)	6519(17)	7683(14)	4979(13)	30(4)
O(2)	7427(13)	6169(13)	3706(10)	61(4)
C(36)	12161(17)	5953(16)	8704(15)	35(5)
C(31)	11382(14)	7250(14)	8711(12)	27(4)
C(4)	8598(18)	4184(17)	7428(17)	44(5)
C(22)	6842(18)	8360(15)	9769(14)	35(4)
C(12)	7892(19)	7663(14)	5080(13)	34(4)
C(14)	5285(18)	8267(14)	5599(15)	40(5)
C(15)	5461(16)	8823(14)	6436(15)	39(5)
O(10)	10859(12)	9477(9)	7013(9)	33(3)
C(16)	6859(16)	8844(14)	6569(12)	30(4)
C(2)	8443(14)	5513(12)	8740(12)	24(4)
C(1)	9144(15)	6360(13)	8070(12)	24(3)
C(26)	8911(18)	7913(14)	10564(13)	36(4)
C(3)	8182(18)	4459(14)	8404(14)	36(4)
C(6)	9592(16)	6089(14)	7068(13)	32(4)
C(11)	8043(17)	8262(14)	5880(13)	32(4)
C(25)	8020(20)	8111(19)	11482(14)	53(5)
C(24)	6477(18)	8478(14)	11533(13)	33(4)
C(35)	13581(19)	5674(18)	8863(15)	48(5)
C(32)	11965(15)	8193(15)	8907(13)	35(4)
C(7)	10376(16)	6924(12)	6313(13)	32(4)
C(23)	5927(19)	8613(15)	10672(15)	45(5)
C(18)	4887(18)	6360(16)	3223(14)	43(5)

C(34)	14159(19)	6607(19)	9075(14)	50(5)
C(33)	13364(17)	7879(16)	9074(14)	42(5)
C(19)	4560(20)	5100(18)	3745(17)	66(6)

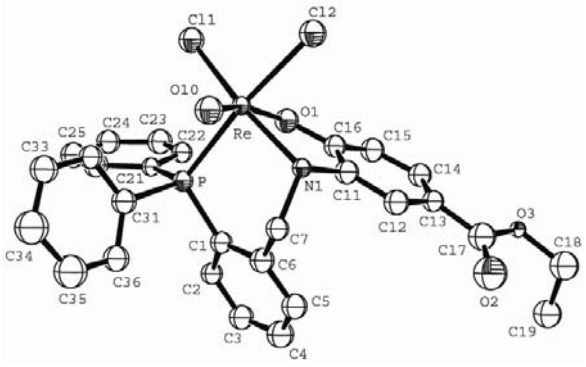

Fig. 15 Ellipsoid plot (50% probability) of $[ReOCl_2(HL^{51}COOEt)]$

$[ReBr(CO)_3(H_2L^{51}COOEt)]$, (16)

Table 31 Crystal data and structure refinement for $[ReBr(CO)_3(H_2L^{51}COOEt)]\cdot NEt_4Br$

Empirical formula	$C_{39}H_{46}Br_2N_2O_6PRe$	
Formula weight	1015.77	
Temperature	200(2) K	
Wavelength	0.71073 Å	
Crystal system	Triclinic	
Space group	$P\bar{1}$	
Unit cell dimensions	a = 8.3459(8) Å	α= 105.002(8)°.
	b = 12.021(1) Å	β= 93.101(8)°.
	c = 21.223(2) Å	γ = 94.161(8)°.
Volume	2045.4(3) $Å^3$	
Z	2	
Density (calculated)	1.649 g/cm^3	
Absorption coefficient	5.008 mm^{-1}	
F(000)	1004	
Crystal size	0.6 x 0.08 x 0.06 mm^3	
Crystal description	Needle	
Crystal color	Pale yellow	
Diff. measurement device type	STOE IPDS 2T	
Theta range for data collection	2.58 to 29.34°.	
Index ranges	-11<=h<=11, -16<=k<=16, -28<=l<=28	
Reflections collected	19711	
Independent reflections	10439 [R(int) = 0.1058]	
Completeness to theta = 29.34°	92.8 %	
Absorption correction	Integration	
Max. and min. transmission	0.6633 and 0.4538	
Refinement method	Full-matrix least-squares on F^2	
Data / restraints / parameters	10439 / 0 / 461	
Goodness-of-fit on F^2	1.132	
Final R indices [I>2sigma(I)]	R1 = 0.0809, wR2 = 0.2152	
R indices (all data)	R1 = 0.1157, wR2 = 0.2300	
Extinction coefficient	0.0054(6)	
Largest diff. peak and hole	3.237 and -3.867 $e.Å^{-3}$	

Table 32 Atomic coordinates (x 10^4) and equivalent isotropic displacement parameters ($Å^2$x 10^3) for $[ReBr(CO)_3(H_2L^{51}COOEt)]\cdot NEt_4Br$. U(eq) is defined as one third of the trace of the orthogonalized U^{ij} tensor.

	x	y	z	U(eq)
Re	3868(1)	6002(1)	2970(1)	36(1)
Br(1)	4504(2)	5185(1)	1740(1)	50(1)
C(10)	5899(17)	5730(11)	3324(6)	43(3)
O(10)	7143(12)	5598(10)	3543(5)	57(3)
C(20)	3245(18)	6697(12)	3848(8)	51(4)
O(20)	2900(14)	7090(10)	4327(6)	62(3)
C(30)	4827(17)	7514(12)	2943(8)	56(4)
O(30)	5407(13)	8401(9)	2930(6)	67(3)
P	2759(4)	4019(3)	2966(2)	37(1)
C(1)	1303(16)	3456(10)	2264(6)	40(3)
C(2)	1293(17)	2370(11)	1846(7)	46(3)
C(3)	246(17)	1996(12)	1293(8)	55(4)
C(4)	-840(20)	2693(14)	1143(7)	60(4)
C(5)	-875(15)	3793(10)	1542(7)	43(3)
C(6)	164(15)	4195(10)	2123(6)	40(3)
C(7)	31(15)	5396(10)	2558(7)	40(3)
N(1)	1427(12)	6231(8)	2502(5)	38(2)
C(11)	1010(16)	7423(9)	2696(7)	42(3)
C(12)	1491(16)	8174(11)	2312(7)	46(3)
C(13)	1143(19)	9310(11)	2475(8)	55(4)
C(14)	216(18)	9665(13)	3014(8)	57(4)
C(15)	-317(16)	8993(13)	3397(7)	50(3)
C(16)	132(17)	7828(11)	3216(7)	47(3)
O(1)	2306(13)	7714(8)	1778(5)	58(3)
C(17)	-1370(20)	9375(14)	3915(9)	68(5)
O(2)	-1830(17)	10331(10)	4043(6)	81(4)
O(3)	-1780(20)	8596(12)	4231(8)	106(6)
C(18)	-3310(40)	8770(20)	4711(13)	117(9)
C(19)	-2350(40)	9320(20)	5236(16)	133(11)
C(21)	1710(16)	3886(10)	3683(7)	44(3)
C(22)	202(17)	3325(12)	3648(8)	53(3)
C(23)	-470(20)	3165(15)	4201(10)	69(5)
C(24)	400(30)	3512(17)	4809(10)	85(7)

C(25)	1910(30)	4105(15)	4850(8)	72(5)
C(26)	2560(20)	4251(14)	4293(7)	57(4)
C(31)	4173(15)	2905(11)	2893(6)	40(3)
C(32)	5529(15)	2951(11)	2535(7)	44(3)
C(33)	6557(16)	2092(11)	2467(7)	46(3)
C(34)	6310(18)	1183(11)	2764(8)	53(3)
C(35)	4970(20)	1175(13)	3141(9)	63(4)
C(36)	3928(19)	2031(12)	3202(8)	58(4)
N(2)	6861(13)	7566(10)	380(6)	47(3)
C(41)	8080(20)	6789(15)	65(9)	64(4)
C(42)	7630(30)	5511(16)	-20(11)	82(6)
C(43)	6380(20)	7326(16)	1015(8)	65(4)
C(44)	7730(30)	7430(20)	1521(10)	87(6)
C(45)	5352(16)	7398(12)	-71(7)	48(3)
C(46)	5530(20)	7750(14)	-705(8)	63(4)
C(47)	7641(18)	8809(13)	485(9)	62(4)
C(48)	6680(20)	9738(14)	810(11)	78(5)
Br(2)	2053(2)	9089(1)	699(1)	54(1)

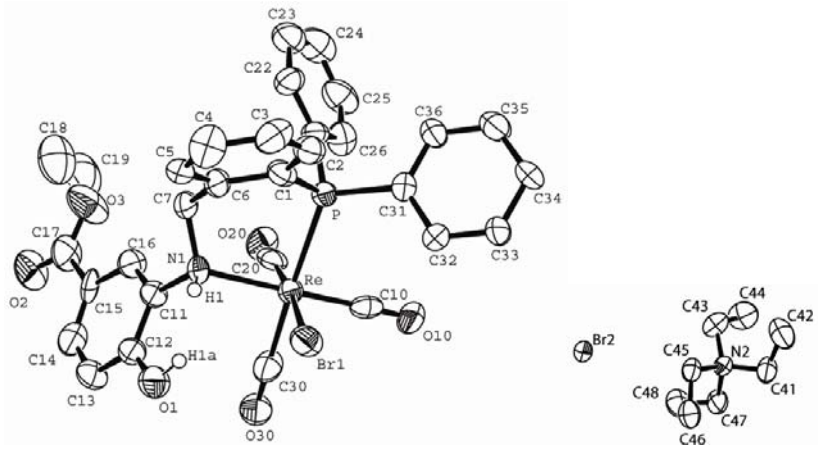

Fig. 16 Ellipsoid plot (50% probability) of $[ReBr(CO)_3(H_2L^{51}COOEt)]\cdot NEt_4Br$.

$[Re(CO)_3(HL^{51}COOMe)]$, (17)

Table 33 Crystal data and structure refinement for $[Re(CO)_3(HL^{51}COOMe)]\cdot 3MeOH$

Empirical formula	$C_{33}H_{35}NO_9PRe$	
Formula weight	806.79	
Temperature	200(2) K	
Wavelength	0.71073 Å	
Crystal system	Triclinic	
Space group	$P\bar{1}$	
Unit cell dimensions	a = 10.3041(7) Å	α= 88.148(6)°.
	b = 10.6852(7) Å	β= 87.243(6)°.
	c = 15.571(1) Å	γ = 79.588(6)°.
Volume	1683.8(2) $Å^3$	
Z	2	
Density (calculated)	1.591 g/cm^3	
Absorption coefficient	3.709 mm^{-1}	
F(000)	804	
Crystal size	0.4 x 0.21 x 0.14 mm^3	
Crystal description	Block	
Crystal color	Colorless	
Diff. measurement device type	STOE IPDS 2T	
Theta range for data collection	1.94 to 29.29°.	
Index ranges	-14<=h<=14, -14<=k<=14, -21<=l<=20	
Reflections collected	17460	
Independent reflections	8951 [R(int) = 0.0599]	
Completeness to theta = 29.29°	97.2 %	
Absorption correction	Integration	
Max. and min. transmission	0.5976 and 0.3905	
Refinement method	Full-matrix least-squares on F^2	
Data / restraints / parameters	8951 / 0 / 413	
Goodness-of-fit on F^2	0.874	
Final R indices [I>2sigma(I)]	R1 = 0.0351, wR2 = 0.0760	
R indices (all data)	R1 = 0.0529, wR2 = 0.0921	
Extinction coefficient	0.0140(6)	
Largest diff. peak and hole	1.415 and -1.620 $e.Å^{-3}$	

Table 34 Atomic coordinates (x 10^4) and equivalent isotropic displacement parameters ($Å^2$x 10^3) for $[Re(CO)_3(HL^{51}COOMe)]\cdot 3MeOH$. U(eq) is defined as one third of the trace of the orthogonalized U^{ij} tensor.

	x	y	z	U(eq)
Re	8324(1)	6210(1)	7445(1)	31(1)
C(10)	7909(5)	5053(5)	8371(3)	43(1)
O(10)	7689(4)	4324(4)	8874(3)	63(1)
C(20)	9555(5)	4839(5)	6944(3)	40(1)
O(20)	10298(4)	4020(4)	6640(3)	59(1)
C(30)	6967(5)	5761(5)	6801(3)	44(1)
O(30)	6117(4)	5501(5)	6417(3)	62(1)
P	8923(1)	7719(1)	6331(1)	30(1)
C(1)	7795(5)	9732(4)	7376(3)	38(1)
C(2)	7800(6)	10874(5)	7779(3)	50(1)
C(3)	8837(7)	11533(5)	7626(4)	55(2)
C(4)	9878(6)	11078(5)	7073(4)	50(1)
C(5)	9890(5)	9939(4)	6663(3)	41(1)
C(6)	8867(4)	9261(4)	6809(3)	33(1)
C(7)	6671(4)	9039(4)	7573(3)	39(1)
N(1)	7090(4)	7848(4)	8102(2)	33(1)
C(11)	7769(4)	8112(4)	8856(3)	31(1)
C(12)	7126(4)	8800(4)	9534(3)	34(1)
C(13)	7845(4)	9105(4)	10204(3)	35(1)
C(14)	9217(5)	8725(5)	10178(3)	39(1)
C(15)	9858(4)	8003(5)	9505(3)	38(1)
C(16)	9142(4)	7658(4)	8842(3)	31(1)
O(1)	9709(3)	6926(3)	8206(2)	35(1)
C(17)	7119(5)	9791(5)	10934(3)	40(1)
O(2)	5942(4)	9907(4)	11078(3)	57(1)
O(3)	7906(4)	10285(4)	11431(2)	55(1)
C(18)	7284(7)	11020(7)	12142(4)	65(2)
C(21)	7880(4)	8063(4)	5409(3)	36(1)
C(22)	7346(5)	9298(5)	5156(3)	46(1)
C(23)	6549(6)	9517(6)	4457(4)	56(1)
C(24)	6280(6)	8513(7)	4008(4)	61(2)
C(25)	6813(6)	7277(6)	4250(4)	57(1)
C(26)	7610(5)	7055(5)	4946(3)	43(1)
C(31)	10597(4)	7303(4)	5865(3)	33(1)

C(32)	10903(5)	7482(5)	5004(3)	44(1)
C(33)	12197(5)	7156(6)	4687(4)	55(1)
C(34)	13188(5)	6661(6)	5227(4)	53(1)
C(35)	12894(5)	6467(5)	6088(4)	46(1)
C(36)	11601(4)	6782(5)	6406(3)	39(1)
C(41)	4444(9)	6828(9)	9659(5)	91(3)
O(4)	5042(5)	6692(5)	8837(3)	74(1)
C(51)	4783(8)	3532(7)	7886(5)	80(2)
O(5)	4256(5)	4800(5)	8030(4)	86(2)
C(61)	8627(9)	5823(10)	932(7)	110(4)
O(6)	8216(5)	4870(5)	1447(4)	87(2)

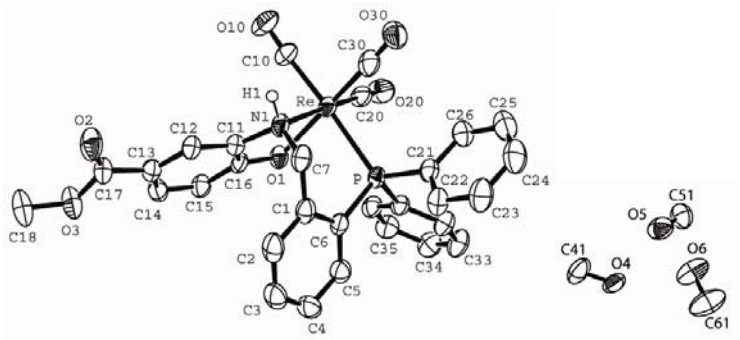

Fig. 17 Ellipsoid plot (50% probability) of $[Re(CO)_3(HL^{51}COOMe)]\cdot 3MeOH$.

$[Re(CO)_3(HL^{51}COOH)]$, (18)

Table 35 Crystal data and structure refinement for $[Re(CO)_3(HL^{51}COOH)]\cdot MeOH$

Empirical formula	$C_{30}H_{25}NO_7PRe$	
Formula weight	728.68	
Temperature	200(2) K	
Wavelength	0.71073 Å	
Crystal system	Monoclinic	
Space group	$P2_1/c$	
Unit cell dimensions	a = 12.078(1) Å	α= 90°.
	b = 12.909(1) Å	β= 108.031(7)°.
	c = 19.242(2) Å	γ = 90°.
Volume	2852.8(4) $Å^3$	
Z	4	
Density (calculated)	1.697 g/cm^3	
Absorption coefficient	4.363 mm^{-1}	
F(000)	1432	
Crystal size	0.150 x 0.097 x 0.050 mm^3	
Crystal description	Block	
Crystal color	Colorless	
Diff. measurement device type	STOE IPDS 2T	
Theta range for data collection	1.77 to 29.28°.	
Index ranges	-16<=h<=16, -15<=k<=17, -26<=l<=17	
Reflections collected	17194	
Independent reflections	7654 [R(int) = 0.1170]	
Completeness to theta = 29.28°	98.2 %	
Absorption correction	Integration	
Max. and min. transmission	0.8043 and 0.5152	
Refinement method	Full-matrix least-squares on F^2	
Data / restraints / parameters	7654 / 0 / 364	
Goodness-of-fit on F^2	0.904	
Final R indices [I>2sigma(I)]	R1 = 0.0574, wR2 = 0.1248	
R indices (all data)	R1 = 0.1172, wR2 = 0.1597	
Extinction coefficient	0.0162(7)	
Largest diff. peak and hole	2.213 and -1.848 $e.Å^{-3}$	

Table 36 Atomic coordinates (x 10^4) and equivalent isotropic displacement parameters ($Å^2$x 10^3) for [Re(CO)3(HL^{51}COOH)]·MeOH. U(eq) is defined as one third of the trace of the orthogonalized U^{ij} tensor.

	x	y	z	U(eq)
Re	1167(1)	1024(1)	8461(1)	34(1)
C(10)	2027(7)	2085(9)	9103(6)	46(2)
O(10)	2486(7)	2739(7)	9491(5)	67(2)
C(20)	-239(8)	1526(9)	8667(7)	49(3)
O(20)	-1016(7)	1804(8)	8801(6)	78(3)
C(30)	1437(8)	131(9)	9285(7)	49(3)
O(30)	1578(8)	-430(8)	9768(5)	67(2)
P	2859(2)	384(2)	8124(1)	35(1)
C(1)	2359(7)	147(7)	7142(5)	36(2)
C(2)	2905(8)	584(9)	6677(6)	44(2)
C(3)	2472(9)	438(9)	5931(6)	51(3)
C(4)	1471(9)	-154(9)	5639(6)	50(3)
C(5)	919(9)	-588(9)	6099(6)	47(2)
C(6)	1346(7)	-429(7)	6850(5)	36(2)
C(7)	684(7)	-886(7)	7330(6)	40(2)
N(1)	87(6)	-72(6)	7641(4)	35(2)
C(11)	-659(7)	552(7)	7049(5)	35(2)
C(12)	-1717(8)	208(8)	6599(5)	42(2)
C(13)	-2343(7)	803(7)	6002(5)	37(2)
C(14)	-1891(8)	1734(8)	5871(6)	44(2)
C(15)	-838(7)	2095(7)	6342(5)	36(2)
C(16)	-216(7)	1531(7)	6951(5)	35(2)
O(1)	753(5)	1881(5)	7436(3)	37(1)
C(17)	-3485(7)	440(8)	5547(6)	44(2)
O(2)	-3980(6)	-278(6)	5782(5)	61(2)
O(3)	-3927(5)	905(6)	4925(4)	49(2)
C(21)	4114(7)	1244(8)	8282(5)	41(2)
C(22)	5252(8)	863(9)	8490(6)	52(3)
C(23)	6179(8)	1526(11)	8629(6)	56(3)
C(24)	6011(8)	2572(10)	8578(6)	56(3)
C(25)	4892(9)	2969(10)	8358(6)	52(3)
C(26)	3945(9)	2292(8)	8212(6)	43(2)
C(31)	3556(7)	-835(7)	8533(5)	39(2)
C(32)	4001(8)	-886(9)	9281(6)	46(2)

C(33)	4704(9)	-1735(9)	9596(6)	51(3)
C(34)	4913(8)	-2511(9)	9167(7)	52(3)
C(35)	4418(9)	-2470(10)	8425(7)	56(3)
C(36)	3747(8)	-1613(9)	8100(6)	49(3)
C(41)	2034(15)	3487(14)	6377(10)	90(5)
O(4)	1517(7)	3615(6)	6939(5)	53(2)

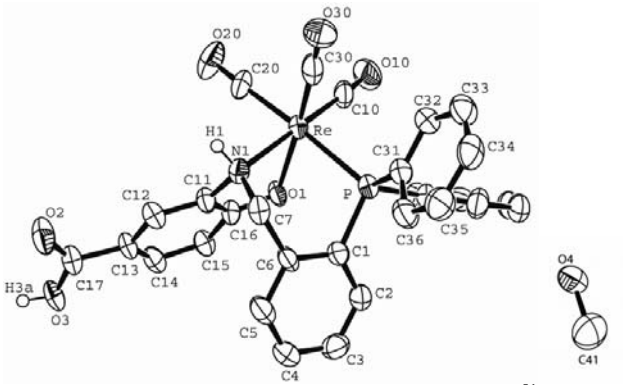

Fig. 18 Ellipsoid plot (50% probability) of $[Re(CO)_3(HL^{51}COOH)]\cdot MeOH$.

$[ReOCl_2(HL^{61})]$, (22)

Table 37 Crystal data and structure refinement for $[ReOCl_2(HL^{61})]\cdot MeOH$

Empirical formula	$C_{26}H_{25}Cl_2NO_3PRe$	
Formula weight	687.54	
Temperature	200(2) K	
Wavelength	0.71073 Å	
Crystal system	Monoclinic	
Space group	P21/n	
Unit cell dimensions	a = 9.288(1) Å	α= 90°.
	b = 17.980(1) Å	β= 96.008(3)°.
	c = 14.897(1) Å	γ = 90°.
Volume	2474.0(4) $Å^3$	
Z	4	
Density (calculated)	1.846 g/cm^3	
Absorption coefficient	5.222 mm^{-1}	
F(000)	1344	
Crystal size	0.3 x 0.2 x 0.09 mm^3	
Crystal description	Block	
Crystal color	Green	
Theta range for data collection	1.78 to 29.18°.	
Index ranges	-12<=h<=11, -24<=k<=24, -19<=l<=20	
Reflections collected	19245	
Independent reflections	6658 [R(int) = 0.1021]	
Completeness to theta = 29.18°	99.5 %	
Absorption correction	Integration	
Max. and min. transmission	0.2754 and 0.1581	
Refinement method	Full-matrix least-squares on F^2	
Data / restraints / parameters	6658 / 0 / 300	
Goodness-of-fit on F^2	0.834	
Final R indices [I>2sigma(I)]	R1 = 0.0394, wR2 = 0.0986	
R indices (all data)	R1 = 0.0520, wR2 = 0.1092	
Extinction coefficient	0.0056(4)	
Largest diff. peak and hole	2.305 and -3.524 $e.Å^{-3}$	

Table 38 Atomic coordinates (x 10^4) and equivalent isotropic displacement parameters ($Å^2$x 10^3) for $[ReOCl_2(HL^{61})]$·MeOH. U(eq) is defined as one third of the trace of the orthogonalized U^{ij} tensor.

	x	y	z	U(eq)
Re	4844(1)	8759(1)	1383(1)	19(1)
O(10)	3260(4)	8807(2)	709(3)	28(1)
Cl(1)	6414(1)	8949(1)	191(1)	29(1)
Cl(2)	5349(1)	7474(1)	1306(1)	29(1)
P	3491(1)	8746(1)	2677(1)	19(1)
C(1)	2968(5)	9715(2)	2713(3)	20(1)
C(2)	1900(5)	9962(3)	3241(3)	25(1)
C(3)	1464(5)	10700(3)	3206(3)	28(1)
C(4)	2073(6)	11194(2)	2637(4)	28(1)
C(5)	3125(5)	10957(3)	2103(3)	23(1)
C(6)	3553(5)	10219(2)	2140(3)	20(1)
N	4619(4)	9968(2)	1530(2)	20(1)
C(17)	6031(5)	10386(3)	1705(3)	25(1)
C(11)	6778(5)	10208(3)	2611(3)	23(1)
C(12)	7283(5)	10754(3)	3228(4)	29(1)
C(13)	8043(5)	10569(3)	4059(3)	30(1)
C(14)	8296(5)	9821(3)	4260(3)	28(1)
C(15)	7800(5)	9267(3)	3670(3)	24(1)
C(16)	7036(4)	9459(2)	2846(3)	20(1)
O(1)	6483(3)	8928(2)	2263(2)	20(1)
C(21)	4550(5)	8501(3)	3720(3)	22(1)
C(22)	4644(5)	8951(3)	4489(3)	26(1)
C(23)	5484(6)	8723(3)	5293(4)	36(1)
C(24)	6203(6)	8058(3)	5295(4)	37(1)
C(25)	6101(6)	7604(3)	4533(4)	35(1)
C(26)	5286(5)	7831(3)	3751(3)	29(1)
C(31)	1779(5)	8257(2)	2703(3)	22(1)
C(32)	1422(5)	7913(3)	3494(3)	27(1)
C(33)	59(6)	7611(3)	3523(4)	36(1)
C(34)	-944(6)	7641(3)	2772(4)	37(1)
C(35)	-598(6)	7968(3)	1975(4)	36(1)
C(36)	769(5)	8275(3)	1946(4)	31(1)
O(3)	9780(6)	202(3)	968(4)	62(1)
C(41)	9767(9)	592(4)	622(6)	57(2)

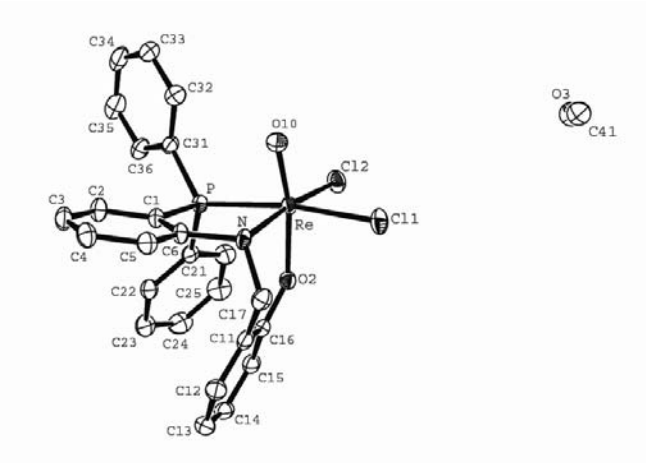

Fig. 19 Ellipsoid plot (50% probability) of $[ReOCl_2(HL^{61})]\cdot MOH$

$[TcOCl_2(HL^{61})]$, (23)

Table 39 Crystal data and structure refinement for $[TcOCl_2(HL^{61})]\cdot Me_2CO$

Empirical formula	$C_{28}H_{27}Cl_2NO_3PTc$	
Formula weight	625.41	
Temperature	200(2) K	
Wavelength	0.71073 Å	
Crystal system	Triclinic	
Space group	P $\bar{1}$	
Unit cell dimensions	a = 9.724(2)Å	α= 82.31(1)°.
	b = 10.654(1) Å	β= 88.13(1)°.
	c = 14.349(2) Å	γ = 67.57(1)°.
Volume	1361.4(4) $Å^3$	
Z	2	
Density (calculated)	1.526 g/cm^3	
Absorption coefficient	0.814 mm^{-1}	
F(000)	636	
Crystal size	0.23 x 0.09 x 0.06 mm^3	
Crystal description	Needle	
Crystal color	Red-violet	
Diff. measurement device type	STOE IPDS 2T	
Theta range for data collection	1.43 to 26.81°.	
Index ranges	-12<=h<=12, -13<=k<=11, -18<=l<=18	
Reflections collected	11195	
Independent reflections	5721 [R(int) = 0.1426]	
Completeness to theta = 26.81°	97.8 %	
Absorption correction	None	
Max. and min. transmission	- and -	
Refinement method	Full-matrix least-squares on F^2	
Data / restraints / parameters	5721 / 0 / 327	
Goodness-of-fit on F^2	0.797	
Final R indices [I>2sigma(I)]	R1 = 0.0573, wR2 = 0.1087	
R indices (all data)	R1 = 0.1502, wR2 = 0.1661	
Largest diff. peak and hole	0.763 and -0.691 $e.Å^{-3}$	

Table 40 Atomic coordinates (x 10^4) and equivalent isotropic displacement parameters ($Å^2$x 10^3) for $[TcOCl_2(HL^{61})]\cdot Me_2CO$. U(eq) is defined as one third of the trace of the orthogonalized U^{ij} tensor.

	x	y	z	U(eq)
Tc	1827(1)	959(1)	7393(1)	27(1)
O(10)	2051(6)	1543(6)	6298(4)	38(2)
Cl(1)	47(2)	30(2)	7140(2)	40(1)
Cl(2)	3821(2)	-1298(2)	7475(2)	41(1)
P(1)	23(2)	3215(2)	7552(2)	28(1)
C(1)	1261(9)	4137(9)	7573(6)	29(2)
C(2)	712(10)	5556(9)	7500(6)	34(2)
C(3)	1697(11)	6223(9)	7454(6)	38(2)
C(4)	3218(10)	5477(10)	7483(7)	39(2)
C(5)	3739(10)	4099(9)	7547(6)	34(2)
C(6)	2776(9)	3427(9)	7613(6)	30(2)
N	3389(7)	1910(7)	7706(5)	28(2)
C(11)	2106(9)	1118(8)	9516(6)	30(2)
C(12)	1278(9)	1153(9)	10323(6)	35(2)
C(13)	1658(10)	1643(9)	11091(6)	37(2)
C(14)	2814(10)	2084(9)	11034(7)	39(2)
C(15)	3646(9)	2013(9)	10226(7)	37(2)
C(16)	3301(9)	1515(9)	9465(6)	32(2)
C(17)	4268(8)	1280(9)	8614(6)	36(2)
O(1)	1752(6)	673(6)	8749(4)	31(1)
C(21)	-1069(9)	3338(9)	8615(6)	33(2)
C(22)	-1816(9)	2451(10)	8805(6)	38(2)
C(23)	-2617(9)	2496(10)	9593(6)	41(2)
C(24)	-2759(10)	3426(9)	10216(6)	40(2)
C(25)	-2026(10)	4316(10)	10035(6)	41(2)
C(26)	-1173(10)	4274(9)	9232(6)	36(2)
C(31)	-1344(9)	4191(9)	6608(6)	33(2)
C(34)	-3334(10)	5712(10)	5164(7)	47(3)
C(35)	-3686(11)	5914(12)	6073(7)	59(3)
C(33)	-2001(13)	4759(12)	4987(7)	69(4)
C(36)	-2705(11)	5154(11)	6808(7)	54(3)
C(32)	-997(11)	4003(12)	5685(7)	60(3)
O(2)	5720(8)	1537(8)	6343(5)	61(2)
C(41)	6613(11)	772(13)	5882(7)	50(3)

C(42)	7001(15)	-723(14)	6051(9)	78(4)
C(43)	7401(11)	1319(13)	5109(7)	63(3)

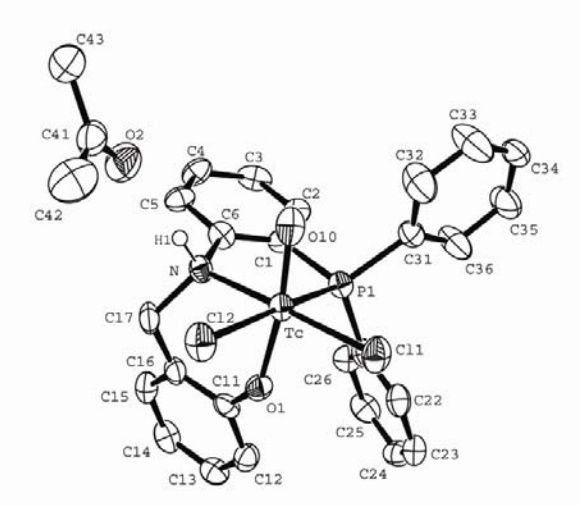

Fig. 20 Ellipsoid plot (50% probability) of $[TcOCl_2(HL^{61})]\cdot Me_2CO$.

[ReOCl(H_2L^{62})], (24)

Table 41 Crystal data and structure refinement for [ReOCl(H_2L^{62})].

Empirical formula	$C_{32}H_{27}ClN_2O_3PRe$	
Formula weight	740.18	
Temperature	200(2) K	
Wavelength	0.71069 Å	
Crystal system	Monoclinic	
Space group	$P2_1/n$	
Unit cell dimensions	a = 9.837(5) Å	α= 90.000(5)°.
	b = 14.775(5) Å	β= 94.047(5)°.
	c = 19.752(5) Å	γ = 90.000(5)°.
Volume	2864.0(2) $Å^3$	
Z	4	
Density (calculated)	1.717 g/cm^3	
Absorption coefficient	4.429 mm^{-1}	
F(000)	1456	
Crystal size	0.3 x 0.1 x 0.1 mm^3	
Crystal description	Block	
Crystal color	Red	
Diff. measurement device type	STOE IPDS 2T	
Theta range for data collection	1.72 to 29.28°.	
Index ranges	-11<=h<=13, -20<=k<=20, -27<=l<=26	
Reflections collected	21802	
Independent reflections	7715 [R(int) = 0.1156]	
Completeness to theta = 29.28°	98.7 %	
Absorption correction	Integration	
Max. and min. transmission	0.6239 and 0.4554	
Refinement method	Full-matrix least-squares on F^2	
Data / restraints / parameters	7715 / 0 / 363	
Goodness-of-fit on F^2	0.870	
Final R indices [I>2sigma(I)]	R1 = 0.0439, wR2 = 0.0792	
R indices (all data)	R1 = 0.1096, wR2 = 0.1161	
Extinction coefficient	0.0056(2)	
Largest diff. peak and hole	1.297 and -1.046 $e.Å^{-3}$	

Table 42 Atomic coordinates (x 10^4) and equivalent isotropic displacement parameters ($Å^2$x 10^3) for [ReOCl(H_2L^{62})]. U(eq) is defined as one third of the trace of the orthogonalized U^{ij} tensor.

	x	y	z	U(eq)
Re	4377(1)	9117(1)	1944(1)	32(1)
O(10)	4797(7)	8178(4)	2389(3)	50(2)
Cl	6640(2)	9301(1)	1505(1)	41(1)
P	4654(2)	10045(1)	2916(1)	34(1)
C(1)	2914(9)	10291(6)	3045(4)	38(2)
C(2)	2513(10)	10956(7)	3492(5)	53(2)
C(3)	1170(12)	11196(7)	3501(6)	64(3)
C(4)	242(11)	10770(8)	3066(6)	68(3)
C(5)	583(10)	10112(7)	2607(6)	57(3)
C(6)	1968(8)	9853(5)	2583(4)	37(2)
N(1)	2441(7)	9252(5)	2110(3)	38(2)
C(17)	1508(10)	8606(7)	1749(5)	53(2)
C(11)	1404(9)	8727(6)	992(5)	49(2)
C(12)	155(11)	8677(8)	631(7)	69(3)
C(13)	65(13)	8749(10)	-71(7)	86(4)
C(14)	1207(13)	8911(9)	-403(6)	77(4)
C(15)	2448(10)	8980(6)	-54(4)	52(2)
C(16)	2571(9)	8879(5)	649(4)	38(2)
O(1)	3848(6)	8939(4)	970(3)	41(1)
C(21)	5505(8)	11055(5)	2694(4)	37(2)
C(22)	6306(10)	11592(6)	3131(5)	49(2)
C(23)	7098(11)	12265(7)	2877(6)	65(3)
C(24)	7084(11)	12394(7)	2179(6)	64(3)
C(25)	6237(9)	11895(6)	1741(6)	53(2)
C(26)	5420(8)	11226(5)	1996(4)	36(2)
N(2)	4479(6)	10682(4)	1578(3)	31(1)
C(37)	3161(8)	11181(5)	1390(4)	36(2)
C(31)	3365(8)	11985(5)	935(4)	36(2)
C(32)	3254(10)	12869(6)	1151(5)	49(2)
C(33)	3515(11)	13601(6)	727(6)	58(3)
C(34)	3831(10)	13422(6)	89(6)	56(3)
C(35)	3968(10)	12563(6)	-149(4)	50(2)
C(36)	3747(9)	11849(5)	287(4)	37(2)
O(2)	3942(8)	10967(4)	105(3)	59(2)

C(41)	5561(9)	9585(6)	3664(4)	41(2)
C(42)	4910(12)	9234(8)	4205(5)	71(3)
C(43)	5670(20)	8767(11)	4699(7)	114(6)
C(44)	7026(19)	8688(11)	4682(7)	101(5)
C(45)	7663(14)	9037(9)	4173(6)	80(4)
C(46)	6961(11)	9484(7)	3669(6)	62(3)

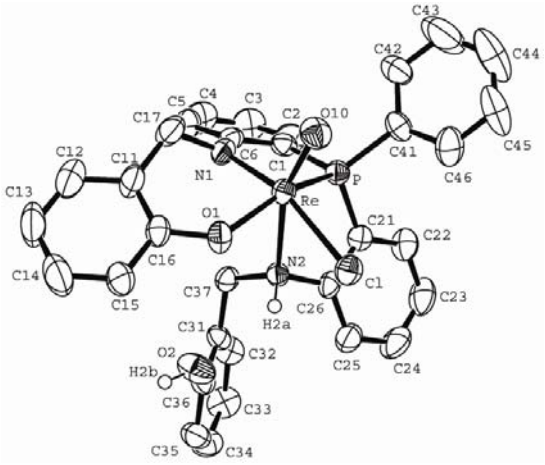

Fig. 21 Ellipsoid plot (50% probability) of [ReOCl(H_2L^{62})]

$[ReOCl_2(H_5L^{63})]$, (26)

Table 43 Crystal data and structure refinement for $[ReOCl_2(H_5L^{72})]\cdot NBu_4Cl.1/2CH_2Cl_2$

Empirical formula	$C_{55.50}H_{72}Cl_4N_4O_4PRe$	
Formula weight	1218.14	
Temperature	200(2) K	
Wavelength	0.71073 Å	
Crystal system	Triclinic	
Space group	$P\bar{1}$	
Unit cell dimensions	a = 12.294(2) Å	α= 86.79(2)°.
	b = 14.395(2) Å	β= 76.31(2)°.
	c = 17.305(2) Å	γ = 88.62(2)°.
Volume	2970.8(7) $Å^3$	
Z	2	
Density (calculated)	1.362 g/cm^3	
Absorption coefficient	2.297 mm^{-1}	
F(000)	1246	
Crystal size	0.4 x 0.28 x 0.2 mm^3	
Crystal description	Block	
Crystal color	Green	
Diff. measurement device type	STOE IPDS 2T	
Theta range for data collection	2.38 to 25.03°.	
Index ranges	-14<=h<=14, -14<=k<=17, -20<=l<=20	
Reflections collected	19429	
Independent reflections	10020 [R(int) = 0.1299]	
Completeness to theta = 25.03°	95.3 %	
Absorption correction	Integration	
Max. and min. transmission	0.7913 and 0.6481	
Refinement method	Full-matrix least-squares on F^2	
Data / restraints / parameters	10020 / 0 / 629	
Goodness-of-fit on F^2	0.876	
Final R indices [I>2sigma(I)]	R1 = 0.0678, wR2 = 0.1510	
R indices (all data)	R1 = 0.1243, wR2 = 0.1821	
Extinction coefficient	0.0146(10)	
Largest diff. peak and hole	1.051 and -1.583 $e.Å^{-3}$	

Table 44 Atomic coordinates (x 10^4) and equivalent isotropic displacement parameters ($Å^2$x 10^3) for $[ReOCl_2(H_5L^{62})]\cdot NBu_4Cl.1/2CH_2Cl_2$. U(eq) is defined as one third of the trace of the orthogonalized U^{ij} tensor.

	x	y	z	U(eq)
Re	5315(1)	6389(1)	7375(1)	49(1)
O(10)	5819(6)	7236(5)	7771(4)	55(2)
Cl(1)	3340(2)	6858(2)	7887(2)	61(1)
Cl(2)	4792(3)	5090(2)	8284(2)	62(1)
P	5602(2)	7221(2)	6124(2)	49(1)
C(1)	6781(9)	6595(7)	5568(7)	56(3)
C(2)	7241(10)	5951(8)	6024(8)	62(3)
C(3)	8204(10)	5465(9)	5640(9)	72(3)
C(4)	8655(12)	5656(11)	4845(11)	91(5)
C(5)	8193(12)	6298(12)	4386(8)	83(4)
C(6)	7257(9)	6765(9)	4759(7)	64(3)
N(1)	6714(8)	5770(6)	6854(6)	56(2)
C(17)	7347(10)	5121(8)	7277(9)	68(3)
C(11)	8416(10)	5550(8)	7386(9)	69(3)
C(12)	8524(12)	6516(10)	7416(11)	89(5)
C(13)	9532(13)	6843(11)	7532(13)	109(6)
C(14)	10371(11)	6324(12)	7647(10)	92(5)
C(15)	10274(10)	5351(12)	7609(9)	82(4)
C(16)	9308(9)	4976(8)	7476(7)	63(3)
O(1)	9157(7)	4043(6)	7432(6)	78(3)
C(21)	4379(9)	7039(7)	5771(6)	47(2)
C(22)	3891(10)	7678(8)	5307(7)	62(3)
C(23)	2864(12)	7487(9)	5181(9)	78(4)
C(24)	2292(11)	6688(10)	5519(9)	77(4)
C(25)	2764(9)	6054(8)	5969(7)	59(3)
C(26)	3790(9)	6235(7)	6096(7)	54(3)
N(2)	4325(7)	5602(5)	6597(5)	51(2)
C(37)	4812(10)	4755(7)	6127(7)	58(3)
C(31)	4920(9)	3910(7)	6633(6)	52(3)
C(32)	5978(10)	3467(8)	6572(8)	61(3)
C(33)	6098(11)	2668(9)	7020(9)	76(4)
C(34)	5148(12)	2277(7)	7509(9)	71(4)
C(35)	4114(12)	2673(8)	7580(8)	68(3)

C(36)	4005(10)	3507(7)	7136(7)	57(3)
O(2)	3004(6)	3934(5)	7163(6)	67(2)
C(41)	5891(9)	8431(8)	6075(7)	57(3)
C(42)	6977(12)	8756(9)	5736(8)	76(4)
C(43)	7259(13)	9670(10)	5710(9)	83(4)
C(44)	6423(13)	10309(9)	6043(9)	80(4)
C(45)	5358(12)	10013(9)	6404(8)	76(4)
C(46)	5085(10)	9071(7)	6437(7)	58(3)
N(3)	4043(8)	8778(7)	6821(6)	67(3)
C(57)	3107(11)	9399(9)	7187(9)	75(4)
C(51)	3263(10)	9782(8)	7931(8)	64(3)
C(52)	4014(10)	9450(9)	8364(8)	68(3)
C(53)	4116(12)	9837(9)	9040(9)	75(4)
C(54)	3437(13)	10535(9)	9359(9)	77(4)
C(55)	2636(13)	10888(9)	8968(9)	83(4)
C(56)	2549(11)	10520(8)	8272(9)	67(3)
O(3)	1791(9)	10797(6)	7820(7)	91(3)
N(4)	2364(7)	7341(7)	382(6)	64(3)
C(61)	1797(10)	6396(9)	589(8)	66(3)
C(62)	1943(11)	5765(9)	-125(8)	74(4)
C(63)	1562(12)	4806(10)	186(9)	81(4)
C(64)	1605(12)	4146(12)	-468(10)	98(5)
C(65)	3607(9)	7256(9)	20(7)	66(3)
C(66)	4271(10)	6591(10)	480(9)	81(4)
C(67)	5521(12)	6494(14)	5(13)	128(8)
C(68)	6154(14)	7254(13)	-260(13)	123(7)
C(69)	1892(10)	7905(9)	-228(8)	69(3)
C(70)	678(13)	8179(14)	0(11)	111(6)
C(71)	414(17)	8640(20)	-800(20)	230(20)
C(72)	-350(50)	8650(30)	-990(30)	340(40)
C(73)	2152(11)	7826(9)	1171(8)	75(4)
C(74)	2671(12)	8768(10)	1131(9)	80(4)
C(75)	2160(15)	9263(11)	1908(10)	99(5)
C(76)	2669(16)	10211(13)	1942(12)	114(6)
Cl(3)	9074(2)	7219(2)	2038(2)	68(1)
Cl(5)	361(14)	9916(13)	6364(11)	195(6)
Cl(4)	-339(18)	11638(16)	5862(14)	237(8)
C(77)	580(30)	11040(20)	6290(20)	102(10)

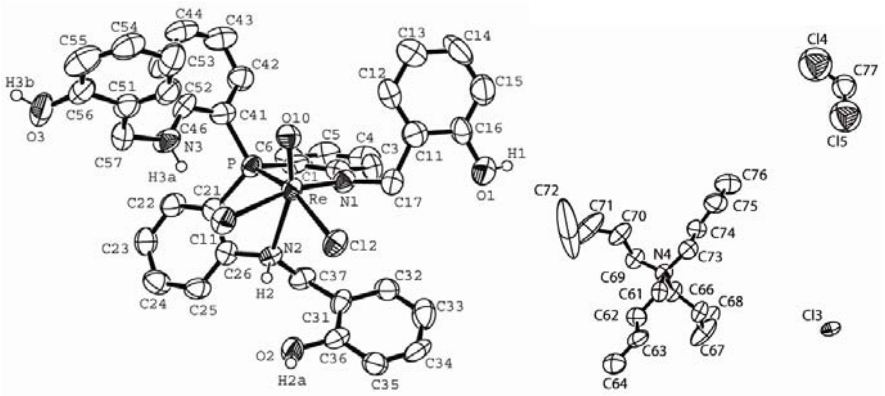

Fig. 22 Ellipsoid plot (50% probability) of $[ReOCl_2(H_5L^{62})]\cdot NBu_4Cl.1/2CH_2Cl_2$.

[ReOCl(H_4L^{63})], (27)

Table 45 Crystal data and structure refinement for [ReOCl(H_5L^{63})]·CH_2Cl_2

Empirical formula	$C_{41}H_{38}Cl_5N_3O_4PRe$	
Formula weight	1031.16	
Temperature	200(2) K	
Wavelength	0.71073 Å	
Crystal system	Triclinic	
Space group	P $\bar{1}$	
Unit cell dimensions	a = 13.3818(9) Å	α= 96.229(6)°.
	b = 13.304(1) Å	β= 111.437(5)°.
	c = 15.316(1) Å	γ = 119.226(5)°.
Volume	2072.1(2) $Å^3$	
Z	2	
Density (calculated)	1.653 g/cm^3	
Absorption coefficient	3.338 mm^{-1}	
F(000)	1024	
Crystal size	0.3 x 0.2 x 0.05 mm^3	
Crystal description	Plate	
Crystal color	Brown	
Diff. measurement device type	STOE IPDS 2T	
Theta range for data collection	1.53 to 26.82°.	
Index ranges	-16<=h<=16, -15<=k<=16, -19<=l<=19	
Reflections collected	17958	
Independent reflections	8705 [R(int) = 0.0941]	
Completeness to theta = 26.82°	97.9 %	
Absorption correction	Integration	
Max. and min. transmission	0.7732 and 0.6391	
Refinement method	Full-matrix least-squares on F^2	
Data / restraints / parameters	8705 / 0 / 498	
Goodness-of-fit on F^2	1.045	
Final R indices [I>2sigma(I)]	R1 = 0.0470, wR2 = 0.0963	
R indices (all data)	R1 = 0.0752, wR2 = 0.1263	
Largest diff. peak and hole	1.240 and -1.986 e.$Å^{-3}$	

Table 46 Atomic coordinates (x 10^4) and equivalent isotropic displacement parameters ($Å^2$x 10^3) for $[ReOCl(H_5L^{63})]\cdot CH_2Cl_2$. U(eq) is defined as one third of the trace of the orthogonalized U^{ij} tensor.

	x	y	z	U(eq)
Re	8297(1)	9774(1)	7111(1)	22(1)
O(10)	7913(5)	8887(5)	6011(4)	33(1)
Cl(1)	10494(2)	10194(2)	7973(2)	31(1)
P	8743(2)	11470(2)	6559(2)	23(1)
C(1)	7322(8)	11458(7)	6355(6)	28(2)
C(2)	7144(9)	12377(9)	6168(7)	36(2)
C(3)	6080(10)	12333(9)	6124(8)	47(2)
C(4)	5175(10)	11359(10)	6272(9)	52(3)
C(5)	5334(9)	10454(9)	6483(8)	44(2)
C(6)	6411(7)	10475(7)	6527(6)	27(2)
N(1)	6649(6)	9601(6)	6770(5)	28(1)
C(17)	5593(8)	8430(7)	6717(6)	32(2)
C(11)	5879(8)	8304(7)	7722(6)	32(2)
C(12)	4951(8)	7926(8)	8054(7)	37(2)
C(13)	5191(9)	7764(8)	8969(7)	43(2)
C(14)	6375(10)	7980(9)	9566(8)	45(2)
C(15)	7329(8)	8393(7)	9269(7)	34(2)
C(16)	7093(7)	8550(7)	8363(6)	28(2)
O(1)	8077(5)	8954(5)	8109(4)	28(1)
C(21)	10135(7)	12845(7)	7600(6)	25(2)
C(22)	10974(8)	13939(8)	7520(7)	35(2)
C(23)	12077(9)	14889(9)	8369(8)	48(2)
C(24)	12349(9)	14759(8)	9297(7)	43(2)
C(25)	11513(8)	13686(8)	9388(7)	38(2)
C(26)	10377(7)	12716(7)	8544(6)	26(2)
N(2)	9419(6)	11556(6)	8560(5)	24(1)
C(37)	8591(8)	11715(7)	8951(6)	29(2)
C(31)	9357(8)	12547(8)	10022(6)	31(2)
C(32)	9428(10)	13623(9)	10311(7)	42(2)
C(33)	10167(12)	14387(10)	11297(8)	60(3)
C(34)	10808(11)	14077(9)	12018(8)	55(3)
C(35)	10760(9)	13026(8)	11769(7)	39(2)
C(36)	10038(8)	12270(7)	10774(6)	31(2)
O(2)	9943(6)	11204(5)	10451(4)	34(1)

C(41)	9038(7)	11595(7)	5503(6)	26(2)
C(42)	8267(8)	11741(8)	4703(6)	33(2)
C(43)	8537(9)	11939(9)	3932(7)	39(2)
C(44)	9626(9)	12018(8)	3962(7)	38(2)
C(45)	10383(8)	11839(7)	4738(6)	31(2)
C(46)	10104(7)	11596(7)	5521(6)	28(2)
N(3)	10834(6)	11385(6)	6273(5)	29(1)
C(57)	11997(8)	11435(7)	6374(7)	31(2)
C(51)	13214(7)	12724(7)	6863(6)	28(2)
C(52)	13914(8)	13240(8)	6371(7)	34(2)
C(53)	15067(9)	14422(9)	6835(8)	45(2)
C(54)	15506(9)	15103(9)	7806(8)	48(2)
C(55)	14819(9)	14614(9)	8304(7)	43(2)
C(56)	13685(8)	13427(8)	7841(7)	35(2)
O(3)	13103(7)	12997(7)	8408(5)	48(2)
C(61)	7205(11)	4951(10)	4187(9)	54(3)
Cl(2)	8218(3)	4424(3)	4380(3)	76(1)
Cl(3)	6887(4)	5090(4)	5195(3)	79(1)
C(62)	6886(15)	525(15)	1079(13)	95(5)
Cl(5)	7465(4)	1960(4)	1379(3)	93(1)
Cl(6)	5825(6)	-460(5)	1436(4)	130(2)

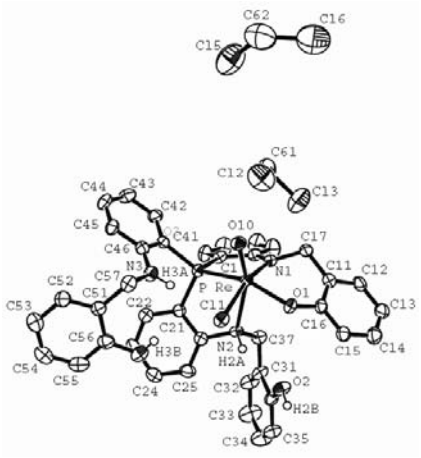

Fig. 23 Ellipsoid plot (50% probability) of $[ReOCl(H_5L^{63})]\cdot CH_2Cl_2$.

[TcOCl(H_4L^{63})], (28)

Table 47 Crystal data and structure refinement for [TcOCl(H_4L^{63})]·3$CHCl_3$

Empirical formula	$C_{84}H_{74}Cl_{20}N_6O_8P_2Tc_2$	
Formula weight	2262.43	
Temperature	200(2) K	
Wavelength	0.71073 Å	
Crystal system	Triclinic	
Space group	P $\bar{1}$	
Unit cell dimensions	a = 14.349(2) Å	α= 61.195(9)°.
	b = 14.479(2) Å	β= 81.71(1)°.
	c = 14.811(2) Å	γ = 61.070(9)°.
Volume	2344.2(5) $Å^3$	
Z	2	
Density (calculated)	1.603 g/cm^3	
Absorption coefficient	0.956 mm^{-1}	
F(000)	1140	
Crystal size	0.5 x 0.24 x 0.1 mm^3	
Crystal description	Needle	
Crystal color	Red	
Diff. measurement device type	STOE IPDS 2T	
Theta range for data collection	1.76 to 29.37°.	
Index ranges	-19<=h<=17, -19<=k<=19, -20<=l<=20	
Reflections collected	24455	
Independent reflections	12422 [R(int) = 0.1568]	
Completeness to theta = 29.37°	96.2 %	
Absorption correction	None	
Max. and min. transmission	noen and none	
Refinement method	Full-matrix least-squares on F^2	
Data / restraints / parameters	12422 / 0 / 553	
Goodness-of-fit on F^2	0.951	
Final R indices [I>2sigma(I)]	R1 = 0.0854, wR2 = 0.2001	
R indices (all data)	R1 = 0.1831, wR2 = 0.2559	
Extinction coefficient	0.0159(14)	
Largest diff. peak and hole	0.956 and -1.432 e.$Å^{-3}$	

Table 48. Atomic coordinates (x 10^4) and equivalent isotropic displacement parameters ($Å^2$x 10^3) for [TcOCl(H_4L^{63})]·3$CHCl_3$. U(eq) is defined as one third of the trace of the orthogonalized U^{ij} tensor.

	x	y	z	U(eq)
Tc	7145(1)	6530(1)	5295(1)	39(1)
O(10)	7227(5)	5655(4)	4849(4)	52(1)
Cl(1)	5199(2)	7241(2)	5451(2)	49(1)
P(1)	7867(2)	4890(2)	6990(1)	39(1)
C(1)	9142(6)	4795(6)	7049(6)	42(2)
C(2)	9854(6)	4138(6)	7942(6)	45(2)
C(3)	10774(7)	4190(7)	7931(7)	57(2)
C(4)	11027(7)	4903(7)	7022(7)	57(2)
C(5)	10347(6)	5585(7)	6119(7)	51(2)
C(6)	9381(6)	5567(6)	6102(6)	44(2)
N(1)	8578(5)	6308(5)	5242(4)	44(2)
C(17)	8838(7)	7018(6)	4217(6)	51(2)
C(11)	8265(7)	8324(6)	3924(6)	50(2)
C(12)	8808(8)	8999(8)	3623(7)	57(2)
C(13)	8244(8)	10215(8)	3328(7)	63(2)
C(14)	7169(8)	10757(7)	3380(7)	62(2)
C(15)	6632(7)	10095(6)	3701(6)	53(2)
C(16)	7154(7)	8883(6)	3989(5)	48(2)
O(1)	6603(4)	8272(4)	4295(4)	48(1)
C(21)	7081(6)	5372(6)	7890(5)	39(2)
C(22)	6889(6)	4641(6)	8846(6)	43(2)
C(23)	6161(7)	5144(7)	9395(6)	48(2)
C(24)	5613(6)	6375(7)	8979(6)	45(2)
C(25)	5810(6)	7113(6)	8044(6)	40(2)
C(26)	6555(6)	6614(6)	7502(5)	41(2)
N(2)	6819(5)	7327(5)	6496(4)	41(1)
C(37)	7621(7)	7658(6)	6632(6)	45(2)
C(31)	7264(6)	8347(6)	7219(5)	43(2)
C(32)	7840(7)	7881(8)	8149(6)	55(2)
C(33)	7541(10)	8502(10)	8697(8)	75(3)
C(34)	6616(9)	9623(9)	8314(8)	69(3)
C(35)	6024(8)	10091(8)	7401(7)	60(2)
C(36)	6364(7)	9446(6)	6855(6)	48(2)
O(2)	5808(5)	9858(5)	5953(4)	57(2)

C(41)	8005(6)	3448(6)	7372(5)	40(2)
C(42)	9001(6)	2428(6)	7742(6)	45(2)
C(43)	9128(7)	1291(6)	8067(6)	51(2)
C(44)	8222(7)	1207(7)	7991(7)	54(2)
C(45)	7233(6)	2201(6)	7594(6)	44(2)
C(46)	7102(6)	3347(6)	7299(6)	43(2)
N(3)	6093(5)	4343(5)	6933(5)	48(2)
C(57)	5218(7)	4349(7)	6508(6)	51(2)
C(51)	4656(6)	3731(6)	7308(5)	43(2)
C(52)	4353(7)	3026(7)	7146(7)	57(2)
C(53)	3819(8)	2474(8)	7816(8)	64(2)
C(54)	3578(8)	2601(9)	8678(8)	66(2)
C(55)	3817(9)	3282(10)	8896(8)	70(3)
C(56)	4380(7)	3846(8)	8202(7)	58(2)
O(3)	4643(7)	4502(8)	8425(6)	82(2)
C(61)	8050(11)	2072(11)	4658(10)	91(3)
Cl(2)	9387(3)	1606(3)	4371(3)	105(1)
Cl(3)	7602(3)	3313(3)	4823(3)	93(1)
Cl(4)	7952(4)	886(4)	5736(3)	131(2)
C(63)	9080(10)	3147(12)	1437(10)	99(4)
Cl(5)	9121(4)	4424(3)	416(3)	113(1)
Cl(6)	7791(3)	3529(3)	1787(3)	113(1)
Cl(7)	9542(4)	2083(3)	1022(5)	150(2)
C(64)	7263(9)	10286(8)	1126(7)	69(3)
Cl(8)	7651(4)	11362(3)	480(3)	131(2)
Cl(9)	5985(3)	10780(4)	655(5)	151(2)
Cl(10)	8153(2)	8978(3)	1061(3)	98(1)

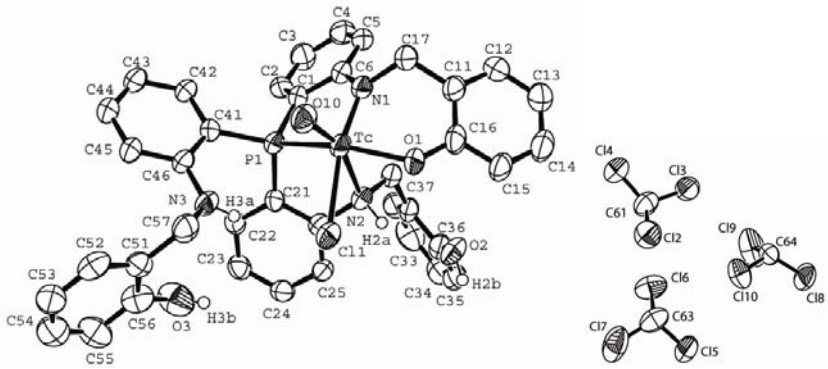

Fig. 24 Ellipsoid plot (50% probability) of $[TcOCl(H_4L^{63})]\cdot 3CHCl_3$

$[ReOCl(L^1)_2]$, (29)

Table 49 Crystal data and structure refinement for $[ReOCl(L^1)_2]\cdot 1/2CH_2Cl_2$

Empirical formula	$C_{76.50}H_{63}Cl_3O_6P_4Re_2$	
Formula weight	1682.01	
Temperature	200(2) K	
Wavelength	0.71073 Å	
Crystal system	Triclinic	
Space group	$P\bar{1}$	
Unit cell dimensions	a = 10.4267(7) Å	α= 98.944(5)°.
	b = 18.026(1) Å	β= 96.120(5)°.
	c = 18.385(1) Å	γ = 92.864(5)°.
Volume	3386.3(4) $Å^3$	
Z	2	
Density (calculated)	1.649 g/cm^3	
Absorption coefficient	3.838 mm^{-1}	
F(000)	1662	
Crystal size	0.34 x 0.10 x 0.04 mm^3	
Crystal description	Needle	
Crystal color	Brown	
Diff. measurement device type	STOE IPDS 2T	
Theta range for data collection	1.73 to 29.29°.	
Index ranges	-14<=h<=13, -24<=k<=24, -24<=l<=25	
Reflections collected	38734	
Independent reflections	18091 [R(int) = 0.1086]	
Completeness to theta = 29.29°	97.7 %	
Absorption correction	Integration	
Max. and min. transmission	0.7954 and 0.3929	
Refinement method	Full-matrix least-squares on F^2	
Data / restraints / parameters	18091 / 2 / 821	
Goodness-of-fit on F^2	0.785	
Final R indices [I>2sigma(I)]	R1 = 0.0444, wR2 = 0.0697	
R indices (all data)	R1 = 0.1119, wR2 = 0.0862	
Extinction coefficient	0.00007(4)	
Largest diff. peak and hole	1.994 and -1.331 $e.Å^{-3}$	

Table 50 Atomic coordinates (x 10^4) and equivalent isotropic displacement parameters ($Å^2$x 10^3) for $[ReOCl(L^1)_2]\cdot 1/2CH_2Cl_2$. U(eq) is defined as one third of the trace of the orthogonalized U^{ij} tensor.

	x	y	z	U(eq)
Re(1)	235(1)	7684(1)	3659(1)	17(1)
O(10)	774(5)	7166(2)	2933(2)	24(1)
Cl(1)	-153(2)	8780(1)	3049(1)	28(1)
P(1)	235(2)	6539(1)	4248(1)	19(1)
C(1)	-1238(7)	5963(3)	3855(3)	19(2)
C(2)	-1234(8)	5175(4)	3657(4)	28(2)
C(3)	-2355(8)	4764(4)	3323(4)	35(2)
C(4)	-3451(8)	5105(4)	3163(4)	35(2)
C(5)	-3475(7)	5873(4)	3356(4)	29(2)
C(6)	-2382(7)	6314(3)	3707(4)	23(2)
C(7)	-2426(7)	7159(4)	3901(4)	30(2)
O(2)	9(5)	8266(2)	4590(2)	23(1)
C(11)	175(7)	6715(3)	5240(4)	24(2)
C(12)	-966(8)	6599(4)	5552(4)	31(2)
C(13)	-1001(9)	6797(5)	6307(4)	42(2)
C(14)	106(9)	7102(4)	6766(4)	39(2)
C(15)	1250(8)	7199(4)	6468(4)	34(2)
C(16)	1292(8)	7002(4)	5708(4)	29(2)
C(21)	1497(7)	5889(4)	4096(4)	22(2)
C(22)	2057(7)	5537(4)	4668(4)	31(2)
C(23)	2963(8)	5034(4)	4533(4)	39(2)
C(24)	3360(8)	4857(4)	3845(5)	40(2)
C(25)	2795(8)	5196(4)	3261(4)	36(2)
C(26)	1871(8)	5700(4)	3404(4)	30(2)
P(2)	2487(2)	8240(1)	4028(1)	19(1)
C(31)	2443(7)	9187(3)	4525(4)	21(2)
C(32)	3287(7)	9770(4)	4412(4)	27(2)
C(33)	3287(8)	10502(4)	4823(5)	39(2)
C(34)	2423(8)	10638(4)	5330(5)	39(2)
C(35)	1564(8)	10066(4)	5435(4)	36(2)
C(36)	1569(7)	9337(3)	5044(3)	24(2)
C(37)	671(7)	8723(4)	5223(3)	26(2)
O(1)	-1676(4)	7558(2)	3474(2)	24(1)
C(41)	3467(7)	8315(3)	3276(4)	23(2)

C(42)	2905(8)	8404(4)	2583(4)	33(2)
C(43)	3637(9)	8473(5)	2010(4)	48(2)
C(44)	4952(9)	8441(5)	2121(4)	45(2)
C(45)	5550(9)	8356(5)	2805(5)	46(2)
C(46)	4783(8)	8308(4)	3373(4)	35(2)
C(51)	3575(7)	7814(3)	4684(4)	25(2)
C(52)	4015(7)	7121(4)	4451(4)	27(2)
C(53)	4790(8)	6776(4)	4937(5)	39(2)
C(54)	5081(9)	7120(4)	5680(5)	43(2)
C(55)	4639(8)	7802(4)	5902(4)	38(2)
C(56)	3906(8)	8164(4)	5413(4)	30(2)
Re(2)	3646(1)	3226(1)	1496(1)	20(1)
O(20)	2650(5)	3352(2)	2165(2)	27(1)
Cl(2)	5411(2)	2807(1)	2278(1)	35(1)
P(3)	2928(2)	1873(1)	1188(1)	24(1)
C(61)	4321(8)	1381(4)	879(4)	31(2)
C(62)	4723(9)	747(4)	1177(5)	44(2)
C(63)	5775(11)	397(5)	945(6)	61(3)
C(64)	6445(10)	676(6)	428(6)	63(3)
C(65)	6038(9)	1293(5)	128(5)	49(2)
C(66)	4996(8)	1657(4)	365(4)	32(2)
C(67)	4643(8)	2345(4)	47(4)	33(2)
O(3)	4487(5)	2948(3)	617(3)	30(1)
C(71)	2383(8)	1405(4)	1917(4)	29(2)
C(72)	1725(10)	707(4)	1752(5)	51(3)
C(73)	1363(10)	342(5)	2312(5)	55(3)
C(74)	1607(9)	675(4)	3043(4)	40(2)
C(75)	2252(9)	1372(4)	3219(4)	41(2)
C(76)	2677(8)	1735(4)	2658(4)	34(2)
C(81)	1663(8)	1568(4)	432(4)	29(2)
C(82)	1877(8)	1132(4)	-241(4)	34(2)
C(83)	858(11)	959(5)	-812(5)	61(3)
C(84)	-364(11)	1215(5)	-719(6)	74(4)
C(85)	-592(9)	1635(5)	-68(6)	64(3)
C(86)	413(9)	1800(4)	504(5)	43(2)
P(4)	2031(2)	3861(1)	761(1)	20(1)
C(91)	2365(8)	4866(4)	1088(4)	26(2)
C(92)	1384(9)	5337(4)	1249(4)	36(2)
C(93)	1688(10)	6093(4)	1551(4)	44(2)

C(94)	2943(10)	6376(4)	1673(4)	44(2)
C(95)	3911(10)	5920(4)	1513(4)	43(2)
C(96)	3649(8)	5152(4)	1228(4)	29(2)
C(97)	4754(8)	4653(4)	1109(4)	30(2)
O(4)	4792(5)	4142(2)	1626(2)	29(1)
C(101)	2065(7)	3759(4)	-236(3)	22(1)
C(102)	2197(8)	4375(4)	-602(4)	32(2)
C(103)	2100(9)	4272(5)	-1367(4)	42(2)
C(104)	1904(8)	3562(5)	-1773(4)	38(2)
C(105)	1763(8)	2944(5)	-1424(4)	39(2)
C(106)	1854(8)	3042(4)	-660(4)	35(2)
C(111)	340(8)	3704(4)	856(4)	27(2)
C(112)	-82(8)	3699(4)	1554(4)	36(2)
C(113)	-1379(8)	3582(5)	1639(5)	43(2)
C(114)	-2298(9)	3501(4)	1028(5)	41(2)
C(115)	-1915(7)	3504(4)	323(4)	35(2)
C(116)	-632(8)	3623(4)	238(4)	31(2)
Cl(3)	4393(6)	9665(3)	7009(3)	81(2)
Cl(4)	1863(9)	9281(5)	7359(5)	134(3)
C(222)	3057	9765	7196	97(8)

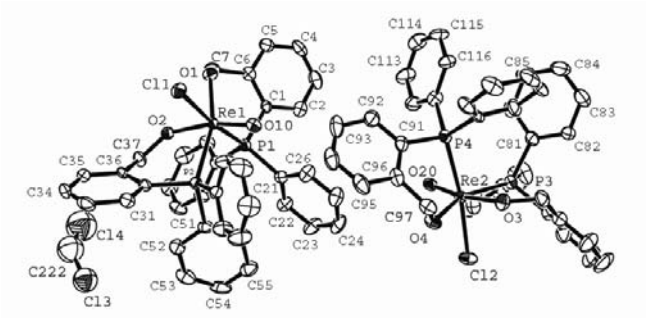

Fig. 25 Ellipsoid plot (50% probability) of $[ReOCl(L^1)_2]\cdot 1/2CH_2Cl_2$

$[TcCl_2(L^1)(HL^1)]\cdot MeOH$, (30)

Table 51 Crystal data and structure refinement for $[TcCl_2(L^1)(HL^1)]\cdot MeOH$

Empirical formula	$C_{39}H_{36}Cl_2O_3P_2Tc$	
Formula weight	783.52	
Temperature	200(2) K	
Wavelength	0.71073 Å	
Crystal system	Triclinic	
Space group	$P\bar{1}$	
Unit cell dimensions	a = 10.4269(9) Å	α= 62.975(6)°.
	b = 14.144(1) Å	β= 79.609(7)°.
	c = 14.526(1) Å	γ = 75.726(7)°.
Volume	1843.7(3) $Å^3$	
Z	2	
Density (calculated)	1.411 g/cm^3	
Absorption coefficient	0.658 mm^{-1}	
F(000)	802	
Crystal size	0.4 x 0.1 x 0.06 mm^3	
Crystal description	Plate	
Crystal color	Orange	
Diff. measurement device type	STOE IPDS 2T	
Theta range for data collection	1.72 to 29.32°.	
Index ranges	-14<=h<=14, -19<=k<=19, -19<=l<=19	
Reflections collected	20943	
Independent reflections	9873 [R(int) = 0.1127]	
Completeness to theta = 29.32°	97.6 %	
Absorption correction	None	
Max. and min. transmission	None and None	
Refinement method	Full-matrix least-squares on F^2	
Data / restraints / parameters	9873 / 0 / 411	
Goodness-of-fit on F^2	1.016	
Final R indices [I>2sigma(I)]	R1 = 0.0692, wR2 = 0.1351	
R indices (all data)	R1 = 0.1292, wR2 = 0.1679	
Extinction coefficient	0.0357(17)	
Largest diff. peak and hole	1.064 and -0.863 $e.Å^{-3}$	

Table 52 Atomic coordinates (x 10^4) and equivalent isotropic displacement parameters ($Å^2$x 10^3) for $[TcCl_2(L^1)(HL^1)]$·MeOH. U(eq) is defined as one third of the trace of the orthogonalized U^{ij} tensor.

	x	y	z	U(eq)
Tc	6825(1)	7312(1)	6865(1)	28(1)
Cl(1)	7752(2)	8571(1)	5326(1)	44(1)
O(2)	5132(4)	8275(3)	6672(3)	38(1)
P(1)	6282(1)	6338(1)	5980(1)	30(1)
C(1)	6497(5)	4891(4)	6838(4)	35(1)
C(2)	6642(6)	4190(5)	6372(5)	41(1)
C(3)	6747(7)	3086(5)	6981(5)	48(2)
C(4)	6702(7)	2685(5)	8032(6)	55(2)
C(5)	6594(7)	3369(5)	8495(5)	47(2)
C(6)	6477(5)	4482(4)	7913(4)	34(1)
C(7)	6374(6)	5135(4)	8525(4)	39(1)
O(1)	5893(4)	6248(3)	7998(3)	35(1)
C(11)	7214(5)	6431(5)	4761(4)	37(1)
C(12)	6608(7)	6611(5)	3914(5)	49(2)
C(13)	7357(8)	6678(6)	3001(5)	57(2)
C(14)	8719(9)	6549(6)	2957(6)	67(2)
C(15)	9330(8)	6375(8)	3788(7)	73(2)
C(16)	8586(6)	6331(6)	4691(5)	53(2)
C(21)	4535(5)	6771(4)	5721(4)	31(1)
C(22)	3657(6)	6059(5)	6132(4)	38(1)
C(23)	2330(6)	6433(6)	5939(5)	46(2)
C(24)	1884(6)	7518(6)	5351(5)	47(2)
C(25)	2753(6)	8232(5)	4936(5)	47(2)
C(26)	4069(6)	7859(5)	5123(5)	41(1)
C(31)	5529(5)	8925(4)	8254(4)	36(1)
C(32)	5196(6)	9008(5)	9185(5)	43(1)
C(33)	4042(7)	9712(6)	9302(6)	54(2)
C(34)	3251(7)	10326(6)	8501(6)	61(2)
C(35)	3578(7)	10234(6)	7580(6)	55(2)
C(36)	4691(6)	9527(5)	7449(5)	39(1)
C(37)	4950(6)	9380(5)	6460(5)	44(1)
Cl(2)	8920(1)	6161(1)	7238(1)	41(1)
P(2)	7108(1)	8121(1)	8031(1)	31(1)
C(41)	8295(5)	9020(4)	7589(4)	36(1)

C(42)	9411(6)	8884(5)	6948(5)	42(1)
C(43)	10312(6)	9558(6)	6606(6)	50(2)
C(44)	10118(6)	10384(5)	6889(5)	47(2)
C(45)	9030(7)	10538(6)	7523(6)	55(2)
C(46)	8112(6)	9868(5)	7852(5)	48(2)
C(51)	7592(5)	7084(4)	9287(4)	33(1)
C(52)	8866(6)	6850(6)	9568(5)	48(2)
C(53)	9243(7)	5975(6)	10486(5)	58(2)
C(54)	8375(7)	5351(6)	11133(5)	52(2)
C(55)	7098(7)	5562(5)	10887(5)	50(2)
C(56)	6685(6)	6418(5)	9964(5)	45(1)
O(3)	6425	3113	1008	68(1)
C(61)	7542	2520	1584	86(3)

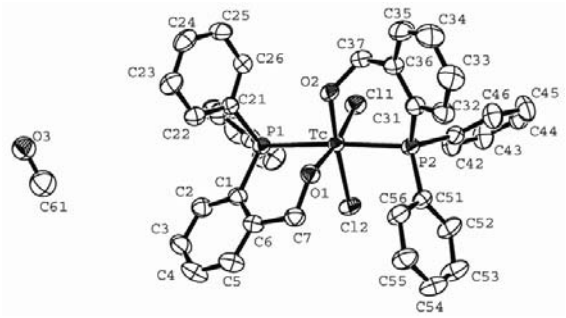

Fig. 26 Ellipsoid plot (50% probability) of $[TcCl_2(L^1)(HL^1)]\cdot MeOH$

$[ReCl_2(NPh)(PPh_3)(L^1)]$, (31)

Table 53 Crystal data and structure refinement for $[Re(Nph)Cl_2(PPh_3)(L^1)]$

Empirical formula	$C_{172}H_{136}Cl_8N_4O_4P_8Re_4$	
Formula weight	3599.05	
Temperature	200(2) K	
Wavelength	0.71073 Å	
Crystal system	Orthorhombic	
Space group	$Pna2_1$	
Unit cell dimensions	a = 18.4610(7) Å	α= 90°.
	b = 9.8858(4) Å	β= 90°.
	c = 20.202(1) Å	γ = 90°.
Volume	3686.9(3) $Å^3$	
Z	4	
Density (calculated)	1.621 g/cm^3	
Absorption coefficient	3.563 mm^{-1}	
F(000)	1784	
Crystal size	0.210 x 0.190 x 0.180 mm^3	
Crystal description	Polyhedron	
Crystal color	Brown	
Diff. measurement device type	STOE IPDS 2T	
Theta range for data collection	2.02 to 29.27°.	
Index ranges	-25<=h<=22, -13<=k<=13, -27<=l<=27	
Reflections collected	37718	
Independent reflections	9979 [R(int) = 0.0619]	
Completeness to theta = 29.27°	99.4 %	
Absorption correction	Integration	
Max. and min. transmission	0.6348 and 0.5040	
Refinement method	Full-matrix least-squares on F^2	
Data / restraints / parameters	9979 / 1 / 452	
Goodness-of-fit on F^2	1.123	
Final R indices [I>2sigma(I)]	R1 = 0.0387, wR2 = 0.0871	
R indices (all data)	R1 = 0.0506, wR2 = 0.1022	
Absolute structure parameter	0.00	
Extinction coefficient	0.0144(4)	
Largest diff. peak and hole	2.114 and -1.169 e.$Å^{-3}$	

Table 54 Atomic coordinates (x 10^4) and equivalent isotropic displacement parameters ($Å^2$x 10^3) for [Re(NPh)Cl_2(PPh_3)(L^1)]. U(eq) is defined as one third of the trace of the orthogonalized U^{ij} tensor.

	x	y	z	U(eq)
Re	-6292(1)	986(1)	732(1)	24(1)
Cl(1)	-5629(1)	2872(2)	268(1)	36(1)
Cl(2)	-7111(1)	-670(2)	1215(1)	37(1)
N(10)	-5545(2)	-86(5)	748(4)	30(1)
C(31)	-4956(3)	-925(6)	733(6)	33(1)
C(32)	-5010(5)	-2245(8)	968(4)	51(2)
C(33)	-4386(6)	-3034(10)	970(5)	67(3)
C(34)	-3744(4)	-2547(10)	752(9)	63(2)
C(35)	-3693(4)	-1273(12)	516(5)	58(2)
C(36)	-4294(4)	-438(10)	504(4)	45(2)
P(1)	-6675(1)	213(2)	-376(1)	26(1)
C(1)	-7661(3)	257(7)	-432(3)	29(1)
C(2)	-8047(4)	-813(7)	-695(3)	36(1)
C(3)	-8806(4)	-766(9)	-697(4)	43(2)
C(4)	-9160(4)	353(10)	-452(4)	48(2)
C(5)	-8766(4)	1416(11)	-188(5)	42(2)
C(6)	-8014(4)	1387(8)	-171(4)	36(1)
C(7)	-7586(4)	2546(8)	145(4)	42(2)
O(1)	-7139(2)	2138(4)	687(4)	36(1)
C(11)	-6411(4)	-1508(7)	-603(3)	33(1)
C(12)	-6186(4)	-1834(9)	-1237(4)	43(2)
C(13)	-5979(5)	-3159(9)	-1384(4)	50(2)
C(14)	-6018(5)	-4123(9)	-914(5)	49(2)
C(15)	-6246(6)	-3835(9)	-287(5)	61(3)
C(16)	-6441(5)	-2504(8)	-137(4)	48(2)
C(21)	-6345(5)	1220(11)	-1072(6)	31(2)
C(22)	-6821(5)	1797(8)	-1541(4)	43(2)
C(23)	-6523(6)	2512(9)	-2064(4)	55(2)
C(24)	-5782(6)	2671(10)	-2131(5)	61(3)
C(25)	-5331(5)	2086(9)	-1669(4)	54(2)
C(26)	-5606(4)	1376(9)	-1146(4)	43(2)
P(2)	-5952(1)	2016(2)	1815(1)	26(1)
C(41)	-6211(3)	3775(7)	1957(4)	33(1)
C(42)	-6603(4)	4530(8)	1501(4)	38(2)

C(43)	-6781(5)	5869(8)	1642(4)	46(2)
C(44)	-6594(5)	6461(8)	2223(5)	49(2)
C(45)	-6215(6)	5723(9)	2679(5)	54(2)
C(46)	-6027(6)	4391(9)	2550(4)	49(2)
C(51)	-6274(5)	1243(12)	2584(7)	33(2)
C(52)	-5822(4)	1052(9)	3137(4)	45(2)
C(53)	-6122(6)	574(13)	3719(5)	64(3)
C(54)	-6840(6)	220(12)	3751(5)	66(3)
C(55)	-7281(5)	421(10)	3209(5)	56(2)
C(56)	-6995(4)	919(8)	2638(4)	43(2)
C(61)	-4963(3)	2023(7)	1869(3)	30(1)
C(62)	-4593(4)	839(8)	2033(4)	37(2)
C(63)	-3841(4)	806(9)	2007(4)	45(2)
C(64)	-3469(4)	1945(11)	1816(4)	54(2)
C(65)	-3828(5)	3105(13)	1652(6)	53(3)
C(66)	-4578(4)	3168(8)	1676(4)	42(2)

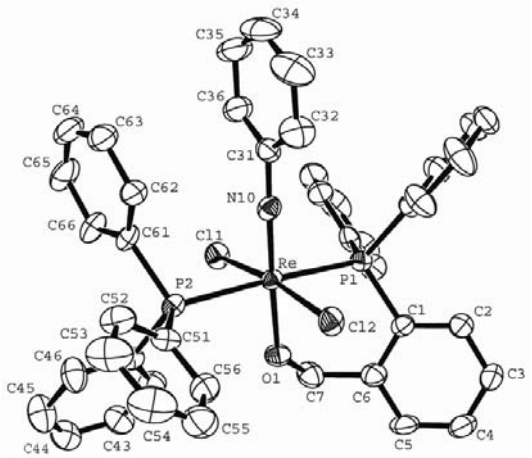

Fig. 27 Ellipsoid plot (50% probability) of [Re(Nph)Cl_2(PPh_3)(L^1)]:

[ReCl(NPh)(L^1)$_2$], (32)

Table 55 Crystal data and structure refinement for [Re(NPh)Cl(L^1)$_2$]

Empirical formula	$C_{44}H_{37}ClNO_2P_2Re$	
Formula weight	895.34	
Temperature	200(2) K	
Wavelength	0.71073 Å	
Crystal system	Monoclinic	
Space group	$P2_1/n$	
Unit cell dimensions	a = 11.551(1) Å	α= 90°.
	b = 18.774(1) Å	β= 94.296(7)°.
	c = 16.733(1) Å	γ = 90°.
Volume	3618.5(5) Å^3	
Z	4	
Density (calculated)	1.643 g/cm^3	
Absorption coefficient	3.561 mm^{-1}	
F(000)	1784	
Crystal size	0.3 x 0.2 x 0.04 mm^3	
Crystal description	Plate	
Crystal color	Green	
Diff. measurement device type	STOE IPDS 2T	
Theta range for data collection	2.07 to 29.28°.	
Index ranges	-15<=h<=15, -25<=k<=25, -20<=l<=22	
Reflections collected	26072	
Independent reflections	9696 [R(int) = 0.2482]	
Completeness to theta = 29.28°	98.2 %	
Absorption correction	Integration	
Max. and min. transmission	0.5317 and 0.4568	
Refinement method	Full-matrix least-squares on F^2	
Data / restraints / parameters	9696 / 0 / 460	
Goodness-of-fit on F^2	0.918	
Final R indices [I>2sigma(I)]	R1 = 0.0999, wR2 = 0.1708	
R indices (all data)	R1 = 0.2182, wR2 = 0.2212	
Largest diff. peak and hole	1.439 and -3.011 e.Å^{-3}	

Table 56 Atomic coordinates (x 10^4) and equivalent isotropic displacement parameters ($Å^2$x 10^3) for [Re(NPh)Cl(L^1)$_2$]. U(eq) is defined as one third of the trace of the orthogonalized U^{ij} tensor.

	x	y	z	U(eq)
Re	880(1)	2410(1)	7062(1)	23(1)
Cl(1)	2768(3)	2982(2)	7382(3)	37(1)
N(10)	251(12)	2780(6)	7870(8)	30(3)
C(31)	-177(14)	3208(9)	8483(10)	34(4)
C(32)	512(16)	3302(11)	9186(10)	43(4)
C(33)	140(20)	3787(12)	9757(12)	62(6)
C(34)	-870(20)	4166(14)	9603(15)	73(8)
C(35)	-1589(18)	4050(11)	8881(13)	51(5)
C(36)	-1192(18)	3584(10)	8332(11)	43(4)
P(1)	515(3)	3469(2)	6227(2)	25(1)
C(1)	1767(14)	3642(11)	5647(9)	36(4)
C(2)	2040(14)	4326(9)	5447(10)	31(3)
C(3)	2983(16)	4513(11)	5015(11)	44(5)
C(4)	3689(16)	3938(10)	4776(11)	40(4)
C(5)	3485(17)	3254(12)	4973(11)	48(5)
C(6)	2524(15)	3103(9)	5414(9)	32(4)
C(7)	2357(15)	2316(10)	5624(12)	47(5)
O(1)	1350(10)	2165(6)	5966(7)	37(3)
C(11)	294(13)	4296(8)	6770(8)	23(3)
C(12)	918(14)	4439(9)	7499(10)	28(4)
C(13)	720(20)	5010(10)	7935(13)	47(5)
C(14)	-15(18)	5540(10)	7634(14)	53(6)
C(15)	-585(18)	5456(11)	6872(15)	54(5)
C(16)	-449(15)	4836(9)	6461(11)	37(4)
C(21)	-682(13)	3471(8)	5456(9)	24(3)
C(22)	-1814(15)	3432(8)	5710(11)	37(4)
C(23)	-2782(17)	3449(10)	5151(12)	46(5)
C(24)	-2604(19)	3468(10)	4361(11)	46(5)
C(25)	-1506(17)	3495(11)	4075(10)	44(5)
C(26)	-583(16)	3501(9)	4633(11)	39(4)
P(2)	-747(3)	1604(2)	6769(2)	24(1)
C(41)	-551(15)	796(9)	7381(9)	32(4)
C(42)	-1487(15)	422(9)	7626(10)	35(4)
C(43)	-1281(19)	-222(12)	8037(11)	51(5)

C(44)	-160(20)	-498(10)	8173(11)	51(5)
C(45)	730(16)	-119(9)	7922(12)	38(4)
C(46)	568(15)	514(9)	7508(11)	31(4)
C(47)	1583(15)	879(10)	7158(13)	45(5)
O(2)	1790(9)	1576(6)	7445(8)	37(3)
C(51)	-2170(13)	1908(9)	7028(10)	31(3)
C(52)	-2286(17)	2061(10)	7817(12)	45(5)
C(53)	-3352(15)	2309(10)	8071(13)	46(4)
C(54)	-4247(15)	2484(11)	7511(15)	58(6)
C(55)	-4092(15)	2349(11)	6700(14)	48(5)
C(56)	-3080(17)	2070(10)	6479(11)	44(5)
C(61)	-968(12)	1221(8)	5750(9)	24(3)
C(62)	-1260(18)	525(10)	5625(11)	44(4)
C(63)	-1460(20)	245(10)	4866(13)	53(5)
C(64)	-1446(19)	701(10)	4241(12)	51(5)
C(65)	-1200(19)	1411(12)	4328(11)	53(6)
C(66)	-938(17)	1665(9)	5100(11)	39(4)

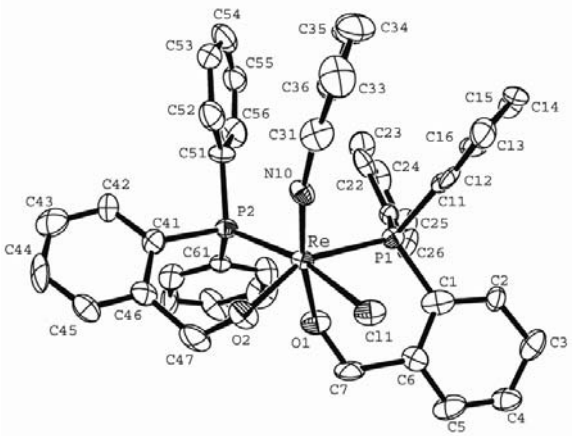

Fig. 28 Ellipsoid plot (50% probability) of [Re(Nph)Cl(L^1)$_2$]

$[ReOCl_2(H_2L^3)]$, (33)

Table 57 Crystal data and structure refinement for $[ReOCl_2(H_2L^3)]\cdot 2MeOH$

Empirical formula	$C_{23}H_{28}Cl_2O_6PRe$	
Formula weight	688.52	
Temperature	200(2) K	
Wavelength	0.71073 Å	
Crystal system	Trigonal	
Space group	$R\bar{3}$:h	
Unit cell dimensions	a = 36.973(5) Å	α= 90°.
	b = 36.973(5) Å	β= 90°.
	c = 9.962(5) Å	γ = 120°.
Volume	11793(6) $Å^3$	
Z	18	
Density (calculated)	1.745 g/cm^3	
Absorption coefficient	4.936 mm^{-1}	
F(000)	6084	
Crystal size	0.3 x 0.2 x 0.04 mm^3	
Crystal description	Plate	
Crystal color	Violet	
Diff. measurement device type	STOE IPDS 2T	
Theta range for data collection	1.91 to 29.27°.	
Index ranges	-50<=h<=50, -50<=k<=50, -12<=l<=13	
Reflections collected	73040	
Independent reflections	7107 [R(int) = 0.1666]	
Completeness to theta = 29.27°	99.2 %	
Absorption correction	Integration	
Max. and min. transmission	0.6816 and 0.5113	
Refinement method	Full-matrix least-squares on F^2	
Data / restraints / parameters	7107 / 0 / 298	
Goodness-of-fit on F^2	1.044	
Final R indices [I>2sigma(I)]	R1 = 0.0633, wR2 = 0.1065	
R indices (all data)	R1 = 0.1171, wR2 = 0.1229	
Extinction coefficient	0.00034(2)	
Largest diff. peak and hole	1.473 and -2.927 $e.Å^{-3}$	

Table 58 Atomic coordinates (x 10^4) and equivalent isotropic displacement parameters ($Å^2$x 10^3) for $[ReOCl_2(H_2L^3)]\cdot 2MeOH$. U(eq) is defined as one third of the trace of the orthogonalized U^{ij} tensor.

	x	y	z	U(eq)
Re	2157(1)	845(1)	2941(1)	21(1)
O(10)	1702(2)	445(2)	2426(7)	35(2)
Cl(1)	2435(1)	1000(1)	705(2)	34(1)
Cl(2)	2015(1)	1418(1)	2777(2)	32(1)
P	2430(1)	389(1)	3418(2)	19(1)
C(1)	2923(3)	582(3)	2545(8)	23(2)
C(2)	3013(3)	311(3)	1823(9)	27(2)
C(3)	3376(3)	462(3)	1119(11)	40(2)
C(4)	3663(3)	879(3)	1144(10)	40(2)
C(5)	3580(3)	1154(3)	1869(9)	30(2)
C(6)	3209(3)	1013(3)	2574(9)	26(2)
C(7)	3142(3)	1320(3)	3371(9)	27(2)
O(1)	2723(2)	1217(2)	3507(6)	24(1)
C(11)	2578(3)	454(2)	5196(8)	23(2)
C(12)	2954(3)	507(3)	5593(9)	30(2)
C(13)	3076(3)	584(3)	6946(10)	36(2)
C(14)	2809(3)	603(3)	7887(9)	35(2)
C(15)	2425(3)	546(3)	7473(8)	32(2)
C(16)	2303(3)	469(2)	6149(8)	21(2)
C(17)	1897(3)	430(3)	5725(9)	27(2)
O(2)	1963(2)	788(2)	4922(6)	26(1)
C(21)	2116(3)	-172(3)	3151(8)	23(2)
C(22)	2039(3)	-433(3)	4254(9)	28(2)
C(23)	1788(3)	-858(3)	4128(11)	42(3)
C(24)	1629(3)	-1036(3)	2903(12)	40(2)
C(25)	1692(3)	-780(3)	1799(12)	45(3)
C(26)	1939(3)	-351(3)	1893(9)	31(2)
C(27)	2006(3)	-99(3)	631(10)	42(2)
O(3)	1619(3)	-174(3)	63(8)	58(2)
O(4)	8997(3)	474(3)	5815(9)	62(2)
O(5)	399(4)	1303(4)	1556(10)	85(3)
C(32)	743(5)	1341(6)	775(18)	99(6)
C(31)	9138(9)	291(9)	5360(30)	161(11)

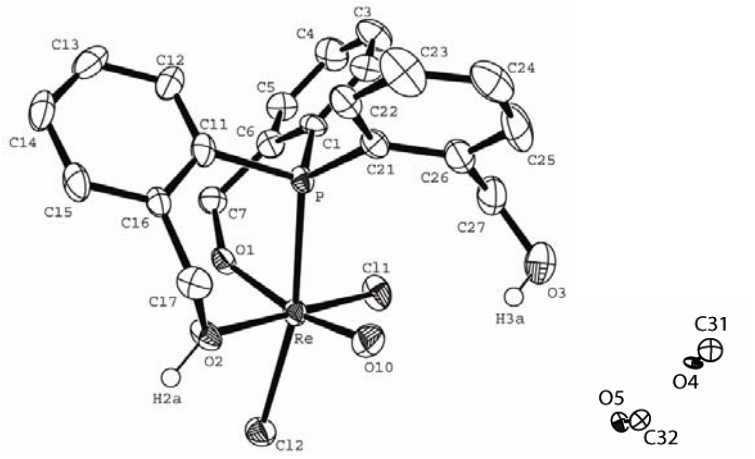

Fig. 29 Ellipsoid plot (50% probability) of $[ReOCl_2(H_2L^3)]\cdot 2MeOH$

$[\{TcOCl\}(\mu\text{-}HL^3)]_2$, (34)

Table 59 Crystal data and structure refinement for $[(TcOCl)(\mu\text{-}HL^3)]_2 \cdot EtOH$

Empirical formula	$C_{21.50}H_{20.50}ClO_{4.25}PTc$	
Formula weight	512.30	
Temperature	200(2) K	
Wavelength	0.71073 Å	
Crystal system	Triclinic	
Space group	$P\bar{1}$	
Unit cell dimensions	a = 9.720(2) Å	α= 86.89(2)°.
	b = 11.852(2) Å	β= 83.18(2)°.
	c = 11.805(3) Å	γ = 80.20(2)°.
Volume	1329.8(5) $Å^3$	
Z	2	
Density (calculated)	1.277 g/cm^3	
Absorption coefficient	0.723 mm^{-1}	
F(000)	517	
Crystal size	0.290 x 0.183 x 0.030 mm^3	
Crystal description	Plate	
Crystal color	Green	
Diff. measurement device type	STOE IPDS 2T	
Theta range for data collection	1.74 to 29.32°.	
Index ranges	-13<=h<=13, -13<=k<=16, -16<=l<=15	
Reflections collected	14055	
Independent reflections	7027 [R(int) = 0.2587]	
Completeness to theta = 29.32°	96.1 %	
Absorption correction	None	
Max. and min. transmission	None and None	
Refinement method	Full-matrix least-squares on F^2	
Data / restraints / parameters	7027 / 0 / 271	
Goodness-of-fit on F^2	0.738	
Final R indices [I>2sigma(I)]	R1 = 0.0757, wR2 = 0.1516	
R indices (all data)	R1 = 0.3242, wR2 = 0.2572	
Extinction coefficient	0.053(4)	
Largest diff. peak and hole	0.687 and -0.666 $e.Å^{-3}$	

Table 60 Atomic coordinates (x 10^4) and equivalent isotropic displacement parameters ($Å^2$x 10^3) for $[(TcOCl)(\mu\text{-}HL^3)]_2 \cdot 1/2EtOH$. U(eq) is defined as one third of the trace of the orthogonalized U^{ij} tensor.

	x	y	z	U(eq)
Tc(1)	5138(1)	8904(1)	5871(1)	60(1)
O(10)	5917(8)	9385(9)	6863(9)	82(3)
Cl(1)	6816(3)	7131(3)	5817(3)	72(1)
P(1)	3416(3)	8298(3)	7269(3)	58(1)
C(1)	3333(12)	6800(11)	7090(12)	54(3)
C(2)	3193(16)	6071(15)	8071(13)	81(5)
C(3)	3160(20)	4914(16)	7961(18)	129(8)
C(4)	3210(20)	4510(14)	6873(18)	107(6)
C(5)	3366(14)	5238(14)	5895(16)	83(5)
C(6)	3407(12)	6415(12)	6009(11)	56(3)
C(7)	3512(14)	7142(12)	4923(13)	72(4)
O(1)	4077(7)	8151(7)	4985(7)	62(2)
C(11)	1726(11)	9075(11)	6930(11)	61(4)
C(12)	545(12)	8527(12)	6962(11)	67(4)
C(13)	-727(11)	9101(15)	6708(11)	66(4)
C(14)	-885(12)	10226(15)	6390(14)	83(5)
C(15)	288(12)	10782(12)	6341(12)	73(4)
C(16)	1565(10)	10247(12)	6582(11)	60(4)
C(17)	2792(12)	10893(11)	6474(12)	72(4)
O(2)	3870(7)	10414(7)	5618(8)	71(3)
C(21)	3499(14)	8558(13)	8771(14)	78(5)
C(23)	2380(20)	9514(18)	10469(18)	115(7)
C(24)	3480(30)	9090(20)	11038(16)	118(7)
C(26)	4662(16)	8090(15)	9349(13)	84(5)
C(25)	4610(20)	8410(20)	10477(15)	128(8)
C(27)	5945(17)	7294(19)	8889(17)	108(7)
C(22)	2352(14)	9241(14)	9346(14)	88(5)
O(3)	6490(20)	6514(16)	9547(14)	191(9)
O(5)	540(40)	3970(30)	380(30)	69(10)
C(52)	810(40)	2570(40)	-920(40)	53(12)
C(51)	300(50)	3020(50)	20(40)	53(12)

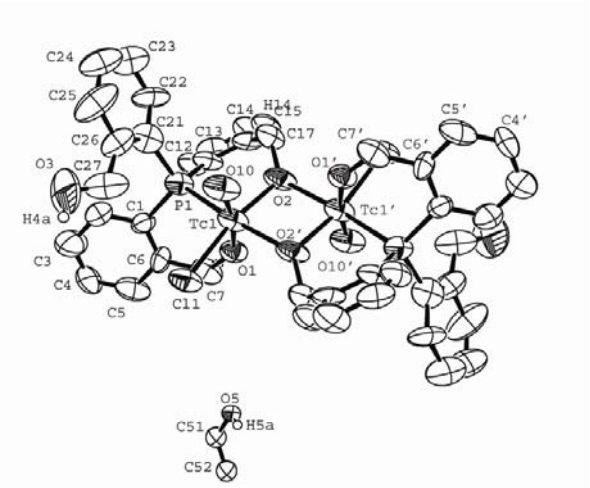

Fig. 30 Ellipsoid plot (50% probability) of $[(TcOCl)(\mu\text{-}HL^3)]_2 \cdot 1/2EtOH$.

$[TcCl_3(H_2L^3)]$, (35)

Table 61 Crystal data and structure refinement for $[TcCl_3(H_2L^3)]$

Empirical formula	$C_{21}H_{19}Cl_3O_3PTc$	
Formula weight	554.68	
Temperature	200(2) K	
Wavelength	0.71073 Å	
Crystal system	Monoclinic	
Space group	$P2_1/c$	
Unit cell dimensions	a = 9.010(2) Å	α= 90.01°.
	b = 15.590(2) Å	β= 105.26(1)°.
	c = 16.184(3) Å	γ = 90.18°.
Volume	2193.1(6) $Å^3$	
Z	4	
Density (calculated)	1.680 g/cm^3	
Absorption coefficient	1.115 mm^{-1}	
F(000)	1112	
Crystal size	0.1 x 0.09 x 0.06 mm^3	
Crystal description	Plate	
Crystal color	Orange	
Diff. measurement device type	STOE IPDS 2T	
Theta range for data collection	2.61 to 26.90°.	
Index ranges	-10<=h<=11, -19<=k<=19, -20<=l<=20	
Reflections collected	17620	
Independent reflections	4587 [R(int) = 0.1932]	
Completeness to theta = 26.90°	96.7 %	
Absorption correction	None	
Max. and min. transmission	None and None	
Refinement method	Full-matrix least-squares on F^2	
Data / restraints / parameters	4587 / 0 / 264	
Goodness-of-fit on F^2	0.963	
Final R indices [I>2sigma(I)]	R1 = 0.0838, wR2 = 0.1604	
R indices (all data)	R1 = 0.1779, wR2 = 0.1996	
Extinction coefficient	0.0043(10)	
Largest diff. peak and hole	1.529 and -0.944 $e.Å^{-3}$	

Table 62 Atomic coordinates (x 10^4) and equivalent isotropic displacement parameters ($Å^2$x 10^3) for [$TcCl_3(H_2L^3)$]. U(eq) is defined as one third of the trace of the orthogonalized U^{ij} tensor.

	x	y	z	U(eq)
Tc	5678(1)	8072(1)	8373(1)	49(1)
Cl(1)	3891(4)	8953(2)	7417(2)	69(1)
Cl(2)	3807(3)	7396(2)	8942(2)	53(1)
Cl(3)	6230(4)	9068(2)	9447(2)	66(1)
P	7799(3)	7050(2)	9061(2)	43(1)
C(1)	9462(13)	7685(6)	9611(6)	49(3)
C(2)	10447(13)	7410(6)	10381(6)	51(3)
C(3)	11698(13)	7872(7)	10791(7)	57(3)
C(4)	12063(13)	8635(7)	10452(7)	58(3)
C(5)	11075(14)	8902(7)	9696(7)	62(3)
C(6)	9759(14)	8460(6)	9248(7)	54(3)
C(7)	8787(14)	8819(8)	8425(7)	66(3)
O(1)	7450(9)	8397(4)	7983(4)	58(2)
C(11)	8372(11)	6554(5)	8198(6)	41(2)
C(12)	9910(13)	6566(6)	8165(6)	49(2)
C(13)	10371(14)	6228(7)	7471(7)	58(3)
C(14)	9213(15)	5889(6)	6800(6)	58(3)
C(15)	7693(14)	5845(7)	6814(6)	53(3)
C(16)	7228(12)	6193(5)	7508(6)	42(2)
C(17)	5578(13)	6244(6)	7474(7)	50(3)
O(2)	5084(8)	7141(4)	7392(4)	46(2)
C(21)	7514(11)	6198(5)	9755(6)	42(2)
C(22)	7646(12)	5331(6)	9514(6)	46(2)
C(23)	7304(13)	4671(6)	9979(6)	56(3)
C(24)	6888(14)	4826(7)	10725(7)	60(3)
C(25)	6784(13)	5650(7)	10981(7)	56(3)
C(26)	7073(12)	6340(6)	10518(6)	46(2)
C(27)	6949(14)	7235(6)	10841(6)	53(3)
O(3)	5440(8)	7413(5)	10935(4)	53(2)

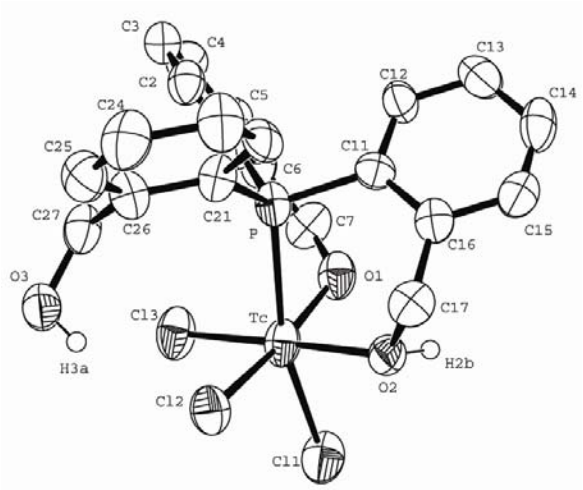

Fig. 31 Ellipsoid plot (50% probability) of $[TcCl_3(H_2L^3)]$

$[Re(CO)_3(H_2L^3)]$, (36)

Table 63 Crystal data and structure refinement for $[Re(CO)_3(H_2L^3)]\cdot MeOH$

Empirical formula	$C_{25}H_{24}O_7PRe$	
Formula weight	653.61	
Temperature	200(2) K	
Wavelength	0.71073 Å	
Crystal system	Monoclinic	
Space group	$P2_1/n$	
Unit cell dimensions	a = 17.354(2) Å	α= 90°.
	b = 8.4670(9) Å	β= 108.207(8)°.
	c = 17.820(2) Å	γ = 90°.
Volume	2487.4(5) $Å^3$	
Z	4	
Density (calculated)	1.745 g/cm^3	
Absorption coefficient	4.992 mm^{-1}	
F(000)	1280	
Crystal size	0.09 x 0.07 x 0.06 mm^3	
Crystal description	Plate	
Crystal color	Colorless	
Diff. measurement device type	STOE IPDS 2T	
Theta range for data collection	1.98 to 26.86°.	
Index ranges	-21<=h<=22, -9<=k<=10, -22<=l<=20	
Reflections collected	11894	
Independent reflections	5208 [R(int) = 0.1002]	
Completeness to theta = 26.86°	97.1 %	
Absorption correction	Integration	
Max. and min. transmission	0.7188 and 0.3940	
Refinement method	Full-matrix least-squares on F^2	
Data / restraints / parameters	5208 / 0 / 310	
Goodness-of-fit on F^2	0.935	
Final R indices [I>2sigma(I)]	R1 = 0.0550, wR2 = 0.1284	
R indices (all data)	R1 = 0.0946, wR2 = 0.1521	
Extinction coefficient	0.0085(6)	
Largest diff. peak and hole	1.545 and -1.876 $e.Å^{-3}$	

Table 64 Atomic coordinates (x 10^4) and equivalent isotropic displacement parameters ($Å^2$x 10^3) for $[Re(CO)_3(H_2L^3)]$·MeOH.. U(eq) is defined as one third of the trace of the orthogonalized U^{ij} tensor.

	x	y	z	U(eq)
Re	8531(1)	642(1)	-48(1)	39(1)
P	8167(1)	-1831(3)	458(2)	38(1)
C(1)	9060(6)	-2869(12)	1083(6)	42(2)
C(2)	9691(5)	-2018(12)	1619(6)	40(2)
C(3)	10296(6)	-2869(14)	2161(7)	52(3)
C(4)	10291(7)	-4503(14)	2178(7)	56(3)
C(5)	9696(7)	-5324(12)	1630(7)	49(3)
C(6)	9078(6)	-4505(12)	1090(6)	43(2)
C(7)	9727(6)	-227(12)	1622(6)	47(3)
O(1)	9659(4)	401(8)	883(4)	46(2)
C(11)	7732(6)	-3178(12)	-366(6)	41(2)
C(12)	7092(7)	-4143(13)	-375(8)	59(3)
C(13)	6746(9)	-5134(16)	-1014(10)	75(4)
C(14)	7027(8)	-5139(15)	-1650(8)	65(4)
C(15)	7660(7)	-4174(12)	-1642(7)	53(3)
C(16)	8019(6)	-3176(13)	-1010(6)	47(2)
C(17)	8751(11)	-2293(19)	-1067(11)	112(7)
O(2)	9069(4)	-1049(9)	-626(5)	57(2)
C(21)	7487(5)	-1873(12)	1075(6)	43(2)
C(22)	7777(7)	-2533(14)	1841(6)	54(3)
C(23)	7327(8)	-2495(18)	2348(8)	70(4)
C(24)	6570(7)	-1815(18)	2106(7)	65(3)
C(25)	6271(7)	-1170(15)	1357(8)	59(3)
C(26)	6707(6)	-1185(12)	831(7)	46(2)
C(27)	6328(6)	-521(13)	8(6)	50(3)
O(3)	5489(4)	-842(11)	-289(5)	68(2)
C(20)	7584(6)	804(11)	-933(6)	43(2)
O(20)	7006(5)	898(10)	-1471(4)	58(2)
C(30)	8968(6)	2544(12)	-418(6)	43(2)
O(30)	9197(5)	3675(9)	-600(5)	55(2)
C(10)	8029(6)	1931(13)	514(6)	47(2)
O(10)	7663(5)	2680(9)	846(5)	60(2)
C(41)	5749(13)	3970(20)	1176(12)	115(7)
O(4)	5088(9)	3834(16)	510(9)	142(6)

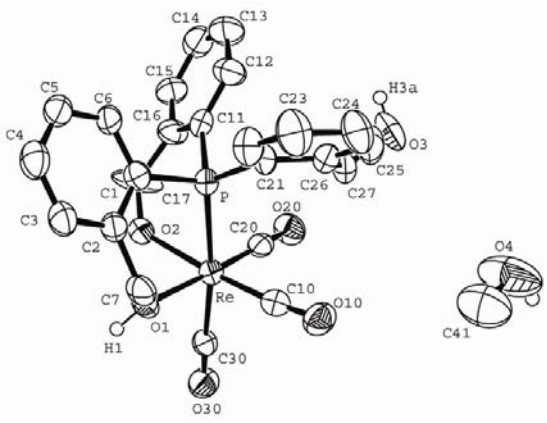

Fig. 32 Ellipsoid plot (50% probability) of $[Re(CO)_3(H_2L^3)]\cdot MeOH$